BCRP (ABCG2) expression, function and regulation in model and intestinal epithelial cells

Jamie A Wright, B.Sc. (Hons)

Submitted for the degree of Doctor of Philosophy

Epithelial Research Group

Institute for Cell and Molecular Biosciences

The Medical School

University of Newcastle upon Tyne

February 2011

Acknowledgements

I would like to thank Prof. Nick Simmons for his continual input, and support throughout my PhD studies. I also would like to thank Dr. Tanya Coleman and Dr. Iain Haslam for their guidance over the 3 years, particularly at AstraZeneca (Alderley Park). I am further thankful to all colleagues from the laboratories I have worked in over the past few years for their help, support and interesting discussions. I would like to acknowledge financial support from Newcastle University, AstraZeneca (Alderley Park) and the BBSRC for funding of this study.

I would also like to say thanks to all my friends who I have met and had the pleasure of knowing during my time in Newcastle and Alderley Park.

Lastly I would like to pass on my gratitude to the most important people in my life which is my family. I am very grateful to Pam and Martyn for their support whilst I have been in Cheshire. Finally a special thank you goes to my Mum and Dad for their continual encouragement and support.

Abstract

The breast cancer resistance protein (BCRP, ABCG2) is a member of the ATP binding cassette transporters (ABC transporters) that functions as an efflux transporter alongside other family members such as MDR1 and MRP2 to remove foreign entities from the cell. These efflux transporters often have overlapping substrate specificity that together comprise a formidable barrier in preventing cell exposure to foreign compounds, but in doing so inevitably influence drug absorption, elimination and distribution of a significant number of prescribed drugs.

This thesis has used established in vitro epithelial cell models such as MDCKII and Caco-2 cells to examine the function and regulation of the less characterised of the three main efflux transporters, BCRP, in the context of epithelial expression with particular focus on human intestinal cells. Several complementary techniques have been used including cellular accumulation of Hoechst 33342, a known MDR1/BCRP bi-substrate in the presence of selective pharmacological inhibitors, together with immunocytochemistry, immunoblotting and PCR techniques. Of most importance were functional assays of transepithelial substrate flux measured across reconstituted epithelial layers.

BCRP substrates were identified by comparing bi-directional transport directly across native MDCKII monolayers to hBCRP/mBcrp and MDR1 transfected MDCKII cell layers in a high throughput assay. This technique identified several BCRP substrates including the selective BCRP agent nitrofurantoin.

The human intestinal Caco-2 cell system was used as a model for BCRP mediated transport and induction of ABC transport activity. BCRP is expressed at differing levels in 2 cell-strains; saturable nitrofurantoin transport was evident in the high-expressing strain. Ko143, a specific BCRP inhibitor, inhibited nitrofurantoin

secretion by this Caco-2 cell strain and allowed partition of BCRP mediated secretory flux from MDR1 for bi-substrates. The aryl hydrocarbon receptor (AhR) agonist β-naphthoflavone (BNF) and the peroxisome proliferator receptor gamma (PPARγ) agonist rosiglitazone increased the BCRP mediated net flux of the selective substrate, nitrofurantoin and this correlated with an increase in both BCRP mRNA and protein expression. BCRP regulation in Caco-2 cells is likely to be controlled by more than one pathway and it appears that in the human gut a complex network of distinct nuclear receptors regulate the expression of BCRP. The present work suggests that the Caco-2 cell model together with nitrofurantoin as a substrate could serve as a screen for potential inducers of BCRP.

Abbreviations

Aa Cellular accumulation across the apical membrane

Ab Cellular accumulation across the basal membrane

ABC ATP-binding cassette

ADME Absorption, distribution, metabolism and excretion

ATP Adenosine triphosphate

AhR Aryl hydrocarbon receptor

ARNT Aryl hydrocarbon receptor nuclear translocator

BBB Blood brain barrier

BCRP Breast cancer resistance protein

BNF β-naphthoflavone

CAR Constitutive androstane receptor

CsA Cyclosporin A

CYP Cytochrome P450

DBM Dibenzoylmethane

DDI Drug-drug interaction

DMEM Dulbecco's Modified Eagle's Medium

DMSO Dimethyl sulphoxide

DNA Dideoxyribonucleic acid

E217βG Estradiol-17-[beta]-glucuronide

EDTA Ethylene-diamintetraacetic acid

EGTA Ethylene glycol-bis(β-aminoethyl ether)-N,N,N′,N′ –tetraacetic acid

EMEM Minimum Essential Eagle's Medium

ER Estrogen receptor

FDA Food and Drug Administration

FITC Fluoroscein isothiocyanate

FTC Fumitremorgin C

FXR Farnesoid x receptor

GSH Glutathione

HBSS Hank's buffered saline solution

HEK Human Embryonic Kidney 293 cells

HEPES N-[2-hydroxyethyl]piperazine-N′-[2-ethanesulphonic acid]

HPLC High-pressure liquid chromatography

HRE Hormone response element

HSP90 Heat shock protein 90

HUGO Human Genome Organisation

IAAP Iodoazidoaryl prazosin

J_{a-b} Flux in the apical-to-basal direction

J_{b-a} Flux in the basal-to-apical direction

J_{net} net flux (secretory, $J_{b-a} - J_{a-b}$)

K_m Michaelis-Menten constant (concentration at which reaction is half maximal)

LXR Liver x receptor

MpkDCT Mouse distal convoluted tubule cells

MpkCCDc14 mouse cortical collecting duct principal cells (clone 14)

MDCK Madin Darby Canine Kidney

MDR1 Multidrug resistance 1

MRP Multidrug resistance-associated protein

MXR Mitoxantrone resistance

NBD Nucleotide binding domain

NCE New chemical entity

NR Nuclear receptor

PA Cell passage

Papp Apparent permeability

PBS Phosphate buffered saline

PPARγ Peroxisome proliferator activated receptor gamma

Pgp P-glycoprotein

PgR Progesterone receptor

PXR Pregnane x receptor

RAR Retinoic acid receptor

RNA Ribonucleic acid

SNP Single nucleotide polymorphism

TBHQ Tert-butylhydroquinone

TBS Tris buffered saline

TEER Transepithelial electrical resistance

TMD Transmembrane domain

WT Wild type

Contents

Abstract....3
Abbreviations....5
Contents....7
Figures....11
Tables....14

1. Introduction....15

1.1 Introduction to the ATP-binding cassette (ABC) transporters....15

1.2 Multidrug resistance protein 1 (MDR1)....20

1.2.1 MDR1 structure....20
1.2.2 Distribution of MDR1 within the body....21
1.2.3 MDR1 function....21

1.3 Multidrug resistance-associated protein (MRP)....24

1.4 Breast cancer resistance protein (BCRP)....28

1.4.1 BCRP structure....29
1.4.2 BCRP function....31
1.4.3 BCRP: a detoxification pathway....32
1.4.4 BCRP: a transporter of endogenous compounds....33

1.5 Implications of the efflux transporters on oral drug delivery....38

1.6 Systems for predicting oral bioavailability....43

1.7 ABC protein nuclear receptor modulation....48

1.8 Objectives of the thesis....50

2. Materials and methods....52

2.1 Materials....52

2.2 Methods....52

2.2.1 Routine cell culture....52

2.2.2 Functional transport assays....54

2.2.2.1 *Hoechst 33342 cellular accumulation assay*....54
2.2.2.2 *Measurement of bi-directional transport across epithelial layers grown on 12-well filter plates*....55

2.2.2.3 *Bi-directional transport across epithelial layers grown on 24 or 96-well filter plates*....58

2.2.3 Induction pre-treatments of Caco-2 cell monolayers 61

2.2.4 Cellular ciprofloxacin accumulation in HEK 293 cells....61

2.2.3 Molecular biology....62

2.2.3.1 *RNA isolation and quantitative PCR*....62
2.2.3.2 *Reverse transcription* 62
2.2.3.3 *Standard polymerase chain reaction*....63
2.2.3.4 *Real-time polymerase chain reaction*....64

2.2.4 Immunoblotting 66

2.2.5 Immunocytochemistry....67

2.2.6 Statistical Methods 68

3. Functional expression of BCRP in epithelial cell-lines....71

3.1 Introduction....71

3.2 Methods....74

3.2.1 Deglycosylation....74

3.3 Results....75

3.3.1 hBCRP/mBcrp mRNA expression in epithelial cell models....75
3.3.2. BCRP/Bcrp protein expression in epithelial cell models 76
3.3.3 Cellular retention of Hoechst 33342 dye: an assay to assess hBCRP/mBcrp function....80
3.3.4 Screening for BCRP substrates using Hoechst 33342 in MDCKII cells....84

3.4 Discussion....116

4. Transepithelial transport mediated by BCRP 122

4.1 Introduction....122

4.2 Methods....125

4.2.1 Cell culture 125
4.2.2 Bi-directional transport across epithelial layers- 24 or 96-well filter plates....125

4.3 Results....126

4.3.1 Identification of BCRP substrates in ABC-transfected MDCKII monolayers 126
4.3.2 Inhibition of BCRP mediated transport in MDCKII cell monolayers using Ko143 132
4.3.3 Determination of the BCRP mediated component of substrate flux across Caco-2 cell monolayers 134

4.4 Discussion.....163

5. The mechanism of transepithelial ciprofloxacin secretion 170

5.1 Introduction.....170

5.2 Methods.....174

5.2.1 Bi-directional transport across epithelial layers grown on 12-well filter plates.....174
5.2.2 Bi-directional transport across epithelial layers grown on 96-well filter plates.....174
5.2.3 Cellular ciprofloxacin accumulation in HEK 293 cells.....174

5.3 Results 176

5.3.1 Bi-directional ciprofloxacin flux across MDCKII cell monolayers 176
5.3.2 Is ciprofloxacin secretion mediated by BCRP in Caco-2 cell monolayers?..179
5.3.3 Is MRP4 involved in ciprofloxacin secretion? 181

5.4 Discussion.....201

6. Regulation of functional BCRP in Caco-2 cells 205

6.1 Introduction.....205

6.2 Methods.....209

6.2.1 Induction pre-treatments of Caco-2 cell monolayers for qPCR, immunoblotting and bi-directional transport assays.....209

6.3 Results 210

6.3.1 The effect of induction agents on BCRP mRNA expression in Caco-2 cells.....211
6.3.2 The effect of induction agents on the mRNA expression of nuclear receptors AhR and PPARγ.....211
6.3.3 The effect of induction agents on BCRP protein expression in Caco-2 cells.....211
6.3.4 Testing the inhibitory effects of induction agents on the bi-directional transport of flavopiridol.....212
6.3.5 The effect of induction agents on the bi-directional transport of BCRP substrates in low passage Caco-2 epithelia.....213

6.3.5.1 *Flavopiridol*.....213
6.3.5.2 *Prazosin*.....214
6.3.5.3 *Nitrofurantoin*.....215

6.4 Discussion.....236

7. Summary and concluding remarks.....243

8. References.....247

Appendix.....270

Figures

Figure 1.1 Schematic diagram of a human enterocyte showing uptake and efflux transporters involved in xenobiotic transport.....18

Figure 1.2 Conformational changes in MsbA.....35

Figure 1.3 Schematic representation of the structure of the ABC efflux transporter BCRP.....36

Figure 1.4 Structures of known BCRP substrates.....37

Figure 2.1 Schematic diagram of an epithelial layer grown on a Transwell filter...69

Figure 3.1 Expression of hBCRP mRNA in MDCKII and Caco-2 cells.....88

Figure 3.2 Expression of mouse Bcrp mRNA in transfected MDCKII cells.....90

Figure 3.3 Western Blot analysis of BCRP protein expression in epithelial cell models.....92

Figure 3.4 Western Blot analysis of deglycosylated mouse Bcrp protein.....94

Figure 3.5 Immunocytochemical detection of BCRP in (A) Native MDCKII, (B) hBCRP-MDCKII and (C) mBcrp1-MDCKII epithelial cell monolayers.....96

Figure 3.6 Immunocytochemical detection of BCRP in low passage Caco-2 epithelial cell monolayers.....98

Figure 3.7 Effect of incubation time on Hoechst 33342 dye retention in native MDCKII cells.....100

Figure 3.8 Effect of seeding density on Hoechst 33342 dye retention in native MDCKII cells.....102

Figure 3.9 Effect of increasing extracellular Hoechst 33342 on cellular dye retention in native MDCKII cells.....104

Figure 3.10 Relationship between Hoeschst 33342 concentration and intracellular Hoeschst 33342 accumulation in human BCRP-transfected MDCKII cells.....106

Figure 3.11 Concentration dependent effect of known ABC transporter inhibitors on cellular Hoechst 33342 dye retention in transfected MDCKII cells.....108

Figure 3.12 Assessment of functional ABC-transporter activity in MDCKII and Caco-2 cell-lines using Hoechst 33342 dye retention.....110

Figure 3.13 Assessment of functional ABC-transporter activity in diverse cell-lines using Hoechst 33342 dye retention.....112

Figure 3.14 Identification of potential BCRP substrates using Hoechst 33342 across A) native MDCKII, B) hBCRP-MDCKII, C) mBcrp1-MDCKII and D) MDR1-MDCKII cells.....114

Figure 4.1 Use of ABC-transfected MDCKII cells to determine substrate specificity; transepithelial flux of diclofenac.....139

Figure 4.2 Dose-dependency of flavopiridol transepithelial flux across confluent native and human BCRP-MDCKII monolayers.....141

Figure 4.3 Action of bi-directional transport of flavopiridol across native and human BCRP-MDCKII monolayers.....143

Figure 4.4 Dose-dependency of prazosin transepithelial flux across confluent native and human BCRP-MDCKII monolayers.....145

Figure 4.5 Action of bi-directional transport of prazosin across native and human BCRP-MDCKII monolayers.....147

Figure 4.6 Bi-directional transport of nitrofurantoin across ABC-transfected MDCKII cells.....149

Figure 4.7 Effect of Ko143 on nitrofurantoin transepithelial flux across confluent human BCRP-MDCKII monolayers.....151

Figure 4.8 Bi-directional and net flux of flavopiridol across confluent Caco-2 cell monolayers.....154

Figure 4.9 Bi-directional and net flux of prazosin across confluent Caco-2 cell monolayers.....156

Figure 4.10 Bi-directional flux of nitrofurantoin across confluent Caco-2 cell monolayers.....158

Figure 4.11 Correlation between Caco-2 and native MDCKII absorptive permeability (Papp) of selected compounds.....160

Figure 4.12 Correlation between absorptive permeability (P_{a-b}) and the partition coefficient (LogP) for select compounds in Caco-2 cells.....162

Figure 5.1 Transepithelial [^{14}C]-ciprofloxacin flux across BCRP transfected MDCKII cell monolayers.....184

Figure 5.2 Concentration dependent curves showing the transepithelial flux of ciprofloxacin across confluent mouse Bcrp1-MDCKII monolayers.....187

Figure 5.3 Effect of known ABC transporter inhibitors on (A) Bi-directional ciprofloxacin flux (B) Ciprofloxacin membrane permeability and (C) Intracellular ciprofloxacin levels across mouse Bcrp1-MDCKII monolayers.....189

Figure 5.4 Transepithelial [^{14}C]-ciprofloxacin flux across high passage Caco-2 cell monolayers…….....191

Figure 5.5 Transepithelial [^{14}C]-ciprofloxacin flux across low passage Caco-2 cell monolayers.....193

Figure 5.6 Effect of BCRP and MRP4 inhibitors on (A) Net ciprofloxacin flux (J_{net}) (B) Ciprofloxacin membrane permeability and (C) Cellular ciprofloxacin uptake across low passage Caco-2 monolayers.....195

Figure 5.7 Demonstration of MRP4 mRNA expression in (A) HEPG2, (B) HEK 293 and (C) Caco-2 cells.....197

Figure 5.8 Effect of MRP4 transfection on [^{14}C]-ciprofloxacin cellular uptake in HEK 293 cells.....199

Figure 5.9 Summary diagram of ciprofloxacin transport across Caco-2 cells.....200

Figure 6.1 qPCR analysis of BCRP mRNA after 72-hour pre-treatments in low passage Caco-2 cells.....218

Figure 6.2 Expression of Ah receptor mRNA in low passage Caco-2 cells.....220

Figure 6.3 Expression of PPAR-gamma receptor mRNA in low passage Caco-2 cells.....222

Figure 6.4 Western Blot analysis of BCRP protein expression in low passage Caco-2 cells after 72-hour pre-treatments.....224

Figure 6.5 Effect of flavopiridol net flux in the presence and absence of potential inhibitors across human BCRP-MDCKII monolayers.....226

Figure 6.6 Effect of pre-treatments on flavopiridol transepithelial flux across confluent Caco-2 cell monolayers ± known ABC transporter inhibitors.....229

Figure 6.7 Effect of pre-treatments on prazosin transepithelial flux across confluent Caco-2 cell monolayers ± known ABC transporter inhibitors.....232

Figure 6.8 Effect of pre-treatments on nitrofurantoin transepithelial flux across confluent Caco-2 cell monolayers ± known ABC transporter inhibitors.....235

Tables

Table 1.1 Human efflux transporter gene, mRNA and protein nomenclature……...49

Table 2.1 Primer sequences used in standard and real-time qPCR reactions.....67

Table 3.1 Identification of potential BCRP substrates using Hoechst 33342 retention in (A) native MDCKII, (B) hBCRP-MDCKII, (C) mBcrp1-MDCKII and (D) MDR1-MDCKII cells.....115

Table 4.1 Absorptive permeabilities of potential BCRP substrates across MDCKII and Caco-2 cell monolayers.....136

Table 4.2 Elucidation of potential BCRP-substrates using MDCKII cell monolayers.....137

Table 4.3 Table showing bi-directional flux of selected compounds in Caco-2 cells.....152

Table 5.1 Table showing bi-directional flux of ciprofloxacin in epithelial cell monolayers measured by HPLC-MS.....185

Table 6.1 Effect of potential BCRP inducing agents after 72hours pre-treatment on flavopiridol transepithelial flux across confluent Caco-2 cell monolayers.....227

Table 6.2 Effect of potential BCRP inducing agents after 72hours pre-treatment on prazosin transepithelial flux across confluent Caco-2 cell monolayers.....230

Table 6.3 Effect of potential BCRP inducing agents after 72hours pre-treatment on nitrofurantoin transepithelial flux across confluent Caco-2 cell monolayers.....233

1. Introduction

1.1 Introduction to the ATP-binding cassette (ABC) transporters

In order for cells, or indeed whole organisms, to survive and proliferate they need to maintain tight control on what enters from the extracellular milieu or environment and also on what needs to be excreted or removed. In order to achieve this, cells and absorptive/secretory organs have a comprehensive catalogue of membrane transport proteins that undertake these functions. As far as we know examples of such transport proteins are expressed in all living organisms and certainly in all cell types of all phyla of the animal kingdom (Jones & George, 2004). Membrane transport proteins are essential to life by the transportation of small ions, nutrients such as peptides, amino acids and sugars, water and xenobiotics to name but a few examples. In human physiology membrane transporters play an essential role in absorption from the intestinal tract, distribution and disposition of nutrients to all the body's organs, and finally elimination of metabolic waste and removal of environmental toxins and drugs via the liver and kidneys (Klaassen & Aleksunes, 2010).

The considerable pharmaceutical interest in drug transport has evolved in the past 20 years, as it is realised that specialised membrane transport mechanisms not passive models, determine drug absorption, distribution, metabolism and excretion (ADME). It is now a legal requirement or at least a strong recommendation from authorities such as the Food and Drug Administration (FDA, 2006; http://www.fda.gov) to ascertain whether new chemical entities (NCEs) are substrates of particular transporters, such as MDR1 (ABCB1) in order to predict pharmacokinetic profiles and potential adverse drug interactions.

The Human Genome Organisation (HUGO) (http://www.genenames.org/) developed a new system of classification of this extensive group of proteins in 1999 and placed these proteins mostly into two basic groups: the solute carrier proteins (SLCs) and ATP-binding cassette (ABC) proteins. Other classified families include the aquaporins and ion channels.

The solute carrier proteins are an extensive collection of proteins with over 350 members grouped into 55 gene families and reside typically on the outer plasma cell membrane, with some members residing intracellularly transporting across organelle membranes (He *et al.*, 2009; Hediger *et al.*, 2004). These transporters typically function on the plasma/organelle membrane by facilitating cellular uptake of an extensive list of nutrients and xenobiotics, see Klaassen and Aleksunes (2010) for xenobiotic substrates. Examples of SLC transporters expressed on the apical and basolateral surface of enterocytes that have an important role in oral drug absorption are shown in Figure 1.1.

The primary active transporter family the ABC transporters are a protein super family that is comprised of 50 members which in turn comprise of further subfamilies such as: ABC1 (ABCA), MDR/TAP (ABCB), MRP/CFTR (ABCC), ALD (ABCD), OABP (ABCE), GCN20 (ABCF) and White (ABCG2) (Chan *et al.*, 2004; Deeley *et al.*, 2006; Klein *et al.*, 1999). The focus of this thesis is with the ABC family members that are responsible for cellular efflux, especially of xenobiotics. The key members involved in enterocytes that limit intestinal absorption so producing an effective barrier are shown in Figure 1.1. An extended list of relevant drug efflux proteins expressed throughout the human body is given in Table 1.1.

All of these ABC transporter proteins are composed of 6, 12 or more transmembrane domains (TMDs) with single or dual nucleotide binding domains

(NBDs), it is this NBD that is highly homologous between all family members, that gives rise to the protein family name ATP-binding cassette (ABC) proteins (Higgins, 1992).

Typical ABC transporters consist of twelve membrane spanning domains (TMD) and two cytosolic ATP binding motifs (NBDs), and this is usually comprised of two halves (a half unit being 6 TMDs and 1 NBD) (Chan *et al.*, 2004; Higgins, 1992). However, not all members follow this structure. For example, MRP1-3 and MRP6-7 possess an extra 5 trans-membrane domain (Deeley *et al.*, 2006). The conserved region that gives rise to the family name is the ATP binding domain that utilises the energy from ATP hydrolysis to morphologically change transporter structure so allowing transport of its substrate. The two ATP binding regions are between 200-250 amino acid conserved regions with particularly important motifs called Walker A and Walker B (units responsible for the adherence of ATP) (Deeley *et al.*, 2006). MDR1 (ABCB1) is an example of a typical ATP binding cassette protein and is expressed as one polypeptide. The enormous interest in this protein has arisen due to its role in chemotherapy-resistance in cancer, but this has lead to studies of the function of many other family members structurally related to MDR1.

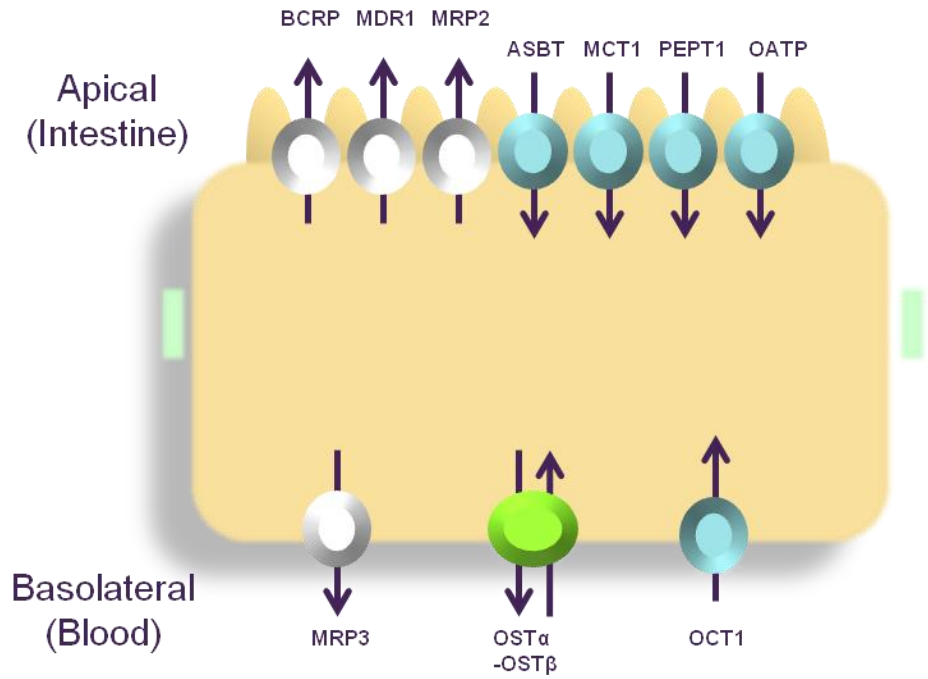

Figure 1.1. Schematic diagram of a human enterocyte showing uptake and efflux transporters involved in xenobiotic transport

Polarised expression of uptake (SLC) and efflux (ABC) transporters (adapted from Giacomini *et al.*, 2010). In the apical (lumen) membrane uptake transporters (shown in blue) the organic anion transporting polypeptides (OATPs, SLCOs) such as OATP2B1 (SLC02B1); the peptide transporter 1 (PEPT1; SLC15A1); the ileal apical sodium/bile acid co-transporter (ASBT; SLC10A2); and the monocarboxylic acid transporter 1 (MCT1; SLC16A1). Expressed alongside the uptake transporters on the apical surface are the main efflux transporters shown in white; BCRP (ABCG2), MDR1 (ABCB1) and MRP2 (ABCC2). On the basolateral (blood) membrane the organic cation transporter 1 in blue (OCT1: SLC22A1); heteromeric organic solute transporter in green (OSTα–OSTβ) and the efflux transporter MRP3 in white (ABCC3) mediate exit from the cytosol or uptake from plasma.

Table 1.1. Human efflux transporter gene, mRNA and protein nomenclature

Table is adapted from Klaassen and Aleksunes (2010) showing the gene names, the chromosomal loci, the mRNA nucleotide accession number and protein names for the efflux transporters typically expressed in humans. Data were originally taken from The National Centre of Biotechnology Information (NCBI).

Human ABC efflux transporters isoforms

Gene		mRNA	Protein	
Name	**Locus**	**Accession number**	**Name**	**Other name**
ABCA1	9q31.1	NM_005502	ABCA1	
ABCB1	7q21.1	NM_000927	MDR1	Pgp
ABCB4	7q21.1	NM_000443	MDR3	PFIC3, PGY3
ABCB11	2q24	NM_003742	BSEP	SPGP, PFIC2
ABCC1	16p13.1	NM_004996	MRP1	MRP, GS-X
ABCC2	10q24	NM_000392	MRP2	cMOAT, DJS
ABCC3	17q22	NM_003786	MRP3	MOAT-D, cMOAT2
ABCC4	13q32	NM_005845	MRP4	MOAT-B
ABCC5	3q27	NM_005688	MRP5	MOAT-C, ABC11
ABCC6	16p13.1	NM_001171	MRP6	MOAT-E, PXE, ARA
ABCC10	6p21.1	NM_033450	MRP7	
ABCC11	16q12.	NM_032583	MRP8	
ABCC12	16q12.	NM_033226	MRP9	
ABCG2	4q22	NM_004827	BCRP	
ABCG5	2p21	NM_022436	ABCG5	Sterolin-1
ABCG8	2p21	NM_022437	ABCG8	Sterolin-2
ATP7B	13q14.3	NM_000053	ATP7B	WD
ATP8B1	18q21-22	NM_005603	ATP8B	1 PFIC1, FIC1, BRIC
OSTα	q29	NM_152672	OSTα	
OSTβ	5q22.31	NM_178859	OSTβ	

1.2 Multidrug resistance protein 1 (MDR1)

The first member of the ABC protein family to be discovered in 1976 by Juliano and Ling was the permeability-glycoprotein (also known as Pgp/MDR1/ABCB1). The term MDR1 will be used in this study for consistency (Juliano & Ling, 1976). A drug resistance phenotype was witnessed in the Chinese hamster ovary cell lines they were studying at the time and this phenotype was revealed to be due to the expression of the cell surface glycoprotein MDR1- hence the term "multidrug resistance" (MDR). It was this interest in chemotherapy-resistance that drove the field forward to discover functionally and structurally related protein family members of MDR1.

1.2.1 MDR1 structure

The human *MDR1* gene on chromosome 7 encodes for a 1280 amino acid polypeptide unit comprising of the typical ATP binding cassette protein structure of two homologous halves (each comprising of a 6 transmembrane domain and one ATP NBD).

The transmembrane domains form the pathway by which solutes cross the membrane, whilst the ATP-binding domains likely use the energy inherent in the hydrolysis of the high-energy phosphates to make conformational changes to the protein. The simplest idea is that the substrate binding sites are in an internal (cytosolic-facing) site, which may become occluded and then transformed into an outward-facing (external) binding site on conformational change. However, both MDR1 and other ABC transporters have been hypothesised to show multiple distinct binding sites. Substrates present in the inner bimolecular leaflet of the membrane may access a binding site within the protein through direct interactions from the hydrophobic membrane interior.

A 3-dimensional X-ray structure of a bacterial ABC transporter, MsbA (Ward *et al.*, 2007), in different conformations may provide a proto-typical structure for all ABC transporters. MsbA is found in Gram-negative bacteria and transports lipopolysaccharide (LPS) from the cytoplasmic leaflet (inward-facing) to the periplasmic leaflet (outward-facing) of the inner membrane. However MsbA transport is not restricted to LPS, in fact it may transport multiple substrates and can actually transport a wide range of drug molecules. This combined with a great sequence similarity with mammalian/human ABC transporters such as MDR1 and even BCRP provides a working model for ABC transporter operation. Figure 1.2 shows the sequential changes in protein structure of MsbA during xenobiotic efflux; whereby the binding and hydrolysis of high-energy phosphates causes a change in structure from an inward facing to an outward facing confirmation.

An X-ray structure of mouse MDR1 at 3.5Å has been reported by Aller *et al.* (2009) without ATP (apo-PgP) (Aller *et al.*, 2009). This structure is very similar to MsbA and for the inner-facing conformation it shows an internal binding site/cavity of ~6000 cubic Å with a wide 30Å separation of the two nucleotide-binding domains. By placing cyclic peptide inhibitors in the internal cavity, 2 distinct binding sites showing stereo-selectivity due to hydrophobic and aromatic interactions were identified. A very important feature of this open inner-facing conformation is that the binding sites are open to the cytoplasm to large molecules up to the size of the pocket, but also open to the inner leaflet of the lipid bilayer. Therefore, MDR1 can "scan" the inner leaflet for drug molecules dissolved within the membrane phase. Substrates may not necessarily even enter the transporter from the cytoplasm but are expelled directly from the membrane phase.

1.2.2 Distribution of MDR1 within the body

MDR1 protein is found in normal and tumour tissues throughout the body (Cordon-Cardo *et al.*, 1990; Thiebaut *et al.*, 1987), expressed on the apical or luminal facing cellular membranes depending on cell type. Particularly high concentrations are found in intestinal epithelia, kidney proximal tubule epithelia, hepatocytes and the blood-brain barrier (brain capillary endothelial cells) (Gatmaitan & Arias, 1993; Hunter *et al.*, 1993; Tatsuta *et al.*, 1992). This localisation suggests a protective excretory role of removing xenobiotics out of the body (Chan *et al.*, 2004).

1.2.3 MDR1 function

The substrate profile of MDR1 is extensive; a list of known MDR1 substrates and inhibitors is given by Mattson *et al.* (2009), substrates being typically hydrophobic and cationic (Matsson *et al.*, 2009). Substrates are known to bind to at least four separate binding sites on the MDR1 protein (Carrier *et al.*, 2003; Martin *et al.*, 2000; Safa, 2004).

MDR1 has a great effect on the absorption, distribution and excretion of these compounds in the human body and is a great consideration in drug design (Fromm, 2004; Polli *et al.*, 2001; Raub, 2006; Schinkel, 1999). For example, MDR1 is responsible for limiting the oral bioavailability of the drugs cyclosporin (Lown *et al.*, 1997; Raub, 2006), digoxin (Cavet *et al.*, 1996), quinidine (Su & Huang, 1996) and paclitaxel (Sparreboom *et al.*, 1997), to name but a few.

Due to the large number of clinically used drugs being MDR1 substrates or inhibitors, this has important implications for drug-drug interactions (DDIs) (Giacomini *et al.*, 2010). These DDIs can have hazardous consequences if the drugs administered have a narrow therapeutic index and a low bioavailability; such as many

of the drugs in cancer treatment. Many cancer agents are potent MDR1 substrates (irinotecan, doxorubicin, vinblastine, paclitaxel). Thus in cancer regimens any change in ADME of the drug via inhibition or induction of MDR1 can affect cancer response and potentially patient survival.

Digoxin is another example of a drug with a narrow therapeutic index, and it is one of the most commonly prescribed drugs in congestive heart failure. Digoxin is also a very good MDR1 substrate and, therefore, agents that affect MDR1 activity through induction or inhibition can lead to digoxin intoxication (Su & Huang, 1996). Agents such as cyclosporin A, quinidine and verapamil are known to be inhibitors of MDR1 in vivo and affect digoxin pharmacokinetics, efficacy and safety (Lown *et al.*, 1997; Su & Huang, 1996; Verschraagen *et al.*, 1999). The interaction between digoxin and verapamil is well documented in medicine and this co-administration is often used to increase digoxin plasma concentration levels to anything between 60-90% (Verschraagen *et al.*, 1999).

However, MDR1 does not operate alone. The *MDR1* gene is known to be tightly regulated in conjunction with the metabolising enzyme CYP3A4 and there is also considerable overlap with substrate specificity (Giacomini *et al.*, 2010; Wacher *et al.*, 1998; Zhang *et al.*, 1998). This has led to the hypothesis that MDR1 has a further indirect role of increasing the rate of metabolism of xenobiotics. By limiting the concentration of xenobiotic in the cell via pumping it back out across the apical membrane it reduces the amount of substrate reaching the metabolising enzymes such as CYP3A4, reducing the possibility of CYP3A4 saturation. This xenobiotic cycling across the apical membrane allows progressive access to metabolic capacity and limits parent compound reaching the systemic circulation (Giacomini *et al.*, 2010; Gomez *et al.*, 1995; Lown *et al.*, 1997). This interaction with the metabolising

enzymes adds another dimension in predicting the pharmacokinetics and safety of MDR1 substrates.

Given the diverse effects MDR1 has on xenobiotic ADME the FDA has guidelines to identify any new drugs that are MDR1 substrates (Giacomini *et al.*, 2010). Currently there are many methods in vitro and in vivo that are used for studying MDR1 activity in drug development, including membrane-based assay systems (ATPase assays and vesicle transport assays), cell-based assay systems (using transfected cell lines, primary cells), in vivo models (animal and human) and even computational models.

1.3 Multidrug resistance-associated protein (MRP)

Following identification of MDR1, many functionally and structurally related ABC protein family members started to be discovered. 1992 saw the discovery of the next drug efflux pump, the multidrug resistance-associated protein (MRP). This MRP efflux pump is classified into the ABCC gene subfamily. This ABCC subfamily consists of 13 members, 9 members belonging to the MRPs (MRP1-6/ABCC1-6 and MRP7-9/ABCC10-12), with the remaining proteins being the cystic fibrosis conductance regulator protein (CFTR/ABCC7) and the sulfonyl urea receptors (SUR1/ABCC8 and SUR2/ABCC9) (Borst *et al.*, 2000, 2007; Toyoda *et al.*, 2008).

Like MDR1 all the MRPs contain two membrane spanning domains each with an ATP-binding domain. However, MRP1, MRP2, MRP3, MRP6 and MRP7 contain an extra N-terminal domain (TMD_0), which is absent in P-glycoprotein (Toyoda *et al.*, 2008).

MRP1 (also known as ABCC1 or GS-X) is a highly characterised member of the MRP family. This transporter expressed on the cell plasma membrane is found in

nearly all tissue types of the human body (Toyoda *et al.*, 2008) and initially it was shown to have a remarkably similar function to MDR1. Further work has shown that its substrates are often different from MDR1, with MRP1 preferring organic anions (such as entities conjugated with glutathione, glucuronide or sulphate) (Ishikawa *et al.*, 1998; Jedlitschky *et al.*, 1994), whereas MDR1 has a low affinity for these negatively charged conjugates (Borst *et al.*, 2000). MRP1 is also thought to play a role in glutathione (GSH) homeostasis and it is this ability to pump GSH out of the cell that explains why it is so efficient at removing drug conjugates such as methotrexate.

MRP2 (ABCC2) also known as the canalicular multispecific organic anion transporter (cMOAT), as the name suggests, is predominantly found in the liver and is involved in the expulsion of metabolites into bile. However, MRP2 is also an important efflux pump in the apical membrane of kidney proximal tubule cells in transporting conjugates into urine and on the apical surface of intestinal epithelia where it cycles agents back into the intestinal lumen (Giacomini *et al.*, 2010).

A mutant Wistar rat strain lacking functional mrp-2 (TR^-/GY) was used to characterise many substrates of this transporter. It turned out that these rats were also shown to be deficient in bilirubin-glucuronide secretion due to the mutation in the *MRP2* gene (Buchler *et al.*, 1996); this gene defect was matched with the human condition Dubin-Johnson syndrome (Kartenbeck *et al.*, 1996; Paulusma *et al.*, 1997).

Over expression of MRP2 in vesicles and transfected cells has further characterised this transporter showing it to be responsible for the resistance seen with many cancer agents, such as resistance to doxorubicin, etoposide, methotrexate and vincristine (Cui *et al.*, 1999; Hooijberg *et al.*, 1999) to name but a few.

MRP3 (ABCC3) also functions as an organic acid transporter that transports many cancer agents similar to MRP1 and MRP2 (Borst *et al.*, 2000; Hirohashi *et al.*, 1999; Kool *et al.*, 1999). MRP3 localisation is also predominantly in the liver. However unlike its family counterpart MRP2, in which it shares 48% amino acid homology (Borst *et al.*, 2000), it resides on the basolateral blood facing membrane of hepatocytes, where it transports organic acids into the bloodstream (Konig *et al.*, 1999), in complete opposition to the protective role of MRP2 which deposits substrates into the bile. Animals deficient in MRP3 have problems in transporting morphine from the liver into the blood stream, suggesting MRP3 to be the major transporter expressed on the basolateral membrane of hepatocytes (Toyoda *et al.*, 2008; Zelcer *et al.*, 2005). MRP3 is also found basolaterally in the intestine and is thought to have a similar function of disposition of organic acids into the blood stream (Giacomini *et al.*, 2010).

The next MRP family member is MRP4 (ABCC4). MRP4 lacks the extra N-terminal domain that the first three members of the MRP family contain. This apparent difference in structure stands it apart and may explain some of the unique characteristics of this transporter compared with MRP1-3.

The localisation of this transporter is tissue dependent. It is found on the basolateral membrane of choroid plexus epithelia, hepatocytes, and prostate tubuloacinar cells, yet it is found on the apical membrane of proximal tubule cells and the luminal side of brain capillary endothelium (Russel *et al.*, 2008). In the colon it has further been found to be localised on both apical and basolateral membranes (Russel *et al.*, 2008). MRP4 is also expressed in the adrenal glands, ovaries, testis, various blood cells and neurons (Ritter *et al.*, 2005).

Due to its variable localisation its function is also not typical for an MRP family member. In vitro, the substrate profile of MRP4, as for other ABC transporters, has been showed to be extensive (Chen *et al.*, 2002; Rius *et al.*, 2003; Russel *et al.*, 2008), transporting pharmaceuticals including antivirals (adefovir), antibiotics (cephalosporins), cardiovascular agents (loop diuretics and thiazides) and cancer agents (methotrexate, 6-mercatopurine and topotecan). However, aside from a role in drug disposition, it has been shown to have a specialist physiological role in transporting endogenous molecules such as; cyclic nucleotides, ADP, eicosanoids, urate and conjugated steroid hormones (Ritter *et al.*, 2005; Zelcer *et al.*, 2003); some of these substrates being distinct from MRP1-3.

MRP5 (ABCC5) similarly to MRP4 also lacks the extra N-terminal domain and too has a role in disposition of cyclic nucleotides (Wijnholds *et al.*, 2000). MRP5 also functions like the other MRPs as a typical organic anion pump, transporting GSH conjugates (Borst *et al.*, 2000, 2007). MRP5, unlike MRP4, is found at relatively low levels ubiquitously in the human body (Borst *et al.*, 2000, 2007). In transfected cells it is found to be expressed on the basolateral surface (Borst *et al.*, 2007).

MRP6 (ABCC6) is found predominantly in the liver and kidneys (Kool *et al.*, 1999). Its physiological function is not well characterised but it is known to transport GSH conjugates, with a lower affinity for glucuronic acid conjugates, such as $E_2$17βG (Belinsky *et al.*, 2002). What is interesting about this transporter is that ABCC6 knockout animal models were shown to have a skin defect that resembled the human condition pseudoxanthoma elasticum (Klement *et al.*, 2005). It has since been confirmed that an ABCC6 mutation results in the condition, although why this mutation results in this phenotype remains unclear (Pfendner *et al.*, 2007).

MRP7 (ABCC10) is known to be expressed ubiquitously but with a higher expression in the pancreas (Hopper *et al.*, 2001). Unlike MRP6 it has a low affinity for glutathione conjugates and a greater affinity for glucuronic acid conjugates. Like most of the MRP family members it has been associated with cancer drug resistance (Toyoda *et al.*, 2008).

MRP8 (ABCC11) and MRP9 (ABCC12) were initially discovered by database search and then cloned from liver cells (Bera *et al.*, 2001; Tammur *et al.*, 2001; Yabuuchi *et al.*, 2001). These two transporters have a predicted structure similar to that of MRP4 and 5, both lacking the extra N-terminal domain (Kruh *et al.*, 2007). The substrate profiles of MRP8 and MRP9 are thought to be very similar to MRP4 and MRP5 also (Toyoda *et al.*, 2008). MRP8 has been shown to transport glutathione and glucuronic acid conjugates like most of the MRP family members, but it also transports cyclic nucleotides like members MRP4 and MRP5 (Chen *et al.*, 2005; Kruh *et al.*, 2007; Toyoda *et al.*, 2008). It seems to have a role in multidrug resistance to 5-Fluorouracil (5-FU) and possibly methotrexate (Guo *et al.*, 2003; Kruh *et al.*, 2007). MRP9 substrates are predicted to be very similar to that of MRP8 but this still needs to be elucidated (Toyoda *et al.*, 2008).

1.4 Breast cancer resistance protein (BCRP)

The focus of this project will be a particular member of the White subfamily called BCRP (ABGG2). BCRP (ABCG2) was discovered in 1998 in the MCF-7 breast cancer cell line, where the phenomenon of multidrug resistance was displayed but in the absence of MDR1 expression (Doyle *et al.*, 1998). RNA fingerprinting revealed a 2.4-kb mRNA; this mRNA encoded a sequence not matching existing members of the ABC transporter family. Due to its initial discovery in an anthracyclin-resistant breast

cancer cell line it was coined BCRP (breast cancer resistance protein). However, this protein name is misleading as it is expressed in a far more ubiquitous fashion, with a background level of the protein found in every tissue examined (Maliepaard *et al.*, 2001). Two other groups (Allikmets *et al.*, 1998; Miyake *et al.*, 1999) cloned the gene denoting it MXR (mitoxantrone resistance) and ABCP (an ABC transporter expressed in the placenta). Honjo *et al.* (2001) showed a functional difference between "BCRP and MXR" due to a mutation at amino acid position 482 (Honjo *et al.*, 2001). The wild type BCRP that has an arginine at position 482 does not actually transport the anthracyclin doxorubicin yet the $BCRP^{R482G}$ mutant does transport doxorubicin (arginine is replaced with a glycine or threonine), this is actually a gain of function mutation only found in drug selected cell lines. For consistency the term BCRP will be used henceforth.

1.4.1 BCRP structure

Although detailed structural information is lacking, it is likely that the 3-dimensional arrangement of BCRP within the membrane will be similar to MsbA (Figure 1.2). BCRP is an example of a ½ ABC transporter that is expressed as more than one peptide forming a dimer or even a multimeric complex. The dimer is thought to possess a structure similar to that of typical ABC transporters. Each polypeptide consists of one membrane spanning region (6 transmembrane helices) and one ATP binding domain (Bates *et al.*, 2001; Chan *et al.*, 2004), (shown in Figure 1.3). There are mixed reports whether BCRP functions as a homodimer bridged by disulphide bonds (Kage *et al.*, 2002; Litman *et al.*, 2002; Ozvegy *et al.*, 2001), heterodimer or even a homotetramer complex (Xu *et al.*, 2004). Several groups have since proved that cysteine residues residing on the extracellular loop between TM5 and TM6 are important for dimer formation, specifically residue Cys603 (Henriksen *et al.*, 2005;

Kage *et al.*, 2005; Wakabayashi *et al.*, 2006). Taken together, this suggests that BCRP functions at least as a homodimer, however, a homotetramer is also possible.

The predicted topology of the 655 amino acid primary sequence of BCRP is shown in Figure 1.3 displaying the 6 predicted transmembrane domains. Amino acids at key sites known to affect BCRP function are highlighted by Hazai and Bikadi (such as the mutations K86M which makes the transporter inactive whilst F431L gives rise to defective methotrexate transport) (Hazai & Bikadi, 2008). As mentioned previously, the mutation at amino acid position 482 on the BCRP polypeptide is thought to be functionally relevant in vitro, giving rise to the anthracyclin resistance phenotype. As seen in Figure 1.3 this residue is present adjacent to the 3rd transmembrane domain in an area that is thought to make up the interior cavity of the transporter. An amino acid change at this site is thought to disrupt shape and size of the cavity which in turn would affect substrate specificity (Hazai & Bikadi, 2008).

Like MDR1, substrates are thought to interact with more than one binding site on BCRP giving rise to a complexity in identifying substrate and inhibitor molecules (Giri *et al.*, 2009). Using the $BCRP^{R482G}$ mutant isoform Clark *et al.* (2006) report 3 distinct pharmacological binding sites using the anthracyclin daunorubicin (a substrate not transported by the wild type variant of BCRP), showing complete, partial or no binding (Clark *et al.*, 2006). Two sites are thought to provide allosteric communication whilst no communication is seen for the third site (Clark *et al.*, 2006). Hazai and Bikadi (2008) published an atomic model of BCRP predicted from the bacterial multidrug transporter Sav-1866 (which is also structurally related to MsbA shown in Figure 1.3) and suggests BCRP to have multiple binding sites. A recent study (Rosenberg *et al.*, 2010), has gone a stage further, using heterologous bacterial expression of BCRP combined with electron crystallography of membranes. 2-D

crystals of BCRP were resolved and a low resolution structure (at 5Å) was obtained. Combining this with homology modelling using the high-resolution MsbA and Pgp structures, inward-facing and outward facing binding sites in combination with the substrate MTX were modelled. It should be noted that the nucleotide-binding sites in the NBDs are separate from the substrate sites. Thus there are 4 and possibly 6 sites if 2 internal sites accessing the hydrophobic membrane phase are present.

Giri *et al.* (2009) predict that the mouse Bcrp protein also has multiple binding sites, showing that the Bcrp substrates prazosin and imatinib bind to sites distinct from the nucleoside analogues abacavir and zidovudine (Giri *et al.*, 2009). Other studies find similar discrepancies in BCRP functional data which are likely due to the multiple binding site phenomenon (Muenster *et al.*, 2008; Xia *et al.*, 2007b). Until a 3-D crystal structure of human BCRP exists this cannot be confirmed but these publications address the need of careful choice of substrate and inhibitor pairs when looking at BCRP function.

1.4.2 BCRP function

BCRP function is atypical in that most "half transporters" associate with organelle membranes instead of residing in the plasma membrane. BCRP is localized on the apical side of the plasma membrane of epithelial cells (Scheffer *et al.*, 2000). It is proposed that substrates bind to BCRP inside the plasma membrane where they are subsequently removed into the extracellular space. Constant cycling between the extracellular space and within the plasma membrane compartment restricts compound entering the cell and further restricts compound reaching the basolateral membrane (Matsson *et al.*, 2007).

BCRP transports an extensive range of structurally diverse ligands. Sophisticated methods of high-speed screening and quantitative structure-activity relationship (QSAR) analysis suggest certain chemical properties required for BCRP binding. An amine group bonded to one carbon of a heterocyclic ring(s) is thought to be important (Giacomini *et al.*, 2010). Furthermore, a fused heterocyclic ring structure with two additional side groups is also an important chemical feature for BCRP binding (Matsson *et al.*, 2007; Nicolle *et al.*, 2009; Saito *et al.*, 2006). An example of a BCRP substrate with this structure is the protein kinase inhibitor gefitinib (Iressa; AstraZeneca). The structure of gefitinib is shown in Figure 1.4 alongside other examples of known BCRP substrates.

1.4.3 BCRP: a detoxification pathway

Many compounds with this heterocyclic ring structure are known to be genotoxic and associated with cancers. Benzo[a]pyrene (BP) is an environmental genotoxin with this heterocyclic structure and it so happens to be a BCRP ligand (Ebert *et al.*, 2007). BCRP expressed on the apical membrane of epithelia (such as enterocytes), actively pumps its substrate from inside the cell back out across the plasma membrane into the surrounding extracellular space (Chan *et al.*, 2004). In this circumstance BCRP has a role in preventing extensive absorption of BP at epithelial barriers and subsequently reduces entry into the systemic circulation.

In the blood-brain barrier (BBB), BCRP is thought to act in conjunction with MDR1 in preventing xenobiotic entry into the brain (Cooray *et al.*, 2002), whilst in the placenta it serves to protect the developing foetus from xenobiotics in the maternal circulation (Jonker *et al.*, 2000) by acting as the rate-limiting barrier. BCRP is also localised in the blood-testis barrier and bile canalicular membrane.

BCRP is up regulated in response to chemotherapy and, unfortunately, protects these cells from chemotherapeutic agents, such as anthracyclins, daunorubicin and doxorubicin, camptothecans such as topotecan/SN-38, and finally mitoxantrone (Doyle & Ross, 2003; Doyle *et al.*, 1998; Hardwick *et al.*, 2007; Litman *et al.*, 2000; Ozvegy *et al.*, 2001; Scheffer *et al.*, 2000).

It is this function and localisation of BCRP that leads us to believe its chief function is to be a protective transporter that removes potentially toxic or otherwise deleterious compounds that have entered the mucosal cells. In human evolution this may explain why the presence of high levels of efflux transporters such as BCRP in the epithelial barriers may have given a survival advantage.

1.4.4 BCRP: a transporter of endogenous compounds

In apparent contradiction to its protective role, BCRP is also expressed in the secretory tissue in the breast of mice, cows and humans (Maliepaard *et al.*, 2001; van Herwaarden & Schinkel, 2006). BCRP in the breast allows the passage of lipophilic xenobiotics into milk and hence will expose suckling neonates. Van Herwaarden *et al.* demonstrated in mice that BCRP substrates such as aflatoxin are actively pumped into milk (van Herwaarden & Schinkel, 2006). However, later work has revealed that the presence of BCRP in the lactating mammary gland is to actually pump a physiologically relevant substrate, riboflavin (Vitamin B2) into milk (van Herwaarden *et al.*, 2007), and it seems unfortunate that other non-therapeutic BCRP substrates might access milk as well as these vitamin components.

It has been hypothesised by Krishnamurthy *et al.* (2005) that the primary role of mouse Bcrp is not necessarily to protect cells from xenobiotics but to transport and regulate porphyrins such as heme (Krishnamurthy & Schuetz, 2005). Porphyrins have

a profound effect on gene expression; therefore, a transporter designated for its transport seems possible. They suggest that the transport of other Bcrp substrates may be infact coincidental and so acts as an advantage that it is able to remove potentially harmful compounds. This, however, has not been supported in human studies.

Aside from this there is accumulating evidence that BCRP has a key role in lipid/sterol transport like other ABCG subfamily members (Klucken *et al.*, 2000; Schmitz *et al.*, 2001). It is known to transport conjugated bile acids, steroids (Imai *et al.*, 2003; Suzuki *et al.*, 2003), and there are reports of interactions with steroidal drugs (Pavek *et al.*, 2005). Furthermore, there are findings from a BCRP over-expressing stomach cell line that this transporter might have a function in cholesterol transport (Woehlecke *et al.*, 2003).

The BCRP transporter is also known to have a role in immature hematopoietic stem cells, giving rise to the defining feature of the "side population" phenotype, with its low BCRP substrate accumulation of Hoechst 33342 (Scharenberg *et al.*, 2002; Zhou *et al.*, 2001). Even though the transporter identifies the side population phenotype, the role of BCRP in stem cells is not well defined.

Taken together, these studies highlight the diverse roles played by BCRP throughout the body; it looks likely that physiological function may depend on the context of its expression.

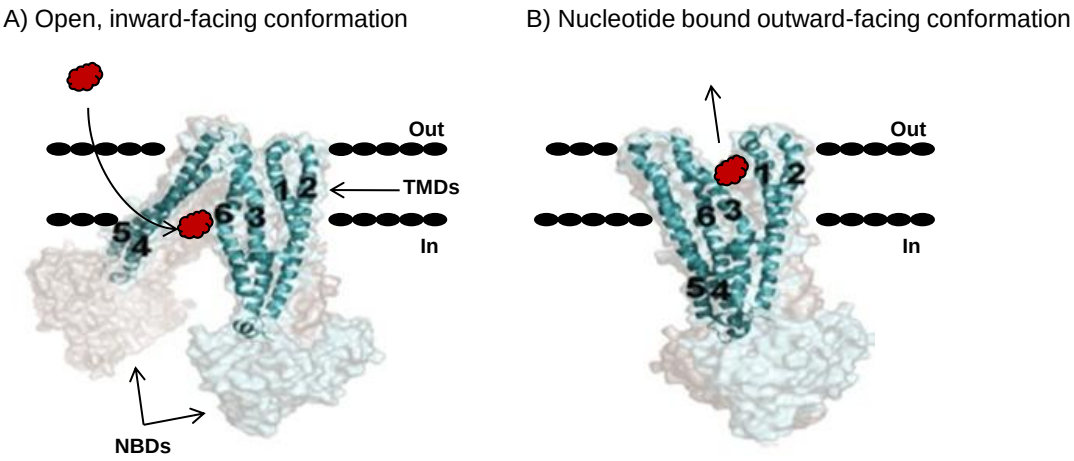

Figure 1.2. Conformational changes in MsbA

Model of inward and outward-facing conformations of MsbA (adapted from Ward *et al.* 2007). Conformational changes of the MsbA dimer in the plasma membrane are a model for the human efflux transporters, especially the half transporter BCRP. Only transmembrane domains (TMDs) 1-6 of one monomer are shown for ease of viewing (shown in blue). In the open state, inward facing confirmation (part A) TMDs 4&5 are separated from TMDs 1&2 and 3&6 rendering a binding pocket available for substrate binding (substrate shown in red). Substrates are thought to bind to BCRP at multiple sites; this figure illustrates substrates gaining access from the lipid bilayer inner membrane leaflet. On nucleotide binding to the NBDs MsbA harnesses the energy inherent in ATP binding and hydrolysis to change protein confirmation causing TMDs 4&5 to shift causing TMDs 3&6 to pull apart from TMDs 1&2 (part B). This change shifts the structure from an inward to outward facing confirmation resulting in the substrate being expelled to the extracellular space.

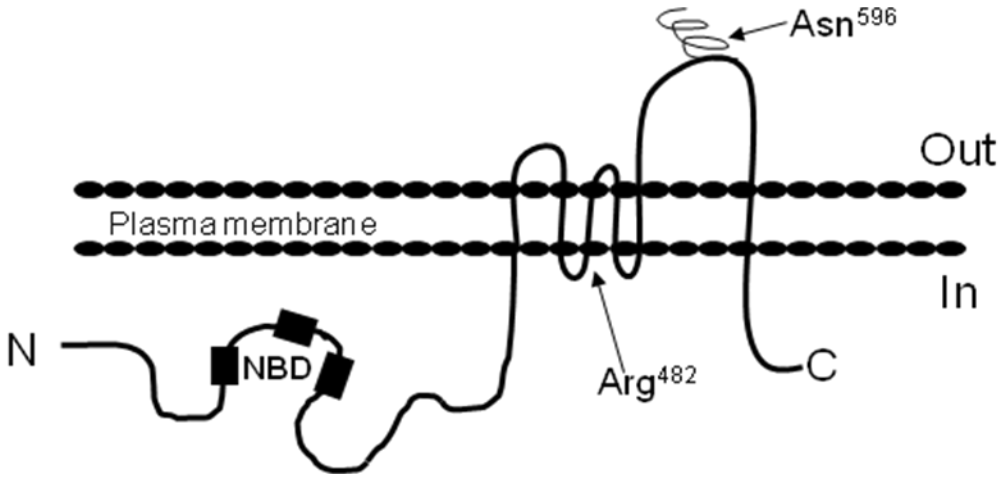

Figure 1.3. Schematic representation of the structure of the ABC efflux transporter BCRP

Figure adapted from Allen and Schinkel (2002a) showing the topological (two-dimensional) structure of the half-transporter BCRP in the plasma membrane, showing the conserved nucleotide binding domain (NBD). N and C denote the NH_2- and COOH- termini. The polymorphism that gives rise to the anthracycline resistance is indicated at position 482, as is the proposed glycosylation site of hBCRP. BCRP is thought to act as a homodimer, in a similar manner to MsbA.

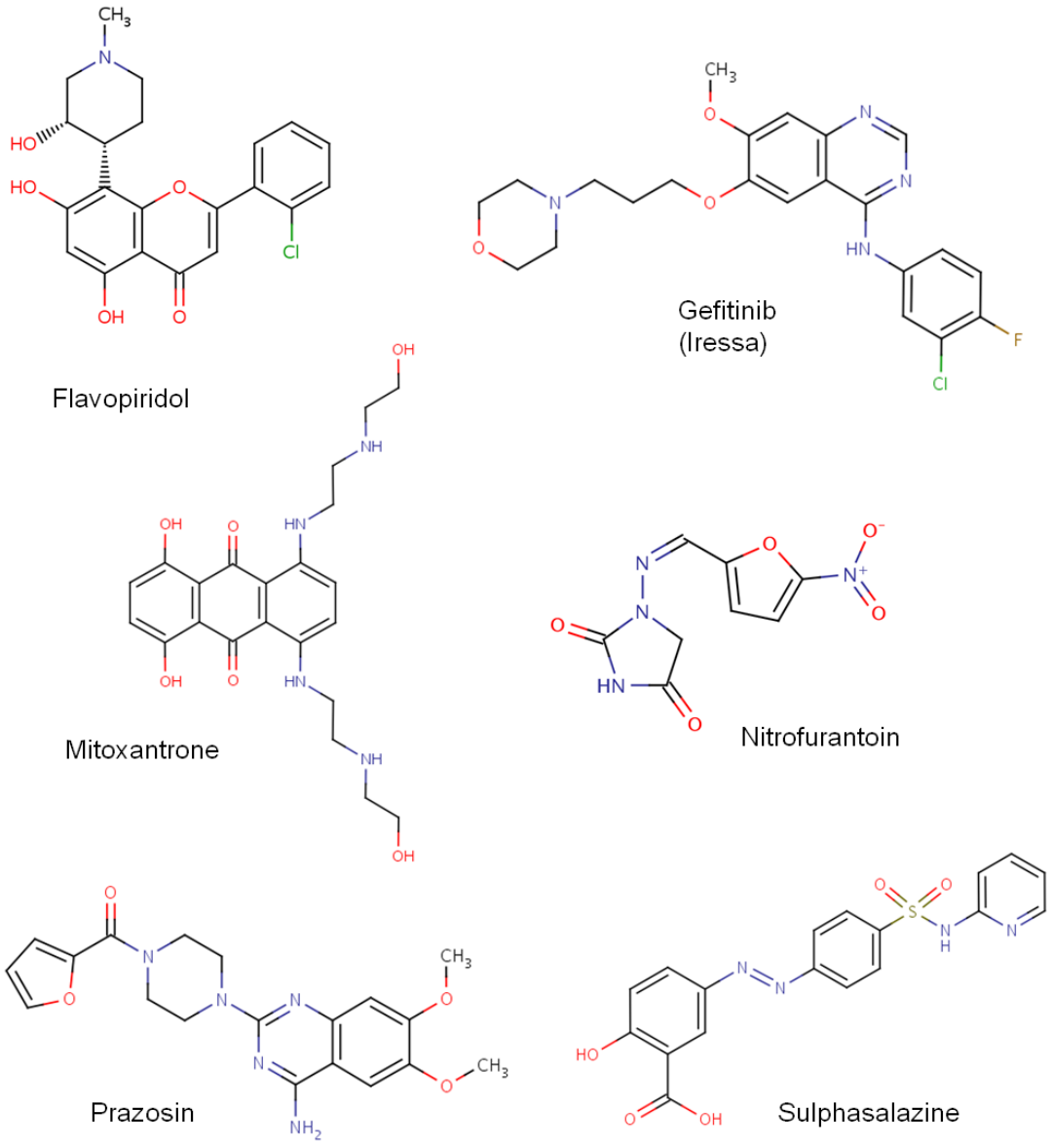

Figure 1.4. Structures of known BCRP substrates

1.5 Implications of the efflux transporters on oral drug delivery

The main efflux transporters expressed on the apical surface of human intestinal cells are BCRP, MDR1 and MRP2 (Dietrich *et al.*, 2003), shown in Figure 1.1. These transporters are distributed along the whole length of the intestine (Dietrich *et al.*, 2003; Doyle & Ross, 2003; Englund *et al.*, 2006; Maliepaard *et al.*, 2001). Studies of relative transporter mRNA expression along the human gastro-intestinal tract have shown that each of the 3 transporters shows segmental differences in expression; BCRP expression is highest in the duodenum and decreases gradually towards the colon (Gutmann *et al.*, 2005; Seithel *et al.*, 2006). Englund *et al.* (Englund *et al.*, 2006) have compared relative mRNA expression levels (normalized to villin) of both ABC and selected SLC transporters and report levels of BCRP > MDR1 and > MRP2 in duodenum, jejunum and colon with comparable levels of BCRP and MDR1 in the ileum and very low levels of MRP2 in colon samples.

All 3 ABC-transporters are highly expressed in intestinal regions that mediates rates of high absorption, so that the site of highest absorption for a particular drug may overlap a region with highest efflux transporter expression (Maliepaard *et al.*, 2001); (Doyle & Ross, 2003). Therefore xenobiotic entering the portal vein and systemic circulation is reduced.

Furthermore, all 3 transporters are present in the liver, or more specifically on the bile canalicular membrane. In this location xenobiotics that have gained entry via the intestine are then metabolised in the liver and cleared into the bile or are cleared as the parent molecule. The expression and function of these efflux transporters in the intestine and liver reduces the body content of potentially harmful compounds from the diet (Dietrich *et al.*, 2003) but consequently provides a potential barrier for oral drug delivery. Factors that can influence transporter expression in the intestine are

likely to account for the variability in the expression data seen in the literature (Berggren *et al.*, 2007; Englund *et al.*, 2006; Gutmann *et al.*, 2005; Taipalensuu *et al.*, 2001). Such factors include gender, ethnic group, genetics, diet, disease state, and multiple medications. Inter-individual variation in the bioavailability of orally delivered drugs which are ABC substrates is, therefore, inherently complex (Chan *et al.*, 2004).

The MDR1 polymorphism C3435T was found in 25% of a Caucasian population and is known to affect the oral bioavailability of the MDR1 substrate digoxin and reduce expression in the duodenum by 2-fold (Dietrich *et al.*, 2003; Hoffmeyer *et al.*, 2000). Many single nucleotide polymorphisms in BCRP have been shown to affect expression and function these being: the polymorphism C421A, C376T, G34A, T1291C and T623C (Adkison *et al.*, 2008; Imai *et al.*, 2002; Kobayashi *et al.*, 2005; Kondo *et al.*, 2004; Mizuarai *et al.*, 2004; Tamura *et al.*, 2007; Yoshioka *et al.*, 2007). Probably the most characterised and frequently occurring polymorphism in the population is the C421A allele. This single nucleotide polymorphism (C421A) was shown to reduce topotecan and rosuvastatin efflux in certain individuals (Sparreboom *et al.*, 1997; Zhang *et al.*, 2006), giving a 1.34 fold increase in topotecan plasma levels. The C421A allele frequency is known to vary with ethnicity. 46% of East Asians, 16-19% of Whites and <2% sub-Saharan Africans are homo- or heterozygous carriers of the variant allele (Adkison *et al.*, 2008; Imai *et al.*, 2002; Lee *et al.*, 2007; Yanase *et al.*, 2006). Thus ethnicity may determine pharmacokinetic profiles following oral drug delivery.

Nonetheless some studies that show that these polymorphisms do not appear to affect function in vivo; Zamber *et al.* looked at the natural variation of BCRP in the human intestine identifying BCRP mRNA and protein variants between patients but

could not detect functional differences, perhaps due to other confounding factors (Zamber *et al.*, 2003).

The polymorphism found in vitro in cell lines occurring at amino acid position 482 and known to affect substrate binding of anthracylines, camptothecans, mitoxantrone and rhodamine 123 (Miwa *et al.*, 2003) has no SNP counterpart (Honjo *et al.*, 2001) and is not found in population studies suggesting it is only found after drug selection in vitro (Kobayashi *et al.*, 2005).

Dubin Johnson syndrome is known to result from a nonsense mutation of the *MRP2* gene (Kartenbeck *et al.*, 1996; Paulusma *et al.*, 1997), thus patients with this condition lack functional MRP2.

Mutations/SNPs in the main efflux transporters suggest a patient's genotype is important in predicting outcome to oral drug therapy, leading to the proposition that testing for these mutations before therapy would be advantageous (Ishikawa *et al.*, 2005).

Disease, itself, may alter ABC transporter expression. All 3 transporters (BCRP, MDR1 and MRP2) are expressed highly on the villus-tip of enterocytes (Fromm, 2004; Krishnamurthy & Schuetz, 2005). The autoimmune disorders Crohn's disease and Coeliac disease are known to cause a blunting of intestinal villi (known as villous atrophy) which results in a reduction in expression of these efflux transporters (Fromm, 2004).

A major factor influencing the oral availability of drugs is an individual's diet. Flavonoids are plant secondary metabolites, primarily natural in origin, which are present in most diets. They are found in chocolate, citrus fruits, liquorice, red wine, tea and vegetables, to name but a few sources, and an average intake of flavonoids have been approximated to be 1g per day (Formica & Regelson, 1995). They are

heavily metabolised by the gut flora and thus active concentrations will be reduced considerably. However, these compounds have been recognised to have beneficial health effects with anti-carcinogenic actions (Havsteen, 2002). Thus foods with high flavonoid content are becoming more popular and even flavonoid supplements, such as quercetin and genistein are available. Many studies link the modulating effects of these flavonoids with the ABC-efflux proteins; they have diverse structures and are known to be substrates, inhibitors and inducers of the ABC-efflux proteins (Alvarez *et al.*, 2009; Ebert *et al.*, 2007; Wang, 2007).

Polypharmacy, where multiple drugs are prescribed for multiple conditions is increasingly common. It is also often the case that drugs are administered orally together to achieve an additive pharmacological effect, such as the two antibiotics amoxicillin and metronidazole, in combination with a proton pump inhibitor such as pantoprazole to treat gastric ulcers. Drug interactions can occur as a result of being substrates of the ABC efflux proteins. Digoxin is a cardiac glycoside used in heart failure that has a narrow therapeutic index that is a good MDR1 substrate (Haslam *et al.*, 2008). Agents such as verapamil and quinidine used in heart conditions, act as potent inhibitors to MDR1 and thus coadministration with digoxin would lead to elevated drug plasma levels and toxicity (Fromm *et al.*, 1999; Klein *et al.*, 1982). Drug-drug or herb-drug interactions can involve inhibition of the efflux activity by one compound, resulting in the increased absorption of a second drug (Haslam *et al.*, 2008). A classic example of a herb-drug interaction is with the herbal supplement St. John's wort, whereby the active component hyperforin is known to induce expression and function of MDR1 and CYP3A4 (Durr *et al.*, 2000). The oral bioavailability of MDR1 substrates such as digoxin will be subsequently reduced resulting in a lack of

drug efficacy or even fatality especially when the absorbed drug has a low therapeutic window (such as digoxin).

Anti-cancer agents often have narrow therapeutic indices and are often substrates of the ABC transporters. These drugs are normally administered in a regimen together and unfortunately drug-drug interactions occur because of the efflux transporters. For example, irinotecan bioavailability is found to increase in the presence of the tyrosine kinase inhibitor (TKI) gefitinib in mice (Stewart *et al.*, 2004). Another report of this interaction showed that the TKI, imatinib mesylate (Gleevec), reversed topotecan resistance (Houghton *et al.*, 2004). This interaction occurs because many of these TKIs, such as gefitinib and imatinib mesylate are potent BCRP inhibitors (Nakamura *et al.*, 2005; Ozvegy-Laczka *et al.*, 2004).

Furthermore, certain anti-viral drugs are shown to be potent MDR1 and BCRP inhibitors (Wang *et al.*, 2003; Weiss *et al.*, 2007), such as lopinavir and nelfinavir. This inhibition can elucidate a drug-drug interaction especially when they are taken often in a HAART (highly active antiretroviral therapy) regimen.

It is often the case that ABC efflux proteins have overlapping substrate specificity and it is quite rare to find substrates specific to a single ABC transporter. By having this system of multiple transporters removing a substrate it probably serves as a survival advantage, as one transporter becomes compromised the other transporter is still operational to remove the xenobiotic. This means the oral bioavailability of drugs can be affected by multiple efflux transporters. For example, the sympatholytic drug prazosin commonly prescribed to treat high blood pressure is known to be transported by both MDR1 and BCRP. In order to understand how the oral availability of drugs is dependent on ABC-transporter action not only is it recommended that all drugs in development are tested as substrates for BCRP and

MDR1, but it is also important to test these directly in an appropriate context e.g. Caco-2 cells or in an intact epithelium.

1.6 Systems for predicting oral bioavailability

Medication is preferentially administered by the oral route for convenience and for patient compliance. In order to predict likely bioavailability and to understand the mechanistic basis of poor oral availability a number of different assays have been developed. It was originally thought that the majority of orally administered drugs were subject to passive absorption (Artursson & Karlsson, 1991), where the physiochemical properties of the drug were the main determinant. Relatively hydrophobic drugs combined with the principal of non-ionic diffusion (where the relative pKa or pKb and the relative concentration of the non-ionic hydrophobic moiety determined permeability) gave adequate oral availability. The role of specific drug transporters was considered to be minimal. Quantitative structure-activity relationship (QSAR) modelling, looking at the physiochemical properties of compounds such as hydrophobicity at a certain pH, pK and hydrogen accepting/donating ability, often give a predictive indication of the permeability of compounds and whether they are likely to interact with efflux transporters (Fujikawa *et al.*, 2007; Ren *et al.*, 1996). To measure permeability the parallel artificial membrane permeability assay (PAMPA) is used as a low cost measure of permeability in the early stages of development of compounds (Avdeef, 2005).

It is now apparent, however, that a decent proportion of drugs taken orally are affected by active and facilitated transporter mechanisms. Typically, hydrophobic drug candidates are often poorly absorbed from the gut lumen. The recognition of the impact of the ABC-family of efflux transporters on the oral absorption of new and

existing xenobiotics has led to the development of new assays incorporating ABC-transporter interaction. 2 such systems are isolated membrane vesicles or tissue cultured human intestinal cells derived from colonic adenocarcinomas e.g. Caco-2 cells.

Inside-out membrane vesicles from heterologously-expressing cells may be used to study the nature of ABC transport; they are relatively cheap and can be used in high throughput (Hegedus *et al.*, 2009; Ozvegy *et al.*, 2001). Transport assays or ATP hydrolysis stimulated by substrate are both utilised. However, these vesicle models are limited when applied to oral drug delivery. Firstly, BCRP is expressed on the extracellular facing membrane in the intestine (Maliepaard *et al.*, 2001) thus cell lines with apical BCRP expression provide us with more physiological data. It is also known that compounds with high passive permeabilities will pass straight through these vesicles and will not be accumulated, giving false positive results (Hegedus *et al.*, 2009). Moreover, this system of looking at one transporter in isolation is not a true representation of what is happening to a compound in a complex cell system such as an enterocyte.

Today the use of polarized cell lines is the first choice when wanting to understand cellular membrane transport in the intestine. The canine kidney cell line MDCKII has a low basal expression of transporters and its formation of a characteristic polarized epithelium has enabled it to be a popular choice in studying the ABC efflux transporters. The low endogenous expression of transporter proteins in these cells provides a good system to look at individual transporters in isolation, even though there are some reports of endogenous transport of drugs, such as digoxin and vinblastine in the native MDCKII cells (Haslam *et al.*, 2008; Lowes *et al.*, 2003). Stable vectorial transfection of MDCKII cells with ABC transporters such as MDR1

(Horio *et al.*, 1989), MRP1 (Bakos *et al.*, 1998), MRP2 (Evers *et al.*, 1998) and the human and mouse BCRP homologues (Jonker *et al.*, 2000; Pavek *et al.*, 2005), have become routine tools in screening for candidate substrates, especially in drug development for the pharmaceutical industry.

Over-expressing MDCKII cells are useful tools for researching ABC-transporters in isolation. However, they do not always give a reliable measure of function in a complex cell system in vivo. Cell lines such as the human colon adenoma carcinoma cell lines Caco-2 and T84 provide much more useful tools when looking at complex cell systems such as the intestine.

The use of the Caco-2 cell line serves today as probably the most popular in vitro tool to study intestinal processes; such as small peptide transport (Ganapathy *et al.*, 1995; Thwaites *et al.*, 1994) and drug transport (Artursson, 1990; Collett *et al.*, 1996; Englund *et al.*, 2006; Hilgers *et al.*, 1990). Early characterization with Caco-2 cells showed extensive transporter expression and due to their expression of the ATP binding cassette transporters MDR1, MRP2, MRP3, MRP5 and BCRP they have been utilized routinely to model these transporters (Ebert *et al.*, 2007; Lowes *et al.*, 2003; Lowes & Simmons, 2002; Prime-Chapman *et al.*, 2004; Xia *et al.*, 2005). Caco-2 cells are frequently used in the pharmaceutical industry in drug permeability assays to model the human intestine (Artursson, 1990; Collett *et al.*, 1996; Hidalgo *et al.*, 1989; Hilgers *et al.*, 1990). Many studies have compared the expression of these transporters in Caco-2 cells to human tissue (Englund *et al.*, 2006; Gutmann *et al.*, 2005; Seithel *et al.*, 2006; Taipalensuu *et al.*, 2001). Reports show that the expression profile of these transporters in Caco-2 cells is very similar to human jejunum (Gutmann *et al.*, 2005; Seithel *et al.*, 2006). On the other hand Taipalensuu *et al.* (2001) conversely show that particular transporters such as BCRP have a 100-fold lower transcript level in Caco-2

cells compared to that of human jejunum (Taipalensuu *et al.*, 2001). These discrepancies and differences show that extrapolation from in vitro cell models to an in vivo situation also is by no means perfect but they are currently the best thing from using human tissue.

To understand the ABC-transporter mediated secretion of compounds in a complex cell system in which multiple ABC transporters exist, such as Caco-2 cells, inhibitors can be used to distinguish between transporter family members. Many agents have been developed or existing agents recognized as BCRP inhibitors. As discussed previously these agents can affect the oral bioavailability of drugs and, therefore, in the clinic could be useful tools to improve oral bioavailability and reverse drug resistance to antibiotics and cancer agents. In the clinic tyrosine kinase inhibitors have been recognized as BCRP inhibitors and so can be used alongside other cancer agents to improve drug efficacy. Nonetheless there are relatively few examples of ABC inhibitors in clinical use.

In vitro specific inhibitors of the ABC transporters are excellent research tools for studying ABC transport. Generating specific inhibitors of particular family members is difficult due to the overlap in substrate specificity, for example, GF120918 (elacridar), a third generation BCRP inhibitor is effective at inhibiting both MDR1 and BCRP in vitro (de Bruin *et al.*, 1999). It often depends on the concentration of an inhibitor to achieve selective inhibition. For example, CsA is known to be an inhibitor of both MDR1 and BCRP and it depends on the concentration as to which family of transporters is inhibited (Ejendal & Hrycyna, 2005; Xia *et al.*, 2007b). Fumitremorgin C, a mycotoxin of *Aspergillus fumigatus*, is an ideal pharmacological research tool, as it is a specific inhibitor of BCRP (Rabindran *et al.*, 1998). However, it possesses neurotoxic effects, which limit its use.

The analogue of FTC, Ko143, is a less toxic and even more effective selective BCRP inhibitor (Allen *et al.*, 2002). A screen by Matsson *et al.* (2007) screened 123 compounds to see whether or not they are BCRP inhibitors and stated that a $logD_{7.4}$ (octanol/water partition coefficient at pH7.4) of at least 0.5 was required for a compound to be a BCRP inhibitor (Matsson *et al.*, 2007).

As already noted, in vitro isolated intestinal segments mounted in Ussing chambers from both animal and human sources provide definitive data as to absorption but do not allow high-throughput capability. In vivo animal/human experiments are yet more expensive but probably serve as the most informative measure of likely oral absorption.

Molecular specificity with respect to ABC-transport proteins may be combined with animal models using both in vivo and in vitro approaches with gene knock-out. This is illustrated by the use of mdr1a or mdr1b knockouts, double knock-outs of mdr1a/b and Bcrp knockout mice in determination of the pharmacokinetics of candidate substrates of ABC transporters in a whole animal system rather than a particular tissue type (Jonker *et al.*, 2005; Marchetti *et al.*, 2008; Zhang *et al.*, 2005). The knock down of a specific ABC transporter clearly shows the contribution of these efflux proteins on the ADME profile of individual drugs. This provides a physiological model that can be extrapolated to man. However, it is not economical to use these animals for all new drugs under development. The use of knockout animals is relatively expensive, is low throughput compared with in vitro methods that are available and, therefore, are only used were necessary.

1.7 ABC protein nuclear receptor modulation

The expression of the ABC efflux transporters is thought to be tightly regulated by a complex network of interacting nuclear receptors (also known as xenosensors), such as constitutive androstane receptor (CAR), farnesoid X receptor (FXR), liver X receptor (LXR), pregnane X receptor (PXR) and vitamin D receptor (VDR). Approximately 50 nuclear receptors working alongside an even greater number of coactivators (which often occur in multiprotein complexes) have been identified, all of which have not been well characterised (Pascussi *et al.*, 2008). These receptors in turn are regulated by a vast array of endogenous and exogenous ligands and it is estimated that approximately 10% of commonly prescribed drugs activate these nuclear receptors. The main structural features of the nuclear receptors are the ligand binding domain at the C-terminal and the more conserved DNA-binding domain (Gibson *et al.*, 2006; Handschin & Meyer, 2003). Nuclear receptors regulate more than the ABC transporter proteins, for example PXR is known to regulate approximately 40 genes (Maglich *et al.*, 2002), such as MDR1, MRP2 and CYP3A4, whilst CAR, 69 genes (Ueda *et al.*, 2002) and LXR regulates approximately 319 genes (Stulnig *et al.*, 2002). Thus nuclear receptors co-ordinate a complex cellular adaptation to xenobiotic exposure by up/down regulation of an array of genes to rid the body of xenobiotics. Expression of cytochrome P450s, conjugation enzymes and ABC transporter proteins show co-ordinate regulation to name but a few (Pascussi *et al.*, 2008). Furthermore, nuclear receptors are thought to work co-operatively in an interacting network of nuclear receptors controlling gene expression (Gibson *et al.*, 2006).

Nuclear receptors are expressed at high concentrations in areas in which there is large ABC transporter expression (Chan *et al.*, 2004). PXR is known to be

expressed in the small intestine and is known to regulate not only MDR1 (Geick *et al.*, 2001) and MRP2 (Kast *et al.*, 2002) but also the drug metabolising enzyme CY3A4 (Greiner *et al.*, 1999). Nuclear receptors when activated by ligands are known to bind to conserved DNA sequences known as hormone response elements (HRE) which are found in the promoter regions of target genes. For example, when PXR is activated by rifampicin it dimerizes with a partner, RXR, to form a heterodimeric complex. This complex then binds to a response element known as PXRE on target genes such as MDR1. The location of these response elements are gene specific and activation also tissue specific, combining this with the multiple endogenous and exogenous ligands that may bind to different binding sites on the same gene, results in a highly complex dynamic method of regulation.

Given the complex nature of nuclear receptor mediated regulation it is unsurprising to find that multiple nuclear receptors have been linked with MDR1 regulation. In the intestinal cell line T84 it has been shown that MDR1 is regulated through PXR activation (Haslam *et al.*, 2008). Whilst there are reports that intestinal regulation of MDR1 is also regulated via the CAR receptor (Burk *et al.*, 2005).

The regulation of MRP2 is also reported to be regulated by PXR activation but also by FXR and CAR (Kast *et al.*, 2002), with reports showing that regulation is dissimilar to that of MDR1 (Haslam *et al.*, 2008).

BCRP has been shown to be regulated via many pathways in different epithelial tissues but no generic pathway of induction has been identified for BCRP between different tissue types. Findings by Albermann *et al.* (2005) correlated PXR with the regulation of BCRP mRNA but no further evidence for the involvement of this nuclear receptor has emerged (Albermann *et al.*, 2005). Perhaps this difference in regulation between MDR1 and MRP2 serves to act as a survival advantage. Providing

alternative gene regulatory pathways for separate efflux transporters will allow one transporter to compensate for the others if any are compromised in any way.

1.8 Objectives of the thesis

Although most work on ABC-transporter function within the intestinal tract has been carried out on MDR1 and MRP2, it is quite clear from expression studies that BCRP is likely to be at least as important to limiting xenobiotic uptake from the diet as MDR1. The primary objective of this thesis is, therefore, to examine the function and regulation of the less characterised of the three main efflux transporters, BCRP in the context of epithelial expression with particular focus on human intestinal cells.

Madin Darby Canine Kidney II (MDCKII) cells transfected with human BCRP and the mouse homologue Bcrp have been characterised for the extent and stability of BCRP/Bcrp expression. In order to identify organ-specific cell-lines in which endogenous BCRP expression occurred, the intestinal Caco-2 cell line, together with several renal epithelial cell lines were assayed for BCRP expression. In order to determine the functional activity of BCRP the fluorescent Hoechst 33342 dye was assessed as an appropriate substrate. Hoechst 33342 was then used as an indirect method of identifying BCRP substrates in the MDCKII cells (Chapter 3).

Since Hoechst 33342 accumulation is only an indirect measure of substrate flux, MDCKII cell models and Caco-2 cells were reconstituted as functional epithelial layers grown upon filter supports to provide an unambiguous assay of BCRP mediated transport function by measurement of net substrate flux. The objectives were to assess the relative contribution of BCRP to ABC-transporter mediated secretion but also to identify a BCRP specific substrate that could be used in isolation

to assess BCRP function despite the existence of multiple ABC transport activities (Chapter 4).

Despite several years of attempting to identify the molecular basis of the fluoroquinolone (ciprofloxacin) secretion, the basis of this secretion in Caco-2 epithelia remained uncertain. The objective of Chapter 5 was, therefore, to determine whether BCRP alone or in conjunction with other ABC transporters mediates this secretion.

Given the existence of a specific BCRP substrate (nitrofurantoin), the final objective addressed in Chapter 6 was to determine whether dynamic regulation of the BCRP pathway occurred in Caco-2 epithelia in response to potential stimuli arising from factors such as dietary components. Such regulation may be used to predict unwanted drug-drug interactions but also may provide insight into methods to improve oral drug delivery.

2. Materials and methods

2.1 Materials

Cell culture media and supplements were purchased from Sigma (Poole, Dorset, UK), and tissue culture plastic flasks and culture plates were supplied by Costar (High Wycombe, UK) and Millipore (Watford, UK). All chemicals were obtained from Sigma (Poole, Dorset, UK), at the highest purity available, unless otherwise stated. Ko143 was given as a gift from the Netherlands Cancer Institute to be used in Chapter 5 only, the remaining work with Ko143 was sourced from AstraZeneca (Alderley Park, Cheshire).

2.2 Methods

2.2.1 Routine cell culture

All cell culture was performed in a class II laminar flow hood (Safeflow1.2, Bio Air Instruments, Italy) under aseptic conditions. Cells were grown in flasks of 175cm^2 surface area and maintained in a sterile incubator at 37ºC with 5% CO_2 in air.

In this study two Caco-2 cell-strains were used; a high-passage (PA) strain (passage 115-120) originating from Dr. I Hassan, as described previously (Cavet *et al.*, 1997) and a low PA strain (passage 34-45) originating from AstraZeneca displaying rapid growth and higher values of transepithelial resistance (American Type Culture Collection, Manassas, VA, 20108, USA). All Caco-2 cells were maintained in high-glucose (4500mg.ml^{-1} D-glucose) Dulbecco's Modified Eagle's Medium (DMEM) supplemented with foetal calf serum (10% v/v), 1mM L-glutamine

(1% v/v), non-essential amino acids (1% v/v) and 30µg.ml^{-1} gentamicin (0.06% v/v). Media was replaced every 3-4 days and cells were passaged every 7-14 days.

MDCKII native, human MDR1-MDCKII, human BCRP-MDCKII and mouse Bcrp1-MDCKII cells were gifts from the Netherlands Cancer Institute. MDCKII cell lines were cultured in Minimum Essential Eagle's Medium (EMEM) supplemented with foetal calf serum (10% v/v), non-essential amino acids (1% v/v), 1mM L-glutamine (1% v/v) and a Penicillin Streptomycin mix (1% v/v). Media was replaced every 3-4 days. MDCKII native cells were used for 15 passages from frozen whilst transfected cells were used for 10 passages.

Native HEK (293/4.59) and MRP4-transfected HEK cells (293/4.63) were a gift from Prof. P. Borst of the Netherlands Cancer Institute (Reid *et al.*, 2003b). HEK 293 cell lines were maintained in high-glucose (4500mg.ml^{-1} D-glucose) Dulbecco's Modified Eagle's Medium (DMEM) supplemented with foetal calf serum (10% v/v) and a Penicillin Streptomycin mix (1% v/v).

The mouse cortical collecting duct principal cell line (mpkCCDc14) and mouse distal convoluted tubule cells (mpkDCT) were kindly provided by Dr. A. Vandewalle (INSERM, Paris). Both cell lines were cultured in a 1:1 (v/v) ratio of low-glucose (1000mg.ml^{-1} D-glucose) Dulbecco's Modified Eagle's Medium (DMEM) and HAMS-F12 nutrient mixture. The mixture was supplemented with 20mM D-glucose (0.0224% v/v), 50nM dexamethasone (0.005% v/v), 10ng.ml^{-1} epidermal growth factor (0.01% v/v), foetal calf serum (2% v/v), 20mM HEPES (0.002%v/v), 2mM L-glutamine (1% v/v), 5µg.ml^{-1} insulin (0.05% v/v), Penicillin/Streptomycin mix (1% v/v), selenium (0.02% v/v), 5µg.ml^{-1} transferrin (0.11% v/v) and 1nM triiodothyronine (0.0014% v/v) (Hasler *et al.*, 2003).

MCF-10A cells were obtained from ATCC (Middlesex, UK) and cultured in a 1:1 (v/v) ratio of low-glucose Dulbecco's Modified Eagle's Medium (DMEM) and HAMS-F12 nutrient. The mixture was supplemented with 20ng.ml^{-1} cholera toxin (0.5% v/v), 20ng.ml^{-1} EGF (0.2% v/v), foetal calf serum (5% v/v), 1µg.ml^{-1} hydrocortisone (0.33% v/v), 10µg.ml^{-1} insulin (0.1% v/v) and a Penicillin and Streptomycin mix (1% v/v). Cholera toxin was added to increase the intracellular levels of cyclic AMP which is thought to promote growth and increase the number of times these cells could be subcultured (Stampfer, 1982).

2.2.2 Functional transport assays

2.2.2.1 Hoechst 33342 cellular accumulation assay

Cell monolayers of all cell types used were seeded at a low density of 5 X 10^4 cells per well onto 24-well plates or 3 X 10^4 cells per well onto 96-well plates and grown for 5-7 days. Caco-2 cells were grown for 7-10 days. The cell monolayers were washed 2 times with warm Krebs' solution then incubated at 37ºC for 30 minutes in 1ml (24-well plates) or 200µl (96-well plates) Krebs' solution (pH 7.4) containing +/- inhibitor. The bathing medium was then aspirated and monolayers were incubated for a further 60 minutes with 1ml (24-well plates) or 200µl (96-well plates) 3µM Hoechst 33342 +/- inhibitor Krebs' solution. At 60 minutes cell medium was again aspirated and monolayers washed 2 times in Krebs' buffer. The 24-well plate's cells were subsequently lysed for between 15-30 minutes with 0.5ml (0.01% Triton X-100 lysis buffer). Typically 40ml of lysis buffer was made for each assay comprising of 1mM EDTA pH 8, 1mM EGTA pH 8, 640µM sucrose, 1mM Tris pH 7.6, 0.05 % Triton X-100, and made up to 40ml with distilled water. Following cell lysis an aliquot of

solution was kept to measure protein levels per well whilst the remainder was transferred to UV-grade cuvettes for Hoechst 33342 fluorescence to be measured on a Perkin Elmer fluorimeter (excitation wavelength 350nm and emission 480nm). Fluorescence was then corrected for protein levels in individual wells using the Bradford Assay for protein concentrations (Thermo). Assays conducted on 96-well plates were not lysed but read straight away on a fluorimetric plate reader (FLUOstar Omega, BMG Labtech), each well was read by a 5x5 well-scan grid system to ensure all areas of the well was read, giving an average fluorescence for each well.

The Bradford assay for protein correction (Bradford, 1976) was performed by producing a bovine serum albumin (BSA) standard curve (0-20µg protein). 50µl of standards were prepared in Eppendorf tubes (1.5ml) and diluted using the lysis buffer used in the assay to remove cells. 10µl of the standards and samples were transferred in triplicate to a 96-well clear round bottomed plate (Fisher Scientific) and to all wells 200µl of Coomassie Brilliant Blue (Thermo) was then added. Any bubbles were removed from the wells by briefly waving over a Bunsen burner flame. Plates were then measured at absorbance 595nm on the fluorimetric plate reader (FLUOstar Omega, BMG Labtech). A BSA standard curve was produced from the standard values and subsequently sample protein concentrations were determined by extrapolation from the curve and correcting for any dilutions (if sample dilutions were made).

2.2.2.2 Measurement of bi-directional transport across epithelial layers grown on 12-well filter plates

Cells were seeded at high density (5 X 10^5 cells per well) onto 12-well permeable polycarbonate membrane filters (Corning, Transwell, 3401, 12mm diameter, 0.4µm

pore size, 1.14cm^2 growth area). Both Caco-2 and MDCKII cells were left until confluency (14 days and 5-7 days post seeding respectively); cells had media changed every 3 days.

Transepithelial electrical resistance (R_T) values were determined for each well as a quality control measure for both MDCKII and Caco-2 monolayer integrity, using a World Precision Instruments EVOM voltohmmeter. Epithelial layers were only accepted if the data were above 200 Ω.cm^2 for Caco-2 epithelia. For MDCKII layers values of < ~100 Ω.cm^2 were more typical. The initial resistance values were corrected for the resistance of the filter alone by subtracting its resistance (81.75 ± 1.68 Ω in Krebs' buffer, n = 8) and adjusting for filter area (1.14 cm^2).

Since transepithelial resistance values for MDCKII monolayers were low an additional quality control measurement was employed to check for confluence. Transepithelial potential differences (PD, mV) were measured after replacement of the basolateral NaCl buffer with D-mannitol (basolateral solution electropositive). Dilution potentials typically greater than 30mV (basolateral solution electropositive) were considered acceptable for confluent monolayers (Carr *et al.*, 2010). Normal PD values ranged between between 40-70mV.

Cell monolayers were washed with warm Krebs' buffer (37°C) and were maintained at this temperature on a hot plate throughout the experiment. Radiolabelled drug was dispensed into the donor solutions. After the addition of the radiolabel-containing donor solutions to either apical or basal compartments, warm Krebs' buffer was added to the opposite compartment (the acceptor solution). The flux of the radiolabelled drug was determined from donor to acceptor compartments (apical or basal), giving a measure of apical to basal or basal to apical flux.

Transport inhibitors included in the experiment were added to both apical and basolateral compartments. Radiolabelled mannitol was included where possible as a measure of paracellular permeability, a mannitol flux greater than 5% into the opposite compartment at the end of the incubation time resulted in these results being discarded (due to poor monolayer integrity).

At 60, 120 and 180 minutes incubation, 50µl samples were removed from both apical and basal compartments of each well. This sample was added to 2.5ml of scintillation cocktail (OptiPhase "Hisafe" 2 Liquid Scintillation Cocktail). After the samples were collected at the end of the 180 minutes, Transwells were washed thoroughly (4 times in ice cold Krebs' buffer), this reduced extracellular isotope to a negligible concentration still remaining on the filter. The filters were then cut out and also added directly to scintillation cocktail. Sample activity was measured using a liquid scintillation counter (Beckman LS 5000 Liquid Scintillation System).

Flux calculations were made as follows and are expressed in moles.cm^{-2}.hr^{-1}:

$$J_{a\text{-}b} = \frac{Db \times M}{Dt \times S}$$

$$J_{b\text{-}a} = \frac{Da \times M}{Dt \times S}$$

$$J_{net} = J_{b\text{-}a} - J_{a\text{-}b}$$

From the formulas $J_{a\text{-}b}$ is the apical to basal flux, $J_{b\text{-}a}$ is the basal to apical flux whilst J_{net} is the net flux. Dt is the total dpm (disintegrations per minute) added to the donor compartment (apical and basal) at the start of the experiment. Da and Db are the activities (in dpm) transported to the apical and basal receiver compartments per

hour, respectively. M is the number of moles of the substrate present and S is the growth area of the filter (1.14cm^2 for 12-well, 0.7cm^2 for 24-well or 0.11cm^2 for 96-well plates).

The accumulation of radiolabelled substrate within the cells was determined using these equations:

$$Aa = \frac{Ta \times M}{Dt \times V}$$

$$Ab = \frac{Tb \times M}{Dt \times V}$$

From the formulas Aa represents accumulation from the apical compartment and Ab accumulation from the basal. Ta is the activity (dpm) of the cell layer exposed to the apical donor solution and Tb the layer exposed to the basal donor solution, V represents the volume of cells on the filter. Cell volumes for Caco-2 and MDCKII grown on 12mm Transwells were approximately 1.98µl and 2µl respectively, calculated previously by using confocal imaging to measure cell height (h) and radius (*r*) of the filter (πr^2.h) (Griffiths *et al.*, 1994; Lowes *et al.*, 2003).

2.2.2.3 Bi-directional transport across epithelial layers grown on 24 or 96-well filter plates

Caco-2 and MDCKII cell-lines were seeded onto 24 or 96-well permeable culture inserts (Millipore, Millicell®-24 and 96 well plates, 0.4µm pore size) at high density. Caco-2 cells were seeded at 2.25 X 10^5 cells per well and 3 X 10^4 cells per well for 24 and 96-wells, respectively. MDCKII cells were seeded at 5 X 10^5 cells per well and 3 X 10^4 cells per well for 24 and 96-well, respectively. Caco-2 and MDCKII cells were

cultured until confluency (14 days and 3-5 days post seeding respectively). Cells had media changed every 3 days.

Caco-2 and MDCKII cell confluence was determined by measurement of transepithelial electrical resistance (R_T) using an automated TEER reader using the REMS system for 96-well plates, the WPI EVOM voltohmmeter (World Precision Instruments, Stevenage, Hertfordshire, UK) was used for the 24-well format. Resistance values for confluent cell monolayers layers on 96-well permeable supports gave TEER values of approx 2500Ω and 450Ω for Caco-2 and MDCKII, respectively without correcting for filter resistance and growth area. Resistance values for confluent cell monolayers layers on 24-well permeable supports gave TEER values of approx 500Ω and 120Ω for Caco-2 and MDCKII, respectively without correcting for filter resistance and growth area. Prior to experimentation MDCKII and Caco-2 cell confluency were determined by the magnitude of the Na^+/choline bi-ionic potential difference (p.d.) (with basal bathing solution replacement), as described previously.

Transport assays measured the compound of interest as the unidirectional (apical to basal, J_{a-b} and basal to apical, J_{b-a}) flux from a donor solution of 10μM unless otherwise stated. Sampling was either performed manually for 24-well assays or for the 96-well format using the Hamilton Starplus robot. Two automated scripts were used for the 96-well format, including a 24 compound substrate assay and a 6 compound substrate assay including ABC transporter inhibitors. Lucifer Yellow (100μM) was included were possible in the transport buffer to allow post-assay determination of paracellular permeability, measured by spectrofluorometry (485-535nm).

Epithelial layers were first washed (3 times) in Hank's Buffered Saline Solution (HBSS) and placed in a fresh base-plate containing HBSS supplemented

with 10mM HEPES. Monolayers were allowed a 15 minute equilibration period at 37ºC. For flux experiments, the buffer composition was identical for apical and basal compartments (HBSS + 10mM HEPES) with the addition of compound of interest to either the donor apical or basal compartments. Samples were taken and at 2 hours incubation at 37°C to determine absorptive (apical to basal, J_{a-b}) and secretory (basal to apical, J_{b-a}) flux. All compounds were made up from solid in DMSO and experimentation volume never exceeded 0.1% DMSO. All assay plates were then prepared for measurement via mass spectroscopy by protein precipitation ("crashing") with MeOH, followed by centrifugation and transferral of supernatants to new sample plates. Samples were optimized and compound analysed by high pressure liquid chromatography-mass spectroscopy (HPLC-MS). Samples were analysed via single or parallel chromatography, using a Phenomenex Gemini 5µ 50 x 2.0 column, in column ovens set at 50°C. The rest of the HPLC unit comprised of: a HP1100 series binary pump, column heater, Diode Array Detector, CTC HTS PAL autosampler. The HPLC stationary phase used was non polar with a polar mobile phase comprising of water and ammonium acetate. The gradient switched from 5% water and 95% ammonium acetate at time 0 to 95% water and 5% ammonium acetate at 3 minutes. Formic acid was added to adjust pH depending on the compound retention. Detection by mass spectroscopy (Waters® Quattro Ultima™) was done by switching between positive or negative ionization modes depending on the individual compound being used. An internal standard was included in samples to ensure injections onto the HPLC-MS system were standardized. C0 samples (concentration at the start of the assay) were also included in the samples to assess the recovery of the compound from the Transwell assay (recoveries were acceptable between 40-120%). Chromatogram data were processed using QuanLynx V4.1 software (Waters Inc. 2008) and flux

values were determined on adjacent layers using the calculations determined in (2.2.2.2).

2.2.3 Induction pre-treatments of Caco-2 cell monolayers

Cell monolayers were incubated between 24-72 hours with different agents, DMSO concentration never exceeding 0.1%. All inducing agents were made up in DMSO and then diluted to the required final concentration using phenol red free Dulbecco's Minimum Essential Media. Cell monolayers were incubated between 24-72 hours depending on the experiment. The washout period consisted of 2 initial washes with pre-warmed media at 37°C and incubated for 60 minutes. 60 minutes washout being long enough to ensure any inducing agent has had adequate dilution and transit time from the cell. The washout duration was not too long as to prevent a reversal of the induction. The protocol was then followed as described in (2.2.2.3).

2.2.4 Cellular ciprofloxacin accumulation in HEK 293 cells

HEK 293 cells were seeded 5 x 10^4 onto 12 well plates (Corning). Cells were grown for 4 days. Media was aspirated and replaced with transport buffer (Krebs' buffer with additional radiolabel and inhibiting agents). Cells were incubated at 37°C for 1 hour and were then washed with ice cold Krebs'. Cells were then treated with 500µl lysis buffer (0.05% Triton X-100) and samples were collected for measurement and protein correction via a Bradford Assay. Cellular accumulation of [^{14}C]-ciprofloxacin (made up to 10µM with unlabelled ciprofloxacin) was determined by scintillation counting.

2.2.3 Molecular biology

2.2.3.1 RNA isolation and quantitative PCR

RNA was isolated from confluent flasks of epithelial cells, using the Qiagen RNeasy mini-kit following the manufacturer's standard protocol. Any contaminating DNA was digested using a DNAse treatment according to the manufacturer's protocol (Promega). RNA was quantified using a NanoDrop ND-1000 spectrophotometer (NanoDrop Technologies Inc., Wilmington, DE, USA) and integrity checked by measurement of the A260/280 nm ratio, which was routinely in the range of 1.8-2.0.

2.2.3.2 Reverse transcription

To synthesise cDNA to be used in the polymerase chain reaction, reverse transcription (RT) was performed using 1µg total purified RNA. Using components from Promega, a 20µl reaction was set up on ice, the final tube contained: 5 X RT reaction buffer (20 % v/v), 2mM dNTP mix (25% v/v), 0.5µg/ml random hexamer primers (5% v/v), RNase inhibitor (1.25% v/v), reverse transcriptase (2.5% v/v) and 1µg template RNA, RNase-free water (to 20µl). Negative controls were also made up at the same time which involved replacing the reverse transcriptase enzyme with an equal volume of RNase-free water.

Note that before all components were added, the RNA template and random hexamer primers were mixed in tubes and then quickly denatured for 5 minutes at 65ºC on a thermal cycler (Px2 thermal cycler, Thermo). The tubes were then transferred to ice for 2 minutes before adding the remaining components. The tubes were then subsequently incubated at 42ºC for 2 hours to allow cDNA synthesis and finally denatured for 3minutes at 95ºC.

2.2.3.3 Standard polymerase chain reaction

Using the cDNA product synthesized from the RT reaction the product was then amplified by standard polymerase chain reaction. The gene region to be amplified was defined by primers that were designed by OligoPerfect™ designer software (Invitrogen). These forward and reverse primers were verified for specificity by BLAST (basic local alignment search tool) and these gene-specific primers were purchased from VH Bio Limited (Gateshead, UK). The primer pairs used in this study are shown in Table 2.1 of methods.

PCR reactions were made up using HotStartaq PCR kits (Qiagen). A 25µl PCR master mix was made on ice, containing: 10 X PCR buffer (10% v/v), 10mM dNTP mix (1% v/v), 10µM forward primer (5% v/v), 10µM reverse primer (5% v/v), HotStarTaq DNA polymerase (0.5% v/v), cDNA sample (8% v/v) and distilled H_20 (to 25µl). Negative controls were again set up for each sample; an RT negative control (described in section) and a second negative in which the cDNA template is replaced with an equal volume of distilled water (this was to confirm the lack of genomic DNA contamination).

The PCR reaction was incubated in a Px2 thermal cycler (Thermo) according to a specific protocol of repeated DNA denaturation, hybridization and extension. The protocol involved 15-minute incubation at 95ºC to activate the Taq Polymerase enzyme. The reaction mix was then cycled between 30-35 times with these 3 steps in sequence; 30 seconds at 94ºC to denature the DNA strands, 30 seconds at a particular cooling temperature depending on the primer pair (shown in Table 2.1 of methods) and then 60 seconds at 72ºC to allow DNA extension. After the cycles were complete the tubes were held for a further 10 minutes at 72ºC and then held at 4ºC until stored in the -20ºC freezer.

PCR products were then separated on a 2% agarose gel containing 0.005% Safeview, whilst a 100 base pair ladder (GeneRuler 100 base pair DNA Ladder plus, Fermentas, Thermo Fisher Scientific) was used to obtain the size of the PCR product. The electrophoresis was run for 70V for 1 hour and viewed using a UV transilluminator (Uvitec, Cambridge).

2.2.3.4 Real-time polymerase chain reaction

Real-time PCR was performed with the same principal as standard PCR, however, as the product can be visualized whilst the reaction is occurring to give a quantitative measure of mRNA when compared with a standard curve. The SYBR green I fluorescence dye is the simplest detection method for RT-PCR; whereby the dye fluoresces when bound to DNA specifically to the minor groove of double stranded DNA (Morrison *et al.*, 1998).

A 10µl reaction mixture was added to a 96-well white PCR analysis plate (Roche) and comprised of: SYBR green (Roche) Master Mix (50%v/v), 10µM forward primer (5% v/v), 10µM reverse primer (5% v/v), 1:4 diluted cDNA sample (20% v/v) and distilled H_20 (to 10µl). Note the cDNA sample was diluted 1:4 to allow samples to go further and to be quantified from the standard curve. Negative controls were again set up for each sample; an RT negative control (described in section 2.2.3.2) and a second negative in which the cDNA template is replaced with an equal volume of distilled water. This was to confirm the lack of genomic DNA contamination.

Amplification was performed over 45 cycles using the Roche Light Cycler 480. Quantification of mRNA was done via two methods. For the MDCKII, Caco-2 and HEK mRNA characterisation, levels were quantified using the Pffafl method of

quantification. This is a mathematical approach that requires no calibration curve (Pfaffl, 2001). The relative expression ratio is calculated only from the real-time PCR efficiencies and the deviation in crossing point of an unknown sample versus a control. The crossing point (CP) is defined as the point at which fluorescence rises appreciably above the background level of florescence. The relative expression ratio of a target gene is calculated using this equation:

$$\text{Ratio(R)} = \frac{(E_{target})^{\Delta CP\text{target (control-sample)}}}{(E_{ref})^{\Delta C\text{ref (control-sample)}}}$$

E_{target} is the real-time PCR efficiency of a target gene transcript (such as hBCRP). E_{ref} is the real-time PCR efficiency of a reference gene transcript (the stable housekeeping gene GAPDH was used). The efficiency was determined from the given slope on the LightCycler software, calculated from the equation $E= 10^{[-1/slope]}$ (Pfaffl, 2001; Tichopad *et al.*, 2003). The ΔCP_{target} is the CP deviation of control-sample of the target gene.

The second method used to quantify changes in BCRP expression in Caco-2 cells shown in Chapter 6 was done via the conventional method of using positive control mRNA to generate standard curves from each primer set, allowing relative quantification (using hBCRP-MDCKII cDNA to generate the standard curve). Sample values were extrapolated from the standard curve and then data were normalised to the expression of the house keeping gene GAPDH and then in turn expressed as relative arbitrary units. Products were verified by electrophoresis on a 2% agarose gel, cut out under UV light, and purified using a Qiagen QIAquick PCR purification kit.

Then 15µl of > 2ng/µl of product was sent off for sequencing (Eurofins MWG DNA Sequencing).

2.2.4 Immunoblotting

Cells were cultured and grown in 75cm^2 flasks as described in Routine Materials and Methods (section 2.2.1). Whole cell extract was lysed using a buffer comprising of 1mM EDTA pH 8, 1mM EGTA pH 8, 640µM sucrose, 1mM Tris pH 7.6, 0.05 % Triton X-100 and ½ a protease inhibitor tablet (Roche), made up to 5ml with distilled water. Cells were washed twice with 1% Phosphate Buffered Saline (PBS) and 1ml of lysis buffer was added to the 75cm^2 flask. Cells were scraped off using a rubber policeman and pippetted into a 15ml Falcon tube. Homogenisation with a needle and syringe was followed by centrifugation at 10,000 x g for 10 minutes. Whole cell lysate was protein quantified using the Bradford Assay (Thermo). Proteins were loaded between 5-40µg onto graded 4% SDS-polyacrylamide (stacking) + 10% SDS-polyacrylamide (running) gels. The Precision Plus Protein^{TM} Dual Colour Standards (Invitrogen) were loaded to allow protein molecular weight to be estimated. Samples were separated by electrophoresis for 1 hour (40mA). Gel transfer onto PVDF membranes (Millipore) was then conducted overnight at 50mA, or for 180 minutes at 250mA. Membranes were blotted in 5% non-fat dry milk in 0.1% Tween 20 phosphate buffered saline (PBS-T) for 1 hour. The membranes were mixed either with the rat-monoclonal anti human/mouse BCRP antibody BXP-53 (Santa Cruz) or BXP-9 (Kamiya), diluted 1:50 and 1:500 respectively in milk PBS-T (both raised against the amino sequence of 221-394 of mouse Bcrp). The mouse-monoclonal antibody BXP-21 (Santa Cruz) was diluted 1:100 in non-fat dry milk PBS-T (raised against the amino sequence 291-396 of human BCRP). Primary incubations were conducted on a

roller mixer at 4°C overnight or for 2 hours at room temperature. Membranes were then washed with PBS and incubated with the appropriate secondary HRP-labelled IgG (Santa Cruz), an anti-rat HRP for BXP-53 and BXP-9, and anti-mouse HRP for BXP-21, diluted 1:10,000. The membrane was then developed using the pico-chemiluminescence substrate (Thermo) and developed using an automatic developer in a dark room. Equal protein loading was confirmed by re-probing membranes for α-tubulin, but before which membranes were stripped with stripping buffer (Thermo) using the manufacturer's guidelines. The primary rabbit anti-human α-tubulin antibody (Abcam) diluted 1:100 in 5% milk was used. Secondary staining was performed with an anti-rabbit HRP-conjugated secondary diluted 1:10,000 (Abcam). Finally the PVDF membranes were copper stained.

2.2.5 Immunocytochemistry

MDCKII and Caco-2 cell monolayers were grown on permeable polycarbonate membrane filters (Transwell, Corning, 3401) for 7 and 14 days respectively. Layers were fixed, prior to staining, with ice cold MeOH for 15minutes. Transwells were then flooded with PBS and blocked in 3% horse serum (HS).

Primary block was followed by the application of a primary antibody either rat-monoclonal anti human/mouse BCRP antibody BXP-53 (Santa Cruz), used at 1:50 dilution in 3% horse serum or mouse-monoclonal anti human BCRP antibody BXP-21 (Santa Cruz) diluted 1:50 and subsequently left in the fridge overnight. Secondary block was done with 3% donkey serum and followed by the secondary antibody; goat anti-rat Alexa Fluor^{TM} 488 (FITC) was diluted 1:100 and used for staining with BXP-53 primary. Secondary block for use with BXP-21 was done with 3% horse serum and followed by the secondary antibody; donkey anti-mouse Alexa Fluor^{TM} 488 (FITC)

and diluted 1:100. Layers were stained with propidium iodide (TRITC) diluted 1:1000 for nuclear staining. Layers were finally mounted onto slides using Vecta Shield and images were taken with a Leica confocal microscope.

2.2.6 Statistical Methods

Results are expressed as mean ± standard error of mean (SEM). Individual experiments were conducted with at least 3 replicates per condition, whilst experiments were repeated at the very least once. Statistical analysis was performed using Student's unpaired t-tests or one-way analysis of variance (ANOVA) with Bonferroni's or Dunnett's post-test for multiple comparisons. Kinetic constants for Michaelis-Menten kinetics and IC_{50} were calculated by non-linear regression with the method of least squares (GraphPad Instat, SanDiego, USA).

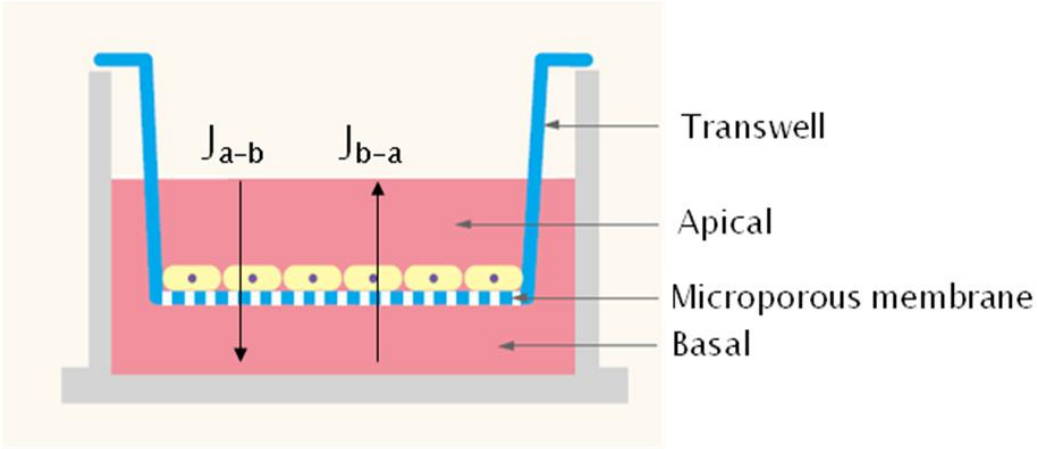

Figure 2.1. Schematic diagram of an epithelial layer grown on a Transwell filter

Table 2.1. Primer sequences used in standard and real-time qPCR reactions

Gene	F Sequence	R Sequence	Product size (bp)	T_A(°C)
hBCRP	5`-AGCTGCAAGGAAAGATCCAA-3`	5`-TCCAGACACACCACGGATAA-3`	289	55
mBcrp	5`-GCATTCTCTGATATGGCTTCA-3`	5`-TTAACACAAGTGCTGTTGTCCG-3`	100	56
hMRP4	5`-CTTGGAGAGGAGTTGCAAGG-3`	5`-GCTGTGTTCAAAGCCACAGA-3`	236	57
hPPAR γ	5`-GACCACTCCCACTCCTTTGA-3`	5`-CGACATTCAATTGCCATGAG-3`	257	55
Ah receptor	5`-CTTCCAAGCGGCATAGAGAC-3`	5`-AGTTATCCTGGCCTCCGTTT-3`	204	56
GAPDH	PrimerDesign Ltd- sequence or product size not given			60

3. Functional expression of BCRP in epithelial cell-lines

3.1 Introduction

Since the discovery of the efflux pump BCRP, in the breast cancer cell line MCF-7 in 1998 (Doyle *et al.*, 1998), many cell models and techniques have been derived and used to model BCRP function in different tissues.

Before ABC transporter function can be assessed in vitro the need to characterise the cell type being used is essential; variations in culture techniques between laboratories has led to differential selection of cells with differing strains arising between laboratories, so resulting in discrepancies in data. For example, the MDCK cell line which was originally derived from a kidney of a female adult cocker spaniel (Madin & Darby, 1972) was shown to have a characteristic low resistance phenotype of 100 $\Omega.cm^2$ (Cereijido *et al.*, 1978, 1980). However, Barker and Simmons (1981) demonstrated that with passage two distinct strains of high and low resistive strains had emerged, displaying differences in size, morphology and expression of Na-K pumps (essentially two distinct cell types) (Barker & Simmons, 1981).

Caco-2 cells are known to be a heterogeneous population of cells, and it is not surprising to find that variant strains of Caco-2 cells have emerged over the years from the original cells, showing inter-laboratory variation in transporter expression and function (Sambuy *et al.*, 2005). This variation highlights the need to characterize protein expression in Caco-2 and other epithelial studies to ensure comparability between laboratories.

In this study two Caco-2 cell-strains were used; a high-passage (PA) strain (115-120 passages) originating from Dr. I Hassan, described previously (Cavet *et al.*, 1997) and a low PA strain (passage 34-45) originating from AstraZeneca displaying rapid growth and higher values of transepithelial resistance (American Type Culture Collection, Manassas, VA, 20108, USA). Caco-2 cells were selected over T84 cells based on the principle they have been shown to express all three main efflux transporters (MDR1, MRP2 and BCRP), whilst expressing multiple nuclear receptors, unlike T84 cells which have been shown to not express MRP2 (Lowes & Simmons, 2002) and BCRP (Haslam, 2007).

The objective of the work in this chapter was to characterise native MDCKII cells, transfected MDCKII cells, Caco-2 cells and other epithelial cell models with respect to BCRP expression and function to ensure their suitability as cell models for the remainder of the project. In order to assess function of BCRP in the chosen epithelial cell lines, the fluorescent dye Hoechst 33342 was used as a substrate. Hoechst 33342 is a dye that is only fluorescent when bound to DNA. Cellular efflux of Hoechst 33342 was initially demonstrated when small populations of bone marrow and peripheral blood cells in mice gave a reduced staining with the dye Hoechst 33342; these cells were then named as side population cells (Goodell *et al.*, 1996). Further investigation by transfecting MDR1 into the murine bone marrow cells increased the number of cells with the side population cell phenotype (Bunting *et al.*, 1999), suggesting Hoechst 33342 to be a substrate of MDR1. However, on closer inspection more than just MDR1 was responsible for Hoechst 33342 efflux and the side population phenotype. Other studies have now shown that both human BCRP and murine Bcrp are responsible for the efflux of Hoechst 33342 dye and the side population phenotype (Kim *et al.*, 2002; Zhou *et al.*, 2001).

Hoechst 33342 is a relatively lipophilic compound displaying an octanol-water coefficient (LogP) of 3.1, it is likely that Hoechst 33342 will partition into the plasma membrane prior to entry into the cell to access BCRP and MDR1 (Matsson *et al.*, 2007). This mechanism of substrate binding to BCRP from the membrane phase as proposed by Matsson *et al.* (2007), and the competition between Hoechst 33342 and substrate can be harnessed to identify potential BCRP substrates. In epithelial cells BCRP is expressed in a polarized manner within the apical plasma membrane whilst for bone-marrow cells and blood cells no such polarity exists. Whether Hoechst 33342 is suitable under all conditions (density of growth, time of growth, etc…) to assay BCRP is unclear.

Thus the secondary aim of this chapter is to determine whether or not the fluorescent Hoechst 33342 dye can be used to assess BCRP function in epithelial cells and furthermore whether it can be used to identify BCRP substrates.

3.2 Methods

3.2.1 Deglycosylation

Cells were cultured and grown in 75cm^2 flasks as described in Materials and Methods (section 2.2.1). Extraction and treatments were done on the same day as instructed by the manufacturer's protocol from the peptide N-glycosidase F kit (PNGase F kit, New England Biolabs). Whole cell extracts were lysed using a buffer comprising of 1mM EDTA pH 8, 1mM EGTA pH 8, 640µM sucrose, 1mM Tris pH 7.6, 0.05 % Triton X-100 and ½ a protease inhibitor tablet (Roche), made up to 5ml with distilled water. Cells were washed twice with 1% PBS and 1ml of lysis buffer was added to the 75cm^2 flask. Cells were scraped off using a rubber policeman and pippetted into a 15ml Falcon tube. Homogenisation with a needle and syringe was followed by centrifugation at 10,000 x g for 10 minutes. Whole cell lysate was protein quantified using the Bradford Assay (Thermo). To the tube 25µg of protein lysate was added to 2µl of denaturing buffer and made up to 20µl with distilled water. Samples were then vortexed and boiled at 100°C for 10 minutes. Samples were then cooled on ice for 1 minute before adding the remaining components (4µl 10x G7 reaction buffer, 4µl 10% NP40, 5µl PNGase F and made up to 40µl with distilled water). Finally samples were incubated at 37°C for 1 hour; samples were then ready for immunoblotting or were frozen at -20°C.

3.3 Results

3.3.1 hBCRP/mBcrp mRNA expression in epithelial cell models

Human BCRP mRNA was analysed in native and hBCRP-transfected MDCKII cells. Measured by real time PCR analysis and adjusted relative to GAPDH levels we found the results were as expected; native cells showed no human BCRP product, with levels no different from the negative controls (RT negative and water control). Human BCRP mRNA was significantly greater in the transfected MDCKII compared with the native cells (Figure 3.1, n = 3 extractions, $P < 0.05$). The other transfect looked at in great detail in this project was the mouse Bcrp protein, the mouse homologue to the human variant. Figure 3.2 shows a significantly higher concentration of murine Bcrp mRNA compared with the native MDCKII (n = 3 extractions, $P < 0.05$), which in turn showed levels no different to the negative controls (RT negatives and water controls).

After confirming hBCRP/mBcrp expression in the MDCKII over-expressing cell lines, human intestinal Caco-2 cells were analysed to confirm BCRP expression. Given the heterogeneous nature of Caco-2 cells and the reported variation of BCRP expression it is unsurprising that differences exist between cell strains arising from different laboratories. This study used two Caco-2 cell strains (high and low passage strains derived from two laboratories, see Materials and Methods). The BCRP levels established by real time PCR (Figure 3.1) showed a dramatic and significant difference in BCRP expression between the two strains of Caco-2 cell (n = 3 extractions, $P < 0.05$). The high passage Caco-2 cell line showing no significant difference in BCRP expression compared with the negative controls (RT negatives and water controls). Whilst BCRP was readily detected in the lower passage Caco-2 cells that was significantly elevated compared with negative controls (n = 3 extractions, $P < 0.05$). The high PA Caco-2 cells expressed little to no BCRP mRNA.

The human small intestine has been shown to express BCRP mRNA (Englund *et al.*, 2006; Gutmann *et al.*, 2005; Maliepaard *et al.*, 2001), thus high PA Caco-2 are an inappropriate model for studying BCRP activity alone, however they could be used as a negative control for BCRP expression. In contrast, the low PA Caco-2 cells, although the BCRP mRNA was not quantified and cannot be compared directly with human intestinal tissue, show a greater BCRP mRNA expression and looked to be a more suitable cell line for studying intestinal BCRP activity.

3.3.2. BCRP/Bcrp protein expression in epithelial cell models

Using antibodies against an internal epitope of hBCRP/mBcrp protein (residues 221-394 of mouse protein); expression was investigated by immunoblotting and immunocytochemistry. Initially BXP-53 (Santa Cruz) which is a rat-monoclonal anti hBCRP/mBcrp antibody was utilised for immunocytochemistry to detect both human and mouse proteins. This antibody was effective for immunohistochemistry of hBCRP/mBcrp but was unable to identify BCRP in Caco-2 cells by immunoblot. BXP-9 which is a rat-monoclonal anti mouse antibody raised against the same epitope as BXP-53 was found to be more effective at detecting both mouse and human BCRP/Bcrp in immunoblotting compared to BXP-53 and was used instead. Figure 3.3 shows that no BCRP band at 72kDa was visible in the native MDCKII cells but a strongly defined band was seen in the human BCRP transfected MDCKII cells at 10μg of protein loaded at 72kDa (n = 3 extractions), with a possible band at lower molecular size. A less intense band was seen at approximately 100kDa. For mBcrp1-MDCKII cells protein loading was reduced (shown with the reduced α-tublin band) together with that of the antibody concentration from 1:50 to 1:500. The band recognised for mBcrp1-MDCKII had an apparent molecular size of approximately

100kDa not 72kD (Figure 3.3.C). Treatment with the deglycosylating enzyme PNGase F reduced the mBcrp apparent molecular size from approximately 100kDa to the expected molecular size of the core mouse Bcrp protein of 72kDa (Figure 3.4). This suggests that the mouse and human proteins are subject to different patterns of glycosylation when expressed in MDCKII cells. According to the literature there are three predicted putative N-linked glycosylation sites at Asn418, Asn557 and Asn596 of human BCRP (Allen & Schinkel, 2002; Mao & Unadkat, 2005), whilst Diop *et al.* (2005) further showed that only Asn 596 is subject to N-linked glycosylation (Diop & Hrycyna, 2005). For mouse Bcrp, two predicted sites for N-glycosylation exist: Asn596 and Asn600 (Allen & Schinkel, 2002). N-glycosylation prediction software (ExPAsy) shows the predicted sites for human BCRP and mouse Bcrp N-glycosylation below.

Predicted N-glycosylation sites on the amino acid sequence of human BCRP and mouse Bcrp (ExPAsy software)

N-linked glycosylation					
hBCRP			mBcrp		
Position		Potential	Position		Potential
338	NSSF	0.5136	316	NKTE	0.5413
418	NDST	0.3618	331	NLSE	0.6974
557	NLTT	0.6748	596	NVTD	0.5798
596	NATG	0.4693	600	NSTC	0.6029

The human BCRP has predicted sites of N-linked glycosylation at positions 418, 557 and 596 (Asn338 is intracellular and is unlikely to be N-glycosylated); these data taken with what is known in the literature shows that Asn596 is likely to be the only N-linked amino acid on the human BCRP sequence. Mouse predictions highlight Asn596 and Asn600 as N-linked glycosylation sites. Asparagines in positions 316 and

331 are located intracellularly and are unlikely to be glycosylated. Thus two closely spaced N-linked glycosylation sites are present on the mouse Bcrp sequence, therefore this predictive data taken with the immunoblotting shows that a greater degree of glycosylation occurs in the mouse protein expressed in MDCKII cells. It is not known whether N-glycosylation of hBCRP\mBcrp affects expression or function (Diop & Hrycyna, 2005) but it is possible it may affect substrate binding.

In agreement with BCRP mRNA expression, in the two Caco-2 cell strains no BCRP protein was detectable in the high passage Caco-2 cells but a band of the apparent correct molecular size for BCRP of ~72kDa was detected in the lower passage Caco-2 cells (Figure 3.3). As expected the expression of BCRP protein was found to be much lower in the Caco-2 cells compared with that of the over-expressing hBCRP-MDCKII cell line (although not quantified, it is clearly shown in Figure 3.3). Note that the hBCRP-MDCKII cells were loaded at 10μg whilst the Caco-2 cells at 40μg (shown visually by the band intensity of α-tubulin). Taken together this result suggests that native hBCRP expressed in Caco-2 cells is not subject to N-glycosylation.

Finally BCRP protein expression at the cell surface was investigated with immunocytochemistry using 2° immunofluorescence with BXP-53 as the primary antibody (Figure 3.5), whilst cell nuclei were stained with propidium iodide (red). No hBCRP/mBcrp immunofluorescence was seen on either XY or XZ sections of native MDCKII cells. In positions 221-394 of the BCRP protein sequence only 15/173 amino acids are not conserved between dog and the human/mouse protein epitopes (shown below). As this is a small difference it would be expected the antibody would detect dog BCRP. It is likely, as no staining is seen, that no dog endogenous BCRP is

expressed in native MDCKII cells. A similar argument applies to the immunoblots with BXP-53 (above).

The MDCKII cells transfected with human BCRP show strong BCRP immunofluorescence localized to the apical cell surface of MDCKII cells (shown on XY and XZ sections Figure 3.5). MDCKII cells transfected with mouse Bcrp cDNA also show localisation of mouse Bcrp to the apical surface of these epithelial cells (shown on XY and XZ sections, Figure 3.5). Caco-2 cell immunocytochemistry with BXP-53 was unsuccessful, but was shown with the human BCRP specific antibody BXP-21 in the low passage Caco-2 cells (Figure 3.6).

The BCRP protein sequence (positions 221-394) showing sequence homology between (A) Mouse/Dog and (B) Mouse/Human/Dog

(A) Epitope area: Mouse/Dog

```
ANAVLLLLKRMSKQGRTIIFSIHQPRYSIFKLFDSLTLLASGKLVFHGPAQKALEYFASA 59  Mouse
ANAVLLLLKRMSEQGRTIIFSIHQPRYSIFKLFDSLTLLAAGKLMFHGPAQEALGFFASV 60  Dog

***********:*****************************:***:******:** :***.


GYHCEPYNNPADFFLDVINGDSSAVMLNREEQDNEANKTEEPSKGEKPVIENLSEFYINS 119 Mouse
GYHCEPYNNPADFFLDVINGDSSAVVLNREDQEGEVKVTEEPSKRGTPFIERIAEFYANS 120 Dog
*************************:****:*:.*.: ******  .*.**.::*** **


AIYGETKAELDQLPGAQEKKGTSAFKEPVYVTSFCHQLRWIARRSFKNLLGNPQASVAQL 178 Mouse
DFCRKTKEELDQLSKSQKRK-SSAFKEITYATSFCQQLKWISKRSFKNLLGNPQASIAQI 179 Dog
 :  :** *****. :*::* :***** .*.****:**:**::**************:**:

IVTVI 184 Mouse
IVTVI 184 Dog
*****
```

42/184 dissimilar 142/184 identical

(B) Epitope area: Mouse/Human/Dog

```
ANAVLLLLKRMSKQGRTIIFSIHQPRYSIFKLFDSLTLLASGKLVFHGPAQKALEYFASA 59 Mouse
ANAVLLLLKRMSKQGRTIIFSIHQPRYSIFKLFDSLTLLASGRLMFHGPAQEALGYFESA 60 Human
ANAVLLLLKRMSEQGRTIIFSIHQPRYSIFKLFDSLTLLAAGKLMFHGPAQEALGFFASV 60 Dog

***********:*****************************:*:*:******:** :* *.

GYHCEPYNNPADFFLDVINGDSSAVMLNREEQDNEANKTEEPSKGEKPVIENLSEFYINS 119 Mouse
```

```
GYHCEAYNNPADFFLDIINGDSTAVALNREE-DFKATEIIEPSKQDKPLIEKLAEIYVNS 119 Human
GYHCEPYNNPADFFLDVINGDSSAVVLNREDQEGEVKVTEEPSKRGTPFIERIAEFYANS 120 Dog
*****.**********:*****:** ****: : :..   ****  .*.**.::*:* **


AIYGETKAELDQLPGAQEKKGTSAFKEPVYVTSFCHQLRWIARRSFKNLLGNPQASVAQL 179 Mouse
SFYKETKAELHQLSGGEKKKKITVFKEISYTTSFCHQLRWVSKRSFKNLLGNPQASIAQI 179 Human
DFCRKTKEELDQLSKSQKRK-SSAFKEITYATSFCQQLKWISKRSFKNLLGNPQASIAQI 179 Dog
 :  :** **.**. .::::*  :.***  *.****:**:*:::**************:**:

IVTVI 184 Mouse
IVTVV 184 Human
IVTVI 184 Dog
****:
```

62/184 dissimilar 122/184 identical

3.3.3 Cellular retention of Hoechst 33342 dye: an assay to assess hBCRP/mBcrp function

The Hoechst 33342 retention assay, as fully described in the Materials and Methods, involved an incubation step without Hoechst 33342 in the presence and absence of a pharmacological inhibitor. This step was followed by incubation with Hoechst 33342 also when appropriate plus inhibitor. During this incubation Hoechst 33342 dye permeates into the cell and binds to DNA whilst the remaining dye is removed from the cells by the efflux transporters BCRP and MDR1. Only DNA-bound Hoechst 33342 shows fluorescence when excited at 350nm. Since both BCRP and MDR1 may transport Hoechst 33342 it was first necessary to optimise the uptake/retention assay.

Figure 3.7 shows the effect of increasing exposure time to Hoechst 33342 in MDCKII cells on dye retention. In controls, increasing incubation time increases Hoechst 33342 cellular retention in a non-linear fashion, the initial rate declines as incubation time increases. This may indicate both attainment of a steady state and saturation of nuclear binding sites. The presence of the ABC transporter inhibitor CsA increases cellular Hoechst 33342 at all time points. After prolonged incubation times it is predicted that curves representing Hoechst 33342 in the presence and absence of CsA

would converge as Hoechst 33342 is bound on all available DNA sites. CsA would increase the rate at which this equilibrium is attained.

Figure 3.8 shows how increasing the seeding density can affect cellular Hoechst 33342 retention. At lower cell numbers the difference in the presence and absence of CsA was not very apparent; for example at 5 x 10^3 cells per well there was only a 6% difference between CsA and non CsA control. However, with higher cell densities, this difference was more marked; at the higher seeding density of 5 x 10^4 cells per well the difference went up to 45% in the presence of CsA compared to the control. An increase in cellular accumulation of Hoechst 33342 was to be expected as nuclear DNA increases. However, there was an apparent saturation with higher seeding density. This is most likely due to monolayer formation resulting in decreased access of dye from the basolateral surfaces, Hoechst 33342 moving into the cell via the apical membrane only. High cell densities were therefore preferable to optimize the effects of inhibition.

Figure 3.9 shows that with increasing Hoechst 33342 bathing concentration in native MDCKII the retention of Hoechst 33342 increases. At all Hoechst 33342 concentrations there was a significant increase in accumulation in the presence of 10μM CsA ($n = 4$ wells per point, $P < 0.05$). Subtracting control data from that in the presence of CsA gives an apparent saturation curve for the CsA-sensitive component (Figure 3.9B); the apparent K_m was 0.3 ± 0.2 μM for Hoechst 33342. The effect of increasing Hoechst 33342 dose in the native cells was also compared to the human BCRP transfected MDCKII cells (Figure. 3.10). The presence of human BCRP significantly reduces the cellular accumulation of Hoechst 33342 dye compared to native MDCKII at all Hoechst 33342 concentrations ($n = 4$ wells per point, $P < 0.05$).

Subtraction of the Hoechst 33342 accumulation from that seen in native cells allows the BCRP-dependent component to be plotted (Figure 3.10B). This component shows saturation with an apparent K_m of 10.3 ± 2.6 µM, this value being substantially greater than the value in the native MDCKII cells (0.3 ± 0.2 µM). The apparent difference in K_m between native and BCRP transfected MDCKII demonstrates that Hoechst 33342 interacts with transfected BCRP with a lower affinity compared to the native ABC transporter in MDCKII cells. Due to the observed saturation with Hoechst 33342, subsequent experiments used a Hoechst 33342 concentration lower than the K_m value (3µM Hoechst 33342 was used).

The dose effect of pharmacological inhibitors was assessed in the BCRP transfected MDCKII cells. Ko143 (Allen *et al.*, 2002) is a known potent hBCRP/mBcrp inhibitor; Figure 3.11A shows that Ko143 increased Hoechst 33342 accumulation in a saturable manner, with an IC_{50} value of 1.06 ± 1.58 µM. Cyclosporin A (CsA) also increased Hoechst 33342 accumulation, but with an IC_{50} of 1.17 ± 1.12 µM (Figure 3.11B). Cyclosporin A is a known MDR1 substrate and inhibitor but also a BCRP inhibitor at higher concentrations (Ejendal & Hrycyna, 2005; Xia *et al.*, 2007a). The increase in Hoechst 33342 observed is therefore a mixture of inhibition of a native ABC-transporter and BCRP. For these reasons a low concentration of CsA (1µM) was used to selectively inhibit MDR1 in other experiments.

Interestingly Ko143 was more effective in the mouse Bcrp1-MDCKII cells than the human BCRP-MDCKII cells (Figure 3.11C), increasing Hoechst 33342 dye retention with an IC_{50} value of 0.15 ± 0.06 µM, a sub micro molar value similar to that previously reported (Allen *et al.*, 2002).

Hoechst 33342 accumulation was then used to assess the functional differences between ABC transporter expression in the different MDCKII cell models and Caco-2 cells (Figure 3.12). In native MDCKII cells Hoechst 33342 retention was significantly increased by 1μM CsA (Figure 3.12A), by 3.1 fold. In contrast no effect was seen with 0.8μM Ko143 treatment. This is consistent with MDR1-like native ABC expression and the absence of BCRP in MDCKII cells. The human BCRP transfected MDCKII cells gave a completely different pattern; unlike the native MDCKII cells no significant effect of CsA was seen in the hBCRP-MDCKII cells whilst Ko143 had a dramatic effect increasing Hoechst 33342 retention by 4.3 fold (Figure 3.12B). This shows that human BCRP is functional in the hBCRP-MDCKII cells and though CsA is effective at inhibition of the native ABC transporter, hBCRP action compensates for its loss. Clearly CsA does not inhibit BCRP at 1μM. The same pattern was seen in the murine Bcrp1-MDCKII with no effect of CsA but an even greater increase in Hoechst 33342 retention to 5.5 fold with Ko143 (Figure 3.12C). For MDR1-MDCKII cells, a 3.4 fold increase in Hoechst 33342 retention was seen with CsA compared with the 3.1 fold increase seen in the native cells (Figure 3.12D). Ko143 had no effect in the MDR1-MDCKII cells confirming that Ko143 (1μM) had no effect on MDR1 in this assay.

The two Caco-2 cell strains were also characterised using the Hoechst 33342 retention assay. Figure 3.12E shows a significant effect of 1μM CsA on Hoechst 33342 retention, increasing Hoechst 33342 fluorescence by 2.8 fold, consistent with an MDR1 component in the high passage Caco-2 cell strain. The absence of Ko143 action on Hoechst 33342 retention shows that there is no functional BCRP activity in the high passage Caco-2 cells. The low passage Caco-2 cell strain shown in Figure 3.12F whilst showing a 2.3 fold increase in fluorescence with CsA, showed a 2.52

fold increase in fluorescence with the selective BCRP agent Ko143. This is consistent with both functional MDR1 and BCRP expression responsible for Hoechst 33342 transport in the low passage Caco-2 cell strain.

Other epithelial cell culture models were characterised using the Hoechst 33342 retention assay to identify cell-lines showing an hBCRP/mBcrp functional component. Figure 3.13A shows a significant 2.6 fold increase in Hoechst 33342 retention with 1μM CsA in the mouse cortical collecting duct principal cell line (mpkCCDc14). A significant 2.3 fold increase in fluorescence with 1μM Ko143 demonstrated a BCRP mediated transport of Hoechst 33342. The mouse distal convoluted tubule cells (mpkDCT) gave a similar pattern of fluorescence retention to that observed with the mpkCCDc14 cells, showing a 1.6 and 1.9 fold increase in fluorescence with CsA and Ko143 respectively. Finally, the human breast cancer cell line MCF-10a, showed a 1.6 and 1.4 fold increase in fluorescence with CsA and Ko143 respectively, again confirming that this cell model could be utilised to further our understanding of BCRP in different tissue types. The MCF cell lines exposed to cytotoxics, such as MTX, have been shown previously to hyper-express BCRP (Robey *et al.*, 2001).

3.3.4 Screening for BCRP substrates using Hoechst 33342 in MDCKII cells

The utility of the Hoechst 33342 retention assay with a high throughput 96-well format was tested to identify substrates or inhibitors of BCRP. In addition, data were compared to native cells and to MDR1-MDCKII cells to identify interaction with the ABC transporter native to MDCKII cells and to identify potential bi-substrates of BCRP/MDR1. All MDCKII cell lines were screened with the same compounds, shown in Table 3.1.

In the native MDCKII cells several compounds increased Hoechst 33342 retention (Figure 3.14A). 1μM Ko143 had no significant effect on accumulation as noted above, however with an increased concentration of 10μM Ko143 a significant increase in Hoechst 33342 retention of 1.36 fold from the control MDCKII cells was observed ($n = 8$ wells, $P < 0.05$). Significant changes were also seen with nitrofurantoin, novobiocin, prazosin, quinidine, risperidone and verapamil. These changes indicate that these compounds are acting as either competitive substrates or non-competitive inhibitors of an endogenous component in native MDCKII cells.

The human BCRP-MDCKII cells showed a more profound effect with the different compounds (Figure 3.14B). All compounds had a significant effect of increasing fluorescence apart from 10μM nitrofurantoin and 10μM risperidone ($n = 8$ wells, $P < 0.05$). The anti-psychotic drug risperidone has been shown to be a BCRP inhibitor with an IC_{50} of 38.1μM in the BCRP over-expressing MCF-7 cell line (Wang *et al.*, 2008b), yet no significant inhibition was seen in this study. This result most likely reflects the multiple binding sites on BCRP whereby substrate access may be via the membrane or from the aqueous cytoplasm (Giri *et al.*, 2009); see Discussion. The greatest change in Hoechst 33342 retention was with Ko143, increasing retention by a 2.51 and 3.84 fold with a 1μM and 10μM dose respectively (Table 3.1).

For the mouse Bcrp1-MDCKII only Ko143, risperidone and verapamil increased Hoechst 33342 retention (Figure 3.14C). Ko143 increased fluorescence by 2.79 and 3.35 fold with a 1μM and 10μM concentration respectively, whilst 10μM risperidone and 100μM verapamil increased arbitrary fluorescence by 1.34 and 1.66 fold respectively (Table 3.1).

In contrast to hBCRP and mBcrp1-MDCKII cells Figure 3.13D shows the MDR1-MDCKII cells did not show an increase in Hoechst 33342 retention with 1µM Ko143. However with 10µM Ko143 fluorescence was significantly increased from 4.7 ± 0.07 to 7.27 ± 0.15 arbitrary units, a 1.54 fold increase (Table 3.1, n = 8 wells, $P < 0.05$). This data shows Ko143 used at 10µM concentration has an unspecific but minor inhibitory effect on MDR1. However, comparing data between cell lines (Table 3.1), it can be seen that 10µM Ko143 had only a marginal effect in the MDR1-MDCKII cells when compared to the increase seen in the human BCRP-MDCKII cells, indicating that even at 10µM Ko143 this agent is more selective to BCRP. Prazosin is a known MDR1 (Feng *et al.*, 2008; Polli *et al.*, 2001; Zhou *et al.*, 2009) substrate and has a significant effect on increasing Hoechst 33342 retention (Figure 3.14, n = 8 wells, $P < 0.05$). The known MDR1 substrate quinidine (Feng *et al.*, 2008; Polli *et al.*, 2001) dramatically increased fluorescence 2.46 fold from control values (Table 3.1). Risperidone has been shown to be a substrate of MDR1 (Feng *et al.*, 2008) and significantly increased fluorescence in this study (Figure 3.14, n = 8 wells, $P < 0.05$). However the greatest effect came from 100µM verapamil which increased fluorescence from 4.7 ± 0.07 to 12.91 ± 0.39 arbitrary units, a 2.74 fold increase (Table 3.1, n = 8 wells, $P < 0.05$). The effect of verapamil on human BCRP and mouse Bcrp at 100µM was minor compared to the dramatic effect seen in the MDR1-MDCKII. Verapamil is therefore selective for MDR1.

In summary, known inhibitors of BCRP (eg. Ko143) and MDR1 (quinidine and verapamil) can be differentiated by the Hoechst 33342 retention assay. However limitations relate to the relative affinity of competitive inhibitors with relation to Hoechst 33342 affinity and to the presence of an endogenous ABC transporter in MDCKII cells.

Figure 3.1. Expression of hBCRP mRNA in MDCKII and Caco-2 cells

(A) An agarose gel image showing PCR product of BCRP mRNA from hBCRP-MDCKII. Lane 1 shows the expected product size of approximately 289 base pairs for the reverse transcriptase positive sample, whilst lane 2 confirms no product in the reverse transcriptase negative sample. PCR product was confirmed by nucleotide sequencing by comparing to the published sequenced, giving 99% identity (see Materials and Methods section 2.2.3.4).

(B) Real time PCR analysis indicating expression of hBCRP mRNA in native MDCKII and human transfected BCRP-MDCKII. Data bars are adjusted relative to GAPDH expression. Quantification was performed using the Pfaffl method (bars represent mean of n = 3 extractions ± SD). Significant difference in hBCRP mRNA expression between native MDCKII and hBCRP-MDCKII cells denoted by * $P < 0.05$.

(C) Real time PCR analysis indicating expression of hBCRP mRNA in Caco-2 epithelia. Data bars are adjusted relative to GAPDH expression. Quantification was done via the Pfaffl method (bars represent mean of n = 3 extractions, ± SD). Significant difference in hBCRP mRNA expression between low and high passage Caco-2 cells denoted by * $P < 0.05$.

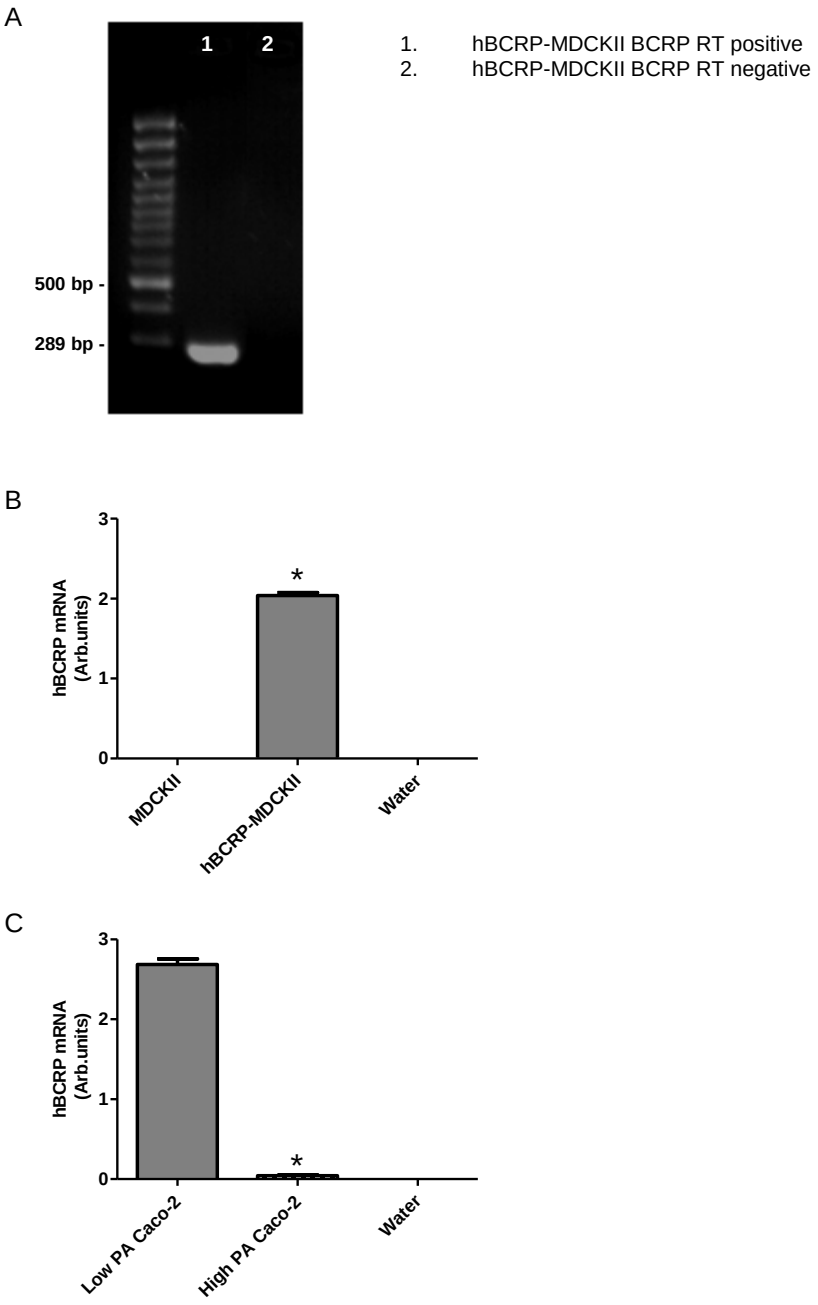

Figure 3.1. Expression of hBCRP mRNA in MDCKII and Caco-2 cells

Figure 3.2. Expression of mouse Bcrp mRNA in transfected MDCKII cells

(A) An agarose gel image showing PCR products from mBcrp1-MDCKII. Lane 1 shows the expected product size of approximately 100 base pairs for the reverse transcriptase positive sample, whilst lane 2 confirms no product in the reverse transcriptase negative sample. PCR product was confirmed by nucleotide sequencing by comparing to the published sequenced, giving 97% identity (see Materials and Methods section 2.2.3.4).

(B) Real time PCR analysis indicating expression of mBcrp mRNA in native and transfected MDCKII cells relative to GAPDH. Data bars are adjusted relative to GAPDH expression. Quantification was performed using the Pfaffl method (bars represent mean of n = 3 extractions, ± SD). Significant difference in mBcrp mRNA expression between native MDCKII and mBcrp-MDCKII cells denoted by * $P < 0.05$.

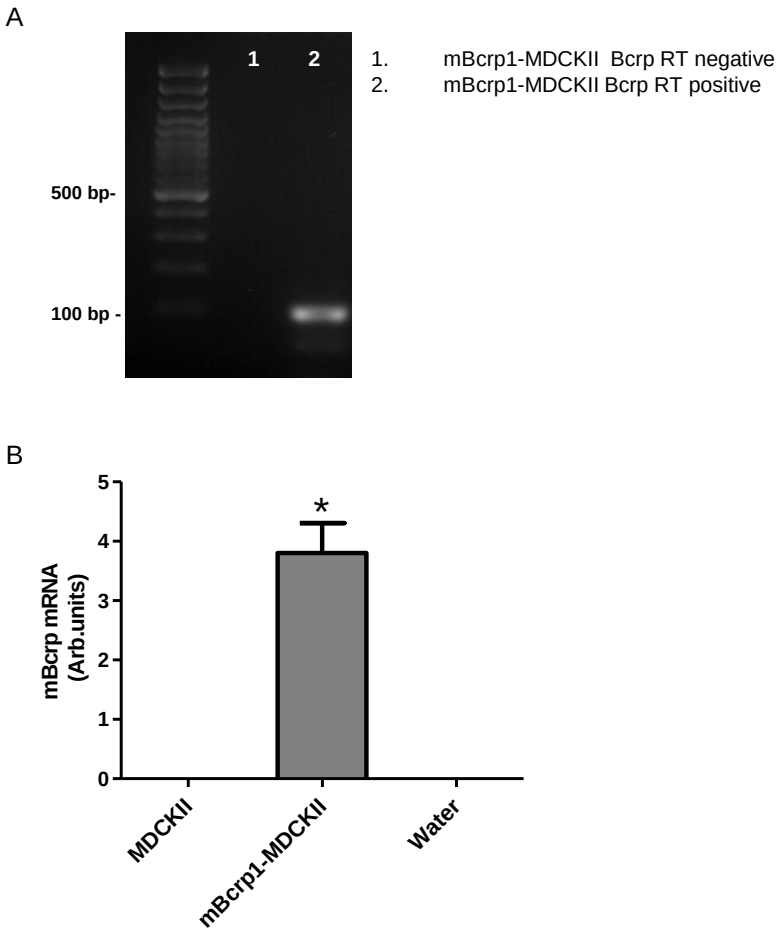

Figure 3.2. Expression of mouse Bcrp mRNA in transfected MDCKII cells

Figure 3.3. Western Blot analysis of BCRP protein expression in epithelial cell models

Images (A) and (B) show BCRP protein and α-tubulin expression respectively. Lane 1 is native MDCKII cell protein (10µg loaded), lane 2 is human BCRP-MDCKII cell protein (10µg loaded), lane 3 is mouse Bcrp1-MDCKII cell protein (5µg loaded), lane 4 is low PA Caco-2 cell protein (40µg loaded) and lane 5 is high PA Caco-2 cell protein (40µg loaded).

(A) Membrane was probed initially with rat-monoclonal anti-mouse Bcrp antibody BXP-9 (Kamiya) at a dilution of 1 in 50 for (samples 1, 2, 4 and 5), whilst the dilution of 1 in 500 was used for sample 3. This image is representative of one gel and shows were the membrane was cut and treated separately (lane 3). BCRP yields bands at approximately 72kDa and 100kDa.

(B) Image shows the membrane from part A stripped and re-probed with a cross species polyclonal anti-α-tubulin antibody (Abcam). The α-tubulin band was visible at approximately 50kDa.

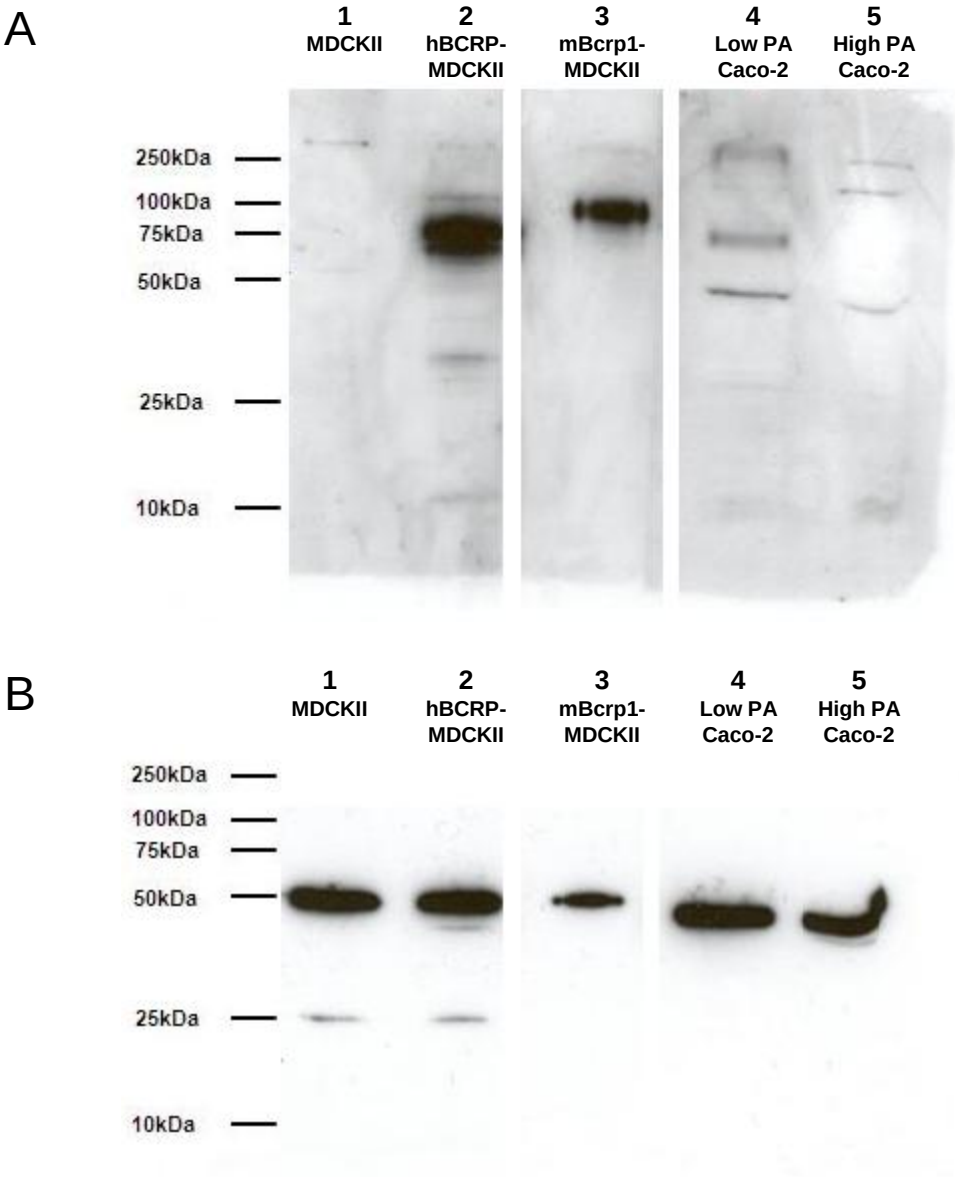

Figure 3.3. Western Blot analysis of BCRP protein expression in epithelial cell models

Figure 3.4. Western Blot analysis of deglycosylated mouse Bcrp protein

Mouse Bcrp is predicted to be glycosylated at two sites within close proximity (Asn596 and Asn600). This image shows (A) Mouse Bcrp1-MDCKII protein lysate treated with the deglycosylating enzyme PNGase F (5µg protein loaded) and (B) Untreated mBcrp1-MDCKII cells (5µg protein loaded). Gel was probed initially with rat-monoclonal anti-mouse Bcrp antibody BXP-9 (Kamiya) at a dilution of 1 in 500. PNGase F treated mBcrp1-MDCKII yields a band of smaller molecular weight (approximately 72kDa) compared with the untreated sample (approximately 100KDa). This Western blot image shown is one gel.

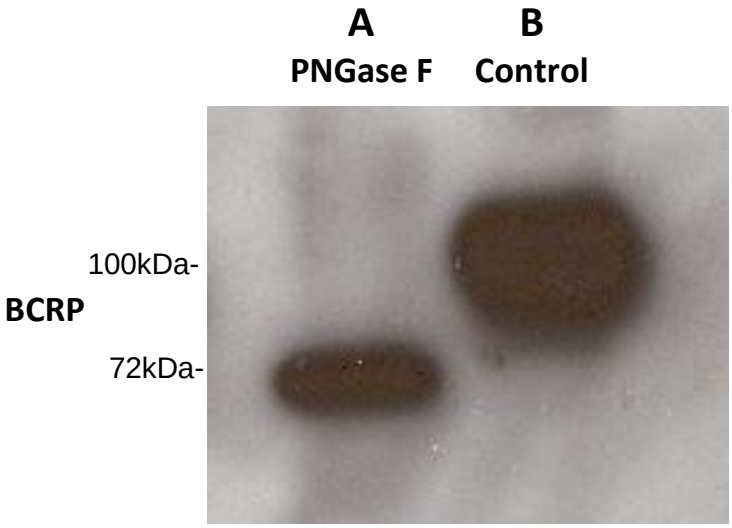

Figure 3.4. Western Blot analysis of deglycosylated mouse Bcrp protein

Figure 3.5. Immunocytochemical detection of BCRP in (A) Native MDCKII, (B) hBCRP-MDCKII and (C) mBcrp1-MDCKII epithelial cell monolayers

Images (A), (B) and (C) display indirect fluorescence staining of (A) Native MDCKII, (B) hBCRP-MDCKII and (C) mBcrp1-MDCKII epithelial cell monolayers with the rat monoclonal primary (1°) antibody BXP-53 directed against human/mouse BCRP (shown in green). Cell nuclei were counterstained with propidium iodide (shown in red). No positive staining with the BXP 53 1° is shown for native MDCKII (A), whilst positive staining with the BXP 53 1° is shown for hBCRP-MDCKII (B) and mBcrp1-MDCKII (C). Negative controls (no BXP 53 1°) are shown alongside the positive staining for native MDCKII (A), hBCRP-MDCKII (B) and mBcrp1-MDCKII (C). Images were viewed using confocal laser scanning microscopy. XY sections were imaged at the apical pole of the cell, XZ images confirm the apical expression (XZ-B_1C). Scale bars = 20µm.

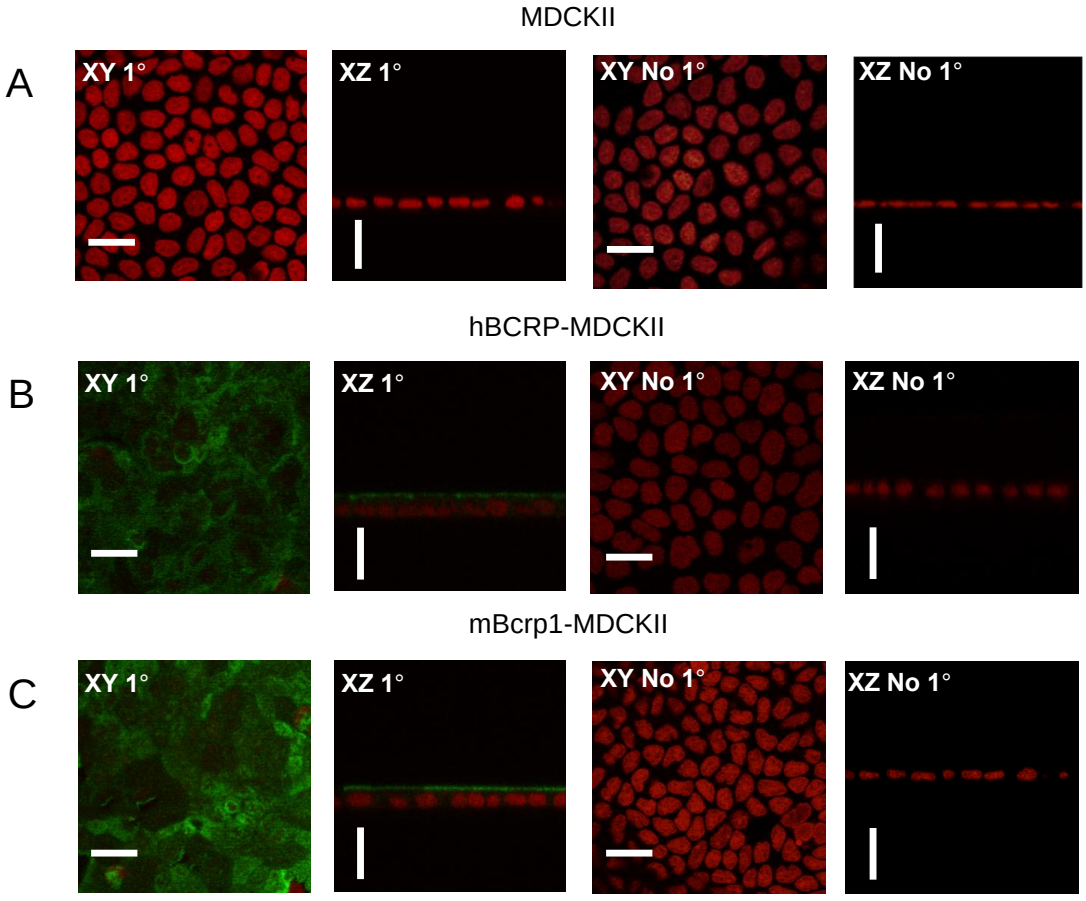

Figure 3.5. Immunocytochemical detection of BCRP in (A) Native MDCKII, (B) hBCRP-MDCKII and (C) mBcrp1-MDCKII epithelial cell monolayers

Figure 3.6. Immunocytochemical detection of BCRP in low passage Caco-2 epithelial cell monolayers

Images display indirect fluorescence staining of the low passage (PA) Caco-2 epithelial cell monolayers with the mouse monoclonal primary (1°) antibody BXP-21 directed against human BCRP (shown in green). Cell nuclei were counterstained with propidium iodide (shown in red). Negative controls (no BXP 21 1°) are displayed alongside the positive staining for XY and XZ sections. Images were viewed using confocal laser scanning microscopy. XY sections were imaged at the apical pole of the cell. XZ images confirm the apical expression (XZ-B_1C). Scale bars = 20μm.

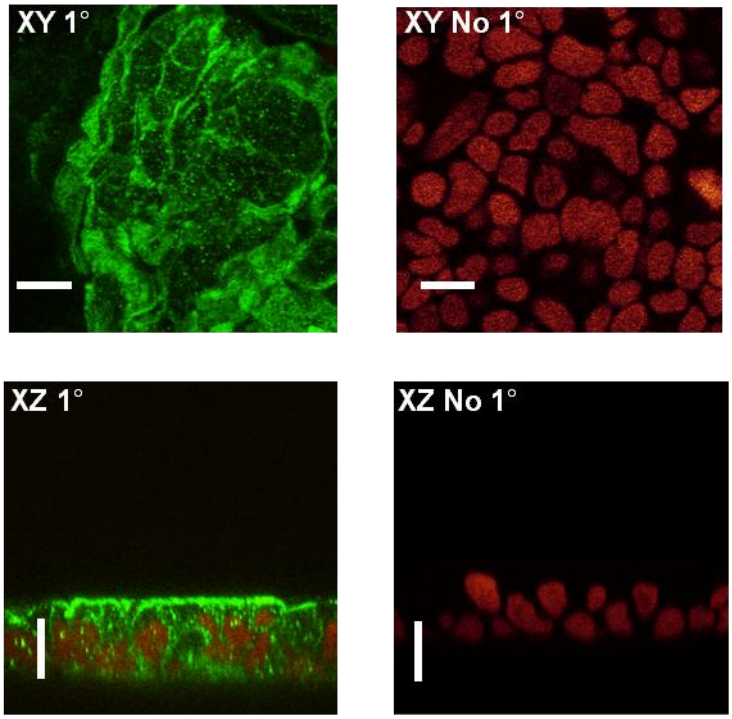

Figure 3.6. Immunocytochemical detection of BCRP in low passage Caco-2 epithelial cell monolayers

Figure 3.7. Effect of incubation time on Hoechst 33342 dye retention in native MDCKII cells

Effect of incubation time (0 to 90 minutes) on Hoechst 33342 retention in native MDCKII cells ± Cyclosporin A (10µM). Cells were incubated in 3µM Hoechst. Data points are means of n = 7 wells, ± SEM. * $P < 0.05$, are significantly different from control values.

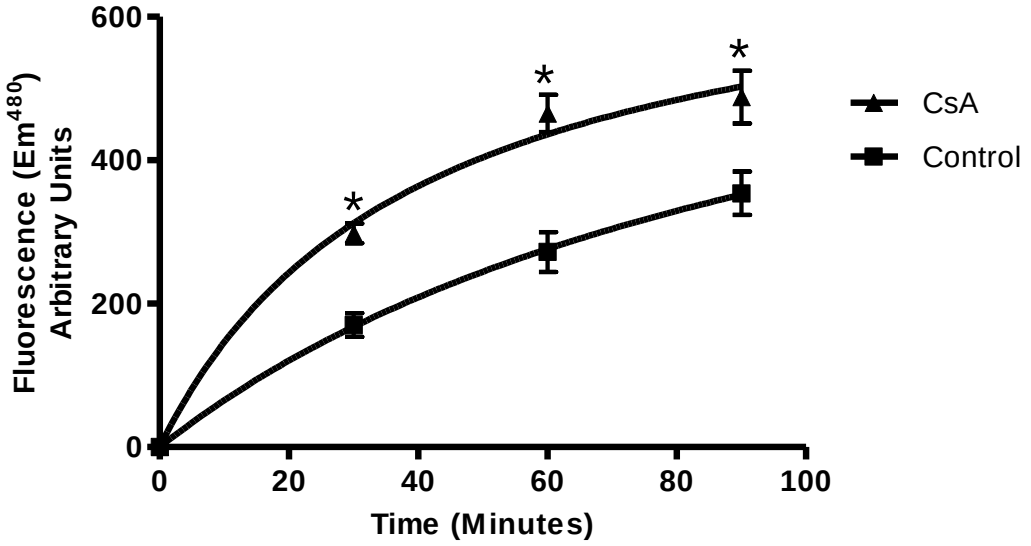

Figure 3.7. Effect of incubation time on Hoechst 33342 dye retention in native MDCKII cells

Figure 3.8. Effect of seeding density on Hoechst 33342 dye retention in native MDCKII cells

Effect of seeding density on Hoechst 33342 retention in MDCKII cells ± Cyclosporin A (10μM). Cells were incubated in 3μM Hoechst. Data points are means of n = 4 wells, ± SEM. * $P < 0.05$, are significantly different from control values.

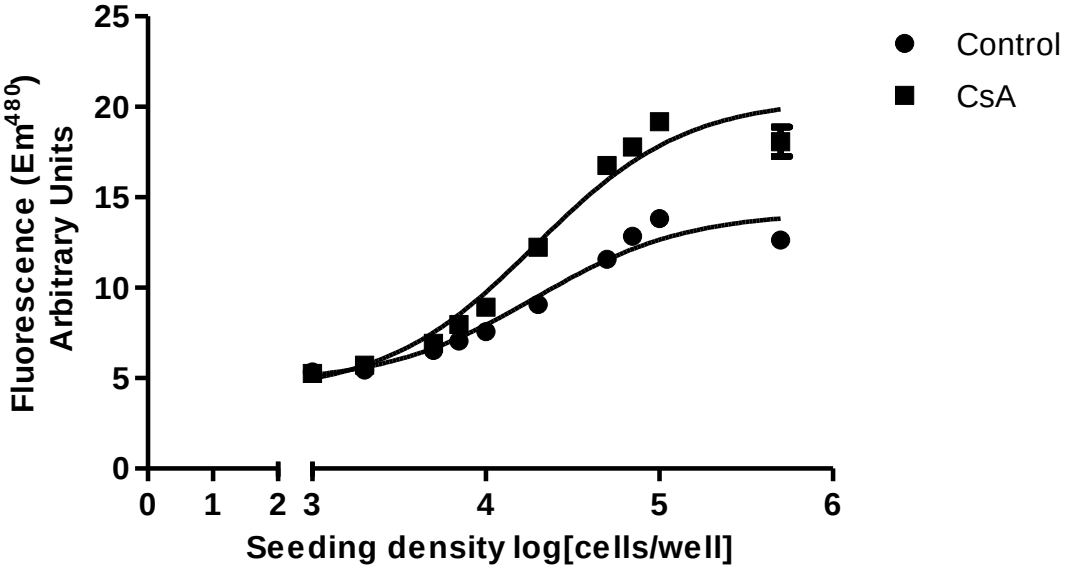

Figure 3.8. Effect of seeding density on Hoechst 33342 dye retention in native MDCKII cells

Figure 3.9. Effect of increasing extracellular Hoechst 33342 on cellular dye retention in native MDCKII cells

(A) Effect of increasing extracellular Hoechst 33342 dye on cellular retention in native MDCKII ± Cyclosporin A (10µM). Circles = control MDCKII cells and filled squares = CsA treated MDCKII cells. Solid lines represent Michaelis-Menten fit of the data. Native control; K_m = 35.5 ± 5.4 µM, V_{max} = 890 ± 85.1 (arb. units) and R^2 = 0.98. CsA treated MDCKII; K_m = 5.7 ± 0.9 µM, V_{max} = 664.5 ± 33.6 (arb. units) and R^2 = 0.97. Data points are means of n = 4 wells, ± SEM.

(B) CsA sensitive component of Hoechst 33342 fluorescence with increasing concentration. Solid lines represent Michaelis-Menten fit of the data; K_m = 0.3 ± 0.2 µM, V_{max} = 198.4 ± 12.8 (arb. units) and R^2 = 0.84. Data points are means of n = 4 wells, ± SEM.

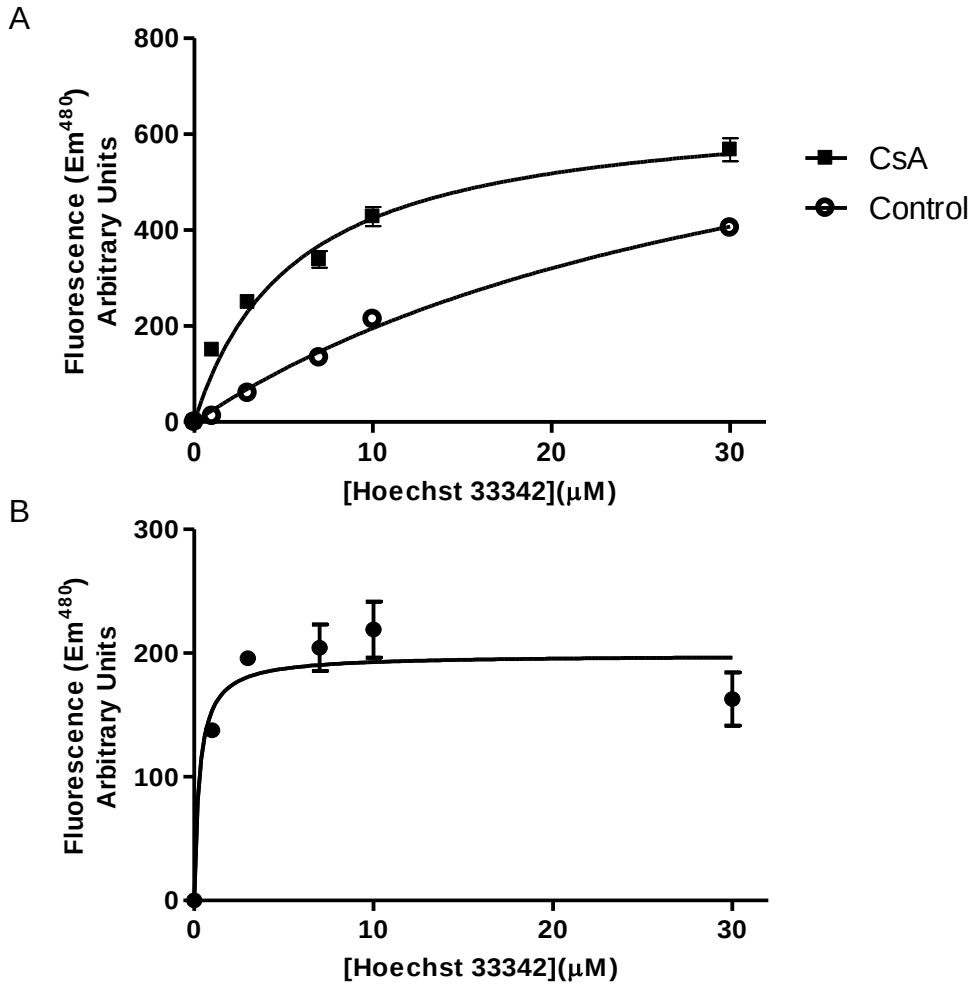

Figure 3.9. Effect of increasing extracellular Hoechst 33342 on cellular dye retention in native MDCKII cells

Figure 3.10. Relationship between Hoeschst 33342 concentration and intracellular Hoeschst 33342 accumulation in human BCRP-transfected MDCKII cells

(A) Effect of increasing extracellular Hoechst 33342 dye on cellular retention in native MDCKII and human transfected MDCKII cells. Solid lines represent Michaelis-Menten fit of the data. Data points are means of n = 4 wells, ± SEM.

(B) Effect of transfection of human BCRP protein in MDCKII cells on Hoechst 33342 dye retention with increasing extracellular Hoechst 33342 concentration. Data points were deduced from subtracting hBCRP-MDCKII Hoechst 33342 retention from native MDCKII values. Solid line represent Michaelis-Menten fit of the data; K_m =10.3 ± 2.6µM, V_{max} = 962.9 ± 92 (arb. units) and R^2 = 0.85. Data points are means of n = 4 wells, ± SEM.

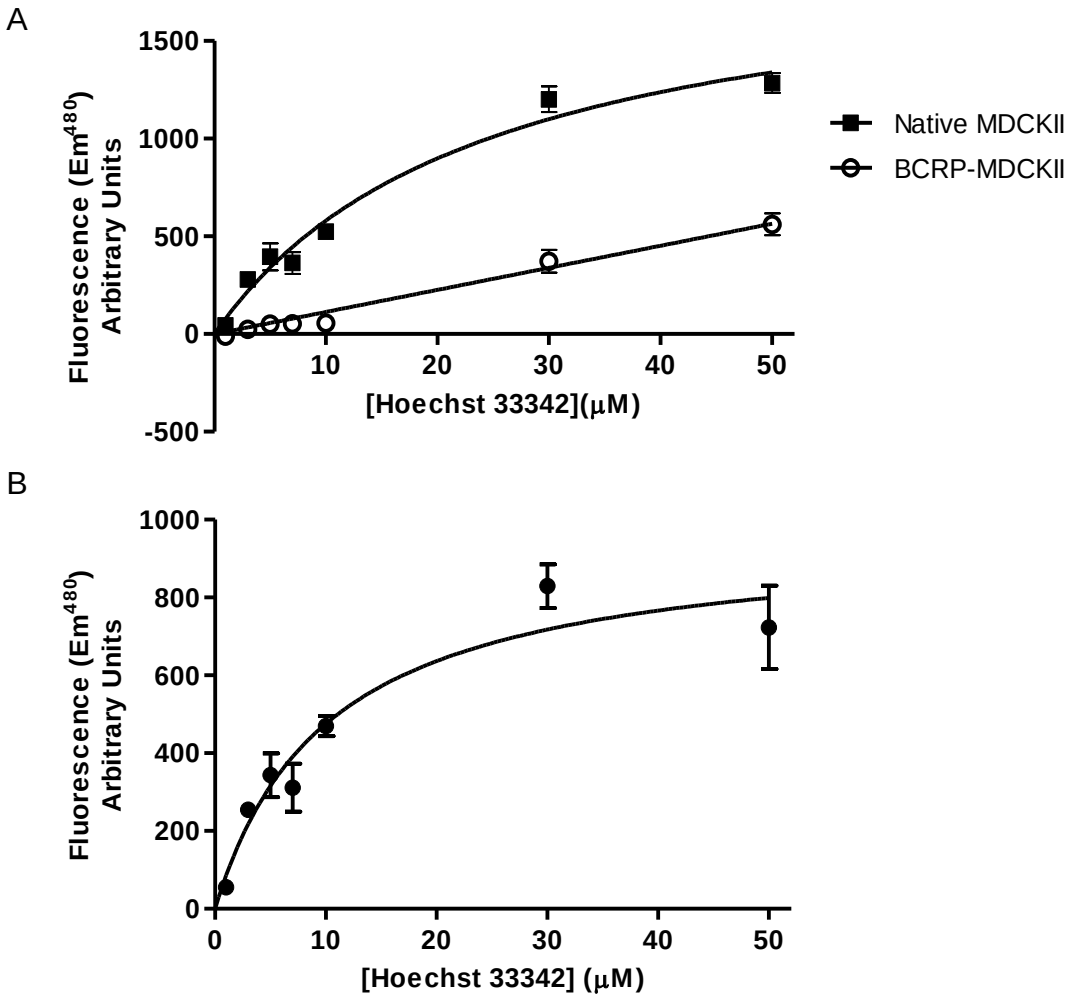

Figure 3.10. Relationship between Hoeschst 33342 concentration and intracellular Hoeschst 33342 accumulation in human BCRP-transfected MDCKII cells

Figure 3.11. Concentration dependent effect of known ABC transporter inhibitors on cellular Hoechst 33342 dye retention in transfected MDCKII cells

(A) Effect of increasing extracellular Ko143 on cellular Hoechst 33342 dye accumulation in human BCRP transfected MDCKII cells. Cells were incubated in 3µM Hoechst. Solid lines represent best-fit lines for Michaelis-Menten kinetics. Data points are means of n = 6 wells, ± SEM. IC_{50} = 1.06 ± 1.58 µM.

(B) Effect of increasing extracellular CsA on cellular Hoechst 33342 dye accumulation in human BCRP transfected MDCKII cells. Cells were incubated in 3µM Hoechst. Solid lines represent best-fit lines for Michaelis-Menten kinetics. Data points are means of n = 6 wells, ± SEM. IC_{50} = 1.17 ± 1.12 µM.

(C) Effect of increasing extracellular Ko143 on cellular Hoechst 33342 dye accumulation in mouse Bcrp transfected MDCKII cells. Cells were incubated in 3µM Hoechst. Solid lines represent best-fit lines for Michaelis-Menten kinetics. Data points are means of n = 6 wells, ± SEM. IC_{50} = 0.15 ± 0.06 µM.

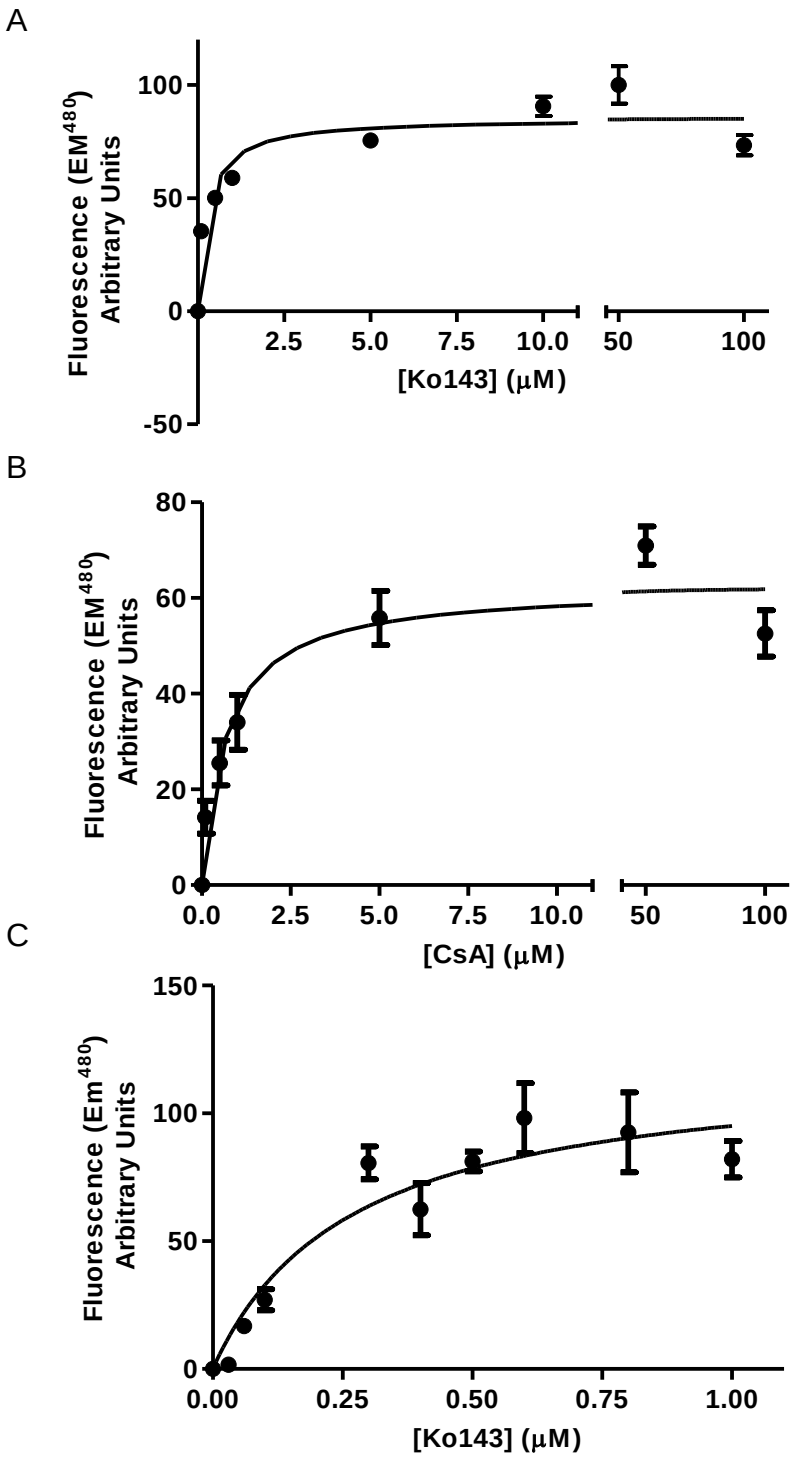

Figure 3.11. Concentration dependent effect of known ABC transporter inhibitors on cellular Hoechst 33342 dye retention in transfected MDCKII cells

Figure 3.12. Assessment of functional ABC-transporter activity in MDCKII and Caco-2 cell-lines using Hoechst 33342 dye retention

Figures (A)-(F) display Hoechst 33342 retention in (A) native MDCKII, (B) human BCRP-MDCKII, (C) mouse Bcrp1-MDCKII, (D) MDR1-MDCKII, (E) high PA Caco-2 and (F) low PA Caco-2 cell strains. Hoechst 33342 retention was assessed in the presence or absence of 1µM CsA (cross-hatched bars), 0.8µM Ko143 (black solid bars) and control bars (unfilled bars). Data bars are means of n = 12 wells, data pooled and normalised from 3 independent experiments ± SEM. * $P < 0.05$, are significantly different from control values.

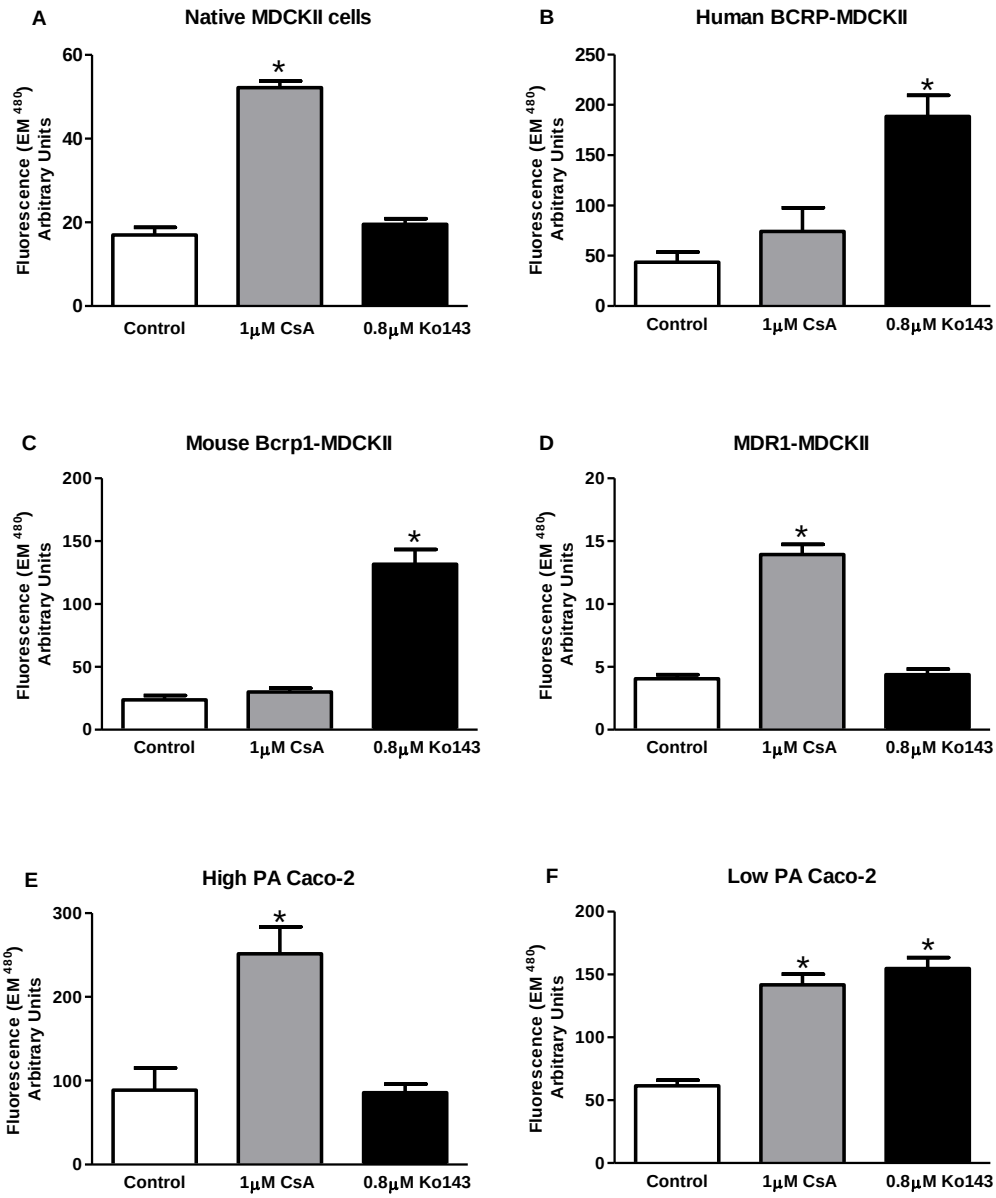

Figure 3.12. Assessment of functional ABC-transporter activity in MDCKII and Caco-2 cell-lines using Hoechst 33342 dye retention

Figure 3.13. Assessment of functional ABC-transporter activity in diverse cell-lines using Hoechst 33342 dye retention

Figures (A)-(C) display Hoechst 33342 retention in (A) MPK CCD, (B) MPK DCT and (C) MCF-10 cells. Hoechst retention was assessed in the presence or absence of 1μM CsA (cross-hatched bars) and 1μM Ko143 (black solid bars), control bars (unfilled bars). Data bars are means of n = 12 wells, data pooled and normalised from 3 independent experiments ± SEM. * $P < 0.05$, are significantly different from control values.

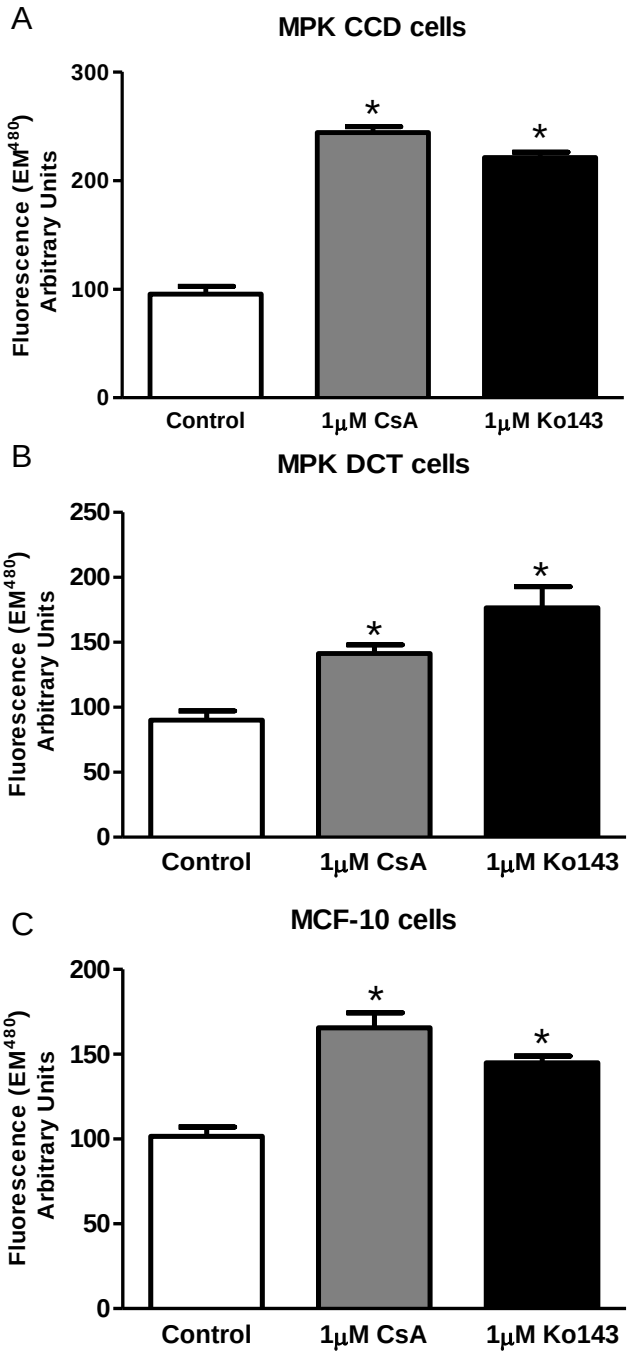

Figure 3.13. Assessment of functional ABC-transporter activity in diverse cell-lines using Hoechst 33342 dye retention

Figure 3.14. Identification of potential BCRP substrates using Hoechst 33342 across A) native MDCKII, B) hBCRP-MDCKII, C) mBcrp1-MDCKII and D) MDR1-MDCKII cells

Figure shows the effect of selected compounds on Hoechst 33342 retention in 96-well plates of (A) MDCKII cells, (B) hBCRP-MDCKII cells, (C) mBcrp1-MDCKII and (D) MDR1-MDCKII cells. All compounds were used at 10µM, Ko143 was used at both 1 and 10µM and verapamil at 100µM. Hoechst 33342 was used at 3µM. Data bars are means of n = 8 wells, data are representative of 2 individual experiments ± SEM. * $P < 0.05$, are significantly different from control (DMSO) values.

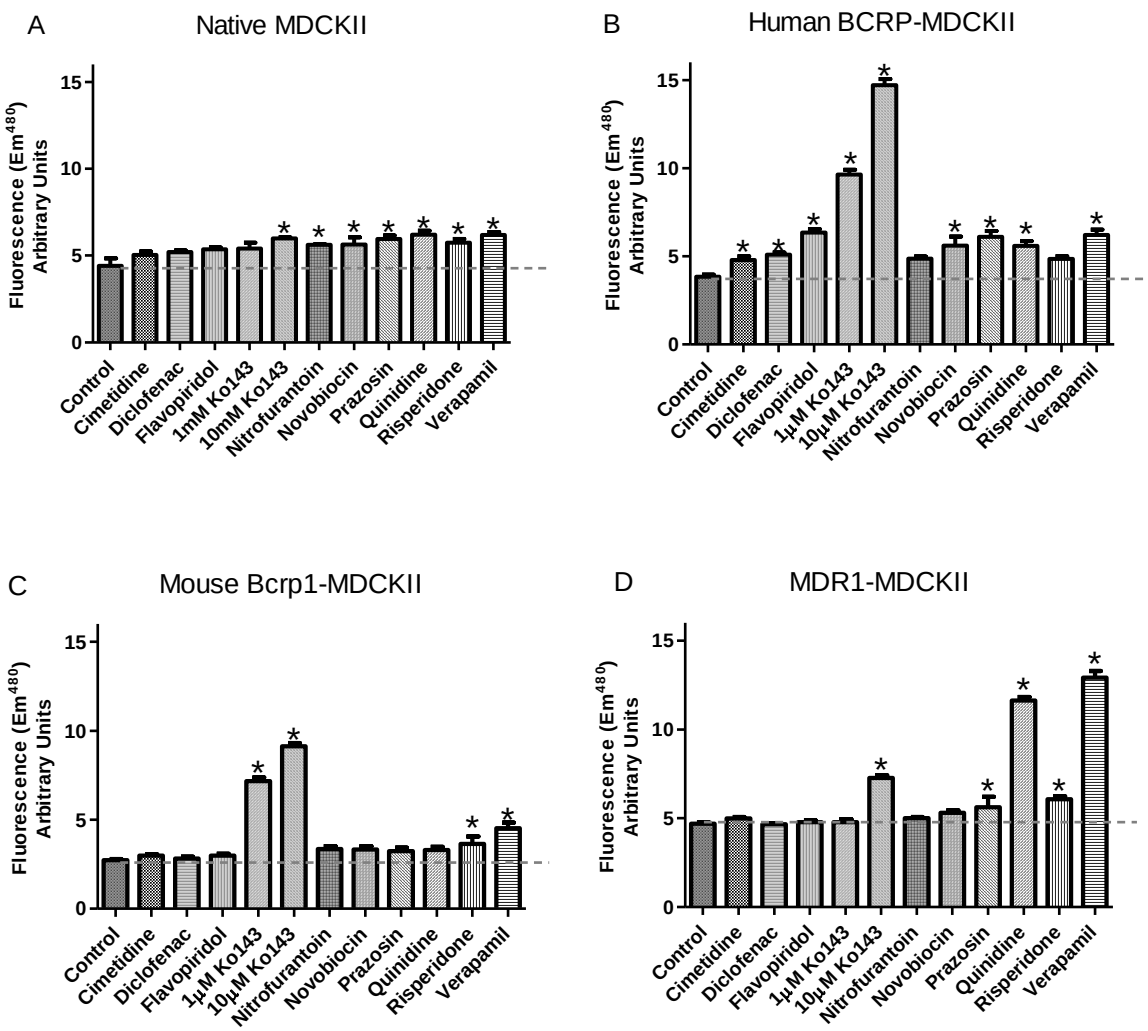

Figure 3.14. Identification of potential BCRP substrates using Hoechst 33342 across A) native MDCKII, B) hBCRP-MDCKII, C) mBcrp1-MDCKII and D) MDR1-MDCKII cells

Table 3.1. Identification of potential BCRP substrates using Hoechst 33342 retention in (A) MDCKII cells, (B) hBCRP-MDCKII cells, (C) mBcrp1-MDCKII and (D) MDR1-MDCKII

Figure shows the effect of select compounds on Hoechst 33342 retention in 96-well plates of (A) MDCKII cells, (B) hBCRP-MDCKII cells, (C) mBcrp1-MDCKII and (D) MDR1-MDCKII cells. All compounds were used at 10µM, Ko143 was used at both 1 and 10µM and verapamil at 100µM. Hoechst 33342 was used at 3µM. Data bars are means of n = 8 wells, data are representative of 2 individual experiments ± SEM. * $P < 0.05$, are significantly different from native MDCKII values.

	Native MDCKII	hBCRP-MDCKII	mBcrp1-MDCKII	MDR1-MDCKII
DMSO	4.41 ± 0.44	3.83 ± 0.13*	2.72 ± 0.07*	4.7 ± 0.07
Cimetidine	5.03 ± 0.2	4.79 ± 0.21	2.99 ± 0.08*	4.99 ± 0.09
Diclofenac	5.21 ± 0.09	5.1 ± 0.1	2.82 ± 0.1*	4.67 ± 0.06*
Flavopiridol	5.37 ± 0.11	6.34 ± 0.2*	2.99 ± 0.1*	4.79 ± 0.09*
1µM Ko143	5.4 ± 0.35	9.63 ± 0.29*	7.16 ± 0.21*	4.79 ± 0.16
10µM Ko143	5.99 ± 0.07	14.72 ± 0.34*	9.13 ± 0.18*	7.27 ± 0.15*
Nitrofurantoin	5.62 ± 0.06	4.87 ± 0.13*	3.36 ± 0.16*	5 ± 0.07*
Novobiocin	5.63 ± 0.43	5.61 ± 0.52	3.33 ± 0.18*	5.32 ± 0.13
Prazosin	5.95 ± 0.2	6.1 ± 0.33	3.24 ± 0.19*	5.63 ± 0.59
Quinidine	6.2 ± 0.23	5.6 ± 0.26	3.3 ± 0.18*	11.6 ± 0.19*
Risperidone	5.74 ± 0.23	4.85 ± 0.15	3.65 ± 0.41*	6.08 ± 0.15
Verapamil	6.19 ± 0.16	6.21 ± 0.3	4.53 ± 0.33	12.91 ± 0.39*

3.4 Discussion

The primary aim of this chapter was to characterize available model systems (eg. MDCKII cells transfected with hBCRP/mBcrp) in relation to the stability and extent of BCRP expression and to establish a functional assay of BCRP to allow substrate/inhibitor specificity to be defined. Since data on the expression of BCRP in the human intestinal Caco-2 cultured line have been ambiguous (Sambuy *et al.*, 2005), BCRP expression and activity was determined in 2 separate strains of these cells to assess BCRP within an appropriate cellular context and as a prerequisite to the use of Caco-2 epithelia for transepithelial transport (Chapters 4 and 5) and as a suitable model to measure regulation of transport activity (Chapter 6).

It was confirmed that both MDCKII transfected cell lines express mRNA and protein of hBCRP/mBcrp whereas native MDCKII cells were negative. HBCRP/mBcrp was expressed at the apical membrane of these epithelial cells and no immunostaining was visible in the native MDCKII cells. The antibodies BXP-9 and BXP-53 used for immunoblotting and immunocytochemistry respectively were raised against an internal protein epitope that was similar between human, mouse and dog. The protein sequence alignment shown in the results indicates that both antibodies are likely to recognise dog protein, as is the case for the human and mouse BCRP protein (although this needs to be confirmed with a positive control). Therefore as no expression was seen with either technique it may be concluded that canine BCRP is not expressed in wild-type MDCKII cells.

Protein immunoblotting with BXP-9 pointed to varied levels of glycosylation in BCRP and Bcrp cDNA transfected MDCKII cells. Glycosylation was minimal in the hBCRP-MDCKII cells compared with mouse Bcrp1-MDCKII cells which revealed a strong band at the higher molecular size of 100kDa which was reduced to

the core protein size of ~72kDa after digestion with PNGase F. The apparent difference in glycosylation revealed by immunoblotting with BXP-9 agrees with what is predicted in the literature (Allen & Schinkel, 2002), showing the mouse Bcrp protein contains additional sites for glycosylation than that of the human protein. This difference in tertiary protein structure may give rise to a difference in transport characteristics between hBCRP-MDCKII cells and mBcrp1-MDCKII cells as the environment of the external facing binding site may be altered with greater glycosylation.

The existence of different Caco-2 cell strains with varied phenotype has been recognized for some years (Sambuy *et al.*, 2005). In the present work it was found that Caco-2 cells which had been cultured for many passages in Newcastle did not express BCRP at neither the mRNA nor protein level. A lower passage strain from AstraZeneca laboratories clearly showed expression at both the RNA and protein level.

Notwithstanding evidence of BCRP expression in Caco-2 cells, the immunoblot in Figure 3.3 shows there is a visible difference in the amount of BCRP protein between the low passage Caco-2 cells and the over-expressing hBCRP-MDCKII cells. This difference in expression may not result in differing levels of substrate flux compared to hBCRP-MDCKII cells if substrate availability is limited by access to the cytosol (e.g. across the basolateral membrane) or from the membrane phase. Nonetheless, the fact that expression appears relatively low in the Caco-2 cells may be an advantage in studies of up-regulation of BCRP where any difference may be more evident from a lower basal level.

After confirming expression of BCRP at the mRNA and protein level in the cell model systems the cell lines were characterised functionally using the

hBCRP/mBcrp substrate Hoechst 33342 (Kim *et al.*, 2002; Zhou *et al.*, 2001). Hoechst 33342 is a substrate that can be easily measured by fluorescence and scaled up to a high through-put assay format at a relatively low cost compared with counterpart assays, such as transepithelial flux and Ussing chamber techniques. However the main problem with Hoechst 33342 is that it is a known substrate of both BCRP and MDR1 (Bunting *et al.*, 1999; Kim *et al.*, 2002; Zhou *et al.*, 2001), given the existence of an endogenous secretory capacity in wild-type MDCKII cells, characterization with selective pharmacological inhibitors to BCRP and MDR1 is essential.

In this study both hBCRP-MDCKII and mBcrp1-MDCKII significantly differed in the retention of Hoechst 33342 compared with the native MDCKII cells in response to Ko143 and verapamil (Figure 3.12). These data confirmed that both human BCRP-MDCKII and mouse Bcrp1-MDCKII express a functionally active transporter not seen in native MDCKII cells.

The endogenous secretory component in the MDCKII cells is inhibited by 1μM CsA. Native MDCKII epithelial layers have been reported previously to secrete the MDR1 substrates digoxin and verapamil (Haslam *et al.*, 2008; Lowes *et al.*, 2003). In this study the effects of CsA were similar to that seen in the MDR1-MDCKII cells, which taken together leads to the conclusion that the endogenous component is MDR1. No effect of 1μM CsA on the endogenous component is seen in the hBCRP/mBcrp transfected cells. Here the lack of CsA effect likely results from the low concentration of CsA used and the compensatory capacity of the transfected hBCRP/mBcrp to transport Hoechst 33342 instead of MDR1. Used at higher concentrations, CsA may inhibit hBCRP/mBcrp as well as the endogenous dog protein. The apparent IC_{50} of 1.17μM in the hBCRP-MDCKII cells represents both

MDR1 and BCRP inhibition (Ejendal & Hrycyna, 2005; Xia *et al.*, 2007a). In contrast 100μM verapamil shown in Figure 3.14 was relatively selective for MDR1 compared with BCRP.

Ko143 used at a low concentration (0.8-1μM) was shown to be a selective inhibitor for hBCRP/mBcrp with little to no effect on the native and MDR1-MDCKII cells. Data from this study are confirmatory to that shown by Mattson *et al.* (2007). At a higher concentration of 10μM the selectivity of Ko143 seems to slightly deteriorate in that there is a slight inhibition seen in MDR1-MDCKII cells on Hoechst 33342 accumulation. However given the affinity of Ko143 to BCRP, shown with the low IC_{50} values, this compound is a powerful tool that can be used to elucidate BCRP mediated secretion in a cell line with multiple transporter systems, such as the low passage Caco-2 cells.

Functional characterisation with Hoechst 33342 (using CsA and Ko143 as MDR1 and BCRP inhibitors respectively) show the low passage Caco-2 cells to have functional MDR1 and BCRP activities, whilst further showing the high passage Caco-2 cells to display only MDR1 function. These functional data are in agreement with the expression data (above).

The concentration-dependent kinetics of Hoechst 33342 retention changed when BCRP was introduced into the parental MDCKII cells; this allows a BCRP-dependent component to be identified with a K_m of 10.3 ± 2.6 μM. This compares with the concentration dependence of the CsA sensitive endogenous Hoechst 33342 retention (due to canine MDR1) of 0.3μM.

To identify a BCRP substrate using this assay a compound has to compete with Hoechst 33342 for the binding site on BCRP or MDR1, or act as a non-competitive inhibitor. The choice of ~3μM for the screening assay should allow all but

the lowest affinity substrates to be able to compete with Hoechst 33342 at the substrate binding site. However it should be noted that multiple binding sites on the BCRP protein may exist (Clark *et al.*, 2006; Hazai & Bikadi, 2008; Xia *et al.*, 2007b) and that Hoechst 33342 may access BCRP from the membrane interior. Therefore the physiochemical properties of the substrate will determine binding to BCRP and whether it will be identified as a substrate/inhibitor in this competitive assay. It is thought that Hoechst 33342 binds to one binding site on the BCRP protein (Clark *et al.*, 2006). The LogP value of Hoechst 33342 is 3.1 suggesting high lipophilicity. The data from this study show that in the hBCRP-MDCKII cells, nitrofurantoin does not affect Hoechst 33342 accumulation, yet nitrofurantoin is shown to be a BCRP substrate (Merino *et al.*, 2005). The LogP value of nitrofurantoin is -0.6. As these compounds are lipophilic and non-lipophilic respectively it is likely that they partition in the plasma membrane differently and bind to distinct binding sites on BCRP. The results from this study fit with the Mattson *et al.* (2007) publication that fails to show that nitrofurantoin increases mitoxantrone accumulation (Matsson *et al.*, 2007). Therefore, problems in BCRP substrate identification may arise when using a competitive assay such as Hoechst 33342 if the site and mode of transport within the BCRP protein differ. Even if this approach identifies a change in Hoechst 33342 accumulation with a compound, this assay alone cannot distinguish between a competitive inhibitor and non competitive inhibitor (Hegedus *et al.*, 2009). This is because it is not a direct measure of cellular transport across the apical surface. Therefore a more direct approach of measuring transport needs to be used.

Further limitations of the Hoechst 33342 assay may arise due to problems with cellular access and membrane leakage (Hegedus *et al.*, 2009). Compounds that gain cell entry through the basal membrane are unlikely identified as substrates/inhibitors

using this method. This is because in a confluent layer of cells access to the basal membrane is limited and thus compound entry is restricted. A way to circumvent this would be to use the cells before reaching maximum confluency to allow better access to the cells; however Figure 3.8 demonstrates that at lower cell seeding density inhibition is difficult to measure. Furthermore as there is no control of cellular integrity, increased passive permeability resulting from toxicity may account for loss of Hoechst 33342 dye.

In summary this chapter states MDCKII cells transfected with the hBCRP/mBcrp cDNA, as well as the low PA Caco-2 cells (AstraZeneca variant shown in this study), all look suitable epithelial cell lines to achieve the aims of this project. The Hoechst 33342 cellular retention assay is an effective method of determining BCRP and MDR1 function and identifying inhibitors of these transporters, however it does not look suitable as an assay for screening for BCRP substrates or understanding BCRP regulation due to the indirect measure of transport having several limitations. Measurement of compounds via bi-directional transport across confluent cell monolayers is a more direct and sensitive method.

4. Transepithelial transport mediated by BCRP

4.1 Introduction

It is now clear that the ABC family of efflux transporters plays a major role in limiting the oral bioavailability, whole body distribution, and subsequent excretion of both potential and novel pharmaceutical agents. The focus of the present thesis is to understand the scope of BCRP with respect to individual agents, but more importantly to understand how the operation of BCRP, within the intestine, acts to limit absorption from the gut lumen to the blood.

The data presented in Chapter 3 has introduced the use of MDCKII cells stably transfected with relevant ABC transporters to identify BCRP-mediated transport and also as a screen to identify compounds able to interact with BCRP (as inhibitors of Hoechst 33342 efflux). However, as already noted, Hoechst 33342 efflux only provides an indirect measure of BCRP function and may fail to distinguish between a competitive substrate and non-competitive inhibitor. Its use is also limited as a screen for novel substrates if the inhibitory potency of the compound being screened is low relative to Hoechst 33342 affinity for BCRP ($K_i > K_m$ for Hoechst 33342). The data presented in Chapter 3 clearly allow high-affinity inhibitors such as Ko143 to be identified, but other potential substrate actions are less clear. In order to overcome such limitations, a direct assay of the transport activity of BCRP is required with respect to potential substrates. Use of excised animal or human intestinal tissue is the gold standard when looking directly at transport of xenobiotics. However the expense and ethical issues point to a more suitable in vitro method of looking at transport, especially in the pharmaceutical industry where throughput of new chemical entities (NCEs) to be tested is high. Cell based in vitro techniques have been

developed and are used for measuring BCRP function; these techniques are fast, high throughput and relatively low cost. The most widely used assay in this respect is the Transwell based monolayer assay. This technique requires epithelial cells to be grown to confluency thereby forming “tight” epithelial layers in which apical tight-junctions are formed and separate brush-border (apical) and basolateral (basal) membrane domains delimit the transcellular pathway for absorption/secretion. The tight junctions form a separate route for passive solute permeation. These epithelial layers therefore simulate the complex transcellular and paracellular barriers that need to be overcome in vivo (Hegedus *et al.*, 2009) to attain oral absorption and therefore act as vital, physiologically appropriate tools in screening for xenobiotic transport. Transwell based assays consist of a porous polycarbonate membrane filter insert of varying size that fits directly into multiwell 6 to 96-well plates. Polarized cells are seeded directly onto the upper surface of the insert, adhere and then grow to confluency. The system has an apical and basolateral compartment representing lumen and interstitial/blood compartments found in vivo (shown in the Fig 2.1 of Materials and Methods).This simple geometry facilitates the investigation of transepithelial transcellular transport by the application of the compound of interest in either the apical or basolateral compartment as the donor compartment, with sampling in the opposite receiver compartment.

As outlined in Chapter 3, MDCKII and ABC-transfected cell-lines provide a suitable means to test directly for substrates of BCRP and other ABC transporters. Caco-2 cells, in contrast, relate such ABC-mediated transport to the context of the human intestine in which multiple ABC-transporters, often with overlapping specificity are expressed. The primary aim, therefore, is to use the parental MDCKII cells alongside the ABC transfected MDCKII cells to determine selective BCRP

substrates from a diverse selection of compounds all associated with BCRP transport from the literature. Screening for ABC-transporter substrates in this way has allowed many studies to identify ABC-transporter substrates and is used frequently in the pharmaceutical industry (Matsson *et al.*, 2007; Polli *et al.*, 2001).

The intestinal processing of such compounds will then be modelled by Caco-2 epithelial cell monolayers. The BCRP mediated fraction of transport may be assessed using selective pharmacological inhibition (Ebert *et al.*, 2007; Giacomini *et al.*, 2010; Lemos *et al.*, 2008). A secondary aim is the identification of a compound exclusively transported by BCRP so that the behaviour of this component can be determined directly in Caco-2 cell layers.

4.2 Methods

4.2.1 Cell culture

MDCKII and Caco-2 cells were cultured as previously described in Methods section 2.2.1.

4.2.2 Bi-directional transport across epithelial layers- 24 or 96-well filter plates

Bi-directional transport across 24-well and 96-well cell monolayers was performed essentially as described in Materials and Methods (Section 2.2.2.3). 96-well transport assays were performed automatically on the Hamilton StarPlus robot. Two robotic scripts were written for the Hamilton StarPlus robot. The first was used in the transport assay for compounds at a selected donor concentration of 10µM. The second robot script allowed the transport assay to be conducted over a range of concentrations in the presence or absence of a pharmacological inhibitor(s). Alternatively transport assays were performed manually in a 24-well format. Donor and receiver concentrations of all compounds were determined by HPLC-MS.

4.3 Results

4.3.1 Identification of BCRP substrates in ABC-transfected MDCKII monolayers

Native MDCKII cell lines together with those stably transfected with human BCRP, mouse Bcrp and human MDR1 were used to identify drug BCRP substrates. The 96-well Transwell format was used for determination of bi-directional flux of potential compounds using protocols implemented on the Hamilton Starplus robot allowing automated solution delivery, exchange and sampling. Initially 21 potential BCRP substrates were selected to include; cimetidine, clozapine, curcumin, diclofenac, estrone-3-sulphate, flavopiridol, gefitinib, methotrexate, mitoxantrone, nitrofurantoin, novobiocin, omeprazole, paclitaxel, pheophorbide A, prazosin, progesterone, quinidine, resveratrol, risperidone, sulphasalazine and zidovudine. However due to limited epithelial permeability and compound levels falling below the detection limit or failure of HPLC/ionisation to allow detection of appropriate m/z intensities, no data for curcumin, estrone-3-sulphate, methotrexate, mitoxantrone, omeprazole, paclitaxel, pheophorbide A, resveratrol, sulphasalazine and zidovudine were obtained. Appendix tables 1-4 summarise the transepithelial flux in the apical to basal direction (J_{a-b}), basal to apical direction (J_{b-a}) and net secretory flux ($J_{net} = J_{b-a} - J_{a-b}$) of those 11 compounds on which data were obtained (appendix tables representative of n = 2 experiments with 4-6 replicates per condition).

Diclofenac has been reported to be a BCRP substrate (Lagas *et al.*, 2009), Figure 4.1 illustrates the utility of native and transfected MDCKII cell layers in the identification of the mechanism of transport. Bi-directional flux across the native (Figure 4.1.A), human BCRP (Figure 4.1.B), mouse Bcrp (Figure 4.1.C) and human MDR1 (Figure 4.1.D) show that whereas no endogenous significant net secretion of

diclofenac across native MDCKII epithelial monolayers is observed, hBCRP-MDCKII, mBcrp1-MDCKII and MDR1-MDCKII cell monolayers all display a significant and elevated net secretory flux ($P < 0.05$, Figure 4.1 E, Table 4.1). The net secretory flux of 132 ± 137 pmol.cm^{-2}.hr^{-1} for the parental cell line was increased to 678.8 ± 57 pmol.cm^{-2}.hr^{-1} for hBCRP transfected, 665.1 ± 37.2 pmol.cm^{-2}.hr^{-1} for mBcrp transfected and 625.6 ± 144.7 pmol.cm^{-2}.hr^{-1} for MDR1 transfected MDCKII cell layers ($n = 2$ experiments, $P < 0.05$). Therefore diclofenac is likely to be a substrate for mouse and human BCRP and for human MDR1 in agreement to the data of Lagas *et al.* (2008).

Table 4.1 summarises the absorptive permeabilities ($P_{a-b} = J_{a-b} / C_a$) of all compounds for which transport data were obtained. A major determinant of epithelial permeability is its lipophilicity. Correlations of partition coefficient (e.g. octanol/water, LogP) have shown a high correlation with % drug absorption in man (Zhao *et al.*, 2002). A high LogP value of 4.5 for diclofenac suggests that passive transcellular absorption across epithelial barriers would predominate and indeed the observed absorptive permeability for diclofenac in native MDCKII cells exceeds that seen for other compounds tested (Table 4.1). The operation of ABC transporters such as MDR1 is generally thought to limit the absorptive permeability (Hunter *et al.*, 1993). A reduction in the apical permeability is generally seen for mBcrp1-MDCKII whilst a modest reduction is generally seen for hBCRP-MDCKII cell layers; no reduction is seen for MDR1-MDCKII cell layers (Table 4.1).

Table 4.2 shows a summary of the net secretory flux for all 11 compounds optimised for HPLC-MS analysis in all four MDCKII cell lines (native, hBCRP-MDCKII, mBcrp1-MDCKII and MDR1-MDCKII). Bi-directional flux data displayed

in Table 4.2 was taken from Appendix Tables 1-4. Each compound may be defined to be either a substrate of hBCRP, mBcrp or MDR1.

Cimetidine is a known hBCRP, mBcrp substrate (Pavek *et al.*, 2005) and also an MDR1 substrate (Dahan & Amidon, 2009), yet only modest and non-significant increments in secretion were seen for mBcrp and hBCRP and MDR1-transfected MDCKII cell layers (Table 4.2). However the retention time for cimetidine in the HPLC system was atypical suggesting that quantification of this compound was in doubt.

Clozapine is an example of an anti-psychotic drug that has been reported to be a BCRP inhibitor (Wang *et al.*, 2008b). It was found not to be a substrate of hBCRP-MDCKII cells. However, it was shown to be a substrate of MDR1-MDCKII cells increasing net secretory flux from 176.3 ± 29.5 pmol.cm^{-2}.hr^{-1} across native MDCKII to 321.5± 26.5 pmol.cm^{-2}.hr^{-1} in MDR1-MDCKII cell layers ($P < 0.05$, Table 4.2).

Flavopiridol net secretion of 872.1± 50.2 pmol.cm^{-2}.hr^{-1} in native MDCKII cell layers increased significantly to 1969.2 ± 315.1 pmol.cm^{-2}.hr^{-1} in hBCRP-MDCKII cells and 1625.2 ± 87.7 pmol.cm^{-2}.hr^{-1} in mBcrp1-MDCKII cells ($P < 0.05$, Table 4.2). Flavopiridol is therefore a substrate of both human BCRP and mouse Bcrp. No significant increase was observed with MDR1-MDCKII cell layers in comparison to wild-type MDCKII cell layers, perhaps due to a very high basal secretion observed in the non-transfected MDCKII cell layers. These findings are similar to Robey *et al.* (2001), whilst Zhou *et al.* (2009) showed flavopiridol transport by human and mouse MDR1/Mdr1a but not to the same extent as human BCRP and mouse Bcrp (Robey *et al.*, 2001; Zhou *et al.*, 2009).

Gefitinib (Iressa™, ZD1839) is an epidermal tyrosine kinase inhibitor used in cancer clinical trials and treatment of non-small cell lung cancers (NSCLC). This

compound has been reported to be an inhibitor of BCRP and MDR1 (Leggas *et al.*, 2006; Ozvegy-Laczka *et al.*, 2004; Yanase *et al.*, 2006), reverses resistance to agents such as topotecan in mice through its interaction with Bcrp (Stewart *et al.*, 2004). Net secretion of gefitinib across all the MDCKII epithelial layers was observed with net flux increasing in the hBCRP, mBcrp and MDR1 transfected MDCKII cells. However only the murine Bcrp1-MDCKII cells showed a significant difference from the native cells with a profound increase in secretion of 1196.4 ± 418.6 pmol.cm^{-2}.hr^{-1} compared to the parental secretion of 81.6 ± 29.4 pmol.cm^{-2}.hr^{-1} ($P < 0.05$, Table 4.2).

In contrast to the other compounds tested, nitrofurantoin is not subject to epithelial secretion in the parental MDCKII cells. In contrast there is a net absorption of nitrofurantoin (see Appendix Table 1 and Figure 4.6). In MDR1-MDCKII cells, no net secretion was observed and there was a similar net absorption compared to native MDCKII epithelial layers (Appendix Table 4, Figure 4.6). Nitrofurantoin is therefore not an MDR1 substrate. However net absorptive flux of -81.3 ± 25.4 pmol.cm^{-2}.hr^{-1} in native layers is converted to substantial net secretions of 269.7 ± 31 pmol.cm^{-2}.hr^{-1} and 232.9 ± 93.7 pmol.cm^{-2}.hr^{-1} in the human and mouse Bcrp1-MDCKII cell monolayers respectively ($P < 0.05$, Table 4.2), showing nitrofurantoin to be a good hBCRP/mBcrp substrate. Nitrofurantoin is a drug used commonly throughout the world to treat bacterial infections and these data confirm findings in previous studies (Merino *et al.*, 2005).

The coumermycin antibiotic novobiocin was included in the substrate screen because of its reported action as a BCRP inhibitor (Shiozawa *et al.*, 2004; Su *et al.*, 2007). In this study no significant effect of hBCRP, mBcrp or MDR1 was seen on novobiocin net secretion, but as with clozapine, novobiocin was subject to epithelial

secretion by the intrinsic secretory transporter(s) present in native MDCKII cells (Table 4.2).

Prazosin is a well known BCRP substrate and is often used with a BODIPY tag to quantify BCRP function (Cerveny *et al.*, 2006; Matsson *et al.*, 2009; Muenster *et al.*, 2008; Staud *et al.*, 2006). It is also reported to be a substrate of MDR1 also but to a lesser degree than BCRP (Feng *et al.*, 2008; Polli *et al.*, 2001; Zhou *et al.*, 2009). Table 4.2 data confirmed these findings for prazosin. Secretion by hBCRP-MDCKII epithelial monolayers (1653.7 ± 117 pmol.cm^{-2}.hr^{-1}) was significantly elevated compared to that (1039.5 ± 92.1 pmol.cm^{-2}.hr^{-1}) seen across the native MDCKII cell monolayers ($P < 0.05$, Table 4.2). Net secretion seen with both mBcrp1-MDCKII and MDR1-MDCKII epithelial layers, (1426.5 ± 50.2 pmol.cm^{-2}.hr^{-1} and 1538.6 ± 30.9 pmol.cm^{-2}.hr^{-1}) were also significantly elevated compared with the parental MDCKII cells ($P < 0.05$, Table 4.2).

Progesterone, though subject to epithelial secretion by native MDCKII cell layers, does not show any significant increase in secretion with mBcrp, hBCRP and MDR1 transfected MDCKII cell monolayers (Table 4.2). Progesterone has been suggested to possess a modulating/regulating role for BCRP in epithelial tissue (Vore & Leggas, 2008; Wang *et al.*, 2008a).

Despite quinidine having being shown to be a good substrate for MDR1 (Polli *et al.*, 2001) Table 4.2 shows that there was no significant difference in secretion between MDR1 transfected and native MDCKII epithelial monolayers. A large net secretion of quinidine was however seen in the native MDCKII cell monolayers, with a ratio of bi-directional flux (J_{b-a} / J_{a-b}, the efflux ratio) of 15.5 (Appendix table 1). This large endogenous secretion observed in the parental MDCKII cells may act to mask secretion mediated by BCRP or MDR1 if flux across the basolateral membrane

is rate-limiting. A significant endogenous secretion is seen with all but one of the other compounds tested and highlights a potential problem with the MDCKII cell model for screening ABC transporter substrates.

As described in Chapter 3 using Hoechst 33342 dye retention, risperidone was found to be a likely BCRP inhibitor at high concentrations (Wang *et al.*, 2008b). The MDCKII substrate screen identified risperidone as a possible hBCRP substrate, this is because net flux significantly increased from 656.4 ± 19.0 $pmol.cm^{-2}.hr^{-1}$ in the native MDCKII cells to 1110.6 ± 218.1 $pmol.cm^{-2}.hr^{-1}$ in the hBCRP-MDCKII cells ($n = 2$, $P < 0.05$, Table 4.1). However it was not identified as a mouse Bcrp or MDR1 substrate. An additional feature of the present data set is the global comparison of absorptive permeabilities between the 11 compounds tested (Table 4.1). Artursson and Karlsson (1991) have found that such permeabilities broadly correlate with a measure of lipophilicity (the partition coefficient, LogP), as can be seen from Table 4.1 this is also fairly true for the compounds shown (Artursson & Karlsson, 1991). Diclofenac is a lipophilic compound displaying high apical to basal permeability whilst cimetidine is a fairly lipophobic compound displaying much lower absorptive values (data shown in Table 4.1) but with notable exceptions (e.g. nitrofurantoin and gefitinib). Nitrofurantoin shows a low LogP (0.5) but an elevated absorptive permeability suggesting that there is a specialised absorptive mechanism for this compound in MDCKII epithelial cells. Conversely the absorptive permeability for gefitinib is low despite a high LogP value (4.9) suggesting that the intrinsic ABC transporters present in the native MDCKII cell-line limit uptake.

In summary the use of ABC transfected MDCKII cell layers as a substrate screen has identified 5 compounds as hBCRP substrates: diclofenac, flavopiridol, nitrofurantoin, prazosin and risperidone. It further identified 5 mouse Bcrp substrates:

diclofenac, flavopiridol, gefitinib, nitrofurantoin and prazosin. 3 compounds were identified as MDR1 substrates: clozapine, diclofenac and prazosin. Flavopiridol and nitrofurantoin are substrates for both human BCRP and mouse Bcrp and provide likely substrates for elucidating directly the functional properties of BCRP within an intact epithelial system. Compounds such as diclofenac and prazosin are secreted by all 3 transporters.

4.3.2 Inhibition of BCRP mediated transport in MDCKII cell monolayers using Ko143

Figure 4.2A shows that when measured over an extended concentration range of 1-100µM flavopiridol was not secreted across the native MDCKII epithelial layers. These data contrast to the high basal level of secretion observed at a donor concentration of 10µM in the substrate screen script giving an efflux ratio of 3.9 (Appendix table 1). However Figure 4.2B shows that for hBCRP-MDCKII cell monolayers a substantial net secretion over the concentration range 1-100µM of flavopiridol ($P < 0.05$) was evident. Flavopiridol net secretion showed non-linear kinetics and a Michaelis-Menten fit (Fig 4.3A) for hBCRP mediated secretion gave a V_{max} of 5.1 ± 1.7 nmol.cm^{-2}.hr^{-1} and apparent K_m of 126 ± 70 µM. This net secretion was significantly reduced in the presence of 1µM Ko143 ($P < 0.05$, Figure 4.3A). Transepithelial flux of flavopiridol was also determined in the 24-well layers in the presence of a higher concentration of 10µM Ko143 (Figure 4.3B) in order to be sure that access did not limit Ko143 action. Flavopiridol net secretion was reduced from 9.01 ± 0.92 nmol.cm^{-2}.hr^{-1} to 4.19 ± 0.27 nmol.cm^{-2}.hr^{-1} in the presence of 10µM Ko143. A Ko143 sensitive and insensitive component of flavopiridol secretion

therefore exists. The Ko143 insensitive component most probably represents endogenous secretion.

Prazosin was shown to be a substrate for hBCRP/mBcrp and MDR1 from the substrate screen shown in Table 4.1. In the native MDCKII cell line at low prazosin concentrations, secretion was limited but a significant net secretion was observed at 100µM ($P < 0.05$, Figure 4.4A). Figure 4.4B shows the concentration dependence of prazosin secretion by hBCRP-MDCKII epithelia; net secretion of prazosin was significantly greater in the hBCRP-MDCKII cells compared with the native MDCKII at all concentrations apart from 3µM ($P < 0.05$, Figure 4.5A, B). Prazosin secretion by hBCRP-MDCKII cell monolayers was also significantly reduced by the BCRP selective 1µM Ko143, reducing secretion at all concentrations (Figure 4.5). In the manual 24-well format (Figure 4.5B) prazosin net secretion by hBCRP-MDCKII cell monolayers was significantly reduced from 10.2 ± 0.62 $nmol.cm^{-2}.hr^{-1}$ to 3.24 ± 0.21 $nmol.cm^{-2}.hr^{-1}$ in the presence of 10µM Ko143, but as with flavopiridol secretion was not completely abolished ($P < 0.05$, Figure 4.5B).

Nitrofurantoin was selected from the MDCKII substrate screen because it was not secreted in the native MDCKII cells but was highly secreted in the human BCRP and mouse Bcrp cDNA transfected MDCKII cell monolayers (Table 4.2 and Figure 4.6A-D). This net secretion of nitrofurantoin across the hBCRP-MDCKII cells was selectively reduced from 1.08 ± 0.12 $nmol.cm^{-2}.hr^{-1}$ in the untreated monolayers to 0.23 ± 0.01 $nmol.cm^{-2}.hr^{-1}$ in the presence of 10µM Ko143 ($P < 0.05$, Figure 4.7).

Taken together this MDCKII data confirms flavopiridol, prazosin and nitrofurantoin as suitable compounds to study functional BCRP activity in a complex cell system such as Caco-2 epithelia.

4.3.3 Determination of the BCRP mediated component of substrate flux across Caco-2 cell monolayers

Data from Chapter 3 confirmed BCRP expression and functionality in the low passage (PA) Caco-2 cells. Table 4.3 summarises the data for transepithelial flux data across Caco-2 cell confluent monolayers. As for MDCKII data, only 12 compounds were amenable to HPLC-MS quantification.

All 12 compounds were secreted across the Caco-2 cell monolayers (Table 4.3). Sulphasalazine, whose low permeability in native MDCKII epithelia precluded measurement, was secreted by Caco-2 cell monolayers. It is known sulphasalazine has a poor absorptive passive permeability (LogP 3.8) (Jani *et al.*, 2009) and this is replicated in the current data (Table 4.3). In contrast there is a high level of basolateral to apical transport and hence secretion of sulphasalazine in Caco-2 cells in agreement with the data of other workers (Dahan & Amidon, 2009; Jani *et al.*, 2009).

The dose dependence of flavopiridol, prazosin and nitrofurantoin were determined over a range of concentrations. Figure 4.8A shows the bi-directional flux of flavopiridol across Caco-2 cells. Secretion shows saturation (Figure 4.8B) and is sensitive to 10μM Ko143 inhibition (Figure 4.8B). Ko143 reduces the V_{max} of flavopiridol secretion from 5.12 ± 0.99 nmol.cm^{-2}.hr^{-1} in untreated cells to 1.59 ± 0.2 nmol.cm^{-2}.hr^{-1} in the presence of 10μM Ko143. The use of Ko143 shows the contribution of BCRP to its secretion in an intact intestinal epithelium and also shows that it is secreted by at least another component (perhaps an MRP family member).

Figure 4.9A shows that prazosin secretion displays saturation kinetics across Caco-2 cell monolayers, with an apparent K_m of 22.1 ± 2.9 μM and a V_{max} of 3.57 ± 0.17 nmol.cm^{-2}.hr^{-1}. In the presence of 10μM Ko143, there is a reduction in the V_{max} of prazosin to 2.54 ± 0.41 nmol.cm^{-2}.hr^{-1}. A substantial Ko143 insensitive component

of prazosin net secretion may represent an MDR1 mediated component (Table 4.2). The effects of Ko143 or verapamil inhibition alone and combined on prazosin flux in the manual 24-well assay format showed that 10µM Ko143 reduced secretion from 1.22 ± 0.06 nmol.cm^{-2}.hr^{-1} to 0.51 ± 0.69 nmol.cm^{-2}.hr^{-1} in the Ko143 treated cells ($P < 0.05$, Figure 4.9C). 100µM verapamil had a marginal but none significant effect at reducing prazosin secretion. However when combined with 10µM Ko143 it reduced net secretion to 0.21 ± 0.02 nmol.cm^{-2}.hr^{-1}. This data shows prazosin is secreted by BCRP in these Caco-2 cells but there is also an alternative route of secretion, likely to be MDR1 due to verapamil sensitivity.

Figure 4.10A shows that nitrofurantoin is subject to saturable secretion by human intestinal Caco-2 cell monolayers. A Michaelis-Menten fit of the net secretion, shown in Figure 4.10B, shows an apparent K_m = 69.4 ± 22.3 µM and a V_{max} = 14.03 ± 2.27 nmol.cm^{-2}.hr^{-1}. The V_{max} of nitrofurantoin was also profoundly reduced by Ko143 to just 1.3 ± 0.19 nmol.cm^{-2}.hr^{-1} across Ko143 treated layers. This effect of 10µM Ko143 shows that the vast majority of nitrofurantoin secretion can be ascribed to BCRP in Caco-2 cells. In the manual 24-well assay format nitrofurantoin flux (donor concentration 10µM) was reduced from 2.28 ± 0.08 nmol.cm^{-2}.hr^{-1} across untreated Caco-2 cell monolayers to 0.18 ± 0.02 nmol.cm^{-2}.hr^{-1} across 10µM Ko143 layers ($P < 0.05$ Figure 4.10B). In contrast to its action on prazosin flux, verapamil had no effect whatsoever on nitrofurantoin flux and did not affect flux even when combined with Ko143.

Therefore nitrofurantoin may be regarded as a selective BCRP substrate and may be used to characterise the functional BCRP component in the context of multiple ABC-transporter expression.

Table 4.1. Absorptive permeabilities of potential BCRP substrates across MDCKII and Caco-2 cell monolayers

Summary table of absorptive permeabilities (P_{a-b} = J_{a-b} / C_a) of potential BCRP substrates in native and transfected MDCKII cells and low passage Caco-2 cells. Partition coefficient at pH 7.4 (LogP) is also displayed for each compound. Cells were grown to confluency on 96-well permeable Transwell supports and assays were conducted via automation on a Hamilton StarPlus Robot. Compounds were used at a concentration of 10µM. Data points are means of n = 6 wells, data were pooled and normalised from 2 independent experiments ± SEM. * P < 0.05, are significantly different from control native values.

	P_{a-b} (10^{-6}cm.h^{-1})					
	MDCKII	**hBCRP-MDCKII**	**mBcrp1-MDCKII**	**MDR1-MDCKII**	**Caco-2**	**LogP**
Cimetidine	1.31 ± 0.07	7.21 ± 2.9	0.14 ± 0.05	6.23 ± 0.79	6.79 ± 0.51	0.4
Clozapine	7.49 ± 0.71	10.38 ± 3.43	6 ± 0.68	22.52 ± 0.57	23.23 ± 0.92	3.2
Diclofenac	33.23 ± 19.72	41.14 ± 3.54	35.66 ± 2.3	80.9 ± 8.04	46.25 ± 14	4.5
Flavopiridol	29.66 ± 1.01	16.57 ± 4.32	0.05 ± 0.01	40.82 ± 4.81	36.54 ± 1.17	3.3
Gefitinib	0.14 ± 0.09	0.73 ± 0.53	0.64 ± 0.39	2.22 ± 1	1.73 ± 0.36	4.9
Nitrofurantoin	17.26 ± 3.54	0.12 ± 0.2	0.15 ± 0.01	16.26 ± 1.28	7.53 ± 0.94	0.5
Novobiocin	1.74 ± 0.54	1.09 ± 0.07	0.06 ± 0.01	2.85 ± 0.6	6.64 ± 0.38	2.5
Prazosin	24.2 ± 2.27	11.01 ± 1.71	0.18 ± 0.05	29.14 ± 0.88	20.93 ± 1.08	1.3
Progesterone	39.0 ± 1.06	33.32 ± 4.88	5.24 ± 0.86	24.33 ± 2.85	21.18 ± 0.38	3.9
Quinidine	11.22 ± 0.93	6.89 ± 1.37	144 ± 11.54	9.93 ± 0.47	35.78 ± 1.57	3.4
Risperidone	30.77 ± 1.84	28.24 ± 1.93	24.77 ± 2.82	52.4 ± 6.86	49.59 ± 1.21	3.5

Table 4.2. Elucidation of potential BCRP-substrates using MDCKII cell monolayers

Summary table of net secretory flux ($J_{net} = J_{b-a} - J_{a-b}$) of potential BCRP substrates in transfected MDCKII cells. Cells were grown to confluency on 96-well permeable Transwell supports and assays were conducted via automation on a Hamilton StarPlus Robot. Compounds were used at a concentration of 10µM. Data points are means of n = 6 wells, data were pooled and normalised from 2 independent experiments ± SEM. * $P < 0.05$, are significantly different from control native values.

	Net secretory flux ($pmol.cm^{-2}.hr^{-1}$)			
Compound	**Native MDCKII (J_{net})**	**BCRP-MDCKII (J_{net})**	**Bcrp1-MDCKII (J_{net})**	**MDR1-MDCKII (J_{net})**
Cimetidine	128.8 ± 21.3	187.4 ± 48.1	220.8 ± 93.1	141.1 ± 71.7
Clozapine	176.3 ± 29.5	237.9 ± 51	226.7 ± 14.1	321.5 ± 26.4 *****
Diclofenac	131.7 ± 137	678.8 ± 57 *****	665.1 ± 37.2 *****	625.6 ± 133.7 *****
Flavopiridol	872.1 ± 50.2	1969.2 ± 315.1 *****	1625.2 ± 87.7 *****	1060.1 ± 145.3
Gefitinib	81.6 ± 29.4	265.8 ± 45	1196.4 ± 418.6 *****	268.6 ± 17.5
Nitrofurantoin	-81.3 ± 25.4	269.7 ± 31 *****	232.9 ± 93.7 *****	-101.3 ± 2.98
Novobiocin	188.8 ± 24.7	236.1 ± 18	162.7 ± 23.1	69.9 ± 8.3
Prazosin	1039.5 ± 92.1	1653.7 ± 117*****	1426.5 ± 50.2 *****	1538.6 ± 30.9 *****
Progesterone	455.4 ± 21.0	468.9 ± 131.1	337.3 ± 52.6	545.2 ± 45.3
Quinidine	1849.1 ± 25.1	2423.1 ± 640	2390.0 ± 421.4	2064.9 ± 38.9
Risperidone	656.4 ± 19.0	1110.6 ± 218.1 *****	407.1 ± 75.5	906.1 ± 27.7

Figure 4.1. Use of ABC-transfected MDCKII cells to determine substrate specificity; transepithelial flux of diclofenac

Figures (A)-(D) show the transepithelial flux of diclofenac in (A) native MDCKII, (B) human BCRP-MDCKII, (C) mouse Bcrp1-MDCKII and (D) MDR1-MDCKII. Cells were grown to confluency on 96-well permeable Transwell supports and assays were conducted via automation on a Hamilton StarPlus Robot. Total diclofenac concentration was 10µM. Horizontal striped bars show flux in the apical to basal direction (J_{a-b}), diagonal stripes represent flux in the basal to apical direction (J_{b-a}) and filled bars represent net flux ($J_{net} = J_{b-a} - J_{a-b}$). Data bars are means of n = 6 wells, data pooled and normalised from 2 independent experiments ± SEM. * $P < 0.05$, are significantly different from control values.

Figure (E) shows net transepithelial flux (J_{net}) of diclofenac across confluent MDCKII monolayers. Black filled bar = native, dark grey = human BCRP-MDCKII, light grey = mouse Bcrp1-MDCKII and unfilled bar = MDR1-MDCKII diclofenac net secretion (J_{net}) respectively. Data bars are means of n = 6 wells, data pooled and normalised from 2 independent experiments ± SEM. * $P < 0.05$ represent significant difference of transfected MDCKII net flux compared to native MDCKII.

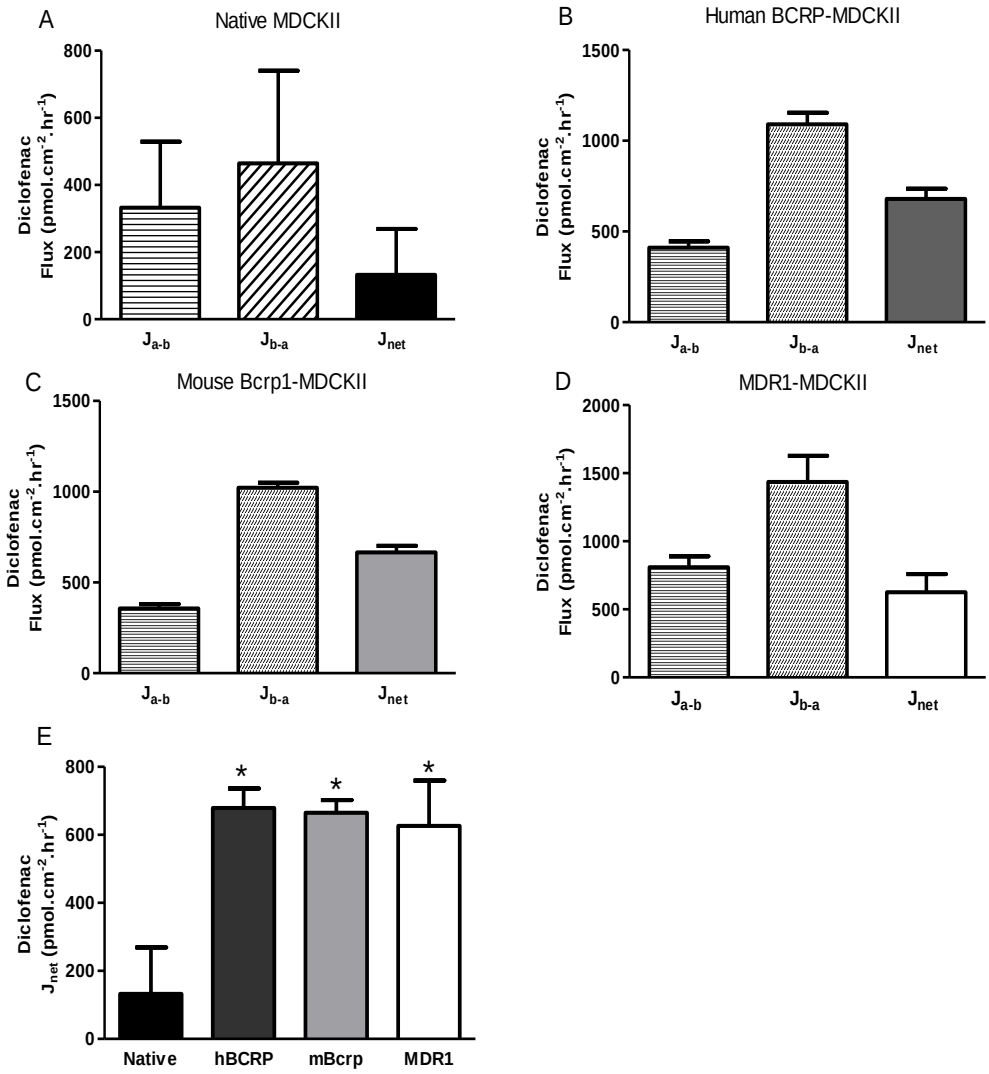

Figure 4.1. Use of ABC-transfected MDCKII cells to determine substrate specificity; transepithelial flux of diclofenac

Figure 4.2. Dose-dependency of flavopiridol transepithelial flux across confluent native and human BCRP-MDCKII monolayers

(A) Dose-dependency of flavopiridol flux in native MDCKII cells grown to confluency on permeable 96-well Transwell supports. Flux were determined in the apical-to-basal (J_{a-b}) and basal-to-apical (J_{b-a}) directions where secretory net flux (J_{net}) = $J_{b-a} - J_{a-b}$. Data points are means of n = 4 monolayers ± SEM.

(B) Dose-dependency of flavopiridol flux in human BCRP-MDCKII cells grown to confluency on permeable 96-well Transwell supports. Flux were determined in the apical-to-basal (J_{a-b}) and basal-to-apical (J_{b-a}) directions where secretory net flux (J_{net}) = $J_{b-a} - J_{a-b}$. Data points are means of n = 4 monolayers ± SEM.

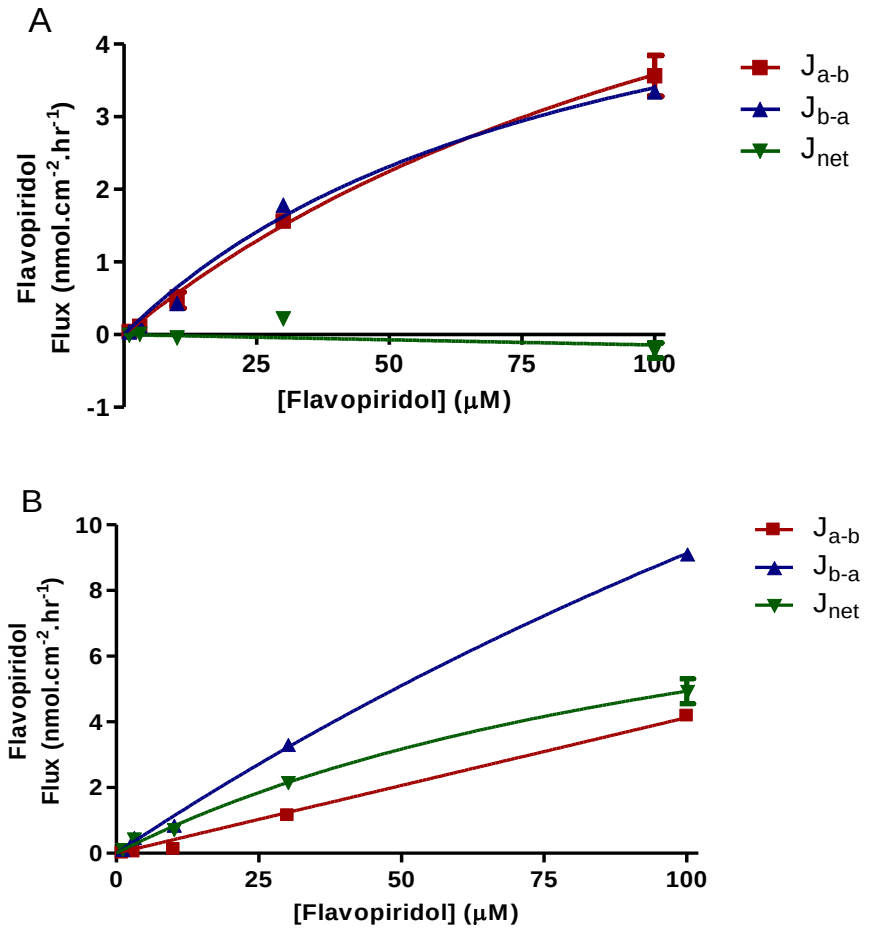

Figure 4.2. Dose-dependency of flavopiridol transepithelial flux across confluent native and human BCRP-MDCKII monolayers

Figure 4.3. Action of bi-directional transport of flavopiridol across native and human BCRP-MDCKII monolayers

(A) Dose-dependency of flavopiridol net secretory flux ($J_{net} = J_{b-a} - J_{a-b}$) across native MDCKII and hBCRP-MDCKII in the presence and absence of the BCRP inhibitor Ko143 (1μM). MDCKII cells were grown to confluency on 96-well Transwell supports. Data points are means of n = 4 monolayers ± SEM.

(B) Transepithelial flux of flavopiridol in hBCRP-MDCKII grown to confluency on permeable 24-well Transwell supports. Donor flavopiridol concentration was 10μM. Flux were determined in the presence and absence of the ABC-transporter inhibitors Ko143 (10μM) and verapamil (100μM). Data bars are means of n = 4 monolayers ± SEM. * $P < 0.05$, significantly different from control.

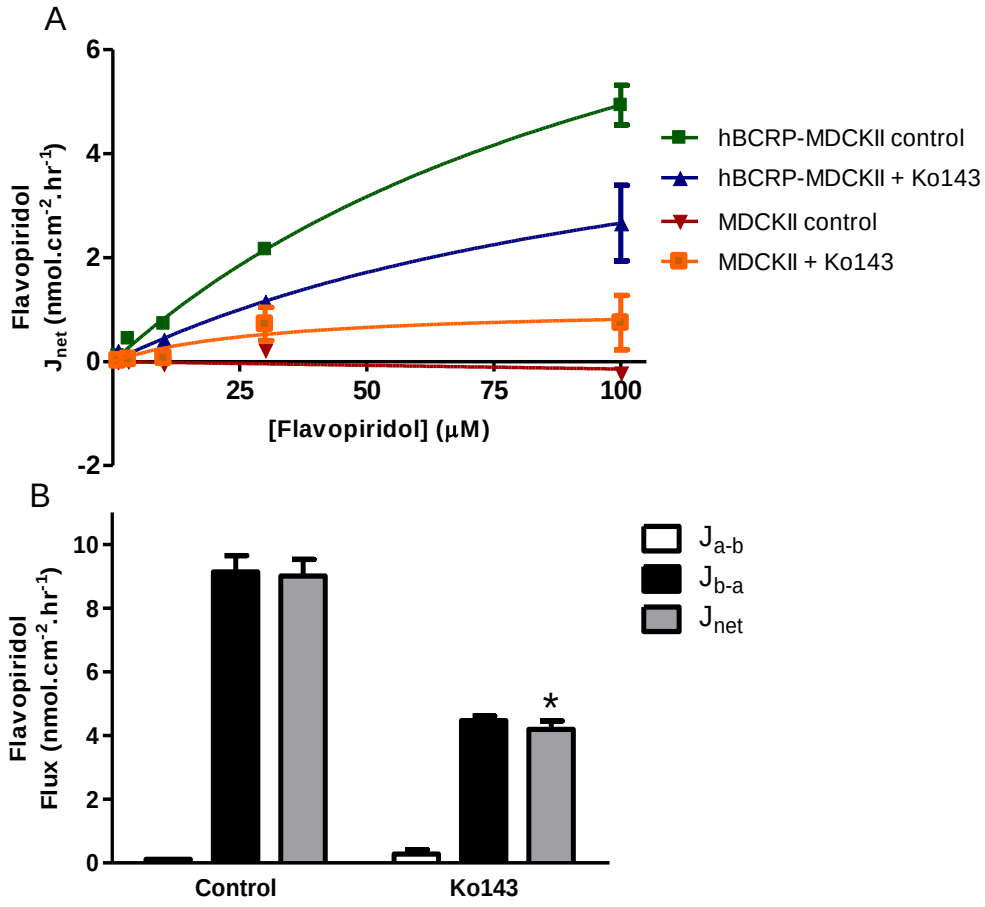

Figure 4.3. Action of bi-directional transport of flavopiridol across native and human BCRP-MDCKII monolayers

Figure 4.4. Dose-dependency of prazosin transepithelial flux across confluent native and human BCRP-MDCKII monolayers

(A) Dose-dependency of prazosin flux across native MDCKII cells grown to confluency on permeable 96-well Transwell supports. Flux were determined in the apical-to-basal (J_{a-b}) and basal-to-apical (J_{b-a}) directions where secretory net flux (J_{net}) = $J_{b-a} - J_{a-b}$. Data points are means of n = 4 monolayers ± SEM.

(B) Dose-dependency of prazosin flux across human BCRP-MDCKII cells grown to confluency on permeable 96-well Transwell supports. Flux were determined in the apical-to-basal (J_{a-b}) and basal-to-apical (J_{b-a}) directions where secretory net flux (J_{net}) = $J_{b-a} - J_{a-b}$. Data points are means of n = 4 monolayers ± SEM.

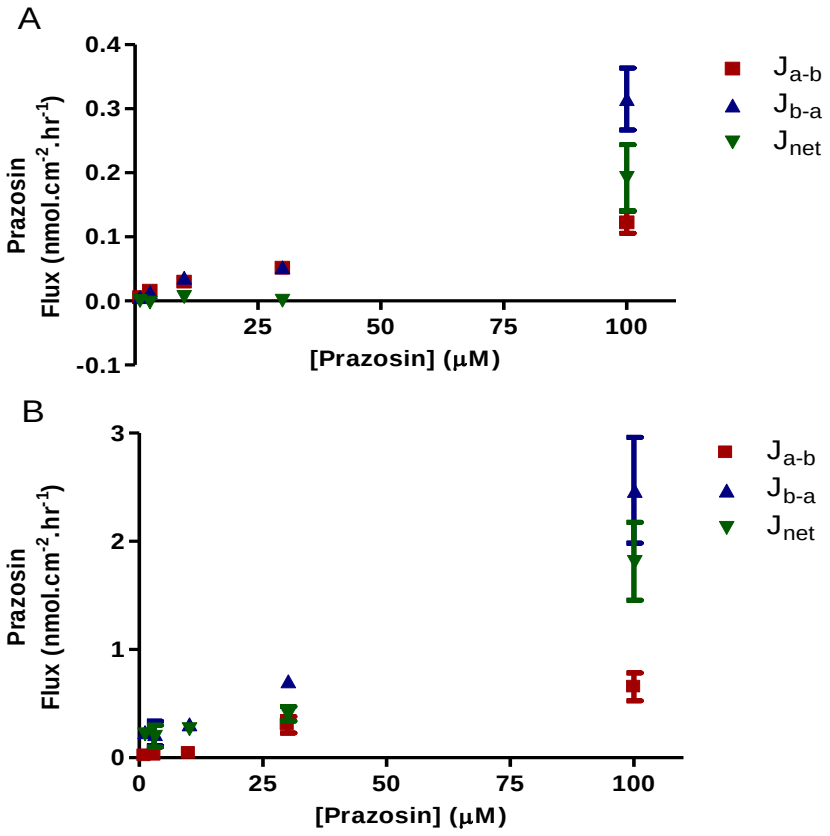

Figure 4.4. Dose-dependency of prazosin transepithelial flux across confluent native and human BCRP-MDCKII monolayers

Figure 4.5. Action of bi-directional transport of prazosin across native and human BCRP-MDCKII monolayers

(A) Dose-dependency of prazosin net secretory flux ($J_{net} = J_{b-a} – J_{a-b}$) across native MDCKII and hBCRP-MDCKII in the presence and absence of the BCRP inhibitor Ko143 (1μM). MDCKII cells were grown to confluency on 96-well Transwell supports. Data points are means of n = 4 monolayers ± SEM.

(B) Transepithelial flux of prazosin across BCRP-MDCKII grown to confluency on permeable 24-well Transwell supports. Donor prazosin concentration was 10μM. Flux were determined in the presence and absence of the known ABC-transporter inhibitors Ko143 (10μM) and verapamil (10μM). Data bars are means of n = 4 monolayers ± SEM. * $P < 0.05$, significantly different from control.

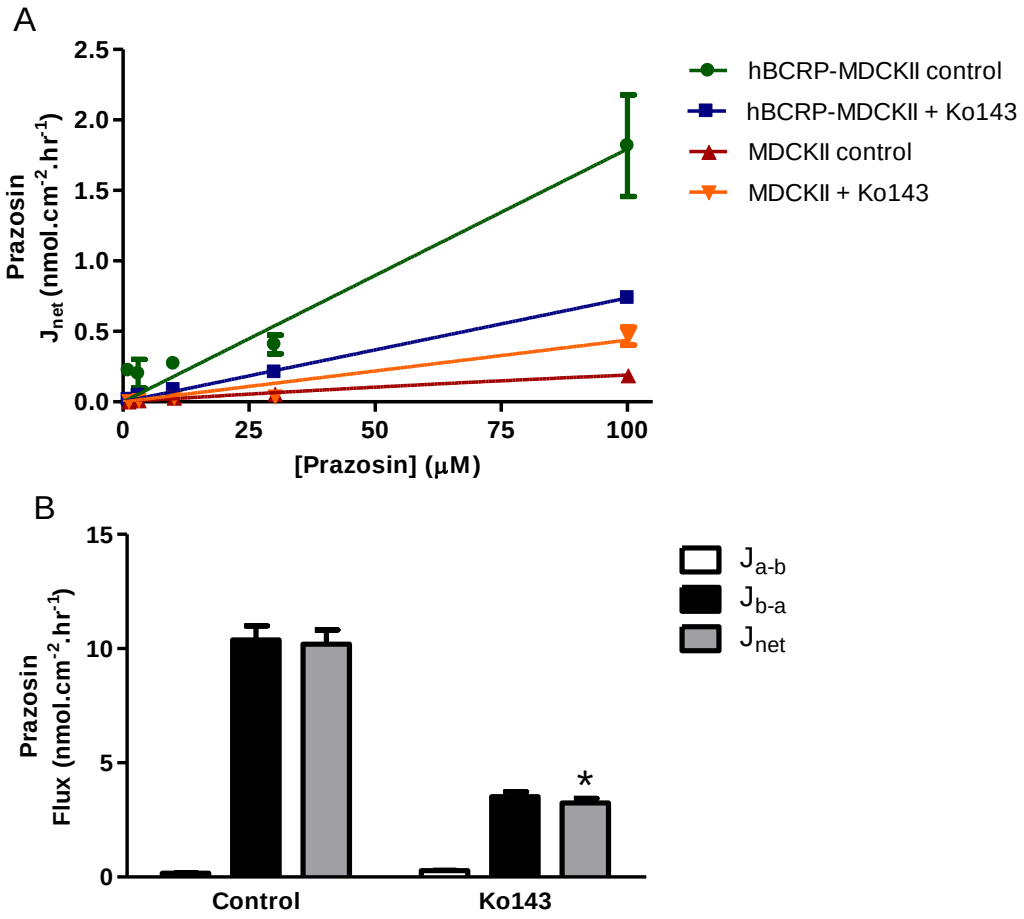

Figure 4.5. Action of bi-directional transport of prazosin across native and human BCRP-MDCKII monolayers

Figure 4.6. Bi-directional transport of nitrofurantoin across ABC-transfected MDCKII cells

Figures (A)-(D) show the transepithelial flux of nitrofurantoin across confluent monolayers of (A) native MDCKII, (B) MDR1-MDCKII, (C) human BCRP-MDCKII and (D) mouse Bcrp1-MDCKII. Donor nitrofurantoin concentration was 10µM. Flux were determined in the apical to basal direction (J_{a-b}), basal to apical direction (J_{b-a}) and net flux was determined by $J_{net} = J_{b-a} - J_{a-b}$. Data bars are means of n = 6 wells, data pooled and normalised from 2 independent experiments ± SEM.

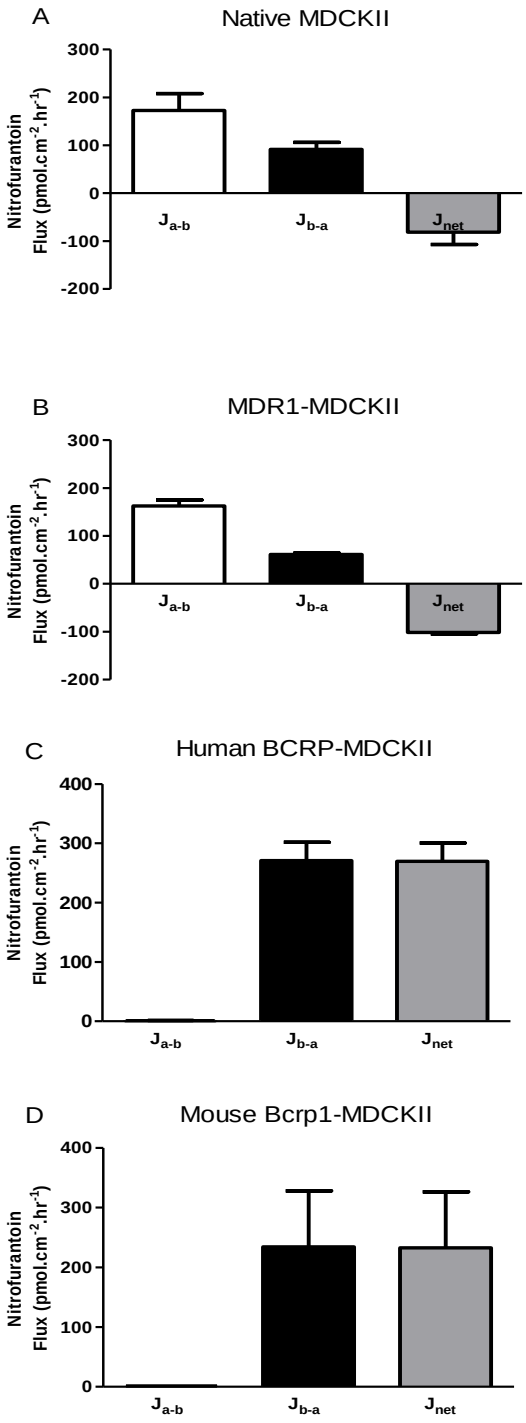

Figure 4.6. Bi-directional transport of nitrofurantoin across ABC-transfected MDCKII cells

Figure 4.7. Effect of Ko143 on nitrofurantoin transepithelial flux across confluent human BCRP-MDCKII monolayers

BCRP-MDCKII cells were cultured on 24-well Transwell supports. Nitrofurantoin donor concentration was 10μM; receiver concentration was measured by HPLC-MS. Flux were determined in the presence and absence of the ABC transporter inhibitors Ko143 (10μM). Data bars are means of n = 4-6 monolayers ± SEM. * $P < 0.05$, significantly different from control.

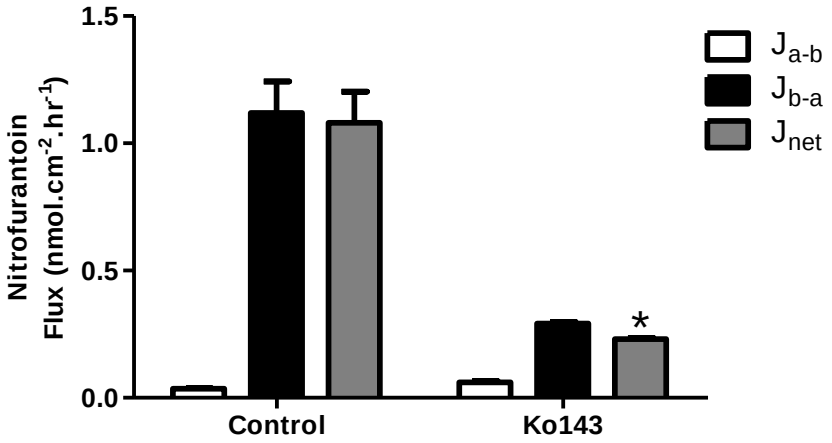

Figure 4.7. Effect of Ko143 on nitrofurantoin transepithelial flux across confluent human BCRP-MDCKII monolayers

Table 4.3. Table showing bi-directional flux of selected compounds in Caco-2 cells

Summary table of bi-directional flux in the apical to basal direction, basal to apical direction, net secretion ($J_{net} = J_{b-a} - J_{a-b}$), efflux ratio ($J_{b-a} / J_{a-b}$) and partition coefficient (LogP) of potential BCRP substrates across Caco-2 monolayers. Cells were grown to confluency on 96-well permeable Transwell supports and assays were conducted via automation on a Hamilton StarPlus Robot. Compounds were used at a concentration of 10µM. Data points are means of n = 4-6 wells, data were pooled and normalised from 2 independent experiments ± SEM.

	Bidirectional Flux ($pmol.cm^{-2}.hr^{-1}$)				
Compound	**J_{a-b}**	**J_{b-a}**	**J_{net}**	**Efflux Ratio**	**logP**
Cimetidine	67.9 ± 5.1	371.7 ± 8.1	303.7 ± 3.1	5.5 ± 0.3	0.4
Clozapine	232.3 ± 9.2	581.7 ± 41.8	349.5 ± 37.8	2.5 ± 0.1	3.2
Diclofenac	462.5 ± 140	828.2 ± 1.3	365.7 ± 138.7	1.8 ± 0.1	4.5
Flavopiridol	365.4 ± 11.7	1333.3 ± 54.8	967.9 ± 55	3.6 ± 0.2	3.3
Gefitinib	17.3 ± 3.6	135.9 ± 10.7	118.7 ± 7.7	7.9 ± 1.1	4.9
Nitrofurantoin	75.3 ± 9.4	1261.5 ± 199.4	1186.2 ± 197.7	16.8 ± 2.9	0.5
Novobiocin	66.4 ± 3.8	451.2 ± 19.1	384.7 ± 19.2	6.8 ± 0.4	2.5
Prazosin	209.3 ± 10.8	1313.6 ± 57.7	1104.3 ± 50.3	6.3 ± 0.2	1.3
Progesterone	211.8 ± 3.8	566.6 ± 51	354.9 ± 54.1	2.7 ± 0.3	3.9
Quinidine	357.8 ± 15.7	1272.5 ± 23.8	914.6 ± 33.1	3.6 ± 0.2	3.4
Risperidone	495.9 ± 12.1	1270.2 ± 40	774.3 ± 46	2.6 ± 0.1	3.5
Sulphasalazine	0.51 ± 0.1	646.3 ± 53.7	645.8 ± 53.7	1267.3 ± 0.1	3.8

Figure 4.8. Bi-directional and net flux of flavopiridol across confluent Caco-2 cell monolayers

(A) Dose-dependence of flavopiridol flux across Caco-2 cells grown to confluency on permeable 96-well Transwell supports. Flux were determined in the apical-to-basal (J_{a-b}) and basal-to-apical (J_{b-a}) directions where secretory net flux (J_{net}) = $J_{b-a} – J_{a-b}$. Data points are means of n = 4-6 monolayers ± SEM.

(B) Effect of the BCRP inhibitor Ko143 (10µM) on flavopiridol net flux (J_{net}) across Caco-2 cell monolayers. Control curve is a Michaelis-Menten fit of the data, K_m = 43.8 ± 2.5 µM and V_{max} = 5.12 ± 0.99 nmol.cm^{-2}.hr^{-1}. Ko143 curve is a Michaelis-Menten fit, K_m = 9.84 ± 4.34 µM and V_{max} = 1.59 ± 0.2 nmol.cm^{-2}.hr^{-1}. Data points are means of n = 4-6 monolayers ± SEM.

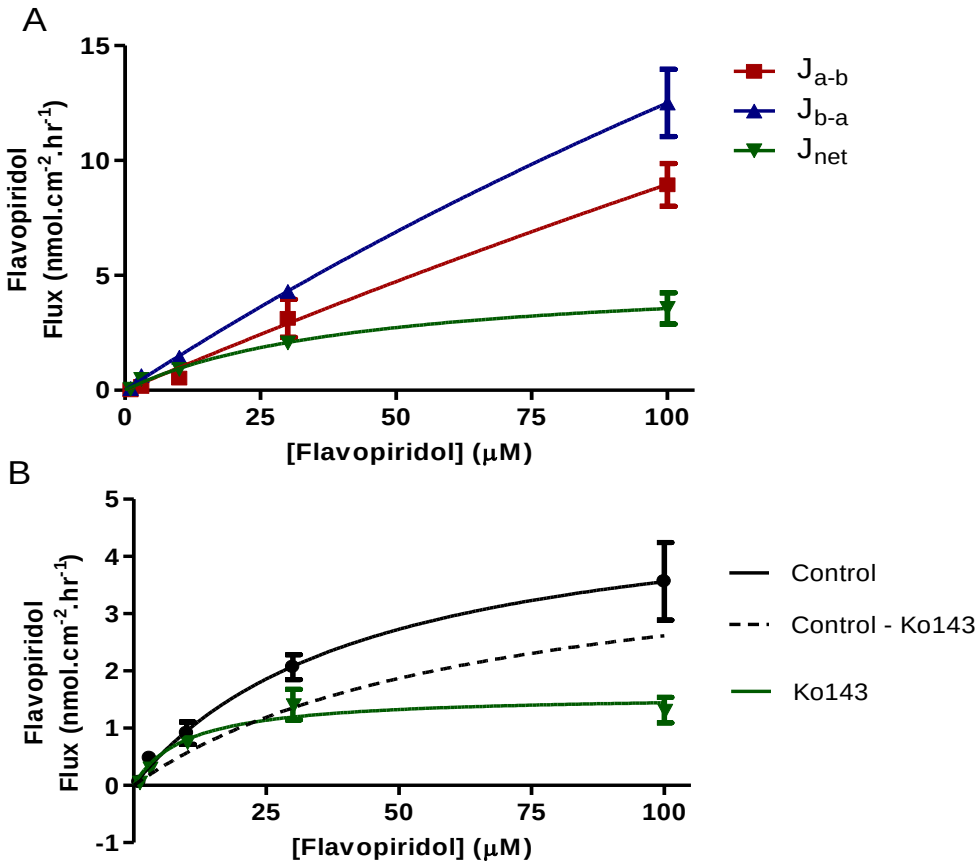

Figure 4.8. Bi-directional and net flux of flavopiridol across confluent Caco-2 cell monolayers

Figure 4.9. Bi-directional and net flux of prazosin across confluent Caco-2 cell monolayers

(A) Dose-dependence of prazosin flux across Caco-2 cell monolayers. Flux were determined in the apical-to-basal (J_{a-b}) and basal-to-apical (J_{b-a}) directions where secretory net flux (J_{net}) = $J_{b-a} - J_{a-b}$. Data points are means of n = 4-6 monolayers ± SEM.

(B) Effect of the BCRP inhibitor Ko143 (10µM) on prazosin net flux (J_{net}) across Caco-2 cell monolayers. Control curve is a Michaelis-Menten fit, K_m = 22.1 ± 2.9µM and V_{max} = 3.57 ± 0.17 nmol.cm^{-2}.hr^{-1}. Ko143 curve is a Michaelis-Menten fit, K_m = 46.8 ± 17.2 µM and V_{max} = 2.54 ± 0.41 nmol.cm^{-2}.hr^{-1}. Data points are means of n = 4-6 monolayers ± SEM.

(C) Effect of the ABC transporter inhibitors Ko143 (10µM) and verapamil (100µM) on prazosin bi-directional flux across Caco-2 cell monolayers cultured on 24-well Transwell supports. Prazosin donor concentration was 10µM. Data are means of n = 4-6 monolayers ± SEM. * $P < 0.05$, significantly different from control.

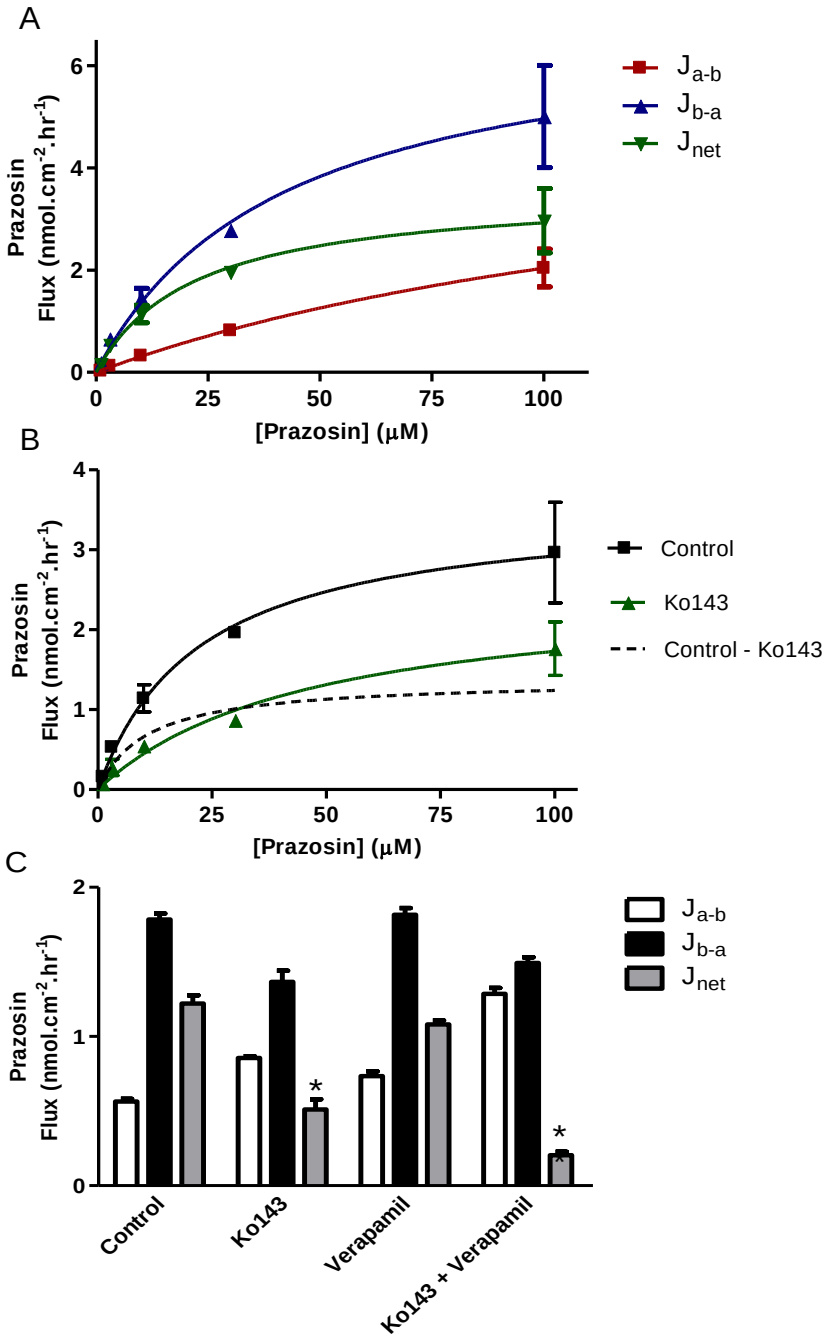

Figure 4.9. Bi-directional and net flux of prazosin across confluent Caco-2 cell monolayers

Figure 4.10. Bi-directional flux of nitrofurantoin across confluent Caco-2 cell monolayers

(A) Dose-dependence of nitrofurantoin flux across Caco-2 cell monolayers grown to confluency on permeable 96-well Transwell supports. Flux were determined in the apical-to-basal (J_{a-b}) and basal-to-apical (J_{b-a}) directions where secretory net flux (J_{net}) = $J_{b-a} - J_{a-b}$. Data points are means of n = 4-6 monolayers ± SEM.

(B) Effect of the BCRP inhibitor Ko143 (10µM) on nitrofurantoin net flux (J_{net}) across Caco-2 cell monolayers. Control curve is a Michaelis-Menten fit, K_m = 69.4 ± 22.3 µM and V_{max} = 14.03 ± 2.27 nmol.cm^{-2}.hr^{-1}. Ko143 curve is a Michaelis-Menten fit, K_m = 34.8 ± 12.4 µM and V_{max} = 1.3 ± 0.19 nmol.cm^{-2}.hr^{-1}. Data points are means of n = 4-6 monolayers ± SEM.

(C) Nitrofurantoin bi-directional and net flux across Caco-2 cells cultured on 24-well Transwell supports in the presence and absence of ABC transporter inhibitors. Nitrofurantoin donor concentration was 10µM. Flux were determined in the presence and absence of the ABC transporter inhibitors Ko143 (10µM) and verapamil (100µM). Data bars are means of n = 4-6 monolayers ± SEM. * $P < 0.05$, significantly different from control.

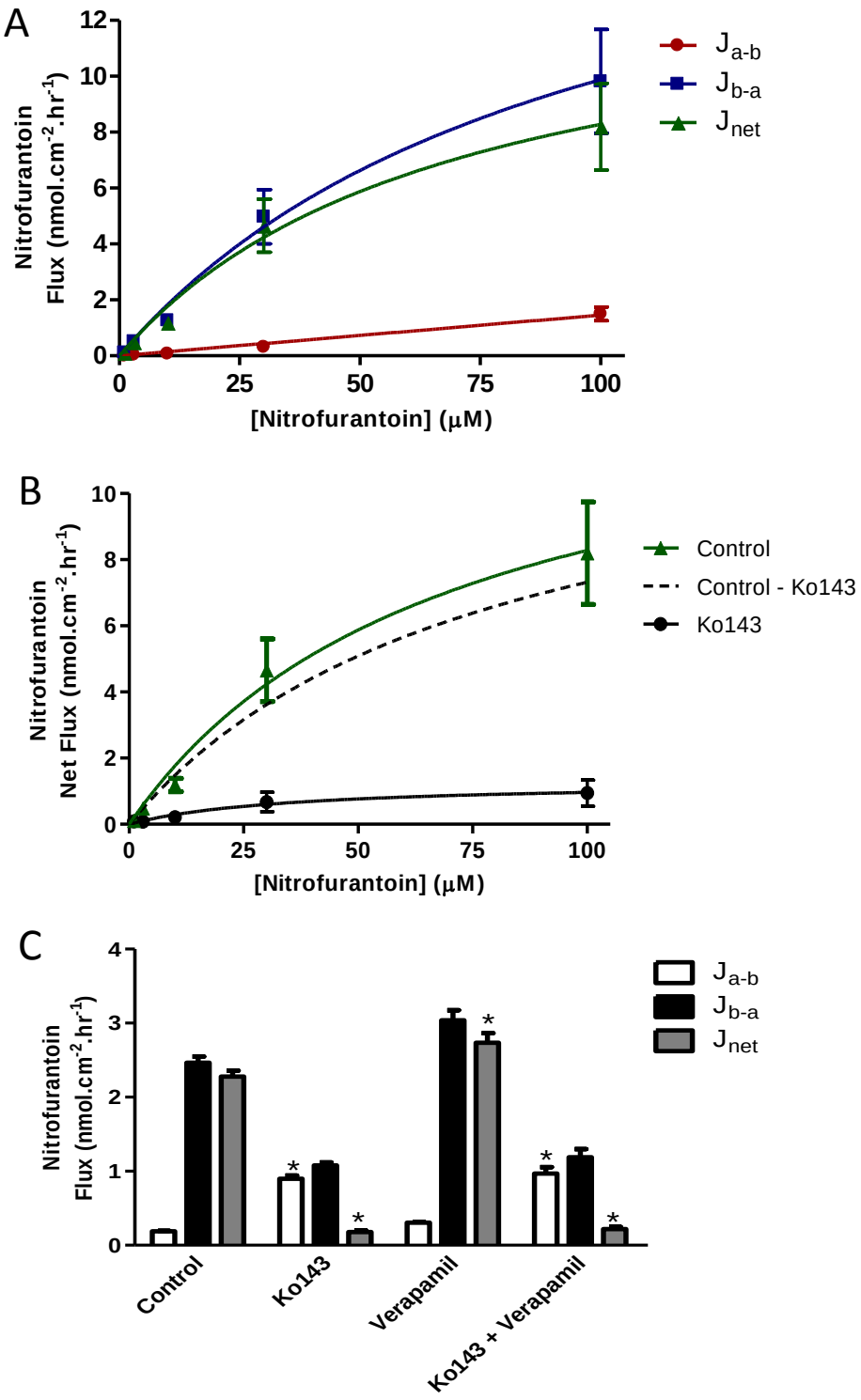

Figure 4.10. Bi-directional flux of nitrofurantoin across confluent Caco-2 cell monolayers

Figure 4.11. Correlation between Caco-2 and native MDCKII absorptive permeability (Papp) of selected compounds

Caco-2 vs. native MDCKII absorptive permeability of compounds. 1. Cimetidine, 2. Clozapine, 3. Diclofenac, 4. Flavopiridol, 5. Gefitinib, 6. Nitrofurantoin, 7. Novobiocin, 8. Prazosin, 9. Progesterone, 10. Quinidine, 11. Risperidone.

Linear regression analysis shows no correlation between the permeability of several compounds across MDCKII and Caco-2 monolayers. Data points are means of 4-6 monolayers of MDCKII and Caco-2 cells, d.f = 9, $P > 0.05$, $R^2 = 0.47$.

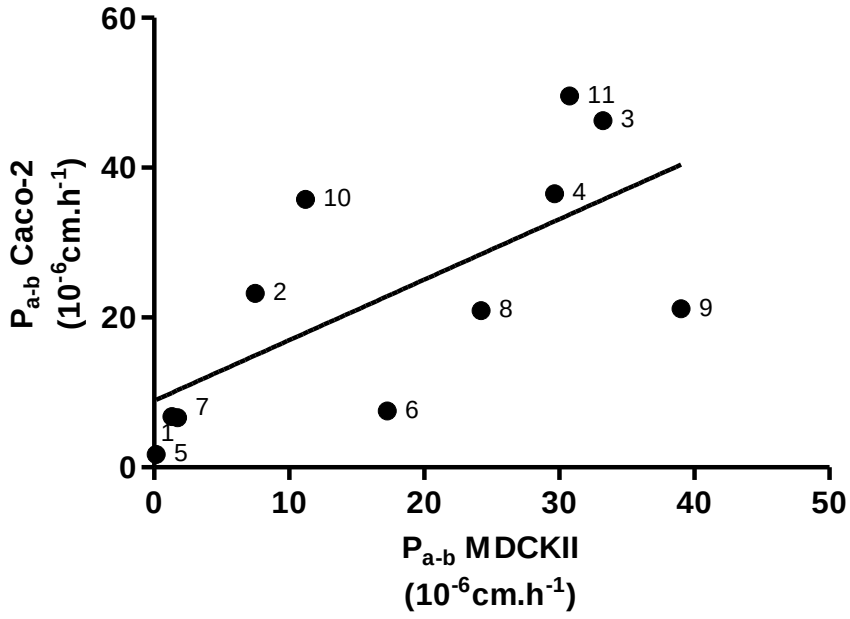

Figure 4.11. Correlation between Caco-2 and native MDCKII absorptive permeability (P_{app}) of selected compounds

Figure 4.12. Correlation between absorptive permeability (P_{a-b}) and the partition coefficient (LogP) for select compounds in (A) native MDCKII and (B) Caco-2 cells

P_{a-b} vs. LogP. 1. Cimetidine, 2. Clozapine, 3. Diclofenac, 4. Flavopiridol, 5. Gefitinib, 6. Nitrofurantoin, 7. Novobiocin, 8. Prazosin, 9. Progesterone, 10. Quinidine, 11. Risperidone, 12. Sulphasalazine. Curve shows an approximate sigmoid relationship and is plotted by hand.

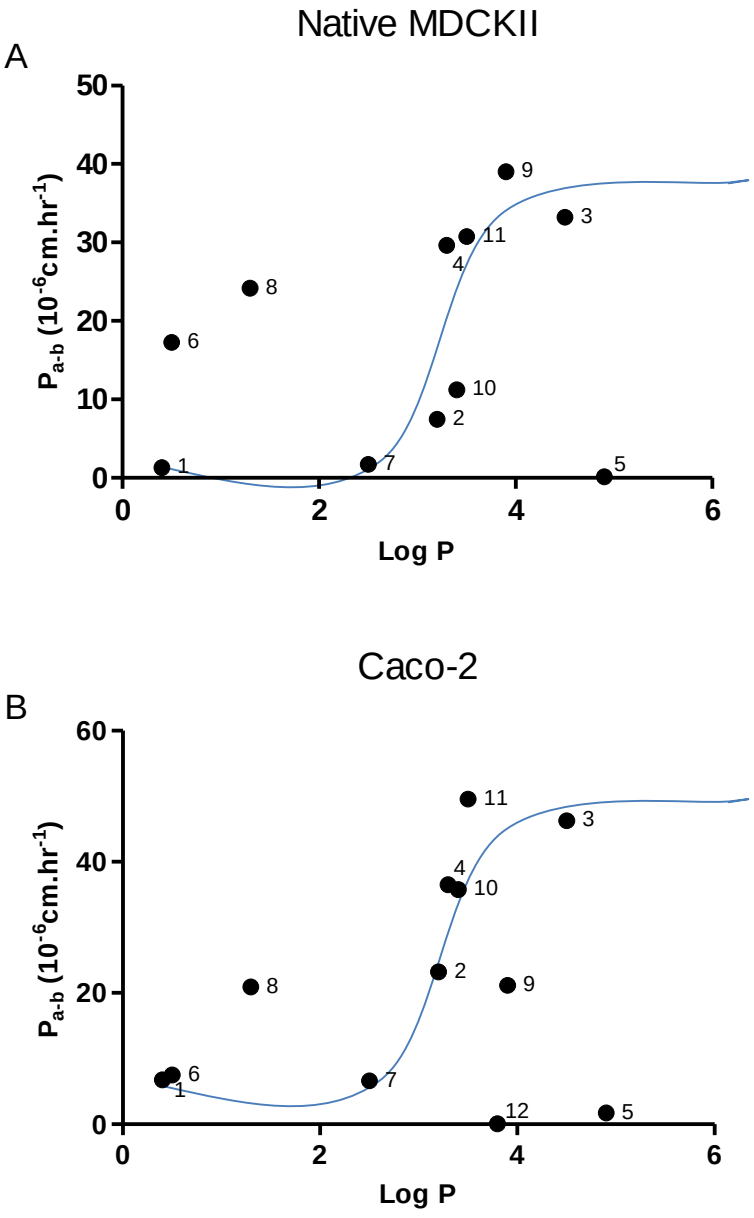

Figure 4.12. Correlation between absorptive permeability (P_{a-b}) and the partition coefficient (LogP) for select compounds in (A) MDCKII and (B) Caco-2 cells

4.4 Discussion

Various methods have been utilised to screen for BCRP substrates. In Chapter 3 the Hoechst 33342 retention assay was shown to have fundamental limitations. Matsson *et al.* (2009), using Saos-2 transfected cells with BCRP, measured the ratio of mitoxantrone accumulation after co-incubation with an inhibitor to the accumulation observed with mitoxantrone only (Matsson *et al.*, 2009). Alternatively cytotoxicity profiles were correlated with BCRP expression levels in the National Cancer Institute anticancer drug screen in 60 cell-lines, positive or negative correlations of enhanced sensitivity or protection indicating interactions with BCRP (Deeken *et al.*, 2009). Another method uses inside-out membrane vesicles prepared from BCRP transfected cell-lines (e.g. HEK 293 cells) which has allowed ATP-dependent substrate accumulation to be studied (Ni *et al.*, 2010). Finally a photo-active compound, [^{125}I]-IAAP may be used to label BCRP in isolated membranes with BCRP substrates or inhibitors used to show inhibition of binding in a concentration-dependent manner (Ni *et al.*, 2010). The data presented in this chapter have used reconstituted parental MDCKII epithelial cell monolayers together with their ABC transfected MDCKII counterparts to determine selective BCRP substrates. By directly comparing native wild-type cell monolayers with their transfected counterparts, transported substrates may be readily and unambiguously identified by HPLC/MS. This method provides many advantages and it may be scaled to multi-well formats (e.g. 24/96 well assays used here). Since HPLC/MS compound identification is used, many substrates may be examined directly without the need to prepare radioisotopes or use of indirect measures such as inhibition of ligand binding. As a live-cell assay, non-specific toxicity may be easily identified (monolayer disruption).

Bi-directional flux were determined to calculate net flux ($J_{net} = J_{b-a} - J_{a-b}$), which in turn was used to compare parental and transfected MDCKII cell lines; significantly higher secretory flux values were deemed to indicate that a compound was a substrate of either human BCRP, mouse Bcrp or human MDR1. Some studies rely on the use of the efflux ratio, whereby the secretory flux is divided by the absorptive flux ($ER = J_{b-a} / J_{a-b}$) (Xiao *et al.*, 2006). Net secretory flux rather than ER was used to determine ABC substrate specificity. The main reason for this was that a small change in the absorptive flux resulting from small leaks/change in paracellular permeability in monolayers may result in a large change in ER. Monolayer integrity was measured using transepithelial electrical resistance (R_T) which allows rejection of leaky monolayers. However, the low transepithelial resistance of MDCKII epithelial monolayers does not allow for accuracy in this regard so that additional controls such as bi-ionic diffusion potentials were used to assess the cation selectivity of the paracellular pathway. Inclusion of an intra-assay measure of paracellular permeability such as lucifer yellow flux is recommended but not all experiments included such a control for passive diffusion during the experiment because of complications with the robotic script. The magnitude of net secretion is largely unaffected by paracellular leak flux so this was used as the primary comparison between parental and transfected MDCKII cell layers.

Fixed measurement parameters were chosen for the screening studies described in this Chapter. Monolayer assays are very sensitive to factors such as time and substrate concentration (Hegedus *et al.*, 2009). Time was fixed at 2 hours which allows low permeability compounds to be detected. A fixed concentration of 10μM compound was chosen for all compounds in the substrate screen. For a high affinity substrate $K_m < 10\mu M$ this concentration may saturate transport via hBCRP/mBcrp or

MDR1 but also via the endogenous efflux system. As explained by Hunter *et al.* (1991) this would not necessarily decrease the ability to discriminate between passive and active transport providing the passive component was low and the V_{max} high (Hunter *et al.*, 1991). For a low affinity substrate K_m > 10μM the active component for a finite V_{max} would be lower so that the discrimination ability would be lower.

One of the noticeable complications in using the MDCKII cell monolayers is the presence of endogenous transporters for the compounds tested. Indeed transepithelial secretion of the majority of the compounds is observed across native MDCKII cell monolayers, an observation corroborated by the data in Chapter 3 with Hoechst 33342 retention. Transepithelial secretion requires both transport across the basal membrane with subsequent ABC-dependent extrusion across the apical membrane. An inability to access a transport step at the basal membrane would render an ABC-substrate to be not secreted. Alternatively the capacity of transport at the basal membrane may rate limit overall secretory transport rate (Xiao *et al.*, 2006). This endogenous ABC dog transporter expressed in MDCKII cells is likely to be MDR1 but additional ABC transporters may exist (Hunter *et al.*, 1991; Pavek *et al.*, 2005). This could well mask the secretion that would normally be seen with BCRP/MDR1 transfected capacity.

Therefore compounds such as cimetidine and quinidine maybe preferentially transported by the endogenous protein but may well be BCRP and MDR1 substrates. Further work is needed to define the nature of secretory flux and their molecular basis in MDCKII cells. However it can be certain that as nitrofurantoin is not secreted in native MDCKII cells, it has different substrate specificity or dog BCRP is not expressed. A final complication may reside in the presence of absorptive transport mechanisms in the brush-border of MDCKII epithelial cells; mitoxantrone has been

shown to be a substrate for an uptake pathway that increases J_{a-b}, above J_{b-a}, so obscuring secretion (Pan *et al.,* 2009). In the present data set nitrofurantoin shows substantial net absorption in native MDCKII monolayers. Species differences between MDR1 function were shown by Feng *et al.* (2008) to be minimal between human and mouse. Furthermore, Zhou *et al.* (2009) showed that there was minimal difference with respect to human BCRP and mouse Bcrp function. Data on the respective dog proteins is however sparse. Out of the 11 compounds screened in this study, 5 compounds were secreted by human BCRP, 5 secreted by mouse Bcrp and 4 of these substrates were shared between human and mouse Bcrp. Human and mouse proteins show 81% identity and as 4 out of 5 substrates were shared between human and mouse BCRP/Bcrp this strong correlation demonstrates that mouse mBcrp can be an important tool in understanding BCRP function in man. The MDCKII substrate screens combined with the pharmacological inhibitors provide additional evidence for compound identification as BCRP substrates. Flavopiridol, prazosin and nitrofurantoin were confirmed as human BCRP substrates in this manner. The substrate screen however failed to identify known substrates perhaps due to the reasons outlined above. Cimetidine is a known BCRP and MDR1 substrate yet was not identified as a substrate, whilst quinidine is a widely used MDR1 substrate and was not identified as an MDR1 substrate.

Caco-2 human intestinal epithelial monolayers have been frequently used to predict the likely bioavailability of compounds from the lumen (oral route). Artursson and Karlsson (1991) have compared the oral bioavailability of 20 compounds with absorptive permeability coefficients measured in Caco-2 cells. The data are best-fit by a sigmoid with an apparent upper limit of permeability $P > 10^{-6}$ cm/sec. In addition these authors correlated Caco-2 permeability with the log octanol/water partition

coefficient (LogP) and found a sigmoid relationship with saturation of Caco-2 permeability at greater than 10^{-5} cm/sec at a log D > 0. However there were exceptions to this for both lipophilic and hydrophilic compounds most probably related to transport phenomena. Table 4.1 summarises absorptive permeabilities measured in both MDCKII and Caco-2 epithelial layers. Figure 4.11 shows the relationship between measurements in these 2 systems. As expected, due to the differences in membrane protein transporter expression between MDCKII cells and Caco-2 cells at the apical and basolateral surfaces (Hilgendorf *et al.*, 2007) there is not a strong relationship in absorptive permeabilities between the 2 cell systems.

Figure 4.12 displays the relationship between the absorptive permeability in Caco-2 cells and the LogP value, as noted by Artursson and Karlsson (1991). However with this data set there is not a clear sigmoid relationship showing saturation (unlike that shown by Artursson and Karlsson, 1991); there are too many exceptions to this, perhaps a larger compound screen would show differently. Prazosin displays higher values of absorptive permeability than expected on the basis of its LogP value. This may relate to either a specific transport system present in the apical membrane/transcellular route or access to the cation-selective paracellular route. Transporters of relevance affecting absorptive permeability may include OATPs, OCTs, and OATs (Hilgendorf *et al.*, 2007). Gefitinib and sulphasalazine, in contrast display markedly reduced absorptive permeabilities on the basis of their LogP values. The most likely reason for this is that the operation of efflux mechanisms at the brush-border limits transcellular transport.

A primary aim of this chapter was to confirm the existence of a BCRP mediated component of secretion in the Caco-2 cells despite the existence of multiple ABC transporters. Flavopiridol, nitrofurantoin and prazosin all showed Ko143

sensitive components of transepithelial secretion. The main route of flavopiridol secretion appeared to be via another ABC transporter such as MRP2. BCRP was only clearly involved at higher concentrations of flavopiridol. Prazosin was shown using Ko143 and verapamil, as BCRP and MDR1 selective inhibitors respectively, to be a substrate for both BCRP and MDR1 substrate as previously reported (Cerveny *et al.*, 2006; Feng *et al.*, 2008; Matsson *et al.*, 2009; Muenster *et al.*, 2008; Polli *et al.*, 2001; Staud *et al.*, 2006; Zhou *et al.*, 2009). However the majority of the secretion in Caco-2 epithelia was via BCRP with only a marginal secretion by MDR1. This compound and its fluorescent derivatives could therefore be a useful tool in further investigations of BCRP function. However nitrofurantoin secretion was shown to be a selective BCRP substrate that was verapamil insensitive. MDR1 and MRP2 have been ruled out as transporters of nitrofurantoin in vitro (Merino *et al.*, 2005; Wang & Morris, 2007), with both studies showing BCRP alone mediates nitrofurantoin transport. However there is some speculation in the literature about the specificity of nitrofurantoin secretion via BCRP. A pharmacogenetic study looking at patients with the C421A polymorphism which reduces functional BCRP activity in vitro, showed human nitrofurantoin pharmacokinetics not to change in those individuals (Adkison *et al.*, 2008). If nitrofurantoin is secreted by only BCRP, this mutation, which is known to widely affect transport of many BCRP substrate in vivo (Sparreboom *et al.*, 2004, 2005; Zhang *et al.*, 2006), should cause the pharmacokinetic profile of nitrofurantoin in these patients to be altered. No MRP transfected MDCKII cell lines were used in the substrate screen to test for MRP involvement in nitrofurantoin secretion. However verapamil at 100μM is known to inhibit both MRP1 and MRP2 (Matsson *et al.*, 2007), and was found to have no effect on secretion in the Caco-2 cells, suggesting no MRP transporter involvement. To further confirm whether the MRP transporters were

not involved in nitrofurantoin secretion, CMFDA accumulation assay described by (Bogman *et al.*, 2003) was used (CMFDA being a fluorescent dye that is a promiscuous MRP substrate). Nitrofurantoin at 1, 10 or 100µM did not affect accumulation of CMFDA in native or MRP2 over expressing MDCKII cells (unpublished data). The near abolition by Ko143 of nitrofurantoin secretion in Caco-2 cells is very good evidence that nitrofurantoin may be used as a selective substrate for BCRP in conditions where there are multiple ABC transporters expressed as is the case for Caco-2 cells.

In summary, the BCRP substrate screen using the MDCKII cells serves as a convenient and direct method for identification of BCRP substrates in vitro. The use of pharmacological inhibitors in Caco-2 cells allowed the characterization of a BCRP mediated component in low-passage epithelia. Nitrofurantoin is identified as a selective BCRP substrate.

5. The mechanism of transepithelial ciprofloxacin secretion

5.1 Introduction

Ciprofloxacin is a widely prescribed fluoroquinolone antibiotic that displays a wide spectrum activity against both Gram positive and negative bacteria. Fluoroquinolones penetrate well into most body tissues and fluids, having a high volume of distribution relative to total body water, making them ideal for treating soft tissue infections. Most fluoroquinolone antibiotics are administered orally with high bioavailability. However ciprofloxacin bioavailability is between 50-80% (Sorgel *et al.*, 1989). Ciprofloxacin is therefore deemed as a low permeability (poor absorption) compound (Volpe, 2004; Zakelj *et al.*, 2006) with an octanol/water partition coefficient (LogP) value of 1.4, typical of a hydrophilic compound (Zhao *et al.*, 2002). Ciprofloxacin undergoes minimal metabolism and is mainly excreted as the parent molecule. Clearance is predominantly renal in vivo (Rohwedder *et al.*, 1990; Sorgel *et al.*, 1989). However, it is also cleared via the intestine (10% of an i.v dose) and into the bile (1% of an i.v dose) (Parry *et al.*, 1988; Rohwedder *et al.*, 1990). The exact nature of ciprofloxacin efflux across the intestine has been investigated by several laboratories and is mediated by ATP-binding cassette (ABC) transporters in common with other fluoroquinolones (Alvarez *et al.*, 2008).

Griffiths *et al.* (1993, 1994) first confirmed an energy dependent secretion of ciprofloxacin in human intestinal Caco-2 cells (Griffiths *et al.*, 1994, 1993). By measurements of ciprofloxacin transport across both apical and basolateral membranes and cellular accumulation, calculation of the unidirectional flux indicated an “active” component at both basolateral and apical membranes (Griffiths *et al.*,

1994). These studies suggest the involvement of an ABC transporter-mediated efflux of ciprofloxacin but not its exact identity.

MDR1 involvement in Caco-2 cell mediated secretion appears unlikely since Cavet *et al.* (1996, 1997) showed no effect of ciprofloxacin on secretion of the known MDR1 substrate vinblastine (Cavet *et al.*, 1997, 1996). Although the anti-MDR1 monoclonal antibodies MRK16 and UIC2 reduced vinblastine secretion neither had any effect on ciprofloxacin secretion. Further investigation confirmed that MDR1 was not involved since with native MDCKII cell monolayers or MDCKII cell monolayers over-expressing human MDR1, no ciprofloxacin secretion was seen (Lowes & Simmons, 2002).

Lowes and Simmons (2002) further investigated the nature of ciprofloxacin secretion in Caco-2 cells and looked at the potential involvement of MRP2. It was shown that MRP2 is unlikely to facilitate ciprofloxacin transport since the MRP selective inhibitor, MK571, had only a minor effect on ciprofloxacin secretion. Furthermore, over-expressing MRP2-MDCKII cell monolayers showed no net secretion of ciprofloxacin (Lowes, 2001).

MRP1 was shown not to be involved in mediating ciprofloxacin transport using J774 macrophages (Michot *et al.*, 2004), although it is suggested that another MRP family member was involved in ciprofloxacin transport since the organic anions gemfibrozil and probenecid inhibited ciprofloxacin efflux (Michot *et al.*, 2004).

Grepafloxacin, a fluoroquinolone only differing from ciprofloxacin by 2 additional methyl groups (Lowes & Simmons, 2002), was shown to be secreted by both MDR1 and MRP2. However, grepafloxacin was shown to competitively inhibit ciprofloxacin secretion, showing that there is a third route of secretion shared by grepafloxacin and ciprofloxacin. This common pathway has yet to be determined.

Ciprofloxacin appears to fit the preferential criteria of a BCRP substrate outlined by the International Transporter Consortium (Giacomini *et al.*, 2010); ciprofloxacin possesses fused heterocyclic rings and amine side groups, characteristic for binding to BCRP. Merino *et al.* (2006) used the MDCKII cell line stably transfected with the human and mouse homologues of BCRP/Bcrp to show that ciprofloxacin was a substrate for mouse Bcrp, whereas hBCRP mediated secretion was, at best, marginal (Merino *et al.*, 2006).

The same group used Bcrp ko (-/-) null mice to show that mouse Bcrp affects ciprofloxacin pharmacokinetics in vivo (Merino *et al.*, 2006). They showed that after subcutaneous injection ciprofloxacin plasma concentrations were elevated 2-fold compared with wild type animals and further showed that wild type lactating dams had a 2-fold higher concentration of ciprofloxacin in their milk compared with Bcrp ko (-/-) lactating mice (Merino *et al.*, 2006). Further work demonstrated mBcrp involvement in the biliary excretion of ciprofloxacin in mice (Ando *et al*, 2007). Therefore, it seems likely that BCRP is involved in intestinal secretion of ciprofloxacin in humans.

Other ABC transporters may also be involved. Using murine J774 macrophages (Marquez *et al.*, 2009) selected for resistance to ciprofloxacin, the nature of ciprofloxacin secretion was examined; gemfibrozil (non-specific MRP inhibitor) inhibited ciprofloxacin excretion but elacridar, a dual P-glycoprotein and BCRP inhibitor was largely ineffective (Marquez *et al.*, 2009). Furthermore ciprofloxacin resistant J774 macrophages had an increased expression of both Mrp2 and Mrp4 family members. Using siRNA knock down it was demonstrated that just Mrp4 was responsible for the drug resistant phenotype by preventing cellular accumulation of ciprofloxacin. Thus ciprofloxacin is a substrate for mouse Mrp4 and

chronic exposure of ciprofloxacin causes an up-regulation of Mrp2 and Mrp4, suggesting this may occur in other eukaryotic cell types.

The main aim of this chapter is to examine the role of hBCRP in mediating ciprofloxacin secretion. Ciprofloxacin transport will be determined in human and mouse BCRP/Bcrp transfected MDCKII cell-layers. Then the mechanism of ciprofloxacin secretion by human intestinal Caco-2 epithelia will be addressed using two variant cell lines, low and high passage (PA) Caco-2 cell, in which BCRP expression is different. Finally the possible involvement of MRP4 in ciprofloxacin transport will be tested.

5.2 Methods

5.2.1 Bi-directional transport across epithelial layers grown on 12-well filter plates

Bi-directional [^{14}C]-ciprofloxacin transport across cell monolayers was determined by scintillation counting in the same way as described in Materials and Methods (Section 2.2.2.2). [^{14}C]-Ciprofloxacin was a gift from Bayer (Wuppertal, Germany).

5.2.2 Bi-directional transport across epithelial layers grown on 96-well filter plates

Bi-directional ciprofloxacin transport across 96-well cell monolayers was determined by HPLC-MS in the same way as described in Materials and Methods (Section 2.2.2.2).

5.2.3 Cellular ciprofloxacin accumulation in HEK 293 cells

HEK 293 cells were seeded at a density of 5 x 10^4 cells into 12-well plates (Corning). Cells were grown for 4 days. Media was aspirated and cells were washed 2x with pre-warmed Krebs' buffer. Transport solutions comprised Krebs' buffer with [^{14}C]-ciprofloxacin (0.1µCi.ml^{-1}, made up to 10µM with unlabelled ciprofloxacin) plus the addition of pharmacological inhibitors. Cells were incubated at 37°C for 1 hour with ciprofloxacin solutions and were then washed 2x with ice cold Krebs' to remove bound isotope from the cell surface. Cells were then treated with 500µl lysis buffer (0.05% Triton X-100) for 15-30 minutes. After lysis a 50µl aliquot was dispensed into 2.5ml of scintillation cocktail and radioactivity was determined by scintillation counting, whilst another 50µl of sample was collected for measurement and protein correction via a Bradford Assay. Cellular accumulation of [^{14}C]-ciprofloxacin (10µM) was determined by scintillation counting. Cellular accumulation was determined as

shown in Material and Methods section 2.2.2.2. Values were then normalised to control values and displayed as arbitrary values.

5.3 Results

5.3.1 Bi-directional ciprofloxacin flux across MDCKII cell monolayers

[^{14}C]-Ciprofloxacin transepithelial flux were determined in both the absorptive (J_{a-b}, apical to basal) and secretory (J_{b-a}, basal to apical) directions in native MDCKII, hBCRP-MDCKII and mBcrp1-MDCKII cell monolayers (Figure 5.1). In wild-type MDCKII cell monolayers and human BCRP-transfected MDCKII cell monolayers the bi-directional flux were similar (0.16 ± 0.03 nmol.cm^{-2}.hr^{-1} and 0.12 ± 0.01 nmol.cm^{-2}.hr^{-1}, for J_{a-b} and J_{b-a}, respectively, and 0.22 ± 0.05 nmol.cm^{-2}.hr^{-1} and 0.18 ± 0.02 nmol.cm^{-2}.hr^{-1}, J_{a-b} and J_{b-a}, respectively) with no significant net secretory flux evident (Figure 5.1 A and B).

However, in contrast to the hBCRP-MDCKII epithelial layers which showed no ciprofloxacin secretion, in murine Bcrp1-MDCKII cell monolayers a marked net secretion of ciprofloxacin was evident (J_{net} = -0.03 ± 0.03 nmol.cm^{-2}.hr^{-1} for WT and 0.24 ± 0.02 nmol.cm^{-2}.hr^{-1} for mBcrp transfected cell layers, n = 3, $P < 0.05$, Figure 5.1 C, D). Over expression of mBcrp increased basal to apical flux to 0.34 ± 0.03 nmol.cm^{-2}.hr^{-1}, (n = 3, $P < 0.05$ vs. control values). Efflux ratios (J_{b-a} / J_{a-b}) for ciprofloxacin transport were 0.78, 0.81 and 3.4 for WT-MDCKII, hBCRP-MDCKII and mBcrp1-MDCKII cells respectively. The findings in this study support the data published by Merino *et al.* (2006) who showed the absorptive ciprofloxacin net flux across the native MDCKII cell monolayers to be reversed to a net secretion of ciprofloxacin with murine Bcrp transfection (Merino *et al.*, 2006). Merino *et al.* (2006) also found a marginal secretion of ciprofloxacin in the human BCRP-MDCKII

cells, but this was only significant after 4 hours of incubation. These authors hypothesised that the cell line had only poor expression of BCRP compared to the murine variant (Bcrp). In order to discount the possibility that the reduced ciprofloxacin secretion was due to a measurement artefact associated with the use of radiolabel, ciprofloxacin flux were also determined in the robotic 96-well assay but with total ciprofloxacin in receiver wells being determined by HPLC-MS (see Methods). Table 5.1 confirms that no net secretion of ciprofloxacin is observed in native MDCKII cell layers and that mBcrp transfected cell-layers maintain a significant secretory flux and enhanced efflux ratio (Table 5.1). Furthermore, in hBCRP-MDCKII epithelial layers a significant but small secretion of ciprofloxacin was observed (Table 5.1).

The kinetics of mBcrp mediated ciprofloxacin secretion is shown in Figure 5.2. Net ciprofloxacin secretion displays saturation kinetics with a K_m of 167 ± 63 µM and a V_{max} of 10.2 ± 1.3 nmol.cm^{-2}.hr^{-1}.

The pharmacological sensitivity of ciprofloxacin secretion by mBcrp1-MDCKII cells was assessed (Figure 5.3). Ko143, a potent and specific BCRP inhibitor (Allen *et al.*, 2002) was shown earlier to have an IC_{50} of 0.15µM for Hoechst 33342 accumulation in mBcrp1-MDCKII cells (see Chapter 3) and 1.06µM for Hoechst 33342 accumulation in hBCRP-MDCKII cells (see Chapter 3). Used at a concentration of 1µM, Ko143 completely abolished net secretory ciprofloxacin flux in mBcrp1-MDCKII cells (0.24 ± 0.02 nmol.cm^{-2}.hr^{-1} to –0.05 ± 0.03 nmol.cm^{-2}.hr^{-1}, n = 3, $P < 0.05$, Figure 5.2A).

The ratio of ciprofloxacin permeability (P_{b-a} / P_{a-b}) was reduced from 2.77 ± 0.16 in control to 0.65 ± 0.24 in the presence of 1µM Ko143, (n = 3, $P < 0.05$, Figure

5.3B). Furthermore 1μM Ko143 increased cellular accumulation across the basolateral membrane from 4.56 ± 0.29 μM to 6.46 ± 0.39 μM (n = 3, P < 0.05, Figure 5.3C), although the concentration never exceeds that of the external medium (10μM). There was no significant change in accumulation across the apical surface in the presence of 1μM Ko143.

Cyclosporin A (CsA) is now known to inhibit both MDR1 and BCRP, albeit with lower affinity (Ejendal & Hrycyna, 2005; Matsson *et al.*, 2009). In the present study, application of a high dose of 50μM CsA greatly reduced net secretory ciprofloxacin flux in mBcrp1-MDCKII cells (0.24 ± 0.02 nmol.cm^{-2}.hr^{-1} to 0.04 ± 0.02 nmol.cm^{-2}.hr^{-1}, n = 3, P < 0.05 versus controls).

It has been previously shown that the anion transport inhibitor 4,4′-diisothiocyanostilbene-2,2′-disulphonic acid (DIDS) at 0.4mM inhibits ciprofloxacin secretion across Caco-2 cell monolayers (Cavet *et al.*, 1997). It was found in this study that DIDS only partially inhibits ciprofloxacin secretion in mBcrp1-MDCKII cells by ~25% (0.24 ± 0.02 nmol.cm^{-2}.hr^{-1} to 0.18 ± 0.02 nmol.cm^{-2}.hr^{-1}, n = 3, P < 0.05). DIDS is therefore not a definitive inhibitor with respect to ciprofloxacin secretion.

MK571 is a known MRP selective inhibitor and was included in the study to confirm the involvement of MRP family members in ciprofloxacin secretion in MDCKII cells. Matsson *et al.* (2009) report MK571 to be also an inhibitor of BCRP (at 50μM), although MK571 has no effect on ciprofloxacin secretion at 10μM or ratio of bi-directional permeabilities (Figure 5.2A and B). MK571 had no significant effect on ciprofloxacin cellular accumulation across the apical and basolateral membranes.

5.3.2 Is ciprofloxacin secretion mediated by BCRP in Caco-2 cell monolayers?

It has already been shown (Chapter 3) that whereas low passage Caco-2 cells express hBCRP, high passage Caco-2 cells have only limited expression in comparison. Both strains of Caco-2 cells used in this study, high passage (111-116 passage) and low passage (34-45 passage), secreted ciprofloxacin (Figure 5.4 and 5.5 respectively). Ciprofloxacin secretion by Caco-2 cells has been the subject of extensive studies in Caco-2 epithelia (Cavet *et al.*, 1997; Griffiths *et al.*, 1993; Lowes & Simmons, 2002). The efflux ratios (J_{b-a} / J_{a-b}) for ciprofloxacin transport were 3.55 and 1.94 for high and low passage Caco-2 cells respectively. Basolateral ciprofloxacin cellular uptake (accumulation) was significantly greater than accumulation across the apical membrane ($p = 0.0314$ and $p = 0.085$ for both high and low passage Caco-2 cells respectively), suggesting the existence of a basolateral uptake mechanism.

Ko143 at 1µM was used to test for a BCRP mediated component of ciprofloxacin secretion in Caco-2 cells of high or low passage Caco-2 cell strains. No significant effect of 1µM Ko143 on ciprofloxacin secretion was seen in the high passage Caco-2 cell monolayers (Figure 5.4) consistent with the low levels of BCRP expression. In contrast, in low PA Caco-2 cells 1µM Ko143 reduced, but did not abolish net ciprofloxacin secretion from 0.26 ± 0.02 $nmol.cm^{-2}.hr^{-1}$ to 0.13 ± 0.02 $nmol.cm^{-2}.hr^{-1}$ ($n = 4$, $P < 0.05$, Figure 5.5). The ratio of bi-directional permeabilities for ciprofloxacin was reduced from 2.29 ± 0.18 to 1.63 ± 0.07 in the presence of 1µM Ko143. No effect upon cellular accumulation across the apical and basolateral membranes in either high or low passage Caco-2 cells was seen for 1µM Ko143 (Figure 5.4C and 5.5C respectively).

The effects of a higher concentration of 10µM Ko143 was also tested in the low passage Caco-2 cells; net ciprofloxacin secretion was reduced from 0.26 ± 0.02 nmol.cm^{-2}.hr^{-1} to 0.11 ± 0.02 nmol.cm^{-2}.hr^{-1} (n = 3, P < 0.05, Figure 5.6). 10µM Ko143 also reduced the ratio of bi-directional permeabilities from 2.29 ± 0.18 to 1.36 ± 0.1 P < 0.05, (Figure 5.6). Therefore, a significant component of ciprofloxacin secretion remains after inhibition by Ko143. The IC_{50} of Ko143 on hBCRP was previously shown to be 1.06µM (Chapter 3 section 3.3.3.3).

Ciprofloxacin flux was sensitive to 50µM CsA in both Caco-2 strains, reducing net secretion from 0.39 ± 0.06 nmol.cm^{-2}.hr^{-1} to 0.14 ± 0.03 nmol.cm^{-2}.hr^{-1}, (n = 3, P < 0.05) and 0.26 ± 0.02 nmol.cm^{-2}.hr^{-1} to 0.08 ± 0.00(7) nmol.cm^{-2}.hr^{-1} (n = 3, P < 0.05) in high and low passage Caco-2 cell monolayers respectively (Figures 5.4B and 5.5B).

It has been previously shown that the anion transport inhibitor 4,4´-diisothiocyanostilbene-2,2´-disulphonic acid (DIDS) at 0.4mM inhibits ciprofloxacin secretion across Caco-2 cell monolayers (Cavet *et al.*, 1997). Secretory ciprofloxacin flux was reduced in both high and low passage Caco-2 cell monolayers from 0.39 ± 0.06 nmol.cm^{-2}.hr^{-1} to 0.14 ± 0.03 nmol.cm^{-2}.hr^{-1}, n = 3, P < 0.05, a ~65% reduction, and 0.26 ± 0.02 nmol.cm^{-2}.hr^{-1} to 0.09 ± 0.02 nmol.cm^{-2}.hr^{-1}, n = 3, P < 0.05, also a ~65% reduction, respectively (Figures 5.4B and 5.5B). DIDS also had a profound effect on cellular ciprofloxacin accumulation in both Caco-2 cell strains. In high passage Caco-2 cell monolayers cellular accumulation across the apical membrane rose from 14.91 ± 1.89 µM to 39.1 ± 9.16 µM, whilst accumulation across the basolateral membrane also increased from 24.59 ± 2.31 µM to 49.05 ± 12.61 µM. The same pattern was seen in the low passage Caco-2 cell-strain with apical accumulation

changing from 11.25 ± 0.55 µM to 26.32 ± 1.38 µM, whilst accumulation across the basolateral membrane also increased from 19.01 ± 1.51 µM to 60.2 ± 0.63 µM. Although DIDS is known to possess diverse pharmacological actions, the contrasting actions of DIDS on ciprofloxacin secretion in mouse Bcrp1-MDCKII and Caco-2 cells of both strains, suggests that DIDS inhibits a component of ciprofloxacin secretion that is unrelated to BCRP.

5.3.3 Is MRP4 involved in ciprofloxacin secretion?

Given the identification by Marquez *et al.* (2009) that MRP4 was involved in active efflux of ciprofloxacin from macrophages, a possible involvement of MRP4 in Caco-2 mediated ciprofloxacin transport was tested. First ciprofloxacin accumulation was investigated in WT-HEK 293 and MRP4-transfected HEK 293 epithelial cells.

Initially qPCR analysis confirmed a significantly greater expression of MRP4 mRNA in the MRP4-HEK 293 cells compared with the wild type cells (Figure 5.7, n = 3 extractions, $P < 0.05$). Net ciprofloxacin uptake was significantly reduced in the MRP4-overexpressing line in relation to the wild-type (Figure 5.8) indicating MRP4-mediated ciprofloxacin export. To confirm MRP4 involvement the addition of MRP inhibitors dipyrimadole (10µM), indomethacin (25µM), quercetin (10µM) and importantly MK571 (10µM) all resulted in significant increases in accumulation above control levels in both wild-type and transfected cells, with MK571 increasing ciprofloxacin accumulation in MRP4-HEK cells to the levels seen in un-transfected cells (Figure 5.8). Ko143 at 1µM was without effect on ciprofloxacin accumulation in either control or MRP4-HEK cells confirming the relative specificity of this agent.

These data therefore indicates that MRP-family members other than MRP4 are expressed in HEK cells and that ciprofloxacin is indeed an MRP4 substrate.

To test for MRP4 involvement in Caco-2 cells firstly qPCR was conducted to find the expression of MRP4 mRNA in both Caco-2 cell variants. Figure 5.7 shows the low passage Caco-2 cells had a greater expression of MRP4 mRNA in comparison to high passage Caco-2 cells ($n = 3$ extractions, $P < 0.05$). Low passage Caco-2 cells were used in the presence of the MRP inhibitors indomethacin (10μM) and MK571 (10μM) to confirm MRP4 involvement (Figure 5.6). No significant changes in ciprofloxacin flux were seen with any of the MRP4 modulating agents, confirming that MRP4 is not involved in Caco-2 cell mediated ciprofloxacin secretion.

Figure 5.1. Transepithelial [^{14}C]-ciprofloxacin flux across BCRP transfected MDCKII cell monolayers

Figures (A)-(C) show the time dependence of [^{14}C]-ciprofloxacin flux (0.1µCi.ml^{-1}, made up to 10µM with unlabelled ciprofloxacin) across confluent monolayers of (A) native MDCKII, (B) human BCRP-MDCKII (C) and mouse Bcrp1-MDCKII cells grown on 12-well permeable supports. Flux were determined in the apical-to-basal (J_{a-b}) and basal-to-apical (J_{b-a}) directions where secretory net flux (J_{net}) = J_{b-a} - J_{a-b}. Data bars are means of 3 independent experiments (n = 9 monolayers) ± SEM.

Figure (D) shows transepithelial [^{14}C]-ciprofloxacin flux averaged over the 3 hours for native MDCKII, human BCRP-MDCKII and mouse Bcrp1-MDCKII. Data bars are means of 3 independent experiments (n = 9 monolayers) ± SEM. * $P < 0.05$ represent significant difference of transfected MDCKII net flux compared to native MDCKII.

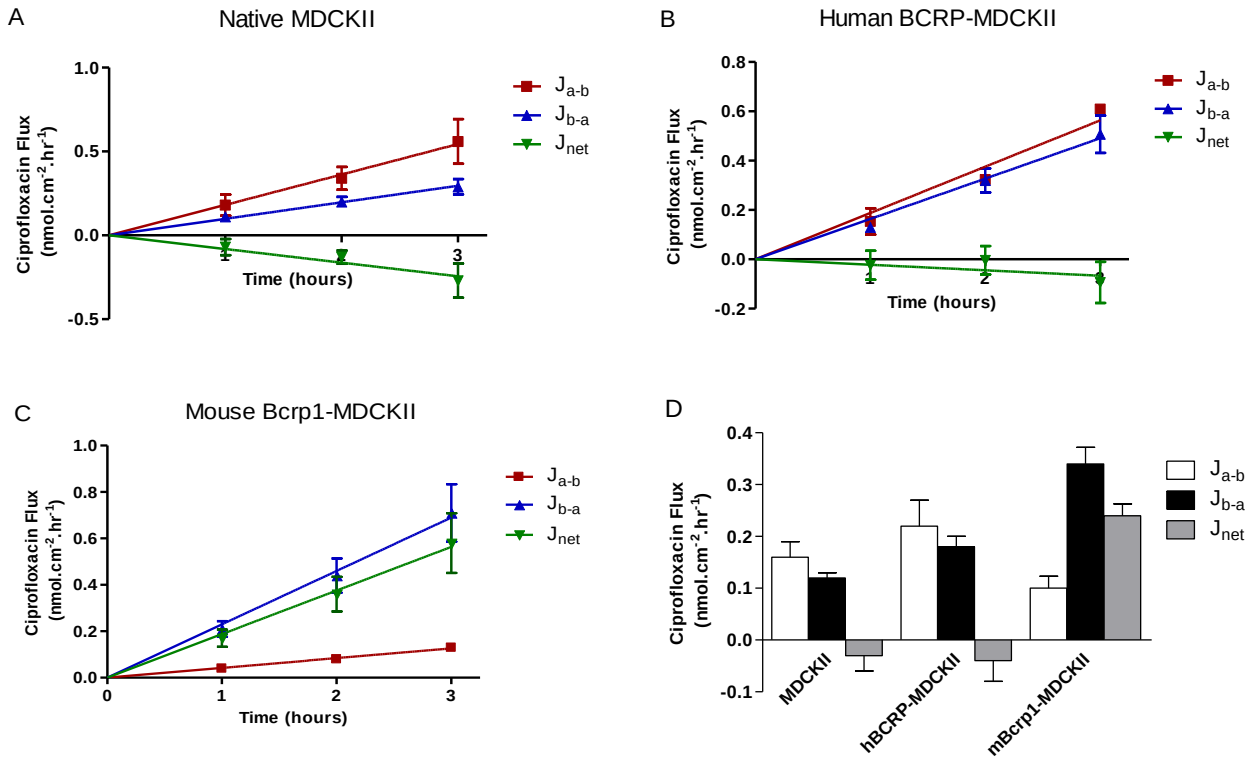

Figure 5.1. Transepithelial [^{14}C]-ciprofloxacin flux across native and BCRP transfected MDCKII cell monolayers

Table 5.1. Table showing bi-directional flux of ciprofloxacin in epithelial cell monolayers measured by HPLC-MS

Summary table of bi-directional flux in the apical to basal direction, basal to apical direction, net secretion (J_{net} = J_{b-a} - J_{a-b}) and efflux ratio (J_{b-a} / J_{a-b}) of ciprofloxacin across MDCKII and low PA Caco-2 cell monolayers. Cells were grown to confluency on 96-well permeable Transwell supports and assays were conducted via automation on a Hamilton StarPlus Robot. Ciprofloxacin was used at a concentration of 10µM. Data points are means of n = 4-6 wells, data were pooled and normalised from 2 independent experiments ± SEM.

	Bidirectional Flux ($pmol.cm^2.hr^{-1}$)			
	J_{a-b}	**J_{b-a}**	**J_{net}**	**Efflux Ratio**
MDCKII	22.3 ± 22.3	12.1 ± 12.1	-10.2 ± 10.2	0.5 ± 0.1
hBCRP-MDCKII	11.4 ± 4.9	28.5 ± 8.7	17.1 ± 4	2.5 ± 2.3
mBcrp1-MDCKII	1.2 ± 0.1	77.7 ± 5.8	76.6 ± 5.8	67 ± 2
Caco-2	1.2 ± 0.2	132.9 ± 23.1	131.8 ± 23	110.8 ± 9.4

Figure 5.2. Concentration dependent curves showing the transepithelial flux of ciprofloxacin across confluent mouse Bcrp1-MDCKII monolayers

Concentration dependence of unidirectional (J_{a-b}, J_{b-a}) and net ciprofloxacin secretion across confluent mouse Bcrp1-MDCKII monolayers. Donor [^{14}C]-ciprofloxacin was made up to concentrations using unlabelled ciprofloxacin. Curves show a Michaelis-Menten fit, net ciprofloxacin, K_m = 169.9 ± 62.7 µM and V_{max} = 10.2 ± 1.3 nmol.cm^{-2}.hr^{-1}. Data points are mean of n = 9 monolayers ± SEM from 3 independent experiments.

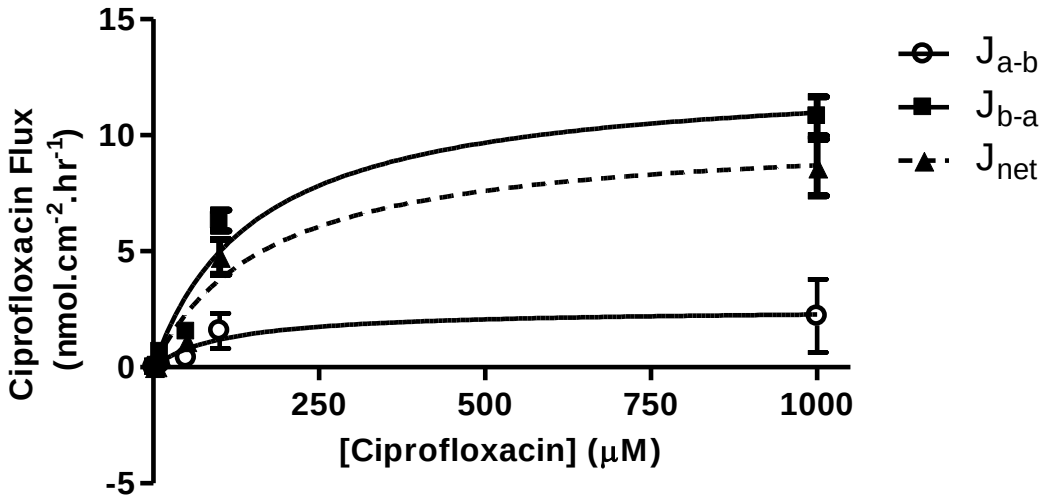

Figure 5.2. Concentration dependent curves showing the transepithelial flux of ciprofloxacin across confluent mouse Bcrp1-MDCKII monolayers

Figure 5.3. Effect of known ABC transporter inhibitors on (A) Bi-directional ciprofloxacin flux (B) Ciprofloxacin membrane permeability and (C) Intracellular ciprofloxacin levels across mouse Bcrp1-MDCKII monolayers

(A) Sensitivity of net transepithelial [^{14}C]-ciprofloxacin flux (0.1µCi.mL^{-1} plus 10µM unlabelled) to pharmacological inhibition across mBcrp1-MDCKII cell monolayers. Net flux (J_{net} = J_{b-a} - J_{a-b}) were determined in the presence and absence of Ko143 (1µM) and MK571 (10µM). Data bars are means of 3 independent experiments (n = 9 monolayers) ± SEM. Significant reductions in J_{net} compared to control values are denoted by * P < 0.05.

(B) Sensitivity of [^{14}C]-ciprofloxacin permeability (0.1µCi.ml^{-1}, made up to 10µM with unlabelled) to pharmacological inhibition across mBcrp1-MDCKII cell monolayers. Cellular permeabilities (P_{b-a} / P_{a-b}) were determined in the presence and absence of Ko143 (1µM) and MK571 (10µM). Data bars are means of 3 independent experiments (n = 9 monolayers) ± SEM. Significant reductions in permeability compared to control values are denoted by * P < 0.05.

(C) Sensitivity of cellular [^{14}C]-ciprofloxacin uptake (0.1µCi.ml^{-1} made up to 10µM with unlabelled) to pharmacological inhibition across the apical and basolateral membranes of mBcrp1-MDCKII cell monolayers. The pharmacological inhibitors used were Ko143 (1µM) and MK571 (10µM). Data bars are means of 3 independent experiments (n = 9 monolayers) ± SEM. Significant reductions in accumulation compared to control values are denoted by * P < 0.05.

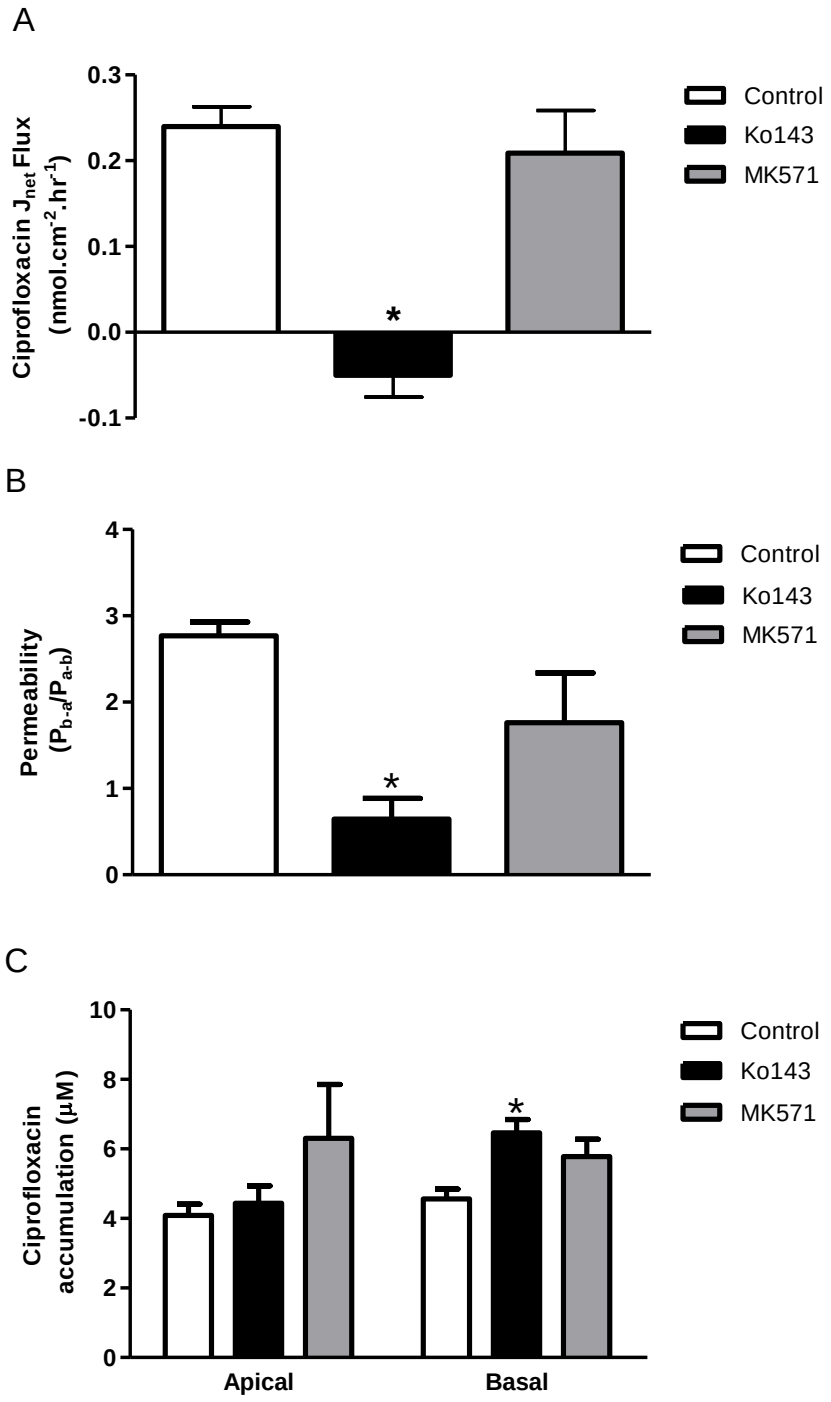

Figure 5.3. Effect of known ABC transporter inhibitors on (A) Bi-directional ciprofloxacin flux (B) Ciprofloxacin membrane permeability and (C) Intracellular ciprofloxacin levels across mouse Bcrp1-MDCKII monolayers

Figure 5.4. Transepithelial [^{14}C]-ciprofloxacin flux across high passage Caco-2 cell monolayers

(A) Time dependence of [^{14}C]-ciprofloxacin unidirectional flux (0.1µCi.ml^{-1}, made up to 10µM with unlabelled) across confluent monolayers of high PA strain Caco-2 cells (passage 111-116) grown on 12-well permeable supports. Flux were determined in the apical-to-basal (J_{a-b}) and basal-to-apical (J_{b-a}) directions where secretory net flux $J_{net} = J_{b-a} – J_{a-b}$. Data points are mean of n = 9 monolayers ± SEM from 3 independent experiments.

(B) Sensitivity of net transepithelial [^{14}C]-ciprofloxacin flux (0.1µCi.ml^{-1}, made up to 10µM with unlabelled) to pharmacological inhibition across high PA Caco-2 cell monolayers. Net flux ($J_{net} = J_{b-a} - J_{a-b}$) were determined in the presence and absence of CsA (50µM), DIDS (0.4mM) and Ko143 (1µM). Data bars are means of 3 independent experiments (n = 9 monolayers) ± SEM. Significant reductions in J_{net} compared to control values are denoted by * $P < 0.05$.

(C) Sensitivity of cellular [^{14}C]-ciprofloxacin uptake (0.1µCi.ml^{-1}, made up to 10µM with unlabelled) to pharmacological inhibition across the apical and basolateral membranes of high PA Caco-2 cell monolayers. The pharmacological inhibitors used were; CsA (50µM), DIDS (0.4mM) and Ko143 (1µM). Data bars are means of 3 independent experiments (n = 9 monolayers) ± SEM. Significant reductions in J_{net} compared to control values are denoted by *$P < 0.05$.

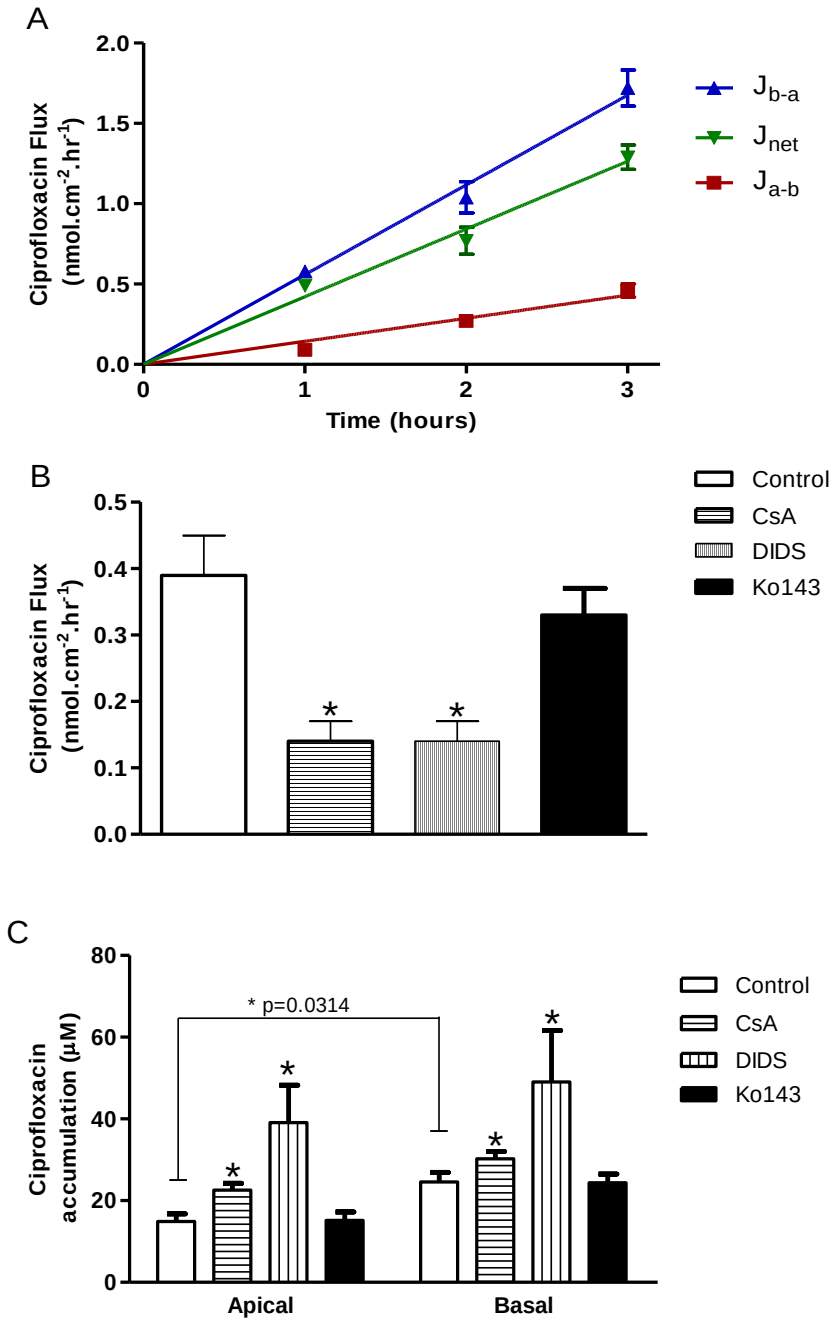

Figure 5.4. Transepithelial [^{14}C]-ciprofloxacin flux across high passage Caco-2 cell monolayers

Figure 5.5. Transepithelial [^{14}C]-ciprofloxacin flux across low passage Caco-2 cell monolayers

(A) Time dependence of [^{14}C]-ciprofloxacin unidirectinal flux (0.1µCi.ml^{-1}, made up to 10µM with unlabelled) across confluent monolayers of low PA strain Caco-2 cells (passage 34-45) grown on 12-well permeable supports. Flux were determined in the apical-to-basal (J_{a-b}) and basal-to-apical (J_{b-a}) directions where secretory net flux (J_{net}) = $J_{b-a} – J_{a-b}$. Data points are mean of n = 9-12 monolayers ± SEM from 3-4 independent experiments.

(B) Sensitivity of net transepithelial [^{14}C]-ciprofloxacin flux (0.1µCi.ml^{-1}, made up to 10µM with unlabelled) to pharmacological inhibition across low PA Caco-2 cell monolayers. Net flux (J_{net} = J_{b-a} - J_{a-b}) were determined in the presence and absence of CsA (50µM), DIDS (0.4mM) and Ko143 (1µM). Data bars are means of 3-4 independent experiments (n = 9-12 monolayers) ± SEM. Significant reductions in J_{net} compared to control values are denoted by * $P < 0.05$.

(C) Sensitivity of cellular [^{14}C]-ciprofloxacin uptake (0.1µCi.ml^{-1}, made up to 10µM with unlabelled) to pharmacological inhibition across the apical and basolateral membranes of low PA Caco-2 cell monolayers. The pharmacological inhibitors used were; CsA (50µM), DIDS (0.4mM) and Ko143 (1µM). Data bars are means of 3-4 independent experiments (n = 9-12 monolayers) ± SEM. Significant reductions in J_{net} compared to control values are denoted by * $P < 0.05$.

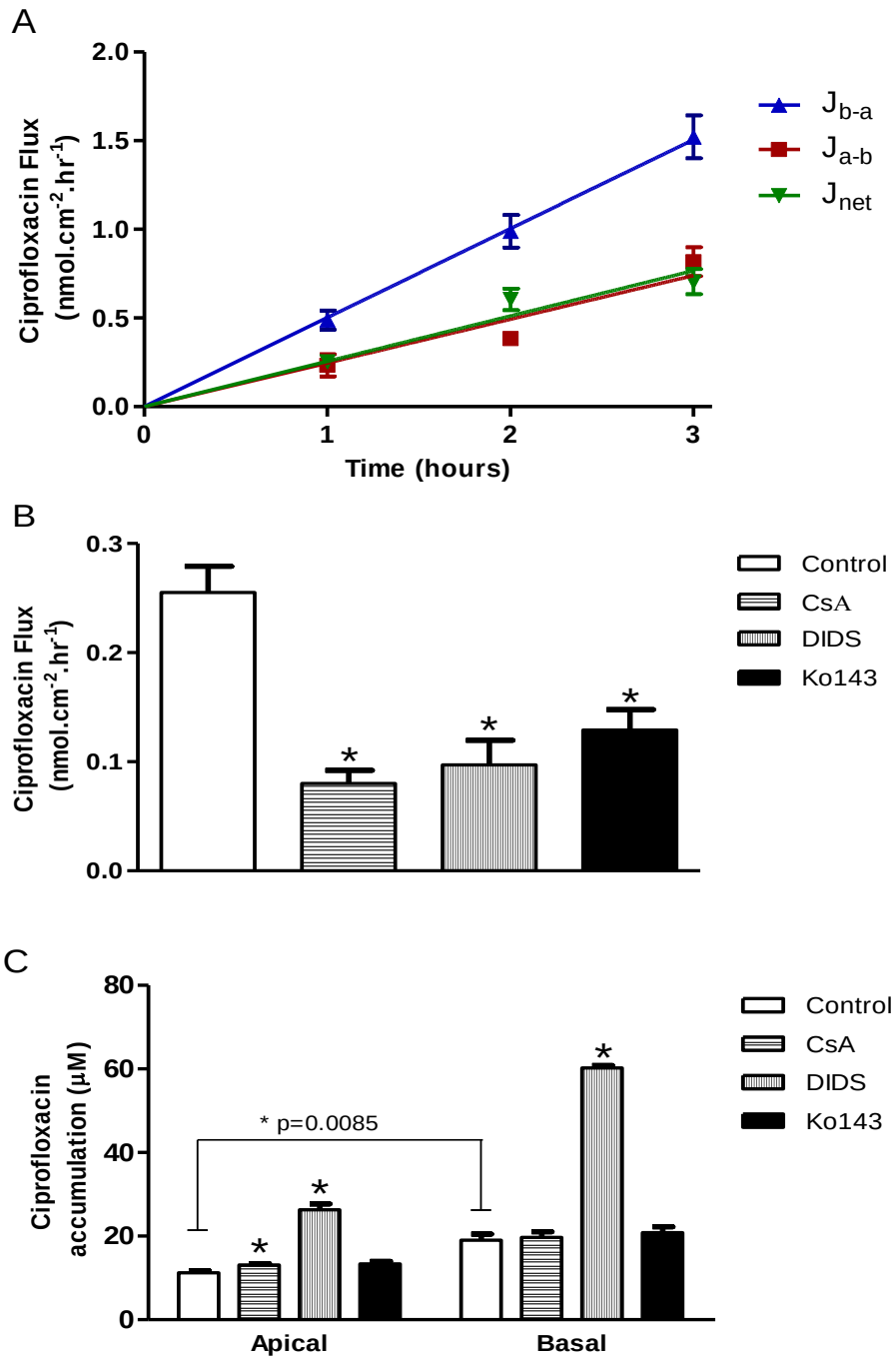

Figure 5.5. Transepithelial [^{14}C]-ciprofloxacin flux across low passage Caco-2 cell monolayers

Figure 5.6. Effect of BCRP and MRP4 inhibitors on (A) Net ciprofloxacin flux (J_{net}) (B) Ciprofloxacin membrane permeability and (C) Cellular ciprofloxacin uptake across low passage Caco-2 monolayers

(A) Sensitivity of net transepithelial [^{14}C]-ciprofloxacin flux (0.1µCi.ml^{-1}, made up to 10µM with unlabelled) to pharmacological inhibition across low PA Caco-2 cell monolayers. Net flux (J_{net} = J_{b-a} - J_{a-b}) were determined in the presence and absence of the MRP4 inhibitors indomethacin (25µM) and MK571 (10µM), and the BCRP inhibitor Ko143 at a higher concentration of 10µM. Data bars are means of 3-4 independent experiments (n = 9-12 monolayers) ± SEM. Significant reductions in J_{net} compared to control values are denoted by * $P < 0.05$.

(B) Sensitivity of [^{14}C]-ciprofloxacin permeability (0.1µCi.ml^{-1}, made up to 10µM with unlabelled) to pharmacological inhibition across low PA Caco-2 cell monolayers. Cellular permeabilities (P_{b-a} / P_{a-b}) were determined in the presence and absence of the MRP4 inhibitors indomethacin (25µM) and MK571 (10µM), and the BCRP inhibitor Ko143 at a higher concentration of 10µM. Data bars are means of 3-4 independent experiments (n = 9-12 monolayers) ± SEM. Significant reductions in permeability compared to control values are denoted by * $P < 0.05$.

(C) Sensitivity of cellular [^{14}C]-ciprofloxacin uptake (0.1µCi.ml^{-1}, made up to 10µM with unlabelled) to pharmacological inhibition across the apical and basolateral membranes of low PA Caco-2 cell monolayers. The pharmacological inhibitors used were the MRP4 inhibitors indomethacin (25µM) and MK571 (10µM), and the BCRP inhibitor Ko143 at a higher concentration of 10µM. Data bars are means of 3-4 independent experiments (n = 9-12 monolayers) ± SEM. Significant reductions in accumulation compared to control values are denoted by * $P < 0.05$.

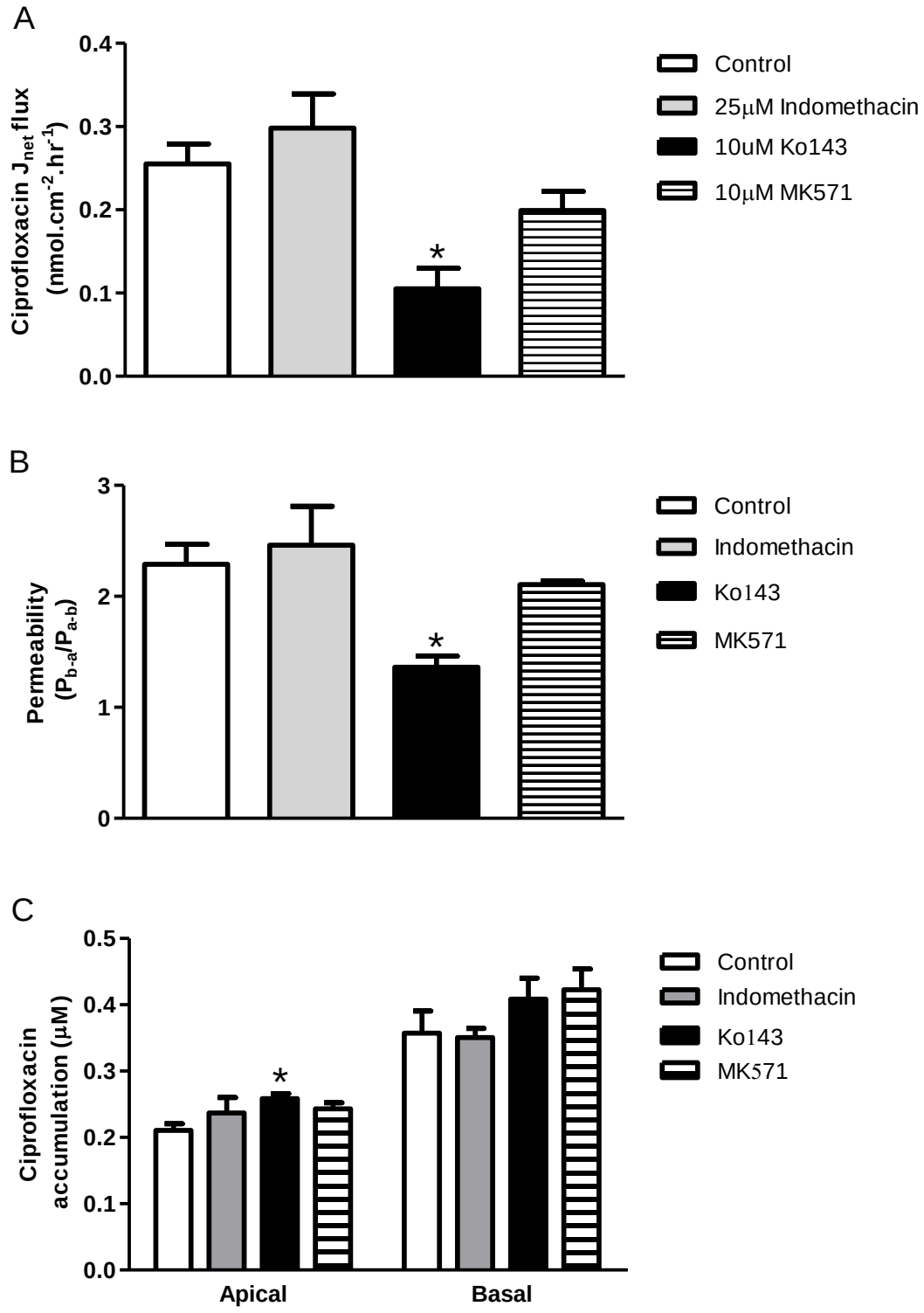

Figure 5.6. Effect of BCRP and MRP4 inhibitors on (A) Net ciprofloxacin flux (J_{net}) (B) Ciprofloxacin membrane permeability and (C) Cellular ciprofloxacin uptake across low passage Caco-2 monolayers

Figure 5.7. Demonstration of MRP4 mRNA expression in (A) HEPG2, (B) HEK 293 and (C) Caco-2 cells

(A) An agarose gel image showing PCR products from HepG2 cells. Lane 1 and 2 are reverse transcriptase negatives showing no bands of MRP4 or GAPDH respectively. Lanes 3 shows the expected MRP4 product at 236 base pairs. Lane 4 shows the expected housekeeping gene product of GAPDH. PCR product of MRP4 was confirmed by nucleotide sequencing by comparing to published sequence, giving 98% identity (see Materials and Methods section 2.2.3.4).

(B) Real time PCR analysis indicating expression of MRP4 mRNA in native HEK and human transfected MRP4-HEK cells. Data bars are adjusted relative to GAPDH expression. Quantification was done via the Pfaffl method (bars represent n = 3 extractions, ± SD). Significant difference in MRP4 mRNA between native HEK and MRP4-HEK cells denoted by * $P < 0.05$.

(C) Real time PCR analysis indicating expression of MRP4 mRNA in Caco-2 epithelia. Data bars are adjusted relative to GAPDH expression. Quantification was done via the Pfaffl method (bars represent n = 3 extractions, ± SD). Significant difference in MRP4 mRNA between low and high passage Caco-2 cells denoted by * $P < 0.05$.

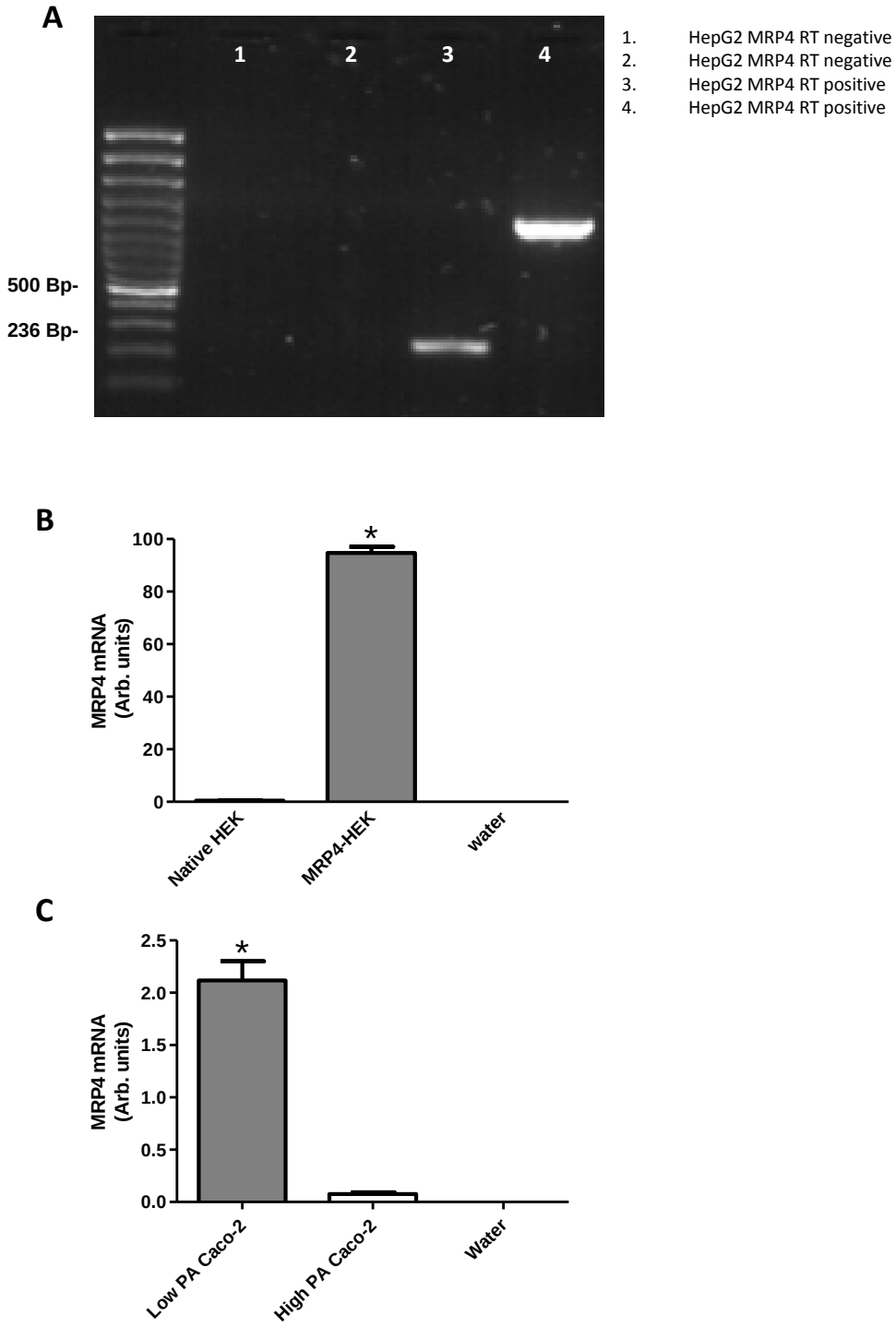

Figure 5.7. Demonstration of MRP4 mRNA expression in (A) HEPG2, (B) HEK 293 and (C) Caco-2 cells

Figure 5.8. Effect of MRP4 transfection on [^{14}C]-ciprofloxacin cellular uptake in HEK 293 cells

(A) Sensitivity of cellular [^{14}C]-ciprofloxacin uptake (0.1µCi.ml^{-1}, made up to 10µM with unlabelled) to pharmacological inhibition across native and MRP4 transfected HEK cells. Cells were grown to confluency on 12-well plates. Uptake was measured in the presence and absence of the MRP inhibitors dypyridamole (10µM), indomethacin (25µM), MK571 (10µM) and quercetin (10µM). Data bars are means of 3 independent experiments (n = 9 wells) ± SEM. Significant reductions in uptake compared to control values are denoted by * $P < 0.05$, whilst significant differences between HEK native cells and MRP4-HEK cells are denoted by #.

(B) Sensitivity of cellular [^{14}C]-ciprofloxacin uptake (0.1µCi.ml^{-1}, made up to 10µM with unlabelled) to pharmacological inhibition across native and MRP4 transfected HEK cells. Cells were grown to confluency on 12-well plates. Uptake was measured in the presence and absence of the BCRP inhibitor Ko143 (1µM).

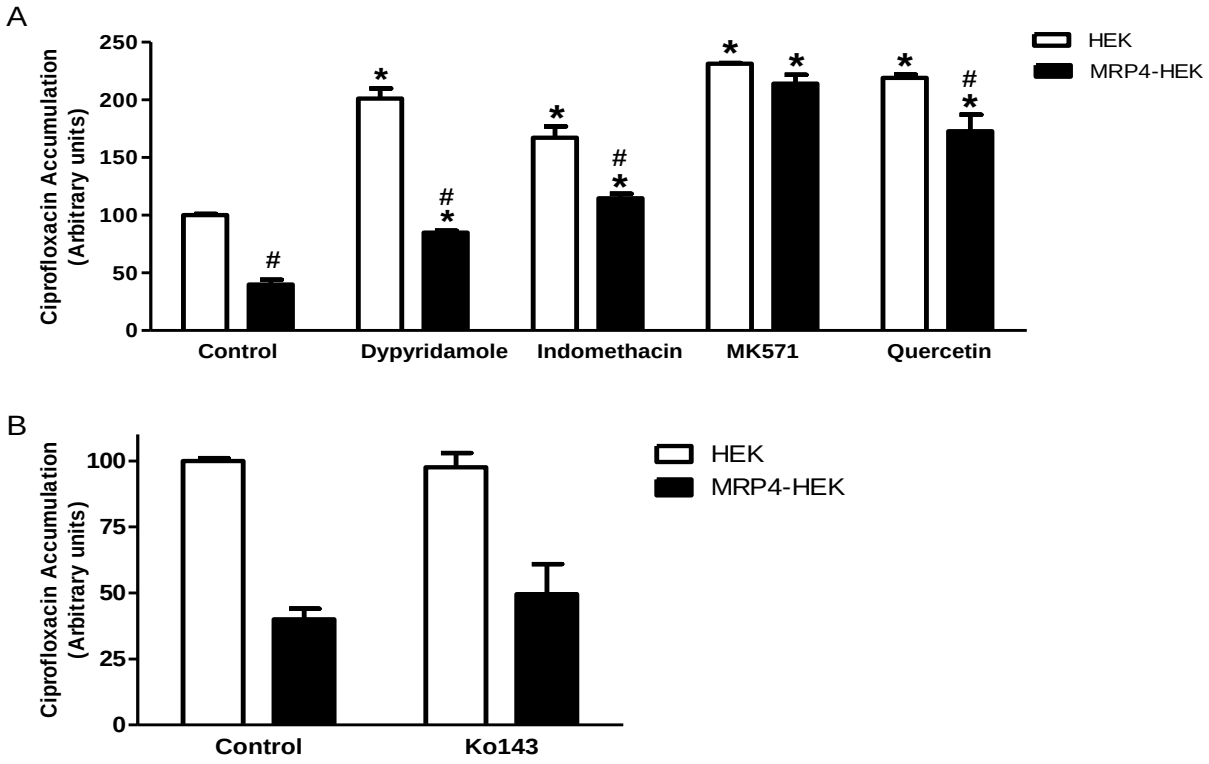

Figure 5.8. Effect of MRP4 transfection on [^{14}C]-ciprofloxacin cellular uptake in HEK 293 cells

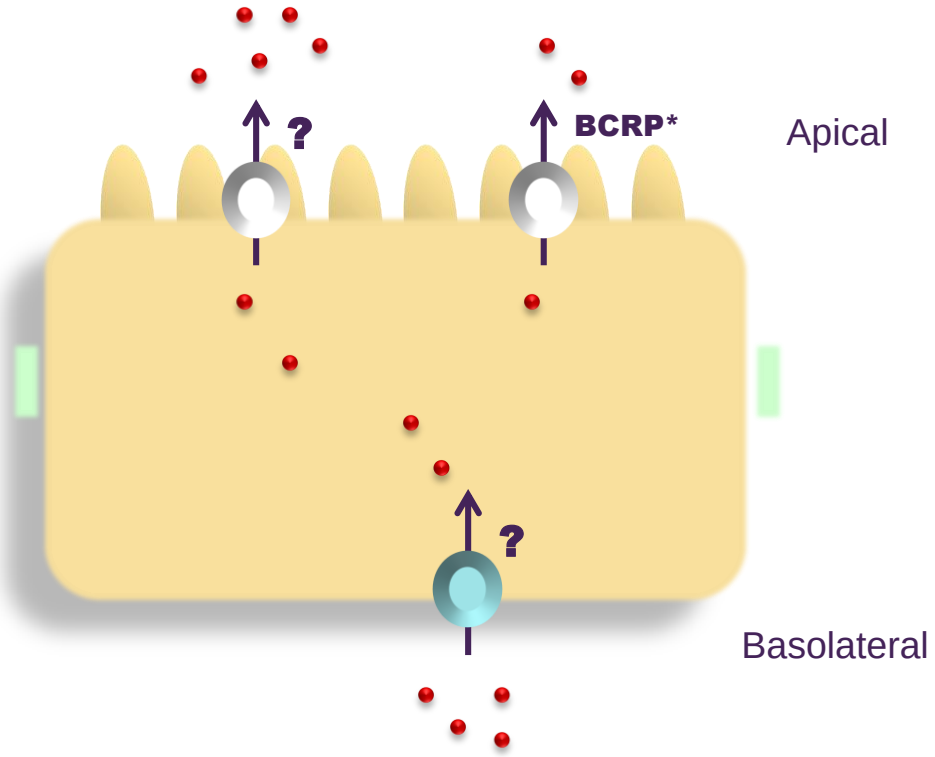

Figure 5.9. Summary diagram of ciprofloxacin transport across Caco-2 cells

Ciprofloxacin (shown in red) was shown to be taken up into both low and high passage Caco-2 cells via an unknown route, mainly across the basolateral membrane. Ciprofloxacin net secretion occurred across the apical membrane and was mediated by BCRP and an unknown mechanism across the low passage Caco-2 cells. Whilst in high passage Caco-2 cells BCRP is not involved in secretion due to a low cellular expression of BCRP. The exit across the apical membrane is energy dependent and remains to be elucidated (candidates that remain include OATPs and MATE transporters).

5.4 Discussion

It has previously been shown that a major route of ciprofloxacin clearance in vivo is secretion across the apical membrane of enterocytes into the intestinal lumen (Sorgel *et al.*, 1989; Sorgel *et al.*, 1991). The primary route of ciprofloxacin clearance is via the kidneys; however the intestinal route of secretion becomes increasingly important in patients that have compromised renal function (Rohwedder *et al.*, 1990). Caco-2 cells have been previously used to investigate the intestinal clearance of ciprofloxacin and demonstrate net secretion of ciprofloxacin across reconstituted Caco-2 epithelia with evidence for an energy-dependent export across the apical surface (Cavet *et al.*, 1997; Griffiths *et al.*, 1993; Lowes & Simmons, 2002). Calculated unidirectional flux show that accumulation is at the basolateral surface. This accumulation compared to the external medium (an observation seen in this study also) likely acts as a driving force across the apical membrane. In this study, two strains of Caco-2 cells have further shown net secretion of ciprofloxacin across the apical membrane and a similar ciprofloxacin accumulation to previous reports (Cavet *et al.*, 1997; Griffiths *et al.*, 1993), resulting in ciprofloxacin cellular concentrations higher than the external medium (Figures 5.5 and 5.6). Differing strains of Caco-2 cells have arisen most likely due to the heterogeneous nature of the original culture and to variable cell selection pressures arising in different laboratories due to differences in growth conditions, seeding densities, and genetic drift from the original cells (Sambuy *et al.*, 2005). The two Caco-2 cell strains used in the present studies have different transporter expression profiles with marked differences in ABC-transporter expression, most notably with respect to BCRP and MRP4. Importantly, despite such differences, both Caco-2 cell strains display net ciprofloxacin secretion across the

apical surface with a similar basolateral accumulation in these cells (summary diagram of ciprofloxacin across Caco-2 cells is shown in Figure 5.9).

This study confirms that mouse Bcrp transports ciprofloxacin across the apical surface of mBcrp1-MDCKII cells, previously shown by Merino *et al.* (2006). Ciprofloxacin exit mediated by mBcrp maintains a low concentration inside the cell. Furthermore it shows that ciprofloxacin accumulation was much lower compared with the Caco-2 cells.

Ko143, a selective BCRP inhibitor, completely abolished net secretion of ciprofloxacin and increased basolateral accumulation in the mBcrp1-MDCKII cells. Conversely ciprofloxacin transport by human BCRP gave mixed results. Human BCRP transfected MDCKII cells did not show secretion of radiolabelled [^{14}C]-ciprofloxacin. Ciprofloxacin measured by the more sensitive approach of HPLC-MS showed a significant net secretion in the hBCRP-MDCKII cells but this was low compared with mBcrp1-MDCKII cells. It may be concluded that human BCRP may transport ciprofloxacin, but that its affinity may be reduced compared to that of the mouse Bcrp protein. In Chapter 3 it has been demonstrated that the hBCRP-MDCKII and mBcrp1-MDCKII cell lines both express BCRP mRNA and protein consistent with functional activity. Therefore it is unlikely that a difference in expression level may explain the difference in ciprofloxacin transport observed between the mBcrp and hBCRP transfected cell lines as suggested by Merino *at el* (2006). One notable difference between the two proteins expressed in MDCK cells is the difference in glycosylation on human BCRP and mouse Bcrp. This difference may result in subtle differences in substrate binding. Further investigation on this aspect is warranted.

The fact that low and high passage Caco-2 cell layers secrete ciprofloxacin suggests that a substantial fraction of such secretion occurs via a BCRP-independent route. A different approach in investigating the nature of Caco-2 cell mediated ciprofloxacin secretion was the use of selective pharmacological inhibitors. Whereas Ko143 was ineffective in reducing ciprofloxacin secretion in the high passage Caco-2 cells, due to the very low expression of BCRP expression in this Caco-2 cell strain (see Chapter 3), in the low passage Caco-2 cell line, which has a greater expression of BCRP, a reduction in net secretion of ~65% was observed with 1μM Ko143. These data show that BCRP may play a significant role in ciprofloxacin secretion across the human intestine, but that additional mechanism(s) of ciprofloxacin secretion are important.

Marquez *et al.* (2009) showed that murine Mrp4 was responsible for ciprofloxacin transport in J774 macrophages. DIDS has been shown both in this study and previously to be effective in reducing net secretion and increasing cellular ciprofloxacin accumulation in Caco-2 cells. DIDS inhibits the exit pathway at both the apical and basolateral membranes whilst active uptake causes the ciprofloxacin concentration to reach levels far greater than the external medium. DIDS is also known to be effective at inhibiting transport by the MRP family members. With this reasoning human MRP4 was investigated as a transport mechanism of ciprofloxacin in this study. MRP4 over-expressing HEK 293 cells (Wielinga *et al.*, 2002) were shown to accumulate less ciprofloxacin compared with native HEK cells. Known MRP inhibiting agents such as MK571 (Reid *et al.*, 2003a; van Aubel *et al.*, 2002; Wu *et al.*, 2005) increased ciprofloxacin accumulation in these HEK cells. Taken together these data confirm ciprofloxacin as a substrate for MRP4 in the over-expressing cell lines. The efficacy of agents such as MK571 in both native and

transfected models suggest endogenous expression of MRP family members besides MRP4 in HEK 293 cells. Ko143 was without effect on MRP4.

MRP4 mRNA was analysed in both Caco-2 cell strains; high passage Caco-2 cells showed poor expression whilst the lower passage Caco-2 cells had a greater expression of MRP4 mRNA. It was found the MRP4 inhibiting agents had no to little effect on net ciprofloxacin secretion across Caco-2 cells and so the involvement of MRP4 in Caco-2 mediated ciprofloxacin efflux can be excluded.

Over-expression of ABC transporters (BCRP, MRP4) in heterologous systems has confirmed ciprofloxacin as a substrate and highlights the complex transport nature of this zwitterion. As already noted ciprofloxacin has a high-volume of distribution suggesting ready access to the intracellular compartment of many cells, thus ABC-mediated efflux must exist with specific influx pathways. In macrophages it is hypothesised that MRP4 up-regulation may render intracellular antibiotic concentrations to be negligible, so providing a bacterial niche inaccessible to therapy (Marquez *et al.*, 2009). It is apparent the major route of secretion from Caco-2 cells is neither via BCRP nor MRP4, even though BCRP may be involved depending on the expression level of BCRP in the Caco-2 cells. The alternative transport pathway still needs to be elucidated and several candidates remain. The alternative role of OATPs (Kalliokoski & Niemi, 2009) and other energy dependent efflux transporters such as MATE1 (Meyer zu Schwabedissen *et al.*, 2010) require further investigation. Human intestinal tissue also needs to be investigated to see if BCRP plays a greater role in ciprofloxacin efflux in vivo compared with the human intestinal Caco-2 cells.

6. Regulation of functional BCRP in Caco-2 cells

6.1 Introduction

The previous chapters have shown that a diverse range of substrates may be transported by BCRP. Additionally since BCRP is highly expressed in gastro-intestinal mucosae, BCRP-mediated excretion will affect the absorption and subsequent disposition of substrates within the body. Data in Chapter 5 show that BCRP expression varies between 2 strains of human intestinal Caco-2 cells resulting in altered transepithelial flux of substrates such as ciprofloxacin. Therefore, factors affecting the expression and amount of BCRP present in its physiological location at the brush-border membrane of enterocytes will impact on substrate absorption from the intestinal lumen.

Many studies on other ABC transporters such as MDR1 have shown that transcription is directly regulated by nuclear receptors (PXR/RXR) that act as 'xenosensors'. MDR1 substrates are invariably regulators of MDR1 expression mediated by nuclear receptor transcriptional activation (Haslam *et al.*, 2008).

A well characterised endogenous mechanism of BCRP transcriptional regulation is mediated via nuclear receptors of sex steroid hormones. Sex hormone (e.g. estrogen, progesterone) regulation of human BCRP would result in sex differences in BCRP expression in the intestine which has not been seen in previous studies (Gutmann *et al.*, 2005). However Merino *et al.* (2005) have shown changes in human liver BCRP expression and there are reports of significantly higher plasma clearance in males than females for the BCRP substrate methotrexate and topotecan (Gallo *et al.*, 2000; Godfrey *et al.*, 1998; Loos *et al.*, 2000; Wall *et al.*, 2000). Furthermore BCRP expression is known to be highest in the placenta and the

expression varies considerably during the different stages of foetal development. Wang *et al.* (2008) have investigated the molecular mechanism underlying this regulation in human placental BeWo cells and have shown that progesterone PRA and PRB receptor isoforms differentially regulate BCRP transcription; PRB regulating transcription in a positive manner whilst PRA having limited effect, but when co-expressed with PRB it suppresses PRB-mediated activation (Wang *et al.*, 2008a). BCRP has been shown to be a survival factor during the formation of the placental syncytium (Evseenko *et al.*, 2007).

Ee *et al.* (2004) have identified an estrogen response element in the promoter region of BCRP that when stimulated causes an increase in BCRP mRNA (Ee *et al.*, 2004). Vore *et al.* (2008) further show that stimulation via 17β-estradiol and progesterone causes a modulation of BCRP expression through this nuclear response element. Several studies report negative regulation of BCRP protein expression by oestrogen; in oestrogen receptor alpha positive MCF cells 17β-estradiol reduces BCRP protein by a post-translational mechanism (Imai *et al.*, 2005). Furthermore 17β-estradiol reduces BCRP mRNA and protein via the oestrogen receptor beta in rat brain capillaries (Mahringer & Fricker, 2010). A potential role for sex hormone regulation of BCRP expression in the intestine can therefore be postulated.

Another mechanism of induction noted for human BCRP and mouse Bcrp is mediated through hypoxia-inducible factor 1/2α (HIF-1/2α) that is activated in hypoxic conditions (Krishnamurthy & Schuetz, 2005). In cardiac stem cells hypoxia-inducible factor (HIF-2α) binds to a conserved HIF-2α response element in the murine Abcg2 promoter to increase Bcrp expression (Martin *et al.*, 2008). Transcriptional assays reveal a dose-dependent activation of Abcg2 expression by HIF-2α. Caco-2 cells arose from a colonic tumour and this cell line is likely to be associated with

hypoxia, however enterocytes are well perfused with blood and therefore unlikely to be subjected to hypoxia under normal physiological conditions. As there were limited facilities to culture Caco-2 cells under hypoxic conditions the HIF-1α pathway was not investigated.

Since enterocytes are exposed to a wide variety of xenobiotics via diet it seems highly likely that dietary components will act to regulate the expression of BCRP along the gastro-intestinal tract. The variability of BCRP expression seen in human intestinal tissue (Zamber *et al.*, 2003) may be down to inter-individual variation in diet and intestinal microflora. Flavonoids are plant secondary metabolites, primarily natural in origin, which are present in most diets. They are found in chocolate, citrus fruits, liquorice, red wine, tea and vegetables to name but a few and an average intake of flavonoids have been approximated to be 1g per day (Formica & Regelson, 1995). They are heavily metabolised by the gut flora and thus active concentrations will be reduced considerably. However these compounds have been recognised to have beneficial health effects with anti-carcinogenic effects (Havsteen, 2002). Thus foods with high flavonoid content are becoming more popular and even flavonoid supplements, such as quercetin and genistein are available, which are often taken over long periods of time. Many studies link the modulating effects of these flavonoids with the ABC-efflux proteins, they have diverse structures and are known to be substrates, inhibitors and inducers of the ABC-efflux proteins (Alvarez *et al.*, 2009; Ebert *et al.*, 2007; Wang, 2007), thus flavonoids may be implicated with drug interactions. Recently the aryl hydrocarbon receptor has been shown to be a transcriptional activator of BCRP expression via a proximal dioxin response element within the BCRP promoter region (Tan *et al.*, 2010). The effects of several flavonoids and aryl hydrocarbon receptor (AhR) agonists on BCRP regulation in Caco-2 cells; β-

naphthoflavone (BNF), chrysin, dibenzoylmethane (DBM), quercetin and tert-butylhydroquinone (TBHQ) have therefore been tested.

Other exogenous factors of BCRP regulation are pharmaceuticals. To date few drugs have been shown to be BCRP regulators but there are one group of compounds that do have an effect in vitro. The thiazolidinediones (glitazones) are used to treat type II diabetes by reducing blood glucose and increasing insulin sensitivity, however they seem to have an alternative role in up-regulating BCRP expression and function in vitro (Szatmari *et al.*, 2006). The thiazolidinediones are PPARγ agonists and thus this pathway was investigated in Caco-2 cells using the thiazolidinedione rosiglitazone.

Dynamic regulation of BCRP transcription in the human gastrointestinal tract is therefore likely, several transcriptional activators (sex steroid nuclear receptors, HIF, AhR, PPARγ) have been identified in various tissues. In this chapter mechanisms of BCRP induction identified in the literature have been investigated in low PA human intestinal Caco-2 cells which both express normal polarised BCRP expression and which may be easily subjected to prolonged exposure to inducing agents by inclusion in the culture medium. Functional activity has been assessed using the BCRP substrates identified in Chapter 3, namely, flavopiridol, prazosin and nitrofurantoin.

6.2 Methods

6.2.1 Induction pre-treatments of Caco-2 cell monolayers for qPCR, immunoblotting and bi-directional transport assays.

Cell monolayers were incubated between 24-72 hours with different agents, the DMSO concentration never exceeding 0.1%. All inducing agents were made up in DMSO and then diluted to the required final concentration using phenol red free Dulbecco's Minimum Essential Media. For measuring changes in mRNA cells were grown in 6-well plates then incubated between 24-72 hours depending on the experiment.

For measuring changes in protein expression, Caco-2 cells were grown in 75cm^2 flasks and were incubated in the presence of inducing agents for 72 hours. Whilst for measuring changes in protein function cells were grown on 96-well Transwell plates until confluency and were incubated between 24-72 hours, again depending on the experiment.

When measuring changes in Caco-2 cell mRNA and protein expression the cells were washed twice with 1% Phosphate Buffered Saline (PBS) and protocols for RNA extraction and protein extraction were followed (shown in Materials and Methods, sections 2.2.3.1 and 2.2.4 respectively).

For measuring changes in protein function cell monolayers had an initial washout period consisting of 2 initial washes with pre-warmed media at 37°C and followed by incubation for 60 minutes. 60 minutes washout being long enough to ensure any inducing agent has had adequate dilution and transit time from the cell. The washout duration was not too long as to prevent a reversal of the induction. The protocol was then followed as described in sections 2.2.2.3.

6.3 Results

6.3.1 The effect of induction agents on BCRP mRNA expression in Caco-2 cells

Since phenol red, or lipophilic impurities in phenol red, possess weak estrogenic activity (Kd 10-20μM on the estrogen receptor in MCF-7 cells) and phenol red concentrations in culture media are 15-45μM (Berthois *et al.*, 1986; Bindal *et al.*, 1988) the effects of BCRP modulating/inducing agents has been determined in custom phenol red free media. Concentrations of inducing agents used had previously been reported to increase BCRP mRNA, protein or function (Ebert *et al.*, 2007; Szatmari *et al.*, 2006). Initially levels of BCRP mRNA were measured using real time PCR analysis after 24 hours of incubation with inducing agents; however limited effects were shown after this time period (data not shown). A longer incubation time of 72 hours was then chosen for BCRP induction (Figure 6.1). Several phytochemicals were used to modulate BCRP expression. β-naphthoflavone (BNF) at 10μM gave a significant increase in BCRP mRNA expression ($n = 3$ extractions, $P < 0.05$, Figure 6.1). The AhR-agonists chrysin (at 10μM), dibenzoylmethane (DBM at 50μM) and quercetin (at 20μM) showed a non-significant increase in BCRP mRNA, in contrast to increases reported by Ebert *et al.* (2006). However the synthetic antioxidant tert-butylhydroquinone (TBHQ at 50μM) which is also an AhR agonist (Gharavi & El-Kadi, 2005) caused a significant increase in BCRP mRNA similar to that shown by Ebert *et al.* (2006). The estrogen, 17-β-estradiol had no effect on BCRP mRNA expression (Figure 6.1) unlike previous findings in different cell types (Vore & Leggas, 2008). The greatest induction of BCRP mRNA was seen with pre-

incubation with the thiazolidinedione rosiglitazone (n = 3 extractions, $P < 0.05$, Figure 6.1).

6.3.2 The effect of induction agents on the mRNA expression of nuclear receptors AhR and PPARγ

The agents with the greatest effect on BCRP mRNA were the AhR agonists β-naphthoflavone (BNF) and TBHQ, and the PPARγ agonist rosiglitazone. In order to confirm expression of the AhR and PPARγ nuclear receptors, RT-PCR and real time PCR analysis were conducted. Figure 6.2A confirms expression of AhR mRNA. AhR mRNA expression levels showed no significant differences with pre-incubation with the phytochemicals BNF, chrysin, DBM and quercetin. Only TBHQ had a significant effect on increasing AhR mRNA (n = 3 extractions, $P < 0.05$, Figure 6.2). Figure 6.3A confirms expression of PPARγ. No significant change in PPARγ mRNA expression was seen in the presence of any of the inducing agents, including the PPARγ agonist rosiglitazone (Figure 6.3B).

6.3.3 The effect of induction agents on BCRP protein expression in Caco-2 cells

Since significant increases in BCRP mRNA were observed, especially with BNF and rosiglitazone pre-incubation, BCRP protein expression was measured by immunoblotting with the mouse anti-human BCRP antibody BXP-21. A faint band for BCRP at ~72kDa was observed in the control low passage Caco-2 cells (Figure 6.4). BCRP-transfected MDCKII cell protein is included as a positive control and a similar band at ~72kDa is observed (Figure 6.4). Caco-2 cells incubated for 72 hours in the presence of BNF and rosiglitazone showed an increase in density of the ~72kDa

BCRP band. Note that protein loading for each sample was at a similar high level as shown by re-probing the blot with an anti-tubulin antibody giving a band at ~50kDa (Figure 6.4).

6.3.4 Testing the inhibitory effects of induction agents on the bi-directional transport of flavopiridol

Flavopiridol was previously shown in this study to be a human BCRP substrate using BCRP-MDCKII transfected layers (Chapter 4); however we have to note that there was a significant endogenous secretion of flavopiridol in native MDCKII epithelial layers indicating that there is more than one component of secretion in hBCRP-MDCKII cells. In order to test inducing agents as potential substrate inhibitors of hBCRP, their effect on the bi-directional transport of flavopiridol in the hBCRP-MDCKII cells was tested (Figure 6.5). Chrysin (10μM) is a potent inhibitor of flavopiridol secretion (donor concentration 10μM), reducing net flavopiridol secretion from 3.3 ± 0.16 nmol.cm^{-1}.hr^{-1} in the control to 1.28 ± 0.03 nmol.cm^{-1}.hr^{-1} ($P < 0.05$), with a similar inhibitory action compared to Ko143 (Figure 6.5). Chrysin acts as a potent BCRP transporter inhibitor (Alvarez *et al.*, 2009; Wang, 2007; Zhang *et al.*, 2005). Other phytochemicals, quercetin and naringenin, both had a significant effect on reducing flavopiridol net secretion at 10μM ($P < 0.05$, Figure 6.5). Quercetin is a known inhibitor of BCRP and MDR1 (Hsiu *et al.*, 2002; Sesink *et al.*, 2005) and naringenin inhibits both BCRP and MDR1 also (Ahmed-Belkacem *et al.*, 2005; de Castro *et al.*, 2007). BNF did not inhibit flavopiridol secretion at the concentration used (10μM). The hormones 17β-estradiol and hydrocortisone had dissimilar effects, with 17β-estradiol showing no effect whilst hydrocortisone (both 10μM) gave significant inhibition of flavopiridol secretion. Rosiglitazone at 10μM gave slight inhibition of flavopiridol transport and has been shown previously to be an inhibitor

of both BCRP and MDR1 (Weiss *et al.*, 2009). It should be noted that these inhibitory actions do not discriminate between hBCRP and the endogenous secretory capacity of MDCKII epithelial cells.

This data set shows that inducing agents, if present, will act as potential inhibitors of BCRP/endogenous secretion. Removal of the external medium and a short period of incubation in drug-free medium are required prior to measurement of secretory capacity.

6.3.5 The effect of induction agents on the bi-directional transport of BCRP substrates in low passage Caco-2 epithelia

6.3.5.1 Flavopiridol

Inducing agents were incubated in the presence of low passage Caco-2 cells for 48 and 72 hours (only 72 hour data are shown). Table 6.1 shows the effect of the inducing agents on the bi-directional transport of flavopiridol in a 96-well format assay. It was found that all 7 inducing agents used increased flavopiridol net secretion from control values, including BNF, chrysin, DBM, estradiol, quercetin, rosiglitazone and TBHQ. The increased net secretion resulted from a reduction in apical to basal transport of flavopiridol and an increase in the basal to apical transport of flavopiridol. Rosiglitazone pre-incubation increased net flavopiridol transport by the greatest magnitude by 1.46 fold from 1.14 ± 0.06 nmol.cm^{-1}.hr^{-1} in the control DMSO treated cells to 1.68 ± 0.05 nmol.cm^{-1}.hr^{-1} (Table 6.1).

In order to assess whether the increased flavopiridol flux resulted from an increased BCRP component, BNF and rosiglitazone induction was performed in the 24-well format. Figure 6.6 shows the effect of selective pharmacological inhibitors,

Ko143 and verapamil, on flavopiridol flux (donor concentration 10µM) after induction. In control layers neither Ko143 nor verapamil reduced flavopiridol secretion showing that at the donor concentration used the non-BCRP and non-MDR1 component of secretion predominated (see also Chapter 4 Figure 4.9B). BNF and rosiglitazone pre-incubation increased the net secretion of flavopiridol significantly by 1.44 and 1.41 fold respectively ($P < 0.05$, Figure 6.6); this increased net secretion was sensitive to Ko143. Ko143 reduced secretion from 10.24 ± 0.26 nmol.cm^{-1}.hr^{-1} in the control BNF treated cell monolayers to 6.42 ± 0.19 nmol.cm^{-1}.hr^{-1}, and from 10.03 ± 0.35 nmol.cm^{-1}.hr^{-1} in the control rosiglitazone treated cell monolayers to 6.7 ± 0.16 nmol.cm^{-1}.hr^{-1}. The increase in the Ko143 sensitive flux component between non-induced and induced monolayers is consistent with BCRP induction. However it should be noted that verapamil also reduces the increased flavopiridol flux, indicating that a MDR1-mediated route for secretion for flavopiridol may have also increased. That flavopiridol may be secreted by BCRP, MDR1 and an additional route in Caco-2 cells, suggests that flavopiridol is not an ideal choice of substrate for investigation of BCRP induction.

6.3.5.2 Prazosin

The affect of inducing agents were also tested upon prazosin secretion in low-passage Caco-2 cells for 48 and 72 hours in the 96-well format assay. At 48 hours of treatment only DBM and rosiglitazone increased the net flux of prazosin significantly. When incubation time was increased to 72 hours DBM, 17-β-estradiol, rosiglitazone and TBHQ all increased prazosin net transport compared to the DMSO treated control layers (Table 6.2). Increased prazosin transport occurred by a reduction in apical to basal transport and increased basal to apical transport of prazosin. As for flavopiridol,

the largest induction was seen with rosiglitazone which increased net secretion of the control from 1.11 ± 0.04 nmol.cm^{-1}.hr^{-1} to 1.68 ± 0.05 nmol.cm^{-1}.hr^{-1} (a 1.51 fold increase).

Figure 6.7 shows the effect of 17-β-estradiol and rosiglitazone pre-incubation for 72 hours on prazosin transport across low passage Caco-2 cells grown in the 24-well format in the presence of ABC transport inhibitors. In the untreated Caco-2 cells prazosin net secretion was reduced significantly in the presence of 10μM Ko143 ($P < 0.05$, Figure 6.7). Verapamil was ineffective on its own on the net secretion of prazosin, however when combined with Ko143, it reduced net secretion significantly. These data imply a large BCRP component for prazosin secretion in Caco-2 cells with a smaller MDR1 route of secretion in these cells. When the Caco-2 cells were treated for 72 hours, 17-β-estradiol had no effect on net secretion of prazosin (unlike the data seen in the 96-well format). However, rosiglitazone increased net secretion by 1.77 fold. The significant increase in prazosin secretion by rosiglitazone was significantly reduced from 2.16 ± 0.08 nmol.cm^{-1}.hr^{-1} to 0.49 ± 0.04 nmol.cm^{-1}.hr^{-1} in the presence of 10μM Ko143 ($P < 0.05$, Figure 6.7). This inhibition reduced net flux levels to that seen in untreated Caco-2 cells. Verapamil had no effect on reducing the net secretion of prazosin after treatment with rosiglitazone, which at 100μM is known to inhibit both MDR1 and MRP2 (Matsson *et al.*, 2007). These data show that the increase in prazosin secretion seen with rosiglitazone is due to an increase in BCRP function.

6.3.5.3 Nitrofurantoin

The data presented in Chapter 4 indicate that nitrofurantoin is a selective BCRP substrate in Caco-2 cells. The affect of inducing agents were also tested upon nitrofurantoin secretion in low-passage Caco-2 cells for 48 and 72 hours in the 96-

well format assay. At 48 hours of treatment BNF, DBM, naringenin and TBHQ increased the net secretion of nitrofurantoin significantly. However, after 72 hours of treatment only BNF and rosiglitazone had an effect of increasing net secretion of nitrofurantoin ($P < 0.05$, Table 6.3). Both compounds increased nitrofurantoin secretion by a significant reduction in the apical to basal transport whilst increasing the basal to apical transport.

Figure 6.8 shows the effects of the pharmacological inhibitors Ko143 and verapamil on the net flux of nitrofurantoin after treatment with BNF and rosiglitazone. In control layers, Ko143 significantly inhibited the bulk of nitrofurantoin secretion, whilst verapamil was ineffective alone or in combination with Ko143. These data confirm nitrofurantoin as a selective BCRP substrate in the low PA Caco-2 cells (as previously described in Chapter 4). BNF increased nitrofurantoin net flux from the control value of 2.28 ± 0.08 nmol.cm^{-1}.hr^{-1} to 3.91 ± 0.36 nmol.cm^{-1}.hr^{-1}, a 1.71 fold increase in secretion ($P < 0.05$, Figure 6.8). This secretion was inhibited in the presence of 10µM Ko143 from 3.91 ± 0.36 nmol.cm^{-1}.hr^{-1} to 0.24 ± 0.03 nmol.cm^{-1}.hr^{-1} ($P < 0.05$). Verapamil had no effect on reducing secretion in the BNF treated Caco-2 cells. Rosiglitazone treatment increased nitrofurantoin net flux from 2.28 ± 0.08 nmol.cm^{-1}.hr^{-1} to 2.95 ± 0.11 nmol.cm^{-1}.hr^{-1}, a 1.29 fold increase in secretion ($P < 0.05$, Figure 6.8). This secretion was inhibited in the presence of 10µM Ko143 from 2.95 ± 0.11 nmol.cm^{-1}.hr^{-1} to 0.24 ± 0.03 nmol.cm^{-1}.hr^{-1} ($P < 0.05$). Verapamil again had no significant effect at reducing the net secretion of nitrofurantoin. BNF and rosiglitazone pre-incubation therefore increased functional BCRP activity in conjunction with increased BCRP mRNA and protein.

Figure 6.1. qPCR analysis of BCRP mRNA after 72-hour pre-treatments in low passage Caco-2 cells

Caco-2 cells were cultured on 6-well plates for 11 days without inducing treatments then treated for a further 3 days (72h) in the presence of the inducing treatments. BNF, chrysin, estradiol and rosiglitazone treatments were used at 10µM, quercetin at 20µM, DBM and TBHQ at 50µM concentrations (diluted in DMSO). Control cells were treated with equal volumes of DMSO. Data bars are means of n = 3 wells ± SD and are corrected relative to GAPDH expression. * $P < 0.05$, significantly different from control.

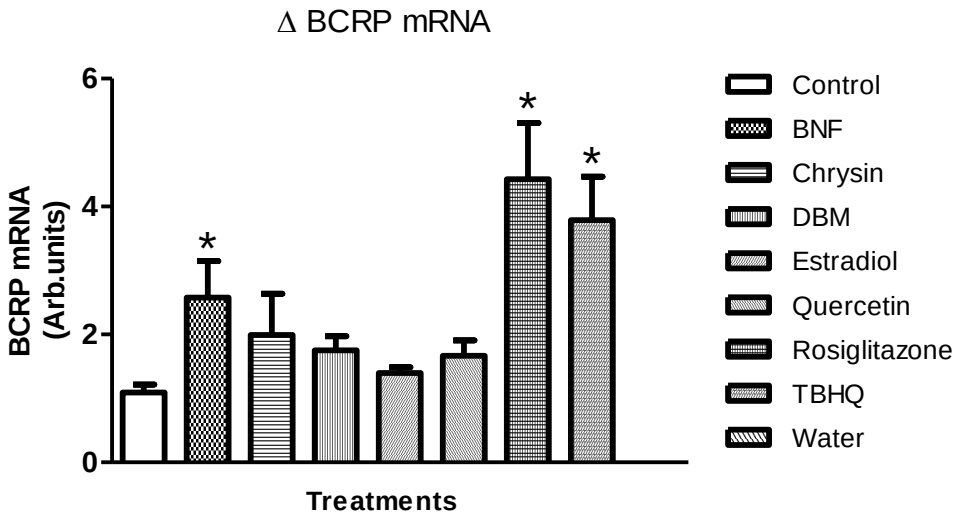

Figure 6.1. qPCR analysis of BCRP mRNA after 72-hour pre-treatments in low passage Caco-2 cells

Figure 6.2. Expression of Ah receptor mRNA in low passage Caco-2 cells

(A) An agarose gel image showing PCR product of Ah receptor from low passage Caco-2 cells, displaying the expected product size of 204 base pairs (see Materials and Methods section 2.2.3.4).

(B) Real time PCR analysis indicating expression of Ah receptor in low passage Caco-2 cells. Caco-2 cells were cultured on 6-well plates for 11 days without inducing treatments then treated for a further 3 days (72hrs) in the presence of the inducing treatments. BNF, chrysin, estradiol and rosiglitazone treatments were used at 10µM, quercetin at 20µM, DBM and TBHQ at 50µM concentrations (diluted in DMSO). Control cells were treated with equal volumes of DMSO. Data bars are means of n = 3 wells ± SD and are corrected relative to GAPDH expression. * $P < 0.05$, significantly different from control.

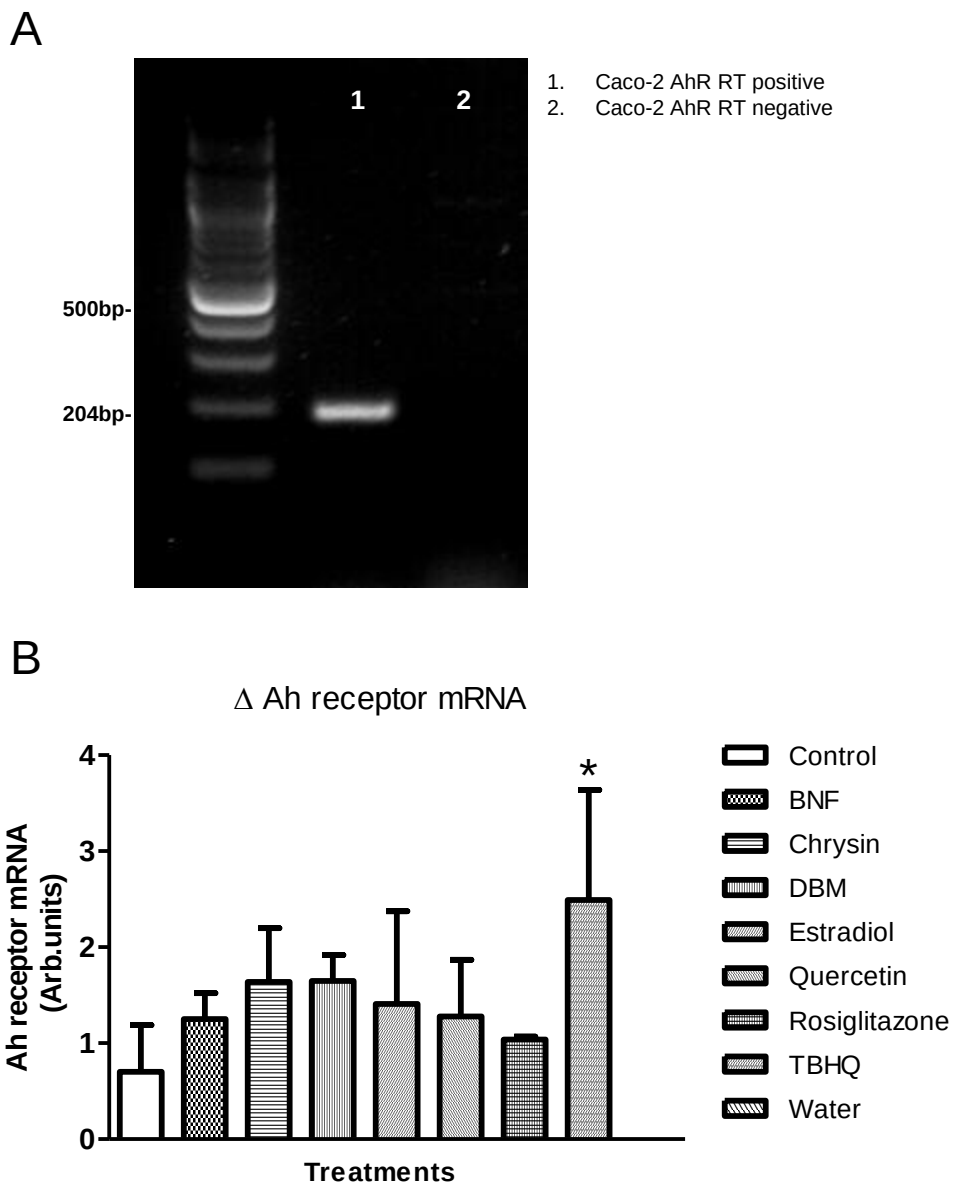

Figure 6.2. Expression of Ah receptor mRNA in low passage Caco-2 cells

Figure 6.3. Expression of PPAR-gamma receptor mRNA in low passage Caco-2 cells

(A) An agarose gel image showing PCR products of PPAR-gamma from low passage Caco-2 cells, displaying the expected product size of 257 base pairs (see Materials and Methods section 2.2.3.4).

(B) Real time PCR analysis indicating expression of PPAR-gamma receptor in low passage Caco-2 cells. Caco-2 cells were cultured on 6 well plates for 11 days without inducing treatments then treated for a further 3 days (72hrs) in the presence of the inducing treatments. BNF, chrysin, estradiol and rosiglitazone treatments were used at 10µM, quercetin at 20µM, DBM and TBHQ at 50µM concentrations (diluted in DMSO). Control cells were treated with equal volumes of DMSO. Data bars are means of n = 3 wells ± SD and are corrected relative to GAPDH expression.

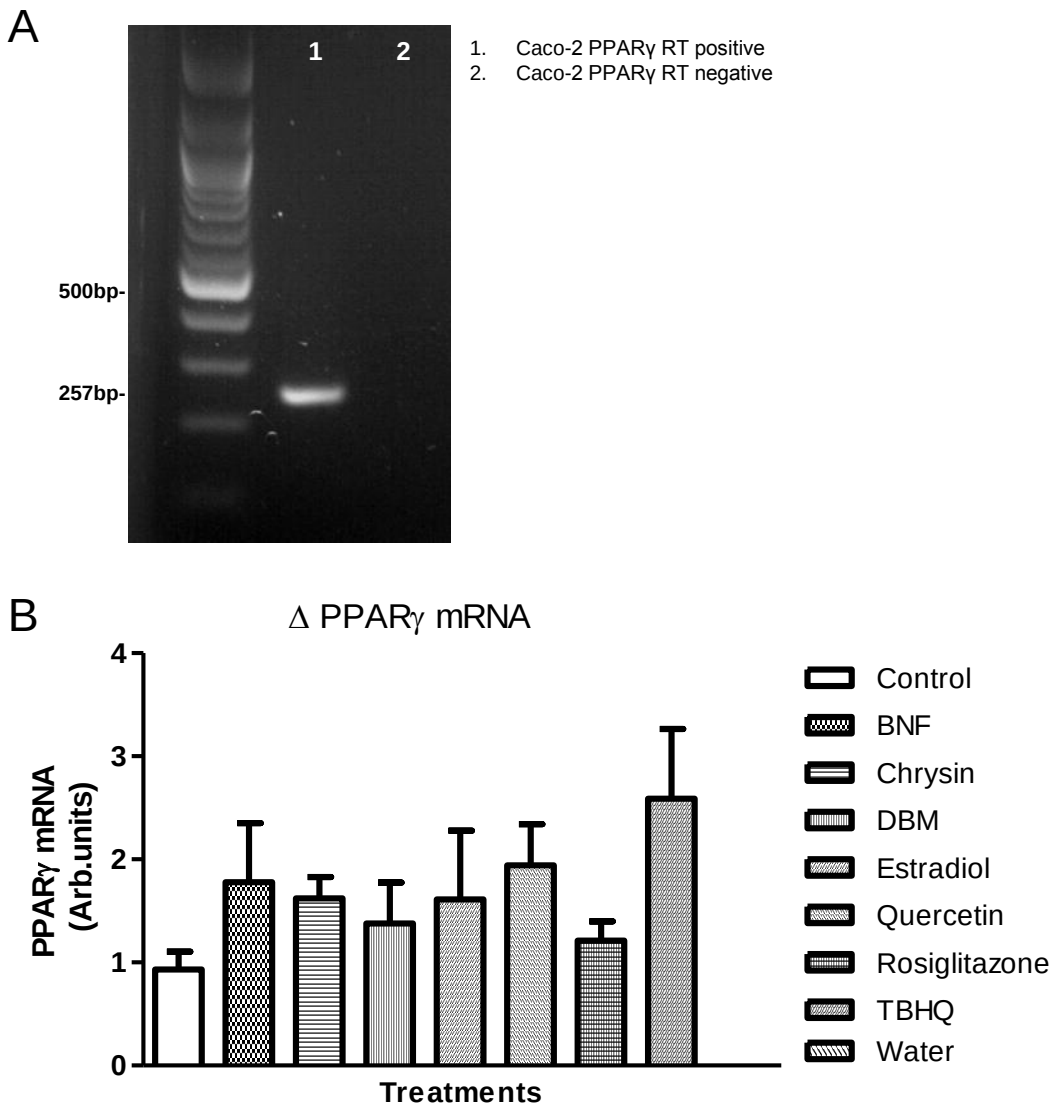

Figure 6.3. Expression of PPAR-gamma receptor mRNA in low passage Caco-2 cells

Figure 6.4. Western Blot analysis of BCRP protein expression in low passage Caco-2 cells after 72-hour pre-treatments

Images (A) and (B) show BCRP protein and α-tubulin expression respectively. Lane 1 is DMSO treated low PA Caco-2 control cells (40µg protein loaded), lane 2 is 10µM BNF treated low PA Caco-2 cells (40µg protein loaded), lane 3 is 10µM rosiglitazone treated low PA Caco-2 cells (40 µg protein loaded) and lane 4 is untreated hBCRP-MDCKII positive control (10µg protein loaded). Low PA Caco-2 cells (shown in lanes 1-3) were grown in 75cm^2 flasks in the presence of the agents indicated for 72 hours then protein was extracted.

(A) Membrane was probed initially with mouse-monoclonal anti-human BCRP antibody BXP-21 (Santa Cruz) at a dilution of 1 in 100. This image is representative of one gel. BCRP yields bands at approximately 72kDa.

(B) Image shows the membrane from part A stripped and re-probed with a cross species polyclonal anti-α-tubulin antibody (Abcam). The α-tubulin band was visible at approximately 50kDa.

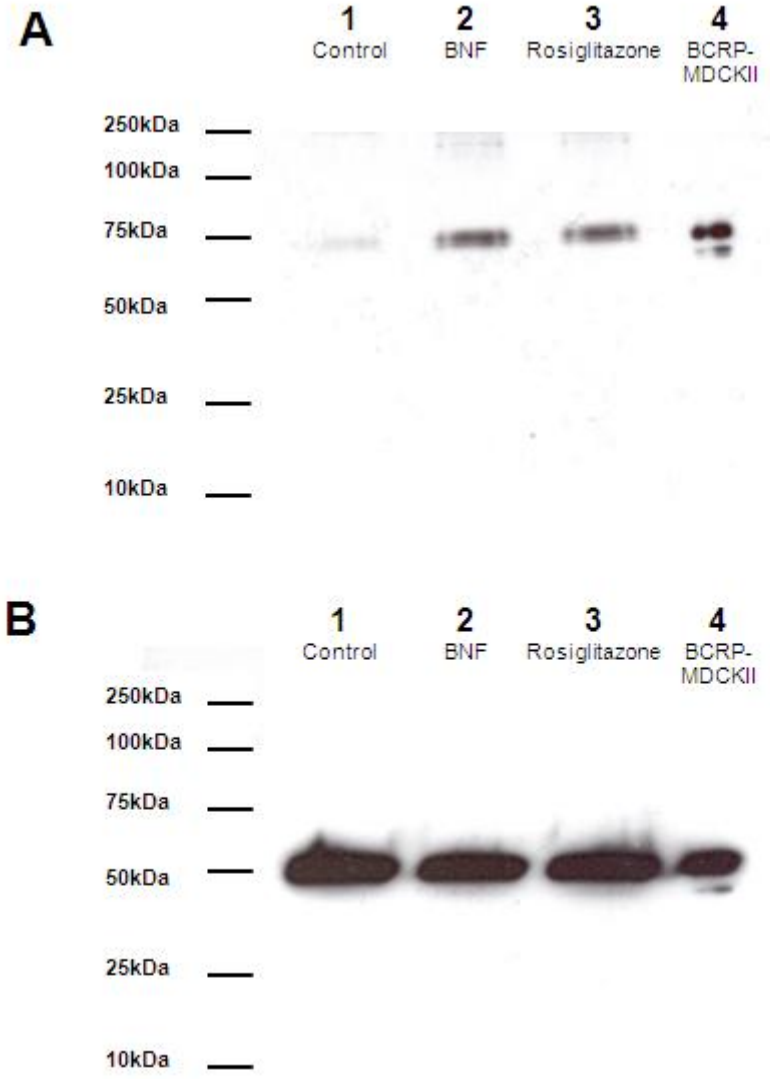

Figure 6.4. Western Blot analysis of BCRP protein expression in low passage Caco-2 cells after 72-hour pre-treatments

Figure 6.5. Effect of flavopiridol net flux in the presence and absence of potential inhibitors across human BCRP-MDCKII monolayers

Human BCRP-MDCKII cells were cultured on 24-well permeable supports until confluency. Data bars represent net flux ($J_{b-a} - J_{a-b}$) and show flavopiridol net flux in the presence and absence of potential inhibitors. All treatment compounds were used at 10µM, aside from quercetin which was used at 20µM. Control cells were treated with equal volumes of DMSO. Flavopiridol donor concentration was 10µM, receiver concentration was measured by HPLC-MS. Data bars are means of n = 4 monolayers ± SEM. * $P < 0.05$, significantly different from control.

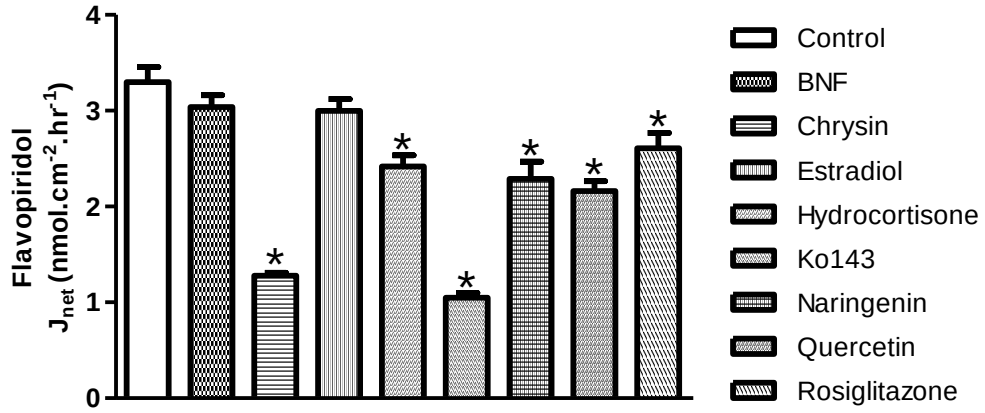

Figure 6.5. Effect of flavopiridol net flux in the presence and absence of potential inhibitors across human BCRP-MDCKII monolayers

Table 6.1. Effect of potential BCRP inducing agents after 72-hours pre-treatment on flavopiridol transepithelial flux across confluent Caco-2 cell monolayers

Caco-2 cells were cultured on 96-well Transwell supports for 11 days without inducing treatments then treated for a further 3 days (72h) in the presence or absence of induction treatments. BNF, chrysin, estradiol and rosiglitazone treatments were used at 10µM, quercetin at 20µM, DBM and TBHQ at 50µM concentrations (diluted in DMSO). Control cells were treated with equal volumes of DMSO. Flavopiridol donor concentration was 10µM, receiver concentration was measured by HPLC-MS. Data bars are means of n = 4-6 monolayers ± SEM. * $P < 0.05$, significantly different from control.

	Transepithelial Flavopiridol Flux (pmol.cm^{-2}.hr^{-1})			
Treatment	**J_{a-b}**	**J_{b-a}**	**J_{net}**	**Δ net flux**
Control	397.5 ± 14.3	1542.1 ± 50.4	1144.6 ± 57.4	NA
BNF	340.4 ± 13.4	1874.9 ± 44.2	1570.7 ± 53.4	**1.37***
Chrysin	314.6 ± 18.4	1755.1 ± 58	1440.5 ± 47.6	**1.26***
DBM	269.8 ± 28.5	1716.8 ± 88.9	1447± 110.7	**1.26***
Estradiol	329.5 ± 9.7	1915.5 ± 35.6	1586 ± 40.4	**1.39***
Quercetin	272.5 ± 35.9	1724.4 ± 15.6	1451.9 ± 46	**1.27***
Rosiglitazone	244.8 ± 25.6	1921.7 ± 67.8	1676.4 ± 46.2	**1.46***
TBHQ	253.5 ± 49.6	1802.6 ± 32.9	1549.1 ± 44.8	**1.35***

Figure 6.6. Effect of pre-treatments on flavopiridol transepithelial flux across confluent Caco-2 cell monolayers ± known ABC transporter inhibitors

Caco-2 cells were cultured on 24-well Transwell supports for 11 days without inducing treatments then treated for a further 3 days (72h) in the presence of induction treatments. BNF and rosiglitazone were used at 10μM concentrations (diluted in DMSO). Control cells were treated with equal volumes of DMSO. Flavopiridol donor concentration was 10μM, receiver concentration was measured by HPLC-MS. Flux were determined in the presence and absence of the ABC transporter inhibitors Ko143 (10μM) and verapamil (100μM). Data bars are means of n = 8 monolayers ± SEM. * $P < 0.05$, significantly different from control values. # $P<0.05$, significantly different from DMSO value.

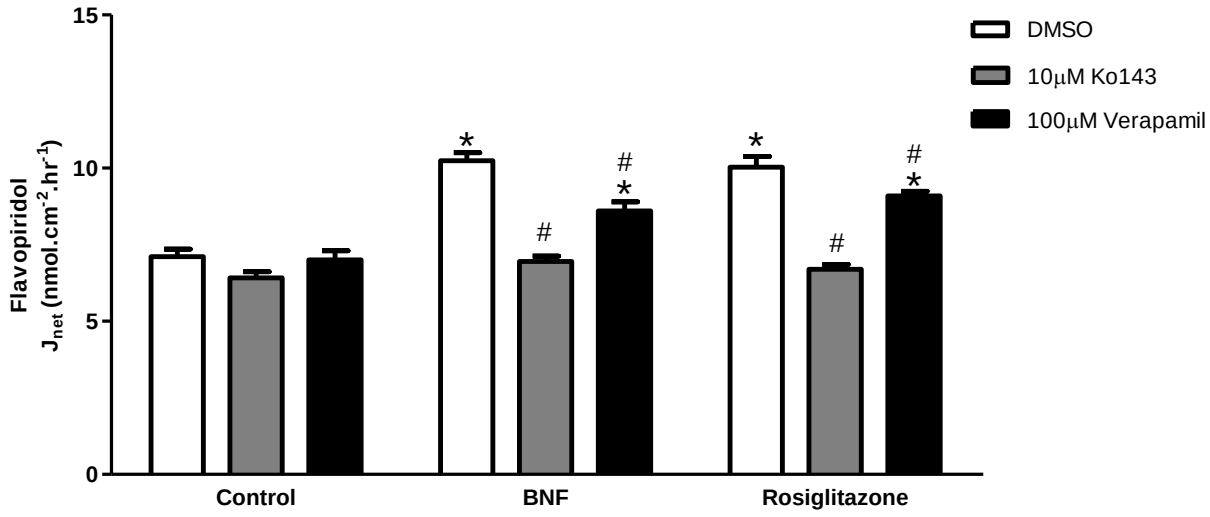

Figure 6.6. Effect of pre-treatments on flavopiridol transepithelial flux across confluent Caco-2 cell monolayers ± known ABC transporter inhibitors

Table 6.2. Effect of potential BCRP inducing agents after 72-hours pre-treatment on prazosin transepithelial flux across confluent Caco-2 cell monolayers

Caco-2 cells were cultured on 96-well Transwell supports for 11 days without inducing treatments then treated for a further 3 days (72h) in the presence or absence of induction treatments. BNF, chrysin, estradiol and rosiglitazone treatments were used at 10µM, quercetin at 20µM, DBM and TBHQ at 50µM concentrations (diluted in DMSO). Control cells were treated with equal volumes of DMSO. Prazosin donor concentration was 10µM, receiver concentration was measured by HPLC-MS. Data bars are means of n = 4-6 monolayers ± SEM. * $P < 0.05$, significantly different from control.

	Transepithelial Prazosin Flux (pmol.cm^{-2}.hr^{-1})			
Treatment	**J_{a-b}**	**J_{b-a}**	**J_{net}**	**Δ net flux**
Control	200.5 ± 8	1308.1 ± 39.6	1114.9 ± 39.2	NA
BNF	105.3 ± 4.1	1347.2 ± 77	1231.6 ± 81.6	1.1
Chrysin	157.4 ± 4.6	1482.5 ± 42.5	1302.3 ± 46.2	1.17
DBM	152.9 ± 7.2	1598.7 ± 66.2	1455.3 ± 83.5	**1.31****
Estradiol	169.4 ± 4.7	1812.4 ± 72	1619.7 ± 82.7	**1.45****
Quercetin	166.2 ± 3.7	1462.3 ± 33.6	1315 ± 26.8	1.18
Rosiglitazone	163.7 ± 11.9	1793.3 ± 50.2	1682.3 ± 48.8	**1.51****
TBHQ	157.3 ± 9.5	1521.8 ± 44.1	1401.2 ± 31.2	**1.26***

Figure 6.7. Effect of pre-treatments on prazosin transepithelial flux across confluent Caco-2 cell monolayers ± known ABC transporter inhibitors

Caco-2 cells were cultured on 24-well Transwell supports for 11 days without inducing treatments then treated for a further 3 days (72h) in the presence of induction treatments. Estradiol and rosiglitazone were used at 10µM concentrations (diluted in DMSO). Control cells were treated with equal volumes of DMSO. Prazosin donor concentration was 10µM, receiver concentration was measured by HPLC-MS. Flux were determined in the presence and absence of the ABC transporter inhibitors Ko143 (10µM) and verapamil (100µM). Data bars are means of n = 8 monolayers ± SEM. * $P < 0.05$, significantly different from control values. # $P < 0.05$, significantly different from DMSO values. Ko143 and Verapamil vs. Ko143 value ** $P < 0.05$, significantly different.

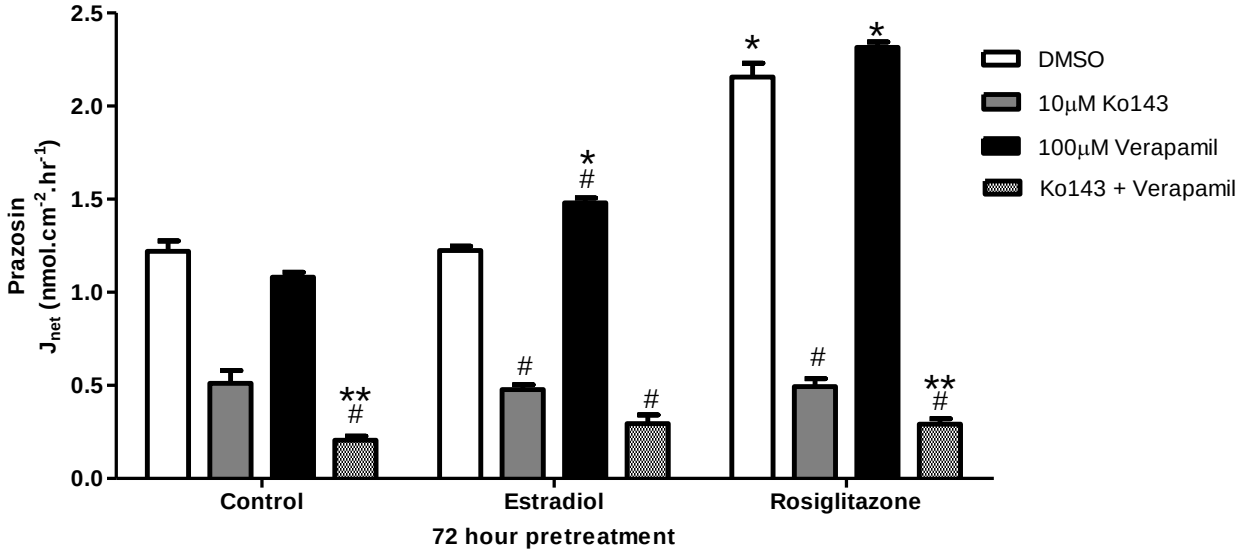

Figure 6.7. Effect of pre-treatments on prazosin transepithelial flux across confluent Caco-2 cell monolayers ± known ABC transporter inhibitors

Table 6.3. Effect of potential BCRP inducing agents after 72-hours pre-treatment on nitrofurantoin transepithelial flux across confluent Caco-2 cell monolayers

Caco-2 cells were cultured on 96-well Transwell supports for 11 days without inducing treatments then treated for a further 3 days (72h) in the presence or absence of induction treatments. BNF, chrysin, estradiol and rosiglitazone treatments were used at 10µM, quercetin at 20µM, DBM and TBHQ at 50µM concentrations (diluted in DMSO). Control cells were treated with equal volumes of DMSO. Nitrofurantoin donor concentration was 10µM, receiver concentration was measured by HPLC-MS. Data bars are means of n = 4-6 monolayers ± SEM. * $P < 0.05$, significantly different from control.

	Transepithelial Nitrofurantoin Flux (pmol.cm^{-2}.hr^{-1})			
Treatment	**J_{a-b}**	**J_{b-a}**	**J_{net}**	**Δ net flux**
Control	63.5 ± 4.7	1345.6 ± 38.3	1283.5 ± 37	NA
BNF	48.1 ± 5.4	1628.3 ± 115.2	1580.2 ± 112.9	**1.23***
Chrysin	49.7 ± 4.0	1385.6 ± 70.6	1335.9 ± 67	1.04
DBM	39.9 ± 6.0	1437.9 ± 58.5	1397.9 ± 56.8	1.09
Estradiol	47.7 ± 7.4	1439.4 ± 56.4	1391.7 ± 50.5	1.08
Quercetin	37.9 ± 0.8	1354.4 ± 50.1	1316.5 ± 50.7	1.03
Rosiglitazone	22.5 ± 1.7	1685.7 ± 45.1	1663.2 ± 45	**1.30****
TBHQ	36.6 ± 6.8	1491.0 ± 62.8	1454.5 ± 58.3	1.13

Figure 6.8. Effect of pre-treatments on nitrofurantoin transepithelial flux across confluent Caco-2 cell monolayers ± known ABC transporter inhibitors

Caco-2 cells were cultured on 24-well Transwell supports for 11 days without inducing treatments then treated for a further 3 days (72h) in the presence of induction treatments. BNF and rosiglitazone were used at 10µM concentrations (diluted in DMSO). Control cells were treated with equal volumes of DMSO. Nitrofurantoin donor concentration was 10µM, receiver concentration was measured by HPLC-MS. Flux were determined in the presence and absence of the ABC transporter inhibitors Ko143 (10µM) and verapamil (100µM). Data bars are means of n = 8 monolayers ± SEM. * $P < 0.05$, significantly different from control values. # $P < 0.05$, significantly different from DMSO value.

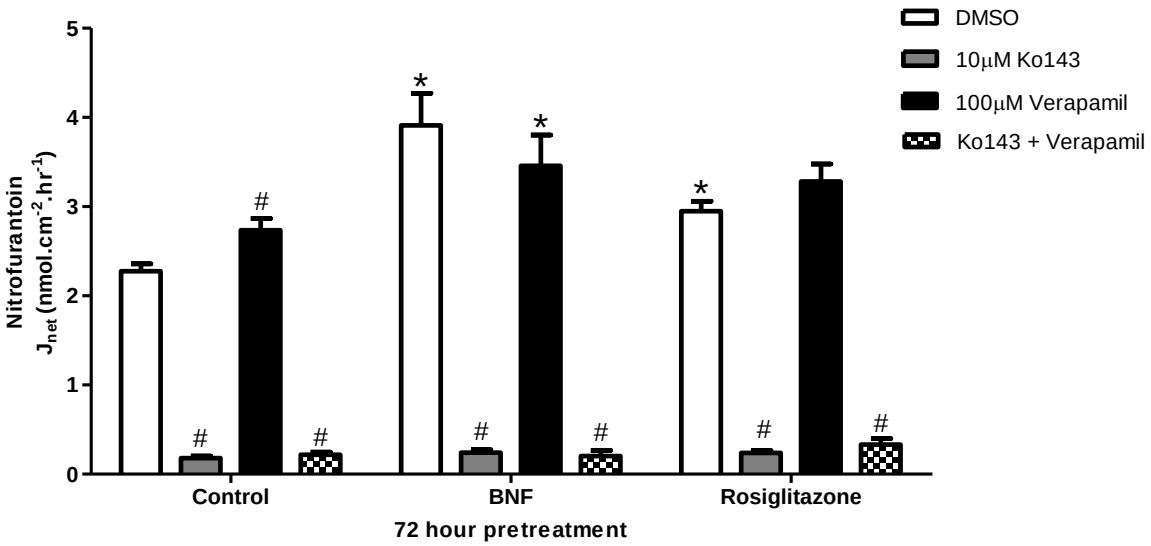

Figure 6.8. Effect of pre-treatments on nitrofurantoin transepithelial flux across confluent Caco-2 cell monolayers ± known ABC transporter inhibitors

6.4 Discussion

The dynamic regulation of BCRP present in its physiological location at the brush-border of enterocytes is associated with ATP-dependent recycling of absorbed substrates back into the lumen. This mode of operation will therefore impact on absorption and bioavailability from the intestinal lumen. Low PA Caco-2 cells have been used as a model of the human intestinal mucosae and pre-treatments with a variety of phytochemicals, sex hormones, AhR agonists BNF and TBHQ (Gharavi & El-Kadi, 2005; Wattenberg *et al.*, 1968) and the PPARγ agonist rosiglitazone were tested for their ability to modulate BCRP expression at the molecular mRNA and protein level, and at the functional level by measurement of BCRP substrate flux. Of the treatments used BNF and rosiglitazone pre-incubation showed the most noticeable up-regulation of BCRP transcription whilst immunoblotting confirmed an increase in protein expression with these agents. These data suggest that the Caco-2 cell system is an appropriate model system to test how the complex lumenal environment and periodic stimuli arising from diet or drug exposure may later affect the barrier function through up-regulation of ABC transporters such as BCRP.

After confirming changes of BCRP expression at the molecular level, the effect of induction agents upon substrate transport was determined. Data in Chapter 4 have established that flavopiridol, prazosin and nitrofurantoin were BCRP substrates of variable specificity. Of the 3 compounds measured flavopiridol is thought to be the least selective, the data in Chapter 4 showing that it is likely secreted by multiple transporters across Caco-2 cell layers. Substrate flux values were measured in both absorptive and secretory directions across the low PA Caco-2 cells. Although all compounds tested in this study were shown to increase flavopiridol net transport, the promiscuous nature of flavopiridol secretion across Caco-2 cells renders it likely that

more than one transporter is being up-regulated, resulting in the increase in flavopiridol secretion. For example, quercetin is a known inducing agent of BCRP, but equally an inducer of the MDR1 and MRP2 transporters. Therefore, the increase in secretion could be the result of the induction of any of these transporters. For this reason selective inhibitors, such as Ko143, described previously in Chapter 3, were tested to elucidate which transporter pathway was being up-regulated. The pre-incubation agents BNF and rosiglitazone increased flavopiridol secretion across Caco-2 cells grown in 24-well plate assays. Ko143 had little effect on the flavopiridol secretion in the control cells, however after pre-treating with BNF and rosiglitazone the increase of flavopiridol secretion was inhibited by 10μM Ko143 but not by 100μM verapamil, which are BCRP and MDR1 selective respectively. Therefore at least BNF and rosiglitazone are responsible for the increase in BCRP mediated flavopiridol secretion in Caco-2 cells. In all cases where there was an increased net transepithelial secretion of flavopiridol, there was a reduction in the apical to basal absorptive flux (and hence permeability) of flavopiridol. This finding links increased functional BCRP activity with a limitation of absorptive permeability.

Prazosin is a known bi-substrate for BCRP and MDR1 (Feng *et al.*, 2008; Matsson *et al.*, 2009; Polli *et al.*, 2001). However, in the low PA Caco-2 cells prazosin was shown to be secreted by BCRP in preference to MDR1, and for this reason served as a useful tool to measure BCRP induction in these cells. Unlike flavopiridol secretion, BNF was ineffective at increasing prazosin secretory transport, but the other AhR agonists DBM and TBHQ were effective in increasing prazosin secretion. Rosiglitazone, as with flavopiridol, increased prazosin secretion and this secretory component was reduced significantly with Ko143. These data increase the evidence that AhR and PPARγ mediated pathways contribute to BCRP regulation in

the intestinal cell line Caco-2. As was the case for flavopiridol, in all cases where there was an increased net transepithelial secretion of prazosin, there was a reduction in the apical to basal absorptive flux (and hence permeability) of prazosin.

Nitrofurantoin proved to be the most useful BCRP substrate for measuring a change in BCRP mediated secretion. Unlike the bi-substrates flavopiridol and prazosin, nitrofurantoin was shown to be secreted only by BCRP across Caco-2 cell layers. For this reason, interpretations of nitrofurantoin flux are without ambiguity. Only pre-incubations with BNF and rosiglitazone increased the nitrofurantoin secretion across the apical membrane, unlike the many compounds that increased secretion of flavopiridol and prazosin. Furthermore this up-regulation in nitrofurantoin secretion by the agents BNF and rosiglitazone was Ko143 sensitive and verapamil insensitive. The increased net transepithelial secretion of nitrofurantoin seen on pre-incubation with rosiglitazone, was associated with a ~60% reduction in the apical to basal absorptive flux (and hence permeability) of nitrofurantoin, emphasising that increased secretory function directly modulates the absorptive permeability.

Taking the transport data as a whole the only agent that consistently increased the net secretion of all 3 compounds was the PPARγ agonist rosiglitazone. The enhancement of secretion with rosiglitazone was also consistently Ko143 sensitive. Therefore this increase in function taken together with the increase in mRNA and protein expression shows rosiglitazone is an effective agent at inducing the BCRP pathway in Caco-2 cells. Svatmari *et al.* (2006) were the first group to link PPARγ with BCRP expression (Szatmari *et al.*, 2006). This group showed PPARγ agonists, such as rosiglitazone to increase mRNA, protein and function of BCRP in human myeloid dendritic cells and monocyclic/macrophage leukaemia cells (MM6), similar

to the findings in Caco-2 cells in this study. The authors further describe that PPARγ binds with RXR to form a heterodimer which in turn binds to a PPAR response element (PPARE) upstream of the *BCRP* gene to cause increased transcription. In order to confirm that PPARγ regulates BCRP in Caco-2 cells the PPARγ antagonist GW9662 could be incubated with rosiglitazone, or a marker gene known to be regulated by PPARγ (such as the fatty acid-binding protein, FABP4) could be monitored to see if it is co-induced alongside BCRP. Furthermore RNA interference to reduce PPARγ expression could be undertaken; PPARγ specific siRNA (Kelly *et al.*, 2004) has previously been shown to be effective (Szatmari *et al.*, 2006). To further establish whether PPARγ partners RXR to induce BCRP in Caco-2 cells, RXR agonists such as LG268 could be used in the presence and absence of rosiglitazone to see if there is an additive effect of induction.

Interestingly PPARγ ligands have been reported to induce the expression of retinoic acid β-receptors in cancer cells (James *et al.*, 2003) and recently a study in Caco-2 cells showed that the non-specific RAR/RXR ligand all-trans retinoic acid induces BCRP expression. Therefore multiple pathways exist which may act synergistically to up-regulate BCRP if the appropriate ligands are present intracellularly.

Aside from PPARγ activation there is likely another different mechanism of BCRP induction that is activated by the flavonoids. This study supports the existing evidence that flavonoids can inhibit and also induce BCRP expression. There are some inconsistencies in the flavonoid induction work seen in this study and the literature for Caco-2 cells. Chrysin and quercetin, for example, are known to induce BCRP mRNA and increase the efflux of the BCRP substrate benzo[a]pyrene-3-sulphate (Ebert *et al.*, 2007), yet in this study these compounds were ineffective at

increasing expression and function of BCRP under the conditions chosen. It is likely this discrepancy is due to the flavonoid concentrations used between studies- 10µM chrysin and 20µM quercetin concentrations used in this study may have been insufficient to elicit an affect. Other flavonoids had a profound effect on mRNA expression in this study, DBM and TBHQ were highly effective and have been shown previously to modulate BCRP expression and function (Ebert *et al.*, 2007). BNF is less well characterised as a BCRP inducer compared with other flavonoids and is often used as an archetype inducer of the AhR (Miller, 1999). BNF at 10µM was an effective inducer of functional BCRP activity. The present flavonoid data shows that BCRP is likely to be up-regulated via the AhR pathway in Caco-2 cells.

Recently the AhR pathway has been proven to regulate BCRP expression and function in a Caco-2 cell sub-type; the C2bbe1 cells (Tan *et al.*, 2010). In brief, the mechanism of AhR induction involves; the exogenous ligand binding to the inactive AhR residing in the cell cytosol; AhR exists as a multimer bound to two chaperone proteins hsp90 (heat shock protein dimer of 90-kDa) and hepatitis B virus X-associated protein 2 (Denison & Nagy, 2003; Tan *et al.*, 2010). This complex undergoes a conformational change and migrates into the nucleus. Within the nucleus the AhR separates from the protein complex and in turn binds to form a heterodimer complex with Arnt. This dimer (AhR-Arnt) has a high affinity to specific DNA recognition sites (DREs) that result in activation of downstream gene expression. Human BCRP was revealed to have 9 putative core DREs (Tan *et al.*, 2010) and of these 4 putative DREs are located in a proximal region within ~200bp from the transcriptional start site and 5′-untranslated region. Interestingly this 'proximal region' covers a region in which HIF1α, ERα and PgR (progesterone receptor) are known to bind (Ee *et al.*, 2004; Krishnamurthy & Schuetz, 2005; Wang *et al.*, 2008a).

As these regions are so close and associated to BCRP induction there may be cross talk between activated DREs resulting in potential for both synergistic and inhibitory actions on BCRP regulation (Tan *et al.*, 2010), especially as the AhR-ARNT heterodimer and ER are known to competitively bind at certain sites (Klinge *et al.*, 2000; Ohtake *et al.*, 2003).

Tan *et al.* (2010) go on to show that one particular DRE activated alone by the AhR agonist TCDD results in an up-regulation of function and expression of BCRP (position -194/-190 of the core DRE in the 5′-flanking region of the *BCRP* gene). Thus BNF action described in this chapter is likely to be mediated via the AhR pathway.

To further confirm BCRP induction of flavonoids through the AhR receptor the cellular cascade through AhR activation could be investigated. For example, one of the gene targets of the AhR-Arnt dimer is a DRE that induces CYP1A1. CYP1A1 is a classic product of AhR regulation and could be quantified to see if this enzyme is being up-regulated alongside BCRP (Denison & Nagy, 2003). An AhR antagonist 3′-methoxy-4′-nitroflavone could be used in the pre-incubations alongside the flavonoids to see if this effects BCRP expression (Ebert *et al.*, 2007).

Hormonal regulation of BCRP via 17β-estradiol seems to be a cell dependent effect; it has been shown to increase BCRP transcription in ER-positive T47D:A18 breast cancer cells (Ee *et al.*, 2004) but reduce its expression in the ER-positive MCF-7 breast cancer cells (Ee *et al.*, 2004; Imai *et al.*, 2005). In this study levels of BCRP mRNA did not change in the presence of the ERα agonist 17β-estradiol, nitrofurantoin transport was unaffected, but it did increase the secretion of the bi-substrates flavopiridol and prazosin across Caco-2 cell monolayers. How 17β-estradiol increases secretion of flavopiridol and prazosin secretion remains to be precisely identified.

However, the lack of affect on the BCRP selective nitrofurantoin suggests that 17β-estradiol action in Caco-2 cells is not mediated by increased BCRP activity. The specific ER expressed in Caco-2 cells needs to be identified and further investigation with other estrogenic compounds and progesterone would confirm any BCRP regulation.

In summary this chapter has shown that various dietary agents and hormones acting through differing signalling targets, particularly AhR and PPARγ, may regulate BCRP expression in Caco-2 cells. Whether these pathways allow cross talk to synergistically regulate BCRP is unknown. However given that the expression of BCRP in the intestine has been shown to vary between individuals (Honjo *et al.*, 2002; Zamber *et al.*, 2003) and that many agents seem to affect its expression, it appears reasonable to suppose that more than one regulatory pathway affects expression of this transporter, and in vivo a combination of endogenous and exogenous ligands act to regulate BCRP dynamically, resulting in a varied expression of BCRP on the apical surface of enterocytes between individuals.

7. Summary and concluding remarks

The main objective of this thesis was to explore the function and regulation of the less characterised of the three main efflux transporters, BCRP, in the context of epithelial expression with a particular focus on the human intestinal epithelial cell line Caco-2. BCRP expressed at the apical brush-border membrane mediates active extrusion of its substrates either from cytosol or directly from the membrane phase, so contributing to the barrier function against xenobiotics from the intestinal lumen.

The data set out in Chapter 3 characterised available cell model systems such as MDCKII cells transfected with hBCRP/mBcrp or Caco-2 cells by assessing the extent of BCRP mRNA and protein expression, with measurements of function being assessed using the cellular extrusion of the MDR1/BCRP bi-substrate, Hoechst 33342. MDCKII cells transfected with hBCRP/mBcrp1 cDNA, as well as the low PA Caco-2 cells expressed BCRP at the apical surface of these epithelial cells. BCRP acts to reduce Hoechst 33342 intercalation into DNA; decreased Hoechst 33342 being observed in BCRP-transfected cell-lines. Since retention of Hoechst 33342 is increased upon BCRP inhibition, this may be used as a convenient assay to screen for BCRP/MDR1 substrates. However, given the existence of endogenous ABC-transport activity in native MDCKII cells or multiple ABC transporters in Caco-2 cells, unambiguous identification of neither novel substrates nor BCRP regulation was possible, though BCRP-selective inhibitors such as Ko143 increased Hoechst 33342 cellular retention.

In Chapter 4, BCRP substrates were screened using transepithelial transport across reconstituted epithelial monolayers of MDCKII cells. Bi-directional transport combined with substrate identification by HPLC-MS provided an unambiguous measurement when wild-type cells were compared to mBcrp or hBCRP MDCKII

epithelia, identifying 5 compounds as hBCRP substrates: diclofenac, flavopiridol, nitrofurantoin, prazosin and risperidone. It further identified 5 mouse Bcrp substrates: diclofenac, flavopiridol, gefitinib, nitrofurantoin and prazosin. Using MDR1-MDCKII epithelia 3 compounds were also identified as MDR1 substrates: clozapine, diclofenac and prazosin.

Flavopiridol and nitrofurantoin were identified as substrates for both human BCRP and mouse Bcrp using the MDCKII cell models and looked the most likely candidates for isolating the BCRP-component of transport in Caco-2 cells. Even though prazosin is an MDR1 substrate it was selected for further study also, on the basis that it was both an hBCRP and mBcrp substrate and is well documented as a BCRP substrate. Further investigation looking at pharmacological inhibition in both MDCKII and Caco-2 cells showed that out of flavopiridol, nitrofurantoin and prazosin, only nitrofurantoin was a selective BCRP substrate.

Chapter 5 sought to test the hypothesis that ciprofloxacin transport in Caco-2 cells was mediated by BCRP. Bi-directional ciprofloxacin transport was initially measured via a Transwell based assay across native and hBCRP/mBcrp cDNA transfected MDCKII cells and it was found that ciprofloxacin net secretion was substantially increased across the mouse transfected cells but only marginally in the human BCRP-transfected cells. These data matched with the findings of Merino *et al*. (2006).

In two Caco-2 cell types, low PA and high PA cells with and without BCRP expression respectively, ciprofloxacin secretion was observed. The low PA Caco-2 cells which express BCRP saw a significant reduction in secretion in the presence of the BCRP inhibitor Ko143. Thus a significant fraction of ciprofloxacin secretion is mediated by BCRP; however the fact that both Caco-2 cell-strains secrete

ciprofloxacin suggests the existence of a BCRP-independent route that remains undefined. In conclusion human BCRP may transport ciprofloxacin depending on its expression; however its affinity may be reduced compared to that of the mouse Bcrp protein.

The final results chapter looked at the effect of pre-incubating different agents on the expression and function of BCRP in Caco-2 cells. Induction of BCRP mRNA expression and protein expression was correlated with functional measurements using the BCRP selective substrate, nitrofurantoin. Several agents with diverse structures and different cellular targets affect BCRP expression in Caco-2 cells, particularly AhR and PPARγ agonists. Given that the expression of BCRP in the intestine has been shown to vary between individuals (Honjo *et al.*, 2002; Zamber *et al.*, 2003) and that many agents seem to affect its expression, it looks reasonable that more than one regulatory site affects expression of this transporter, and in vivo it is likely a combination of endogenous and exogenous ligands act to regulate BCRP dynamically, resulting in a varied expression of BCRP on the apical surface of enterocytes, resulting in both within and between individual variation.

A detailed understanding of such BCRP function may lead, ultimately, to improvements to oral drug delivery regimes and to avoidance of unwanted drug-drug and herb-drug interactions. For example leflunomide, a disease modifying anti-rheumatic drug and its metabolite A771726 are known BCRP substrates (Kim *et al.*, 2010; Kis *et al.*, 2009). In the clinic these agents could lead to liver damage when administered with other commonly prescribed BCRP substrates and inhibitors such as nitrofurantoin, methotrexate, proton pump inhibitors (pantoprazole) and statins (pravastatin). Having a detailed understanding of what compounds are substrates and

inhibitors of the main efflux transporters such as MDR1 and BCRP in vitro may circumvent such interactions in the clinic.

Alternatively some agents can increase BCRP expression and function as shown in this study and previous studies (Ebert *et al.*, 2007; Szatmari *et al.*, 2006; Tan *et al.*, 2010). For MDR1 it is known that pre-exposure of Caco-2 cells with rifampicin can lead to an up-regulation of MDR1 expression and function. Rifampicin in the clinical setting could potentially have grave consequences when it is administered over time alongside a drug with a narrow therapeutic index such as digoxin. Where both impaired absorption or elimination of digoxin could lead to failure of therapy or toxicity respectively (Greiner *et al.*, 1999). In a similar manner to MDR1 induction by rifampicin, BCRP induction by agents such as dietary flavonoids could lead to failure in the absorption of substrates such as methotrexate given orally. The large inter-individual variability in oral absorption of methotrexate (Balis *et al.*, 1983) may in part result from variable BCRP expression. Understanding which agents can cause induction of BCRP/MDR1 even in vitro could be used as a flag that such induction is occurring in the clinic and maybe a useful screen in the development of new chemical entities to prevent drug-drug interactions.

8. References

Adkison, KK, Vaidya, SS, Lee, DY, Koo, SH, Li, L, Mehta, AA, Gross, AS, Polli, JW, Lou, Y, Lee, EJ (2008) The ABCG2 C421A polymorphism does not affect oral nitrofurantoin pharmacokinetics in healthy Chinese male subjects. *Br J Clin Pharmacol* **66**(2)**:** 233-239.

Ahmed-Belkacem, A, Pozza, A, Munoz-Martinez, F, Bates, SE, Castanys, S, Gamarro, F, Di Pietro, A, Perez-Victoria, JM (2005) Flavonoid structure-activity studies identify 6-prenylchrysin and tectochrysin as potent and specific inhibitors of breast cancer resistance protein ABCG2. *Cancer Res* **65**(11)**:** 4852-4860.

Albermann, N, Schmitz-Winnenthal, FH, Z'Graggen, K, Volk, C, Hoffmann, MM, Haefeli, WE, Weiss, J (2005) Expression of the drug transporters MDR1/ABCB1, MRP1/ABCC1, MRP2/ABCC2, BCRP/ABCG2, and PXR in peripheral blood mononuclear cells and their relationship with the expression in intestine and liver. *Biochem Pharmacol* **70**(6)**:** 949-958.

Allen, JD, Schinkel, AH (2002) Multidrug resistance and pharmacological protection mediated by the breast cancer resistance protein (BCRP/ABCG2). *Mol Cancer Ther* **1**(6)**:** 427-434.

Allen, JD, van Loevezijn, A, Lakhai, JM, van der Valk, M, van Tellingen, O, Reid, G, Schellens, JH, Koomen, GJ, Schinkel, AH (2002) Potent and specific inhibition of the breast cancer resistance protein multidrug transporter in vitro and in mouse intestine by a novel analogue of fumitremorgin C. *Mol Cancer Ther* **1**(6)**:** 417-425.

Aller, SG, Yu, J, Ward, A, Weng, Y, Chittaboina, S, Zhuo, R, Harrell, PM, Trinh, YT, Zhang, Q, Urbatsch, IL, Chang, G (2009) Structure of P-glycoprotein reveals a molecular basis for poly-specific drug binding. *Science* **323**(5922)**:** 1718-1722.

Allikmets, R, Schriml, LM, Hutchinson, A, Romano-Spica, V, Dean, M (1998) A human placenta-specific ATP-binding cassette gene (ABCP) on chromosome 4q22 that is involved in multidrug resistance. *Cancer Res* **58**(23)**:** 5337-5339.

Alvarez, AI, Perez, M, Prieto, JG, Molina, AJ, Real, R, Merino, G (2008) Fluoroquinolone efflux mediated by ABC transporters. *J Pharm Sci* **97**(9)**:** 3483-3493.

Alvarez, AI, Real, R, Perez, M, Mendoza, G, Prieto, JG, Merino, G (2009) Modulation of the activity of ABC transporters (P-glycoprotein, MRP2, BCRP) by flavonoids and drug response. *J Pharm Sci* **99**(2)**:** 598-617.

Artursson, P (1990) Epithelial transport of drugs in cell culture. I: A model for studying the passive diffusion of drugs over intestinal absorptive (Caco-2) cells. *J Pharm Sci* **79**(6)**:** 476-482.

Artursson, P, Karlsson, J (1991) Correlation between oral drug absorption in humans and apparent drug permeability coefficients in human intestinal epithelial (Caco-2) cells. *Biochem Biophys Res Commun* **175**(3)**:** 880-885.

Avdeef, A (2005) The rise of PAMPA. *Expert Opin Drug Metab Toxicol* **1**(2)**:** 325-342.

Bakos, E, Evers, R, Szakacs, G, Tusnady, GE, Welker, E, Szabo, K, de Haas, M, van Deemter, L, Borst, P, Varadi, A, Sarkadi, B (1998) Functional multidrug resistance protein (MRP1) lacking the N-terminal transmembrane domain. *J Biol Chem* **273**(48)**:** 32167-32175.

Balis, FM, Savitch, JL, Bleyer, WA (1983) Pharmacokinetics of oral methotrexate in children. *Cancer Res* **43**(5)**:** 2342-2345.

Barker, G, Simmons, NL (1981) Identification of two strains of cultured canine renal epithelial cells (MDCK cells) which display entirely different physiological properties. *Q J Exp Physiol* **66**(1)**:** 61-72.

Bates, SE, Robey, R, Miyake, K, Rao, K, Ross, DD, Litman, T (2001) The role of half-transporters in multidrug resistance. *J Bioenerg Biomembr* **33**(6)**:** 503-511.

Belinsky, MG, Chen, ZS, Shchaveleva, I, Zeng, H, Kruh, GD (2002) Characterization of the drug resistance and transport properties of multidrug resistance protein 6 (MRP6, ABCC6). *Cancer Res* **62**(21)**:** 6172-6177.

Bera, TK, Lee, S, Salvatore, G, Lee, B, Pastan, I (2001) MRP8, a new member of ABC transporter superfamily, identified by EST database mining and gene prediction program, is highly expressed in breast cancer. *Mol Med* **7**(8)**:** 509-516.

Berggren, S, Gall, C, Wollnitz, N, Ekelund, M, Karlbom, U, Hoogstraate, J, Schrenk, D, Lennernas, H (2007) Gene and protein expression of P-glycoprotein, MRP1, MRP2, and CYP3A4 in the small and large human intestine. *Mol Pharm* **4**(2)**:** 252-257.

Berthois, Y, Katzenellenbogen, JA, Katzenellenbogen, BS (1986) Phenol red in tissue culture media is a weak estrogen: implications concerning the study of estrogen-responsive cells in culture. *Proc Natl Acad Sci U S A* **83**(8)**:** 2496-2500.

Bindal, RD, Carlson, KE, Katzenellenbogen, BS, Katzenellenbogen, JA (1988) Lipophilic impurities, not phenolsulfonphthalein, account for the estrogenic activity in commercial preparations of phenol red. *J Steroid Biochem* **31**(3)**:** 287-293.

Bogman, K, Erne-Brand, F, Alsenz, J, Drewe, J (2003) The role of surfactants in the reversal of active transport mediated by multidrug resistance proteins. *J Pharm Sci* **92**(6)**:** 1250-1261.

Borst, P, de Wolf, C, van de Wetering, K (2007) Multidrug resistance-associated proteins 3, 4, and 5. *Pflugers Arch* **453**(5)**:** 661-673.

Borst, P, Evers, R, Kool, M, Wijnholds, J (2000) A family of drug transporters: the multidrug resistance-associated proteins. *J Natl Cancer Inst* **92**(16)**:** 1295-1302.

Bradford, MM (1976) A rapid and sensitive method for the quantitation of microgram quantities of protein utilizing the principle of protein-dye binding. *Anal Biochem* **72:** 248-254.

Buchler, M, Konig, J, Brom, M, Kartenbeck, J, Spring, H, Horie, T, Keppler, D (1996) cDNA cloning of the hepatocyte canalicular isoform of the multidrug resistance protein, cMrp, reveals a novel conjugate export pump deficient in hyperbilirubinemic mutant rats. *J Biol Chem* **271**(25)**:** 15091-15098.

Bunting, KD, Galipeau, J, Topham, D, Benaim, E, Sorrentino, BP (1999) Effects of retroviral-mediated MDR1 expression on hematopoietic stem cell self-renewal and differentiation in culture. *Ann N Y Acad Sci* **872:** 125-140; discussion 140-121.

Burk, O, Arnold, KA, Geick, A, Tegude, H, Eichelbaum, M (2005) A role for constitutive androstane receptor in the regulation of human intestinal MDR1 expression. *Biol Chem* **386**(6)**:** 503-513.

Carr, G, Wright, JA, Simmons, NL (2010) Epithelial barrier resistance is increased by the divalent cation zinc in cultured MDCKII epithelial monolayers. *J Membr Biol* **237**(2-3)**:** 115-123.

Carrier, I, Julien, M, Gros, P (2003) Analysis of catalytic carboxylate mutants E552Q and E1197Q suggests asymmetric ATP hydrolysis by the two nucleotide-binding domains of P-glycoprotein. *Biochemistry* **42**(44)**:** 12875-12885.

Cavet, ME, West, M, Simmons, NL (1997) Fluoroquinolone (ciprofloxacin) secretion by human intestinal epithelial (Caco-2) cells. *Br J Pharmacol* **121**(8)**:** 1567-1578.

Cavet, ME, West, M, Simmons, NL (1996) Transport and epithelial secretion of the cardiac glycoside, digoxin, by human intestinal epithelial (Caco-2) cells. *Br J Pharmacol* **118**(6)**:** 1389-1396.

Cereijido, M, Robbins, ES, Dolan, WJ, Rotunno, CA, Sabatini, DD (1978) Polarized monolayers formed by epithelial cells on a permeable and translucent support. *J Cell Biol* **77**(3)**:** 853-880.

Cereijido, M, Stefani, E, Palomo, AM (1980) Occluding junctions in a cultured transporting epithelium: structural and functional heterogeneity. *J Membr Biol* **53**(1)**:** 19-32.

Cerveny, L, Pavek, P, Malakova, J, Staud, F, Fendrich, Z (2006) Lack of interactions between breast cancer resistance protein (bcrp/abcg2) and selected antiepileptic agents. *Epilepsia* **47**(3)**:** 461-468.

Chan, LM, Lowes, S, Hirst, BH (2004) The ABCs of drug transport in intestine and liver: efflux proteins limiting drug absorption and bioavailability. *Eur J Pharm Sci* **21**(1)**:** 25-51.

Chen, ZS, Guo, Y, Belinsky, MG, Kotova, E, Kruh, GD (2005) Transport of bile acids, sulfated steroids, estradiol 17-beta-D-glucuronide, and leukotriene C4 by human multidrug resistance protein 8 (ABCC11). *Mol Pharmacol* **67**(2)**:** 545-557.

Chen, ZS, Lee, K, Walther, S, Raftogianis, RB, Kuwano, M, Zeng, H, Kruh, GD (2002) Analysis of methotrexate and folate transport by multidrug resistance protein 4 (ABCC4): MRP4 is a component of the methotrexate efflux system. *Cancer Res* **62**(11)**:** 3144-3150.

Clark, R, Kerr, ID, Callaghan, R (2006) Multiple drugbinding sites on the R482G isoform of the ABCG2 transporter. *Br J Pharmacol* **149**(5)**:** 506-515.

Collett, A, Sims, E, Walker, D, He, YL, Ayrton, J, Rowland, M, Warhurst, G (1996) Comparison of HT29-18-C1 and Caco-2 cell lines as models for studying intestinal paracellular drug absorption. *Pharm Res* **13**(2)**:** 216-221.

Cooray, HC, Blackmore, CG, Maskell, L, Barrand, MA (2002) Localisation of breast cancer resistance protein in microvessel endothelium of human brain. *Neuroreport* **13**(16)**:** 2059-2063.

Cordon-Cardo, C, O'Brien, JP, Boccia, J, Casals, D, Bertino, JR, Melamed, MR (1990) Expression of the multidrug resistance gene product (P-glycoprotein) in human normal and tumor tissues. *J Histochem Cytochem* **38**(9)**:** 1277-1287.

Cui, Y, Konig, J, Buchholz, JK, Spring, H, Leier, I, Keppler, D (1999) Drug resistance and ATP-dependent conjugate transport mediated by the apical multidrug resistance protein, MRP2, permanently expressed in human and canine cells. *Mol Pharmacol* **55**(5)**:** 929-937.

Dahan, A, Amidon, GL (2009) Small intestinal efflux mediated by MRP2 and BCRP shifts sulfasalazine intestinal permeability from high to low, enabling its colonic targeting. *Am J Physiol Gastrointest Liver Physiol* **297**(2)**:** G371-377.

de Bruin, M, Miyake, K, Litman, T, Robey, R, Bates, SE (1999) Reversal of resistance by GF120918 in cell lines expressing the ABC half-transporter, MXR. *Cancer Lett* **146**(2)**:** 117-126.

de Castro, WV, Mertens-Talcott, S, Derendorf, H, Butterweck, V (2007) Grapefruit juice-drug interactions: Grapefruit juice and its components inhibit P-glycoprotein (ABCB1) mediated transport of talinolol in Caco-2 cells. *J Pharm Sci* **96**(10)**:** 2808-2817.

Deeken, JF, Robey, RW, Shukla, S, Steadman, K, Chakraborty, AR, Poonkuzhali, B, Schuetz, EG, Holbeck, S, Ambudkar, SV, Bates, SE (2009) Identification of compounds that correlate with ABCG2 transporter function in the National Cancer Institute Anticancer Drug Screen. *Mol Pharmacol* **76**(5)**:** 946-956.

Deeley, RG, Westlake, C, Cole, SP (2006) Transmembrane transport of endo- and xenobiotics by mammalian ATP-binding cassette multidrug resistance proteins. *Physiol Rev* **86**(3)**:** 849-899.

Denison, MS, Nagy, SR (2003) Activation of the aryl hydrocarbon receptor by structurally diverse exogenous and endogenous chemicals. *Annu Rev Pharmacol Toxicol* **43:** 309-334.

Dietrich, CG, Geier, A, Oude Elferink, RP (2003) ABC of oral bioavailability: transporters as gatekeepers in the gut. *Gut* **52**(12)**:** 1788-1795.

Diop, NK, Hrycyna, CA (2005) N-Linked glycosylation of the human ABC transporter ABCG2 on asparagine 596 is not essential for expression, transport activity, or trafficking to the plasma membrane. *Biochemistry* **44**(14)**:** 5420-5429.

Doyle, LA, Ross, DD (2003) Multidrug resistance mediated by the breast cancer resistance protein BCRP (ABCG2). *Oncogene* **22**(47)**:** 7340-7358.

Doyle, LA, Yang, W, Abruzzo, LV, Krogmann, T, Gao, Y, Rishi, AK, Ross, DD (1998) A multidrug resistance transporter from human MCF-7 breast cancer cells. *Proc Natl Acad Sci U S A* **95**(26)**:** 15665-15670.

Durr, D, Stieger, B, Kullak-Ublick, GA, Rentsch, KM, Steinert, HC, Meier, PJ, Fattinger, K (2000) St John's Wort induces intestinal P-glycoprotein/MDR1 and intestinal and hepatic CYP3A4. *Clin Pharmacol Ther* **68**(6)**:** 598-604.

Ebert, B, Seidel, A, Lampen, A (2007) Phytochemicals induce breast cancer resistance protein in Caco-2 cells and enhance the transport of benzo[a]pyrene-3-sulfate. *Toxicol Sci* **96**(2)**:** 227-236.

Ee, PL, Kamalakaran, S, Tonetti, D, He, X, Ross, DD, Beck, WT (2004) Identification of a novel estrogen response element in the breast cancer resistance protein (ABCG2) gene. *Cancer Res* **64**(4)**:** 1247-1251.

Ejendal, KF, Hrycyna, CA (2005) Differential sensitivities of the human ATP-binding cassette transporters ABCG2 and P-glycoprotein to cyclosporin A. *Mol Pharmacol* **67**(3)**:** 902-911.

Englund, G, Rorsman, F, Ronnblom, A, Karlbom, U, Lazorova, L, Grasjo, J, Kindmark, A, Artursson, P (2006) Regional levels of drug transporters along the human intestinal tract: co-expression of ABC and SLC transporters and comparison with Caco-2 cells. *Eur J Pharm Sci* **29**(3-4)**:** 269-277.

Evers, R, Kool, M, van Deemter, L, Janssen, H, Calafat, J, Oomen, LC, Paulusma, CC, Oude Elferink, RP, Baas, F, Schinkel, AH, Borst, P (1998) Drug export activity of the human canalicular multispecific organic anion transporter in polarized kidney MDCK cells expressing cMOAT (MRP2) cDNA. *J Clin Invest* **101**(7)**:** 1310-1319.

Evseenko, DA, Murthi, P, Paxton, JW, Reid, G, Emerald, BS, Mohankumar, KM, Lobie, PE, Brennecke, SP, Kalionis, B, Keelan, JA (2007) The ABC transporter

BCRP/ABCG2 is a placental survival factor, and its expression is reduced in idiopathic human fetal growth restriction. *FASEB J* **21**(13)**:** 3592-3605.

Feng, B, Mills, JB, Davidson, RE, Mireles, RJ, Janiszewski, JS, Troutman, MD, de Morais, SM (2008) In vitro P-glycoprotein assays to predict the in vivo interactions of P-glycoprotein with drugs in the central nervous system. *Drug Metab Dispos* **36**(2)**:** 268-275.

Formica, JV, Regelson, W (1995) Review of the biology of Quercetin and related bioflavonoids. *Food Chem Toxicol* **33**(12)**:** 1061-1080.

Fromm, MF (2004) Importance of P-glycoprotein at blood-tissue barriers. *Trends Pharmacol Sci* **25**(8)**:** 423-429.

Fromm, MF, Kim, RB, Stein, CM, Wilkinson, GR, Roden, DM (1999) Inhibition of P-glycoprotein-mediated drug transport: A unifying mechanism to explain the interaction between digoxin and quinidine [seecomments]. *Circulation* **99**(4)**:** 552-557.

Fujikawa, M, Nakao, K, Shimizu, R, Akamatsu, M (2007) QSAR study on permeability of hydrophobic compounds with artificial membranes. *Bioorg Med Chem* **15**(11)**:** 3756-3767.

Gallo, JM, Laub, PB, Rowinsky, EK, Grochow, LB, Baker, SD (2000) Population pharmacokinetic model for topotecan derived from phase I clinical trials. *J Clin Oncol* **18**(12)**:** 2459-2467.

Ganapathy, ME, Brandsch, M, Prasad, PD, Ganapathy, V, Leibach, FH (1995) Differential recognition of beta -lactam antibiotics by intestinal and renal peptide transporters, PEPT 1 and PEPT 2. *J Biol Chem* **270**(43)**:** 25672-25677.

Gatmaitan, ZC, Arias, IM (1993) Structure and function of P-glycoprotein in normal liver and small intestine. *Adv Pharmacol* **24:** 77-97.

Geick, A, Eichelbaum, M, Burk, O (2001) Nuclear receptor response elements mediate induction of intestinal MDR1 by rifampin. *J Biol Chem* **276**(18)**:** 14581-14587.

Gharavi, N, El-Kadi, AO (2005) tert-Butylhydroquinone is a novel aryl hydrocarbon receptor ligand. *Drug Metab Dispos* **33**(3)**:** 365-372.

Giacomini, KM, Huang, SM, Tweedie, DJ, Benet, LZ, Brouwer, KL, Chu, X, Dahlin, A, Evers, R, Fischer, V, Hillgren, KM, Hoffmaster, KA, Ishikawa, T, Keppler, D, Kim, RB, Lee, CA, Niemi, M, Polli, JW, Sugiyama, Y, Swaan, PW, Ware, JA, Wright, SH, Yee, SW, Zamek-Gliszczynski, MJ, Zhang, L (2010) Membrane transporters in drug development. *Nat Rev Drug Discov* **9**(3)**:** 215-236.

Gibson, GG, Phillips, A, Aouabdi, S, Plant, K, Plant, N (2006) Transcriptional regulation of the human pregnane-X receptor. *Drug Metab Rev* **38**(1-2)**:** 31-49.

Giri, N, Agarwal, S, Shaik, N, Pan, G, Chen, Y, Elmquist, WF (2009) Substrate-dependent breast cancer resistance protein (Bcrp1/Abcg2)-mediated interactions: consideration of multiple binding sites in in vitro assay design. *Drug Metab Dispos* **37**(3)**:** 560-570.

Godfrey, C, Sweeney, K, Miller, K, Hamilton, R, Kremer, J (1998) The population pharmacokinetics of long-term methotrexate in rheumatoid arthritis. *Br J Clin Pharmacol* **46**(4)**:** 369-376.

Gomez, DY, Wacher, VJ, Tomlanovich, SJ, Hebert, MF, Benet, LZ (1995) The effects of ketoconazole on the intestinal metabolism and bioavailability of cyclosporine. *Clin Pharmacol Ther* **58**(1)**:** 15-19.

Goodell, MA, Brose, K, Paradis, G, Conner, AS, Mulligan, RC (1996) Isolation and functional properties of murine hematopoietic stem cells that are replicating in vivo. *J Exp Med* **183**(4)**:** 1797-1806.

Greiner, B, Eichelbaum, M, Fritz, P, Kreichgauer, HP, von Richter, O, Zundler, J, Kroemer, HK (1999) The role of intestinal P-glycoprotein in the interaction of digoxin and rifampin. *J Clin Invest* **104**(2)**:** 147-153.

Griffiths, NM, Hirst, BH, Simmons, NL (1994) Active intestinal secretion of the fluoroquinolone antibacterials ciprofloxacin, norfloxacin and pefloxacin; a common secretory pathway? *J Pharmacol Exp Ther* **269**(2)**:** 496-502.

Griffiths, NM, Hirst, BH, Simmons, NL (1993) Active secretion of the fluoroquinolone ciprofloxacin by human intestinal epithelial Caco-2 cell layers. *Br J Pharmacol* **108**(3)**:** 575-576.

Guo, Y, Kotova, E, Chen, ZS, Lee, K, Hopper-Borge, E, Belinsky, MG, Kruh, GD (2003) MRP8, ATP-binding cassette C11 (ABCC11), is a cyclic nucleotide efflux pump and a resistance factor for fluoropyrimidines 2',3'-dideoxycytidine and 9'-(2'-phosphonylmethoxyethyl)adenine. *J Biol Chem* **278**(32)**:** 29509-29514.

Gutmann, H, Hruz, P, Zimmermann, C, Beglinger, C, Drewe, J (2005) Distribution of breast cancer resistance protein (BCRP/ABCG2) mRNA expression along the human GI tract. *Biochem Pharmacol* **70**(5)**:** 695-699.

Handschin, C, Meyer, UA (2003) Induction of drug metabolism: the role of nuclear receptors. *Pharmacol Rev* **55**(4)**:** 649-673.

Hardwick, LJ, Velamakanni, S, van Veen, HW (2007) The emerging pharmacotherapeutic significance of the breast cancer resistance protein (ABCG2). *Br J Pharmacol* **151**(2)**:** 163-174.

Haslam, IS Regulation of the expression and function of P-glycoprotein by the nuclear receptor PXR. Physiology/Pharmacology PhD, Newcastle University, Newcastle upon Tyne, 2007.

Haslam, IS, Jones, K, Coleman, T, Simmons, NL (2008) Induction of P-glycoprotein expression and function in human intestinal epithelial cells (T84). *Biochem Pharmacol* **76**(7)**:** 850-861.

Hasler, U, Mordasini, D, Bianchi, M, Vandewalle, A, Feraille, E, Martin, PY (2003) Dual influence of aldosterone on AQP2 expression in cultured renal collecting duct principal cells. *J Biol Chem* **278**(24)**:** 21639-21648.

Havsteen, BH (2002) The biochemistry and medical significance of the flavonoids. *Pharmacol Ther* **96**(2-3)**:** 67-202.

Hazai, E, Bikadi, Z (2008) Homology modeling of breast cancer resistance protein (ABCG2). *J Struct Biol* **162**(1)**:** 63-74.

Hegedus, C, Szakacs, G, Homolya, L, Orban, TI, Telbisz, A, Jani, M, Sarkadi, B (2009) Ins and outs of the ABCG2 multidrug transporter: an update on in vitro functional assays. *Adv Drug Deliv Rev* **61**(1)**:** 47-56.

Henriksen, U, Gether, U, Litman, T (2005) Effect of Walker A mutation (K86M) on oligomerization and surface targeting of the multidrug resistance transporter ABCG2. *J Cell Sci* **118**(Pt 7)**:** 1417-1426.

Hidalgo, IJ, Raub, TJ, Borchardt, RT (1989) Characterization of the human colon carcinoma cell line (Caco-2) as a model system for intestinal epithelial permeability. *Gastroenterology* **96**(3)**:** 736-749.

Higgins, CF (1992) ABC transporters: from microorganisms to man. *Annu Rev Cell Biol* **8:** 67-113.

Hilgendorf, C, Ahlin, G, Seithel, A, Artursson, P, Ungell, AL, Karlsson, J (2007) Expression of thirty-six drug transporter genes in human intestine, liver, kidney, and organotypic cell lines. *Drug Metab Dispos* **35**(8)**:** 1333-1340.

Hilgers, AR, Conradi, RA, Burton, PS (1990) Caco-2 cell monolayers as a model for drug transport across the intestinal mucosa. *Pharm Res* **7**(9)**:** 902-910.

Hirohashi, T, Suzuki, H, Sugiyama, Y (1999) Characterization of the transport properties of cloned rat multidrug resistance-associated protein 3 (MRP3). *J Biol Chem* **274**(21)**:** 15181-15185.

Hoffmeyer, S, Burk, O, von Richter, O, Arnold, HP, Brockmoller, J, Johne, A, Cascorbi, I, Gerloff, T, Roots, I, Eichelbaum, M, Brinkmann, U (2000) Functional polymorphisms of the human multidrug-resistance gene: multiple sequence variations and correlation of one allele with P-glycoprotein expression and activity in vivo. *Proc Natl Acad Sci U S A* **97**(7)**:** 3473-3478.

Honjo, Y, Hrycyna, CA, Yan, QW, Medina-Perez, WY, Robey, RW, van de Laar, A, Litman, T, Dean, M, Bates, SE (2001) Acquired mutations in the MXR/BCRP/ABCP gene alter substrate specificity in MXR/BCRP/ABCP-overexpressing cells. *Cancer Res* **61**(18)**:** 6635-6639.

Honjo, Y, Morisaki, K, Huff, LM, Robey, RW, Hung, J, Dean, M, Bates, SE (2002) Single-nucleotide polymorphism (SNP) analysis in the ABC half-transporter ABCG2 (MXR/BCRP/ABCP1). *Cancer Biol Ther* **1**(6)**:** 696-702.

Hooijberg, JH, Broxterman, HJ, Kool, M, Assaraf, YG, Peters, GJ, Noordhuis, P, Scheper, RJ, Borst, P, Pinedo, HM, Jansen, G (1999) Antifolate resistance mediated by the multidrug resistance proteins MRP1 and MRP2. *Cancer Res* **59**(11)**:** 2532-2535.

Hopper, E, Belinsky, MG, Zeng, H, Tosolini, A, Testa, JR, Kruh, GD (2001) Analysis of the structure and expression pattern of MRP7 (ABCC10), a new member of the MRP subfamily. *Cancer Lett* **162**(2)**:** 181-191.

Horio, M, Chin, KV, Currier, SJ, Goldenberg, S, Williams, C, Pastan, I, Gottesman, MM, Handler, J (1989) Transepithelial transport of drugs by the multidrug transporter in cultured Madin-Darby canine kidney cell epithelia. *J Biol Chem* **264**(25)**:** 14880-14884.

Houghton, PJ, Germain, GS, Harwood, FC, Schuetz, JD, Stewart, CF, Buchdunger, E, Traxler, P (2004) Imatinib mesylate is a potent inhibitor of the ABCG2 (BCRP) transporter and reverses resistance to topotecan and SN-38 in vitro. *Cancer Res* **64**(7)**:** 2333-2337.

Hsiu, SL, Hou, YC, Wang, YH, Tsao, CW, Su, SF, Chao, PD (2002) Quercetin significantly decreased cyclosporin oral bioavailability in pigs and rats. *Life Sci* **72**(3)**:** 227-235.

Hunter, J, Hirst, BH, Simmons, NL (1993) Drug absorption limited by P-glycoprotein-mediated secretory drug transport in human intestinal epithelial Caco-2 cell layers. *Pharm Res* **10**(5)**:** 743-749.

Hunter, J, Hirst, BH, Simmons, NL (1991) Epithelial secretion of vinblastine by human intestinal adenocarcinoma cell (HCT-8 and T84) layers expressing P-glycoprotein. *Br J Cancer* **64**(3)**:** 437-444.

Imai, Y, Asada, S, Tsukahara, S, Ishikawa, E, Tsuruo, T, Sugimoto, Y (2003) Breast cancer resistance protein exports sulfated estrogens but not free estrogens. *Mol Pharmacol* **64**(3)**:** 610-618.

Imai, Y, Ishikawa, E, Asada, S, Sugimoto, Y (2005) Estrogen-mediated post transcriptional down-regulation of breast cancer resistance protein/ABCG2. *Cancer Res* **65**(2)**:** 596-604.

Imai, Y, Nakane, M, Kage, K, Tsukahara, S, Ishikawa, E, Tsuruo, T, Miki, Y, Sugimoto, Y (2002) C421A polymorphism in the human breast cancer resistance protein gene is associated with low expression of Q141K protein and low-level drug resistance. *Mol Cancer Ther* **1**(8)**:** 611-616.

Ishikawa, T, Akimaru, K, Nakanishi, M, Tomokiyo, K, Furuta, K, Suzuki, M, Noyori, R (1998) Anti-cancer-prostaglandin-induced cell-cycle arrest and its modulation by an inhibitor of the ATP-dependent glutathione S-conjugate export pump (GS-X pump). *Biochem J* **336 (Pt 3):** 569-576.

Ishikawa, T, Sakurai, A, Kanamori, Y, Nagakura, M, Hirano, H, Takarada, Y, Yamada, K, Fukushima, K, Kitajima, M (2005) High-speed screening of human ATP-binding cassette transporter function and genetic polymorphisms: new strategies in pharmacogenomics. *Methods Enzymol* **400:** 485-510.

James, SY, Lin, F, Kolluri, SK, Dawson, MI, Zhang, XK (2003) Regulation of retinoic acid receptor beta expression by peroxisome proliferator-activated receptor gamma ligands in cancer cells. *Cancer Res* **63**(13)**:** 3531-3538.

Jani, M, Szabo, P, Kis, E, Molnar, E, Glavinas, H, Krajcsi, P (2009) Kinetic characterization of sulfasalazine transport by human ATP-binding cassette G2. *Biol Pharm Bull* **32**(3)**:** 497-499.

Jedlitschky, G, Leier, I, Buchholz, U, Center, M, Keppler, D (1994) ATP-dependent transport of glutathione S-conjugates by the multidrug resistance-associated protein. *Cancer Res* **54**(18)**:** 4833-4836.

Jones, PM, George, AM (2004) The ABC transporter structure and mechanism: perspectives on recent research. *Cell Mol Life Sci* **61**(6)**:** 682-699.

Jonker, JW, Freeman, J, Bolscher, E, Musters, S, Alvi, AJ, Titley, I, Schinkel, AH, Dale, TC (2005) Contribution of the ABC transporters Bcrp1 and Mdr1a/1b to the side population phenotype in mammary gland and bone marrow of mice. *Stem Cells* **23**(8)**:** 1059-1065.

Jonker, JW, Smit, JW, Brinkhuis, RF, Maliepaard, M, Beijnen, JH, Schellens, JH, Schinkel, AH (2000) Role of breast cancer resistance protein in the bioavailability and fetal penetration of topotecan. *J Natl Cancer Inst* **92**(20)**:** 1651-1656.

Juliano, RL, Ling, V (1976) A surface glycoprotein modulating drug permeability in Chinese hamster ovary cell mutants. *Biochim Biophys Acta* **455**(1)**:** 152-162.

Kage, K, Fujita, T, Sugimoto, Y (2005) Role of Cys-603 in dimer/oligomer formation of the breast cancer resistance protein BCRP/ABCG2. *Cancer Sci* **96**(12)**:** 866-872.

Kage, K, Tsukahara, S, Sugiyama, T, Asada, S, Ishikawa, E, Tsuruo, T, Sugimoto, Y (2002) Dominant-negative inhibition of breast cancer resistance protein as drug efflux pump through the inhibition of S-S dependent homodimerization. *Int J Cancer* **97**(5)**:** 626-630.

Kalliokoski, A, Niemi, M (2009) Impact of OATP transporters on pharmacokinetics. *Br J Pharmacol* **158**(3)**:** 693-705.

Kartenbeck, J, Leuschner, U, Mayer, R, Keppler, D (1996) Absence of the canalicular isoform of the MRP gene-encoded conjugate export pump from the hepatocytes in Dubin-Johnson syndrome. *Hepatology* **23**(5)**:** 1061-1066.

Kast, HR, Goodwin, B, Tarr, PT, Jones, SA, Anisfeld, AM, Stoltz, CM, Tontonoz, P, Kliewer, S, Willson, TM, Edwards, PA (2002) Regulation of multidrug resistance-associated protein 2 (ABCC2) by the nuclear receptors pregnane X receptor, farnesoid X-activated receptor, and constitutive androstane receptor. *J Biol Chem* **277**(4)**:** 2908-2915.

Kelly, D, Campbell, JI, King, TP, Grant, G, Jansson, EA, Coutts, AG, Pettersson, S, Conway, S (2004) Commensal anaerobic gut bacteria attenuate inflammation by regulating nuclear-cytoplasmic shuttling of PPAR-gamma and RelA. *Nat Immunol* **5**(1)**:** 104-112.

Kim, KA, Joo, HJ, Park, JY (2010) Effect of ABCG2 genotypes on the pharmacokinetics of A771726, an active metabolite of prodrug leflunomide, and association of A771726 exposure with serum uric acid level. *Eur J Clin Pharmacol* **67**(2)**:** 129-134.

Kim, M, Turnquist, H, Jackson, J, Sgagias, M, Yan, Y, Gong, M, Dean, M, Sharp, JG, Cowan, K (2002) The multidrug resistance transporter ABCG2 (breast cancer resistance protein 1) effluxes Hoechst 33342 and is overexpressed in hematopoietic stem cells. *Clin Cancer Res* **8**(1)**:** 22-28.

Kis, E, Nagy, T, Jani, M, Molnar, E, Janossy, J, Ujhellyi, O, Nemet, K, Heredi-Szabo, K, Krajcsi, P (2009) Leflunomide and its metabolite A771726 are high affinity substrates of BCRP: implications for drug resistance. *Ann Rheum Dis* **68**(7)**:** 1201-1207.

Klaassen, CD, Aleksunes, LM (2010) Xenobiotic, bile acid, and cholesterol transporters: function and regulation. *Pharmacol Rev* **62**(1)**:** 1-96.

Klein, HO, Lang, R, Weiss, E, Di Segni, E, Libhaber, C, Guerrero, J, Kaplinsky, E (1982) The influence of verapamil on serum digoxin concentration. *Circulation* **65**(5)**:** 998-1003.

Klement, JF, Matsuzaki, Y, Jiang, QJ, Terlizzi, J, Choi, HY, Fujimoto, N, Li, K, Pulkkinen, L, Birk, DE, Sundberg, JP, Uitto, J (2005) Targeted ablation of the abcc6 gene results in ectopic mineralization of connective tissues. *Mol Cell Biol* **25**(18)**:** 8299-8310.

Klinge, CM, Kaur, K, Swanson, HI (2000) The aryl hydrocarbon receptor interacts with estrogen receptor alpha and orphan receptors COUP-TFI and ERRalpha1. *Arch Biochem Biophys* **373**(1)**:** 163-174.

Klucken, J, Buchler, C, Orso, E, Kaminski, WE, Porsch-Ozcurumez, M, Liebisch, G, Kapinsky, M, Diederich, W, Drobnik, W, Dean, M, Allikmets, R, Schmitz, G (2000) ABCG1 (ABC8), the human homolog of the Drosophila white gene, is a regulator of

macrophage cholesterol and phospholipid transport. *Proc Natl Acad Sci U S A* **97**(2)**:** 817-822.

Kobayashi, D, Ieiri, I, Hirota, T, Takane, H, Maegawa, S, Kigawa, J, Suzuki, H, Nanba, E, Oshimura, M, Terakawa, N, Otsubo, K, Mine, K, Sugiyama, Y (2005) Functional assessment of ABCG2 (BCRP) gene polymorphisms to protein expression in human placenta. *Drug Metab Dispos* **33**(1)**:** 94-101.

Kondo, C, Suzuki, H, Itoda, M, Ozawa, S, Sawada, J, Kobayashi, D, Ieiri, I, Mine, K, Ohtsubo, K, Sugiyama, Y (2004) Functional analysis of SNPs variants of BCRP/ABCG2. *Pharm Res* **21**(10)**:** 1895-1903.

Konig, J, Rost, D, Cui, Y, Keppler, D (1999) Characterization of the human multidrug resistance protein isoform MRP3 localized to the basolateral hepatocyte membrane. *Hepatology* **29**(4)**:** 1156-1163.

Kool, M, van der Linden, M, de Haas, M, Baas, F, Borst, P (1999) Expression of human MRP6, a homologue of the multidrug resistance protein gene MRP1, in tissues and cancer cells. *Cancer Res* **59**(1)**:** 175-182.

Krishnamurthy, P, Schuetz, JD (2005) The ABC transporter Abcg2/Bcrp: role in hypoxia mediated survival. *Biometals* **18**(4)**:** 349-358.

Kruh, GD, Guo, Y, Hopper-Borge, E, Belinsky, MG, Chen, ZS (2007) ABCC10, ABCC11, and ABCC12. *Pfluegers Arch* **453**(5)**:** 675-684.

Lagas, JS, van der Kruijssen, CM, van de Wetering, K, Beijnen, JH, Schinkel, AH (2009) Transport of diclofenac by breast cancer resistance protein (ABCG2) and stimulation of multidrug resistance protein 2 (ABCC2)-mediated drug transport by diclofenac and benzbromarone. *Drug Metab Dispos* **37**(1)**:** 129-136.

Lee, SS, Jeong, HE, Yi, JM, Jung, HJ, Jang, JE, Kim, EY, Lee, SJ, Shin, JG (2007) Identification and functional assessment of BCRP polymorphisms in a Korean population. *Drug Metab Dispos* **35**(4)**:** 623-632.

Leggas, M, Panetta, JC, Zhuang, Y, Schuetz, JD, Johnston, B, Bai, F, Sorrentino, B, Zhou, S, Houghton, PJ, Stewart, CF (2006) Gefitinib modulates the function of multiple ATP-binding cassette transporters in vivo. *Cancer Res* **66**(9)**:** 4802-4807.

Lemos, C, Jansen, G, Peters, GJ (2008) Drug transporters: recent advances concerning BCRP and tyrosine kinase inhibitors. *Br J Cancer* **98**(5)**:** 857-862.

Litman, T, Brangi, M, Hudson, E, Fetsch, P, Abati, A, Ross, DD, Miyake, K, Resau, JH, Bates, SE (2000) The multidrug-resistant phenotype associated with overexpression of the new ABC half-transporter, MXR (ABCG2). *J Cell Sci* **113 (Pt 11):** 2011-2021.

Litman, T, Jensen, U, Hansen, A, Covitz, KM, Zhan, Z, Fetsch, P, Abati, A, Hansen, PR, Horn, T, Skovsgaard, T, Bates, SE (2002) Use of peptide antibodies to probe for

the mitoxantrone resistance-associated protein MXR/BCRP/ABCP/ABCG2. *Biochim Biophys Acta* **1565**(1)**:** 6-16.

Loos, WJ, Gelderblom, HJ, Verweij, J, Brouwer, E, de Jonge, MJ, Sparreboom, A (2000) Gender-dependent pharmacokinetics of topotecan in adult patients. *Anticancer Drugs* **11**(9)**:** 673-680.

Lowes, S Multiple pathways for organic solute secretion by human intestinal epithelium (Caco-2) cells, Newcastle University, 2001.

Lowes, S, Cavet, ME, Simmons, NL (2003) Evidence for a non-MDR1 component in digoxin secretion by human intestinal Caco-2 epithelial layers. *Eur J Pharmacol* **458**(1-2)**:** 49-56.

Lowes, S, Simmons, NL (2002) Multiple pathways for fluoroquinolone secretion by human intestinal epithelial (Caco-2) cells. *Br J Pharmacol* **135**(5)**:** 1263-1275.

Lown, KS, Mayo, RR, Leichtman, AB, Hsiao, HL, Turgeon, DK, Schmiedlin-Ren, P, Brown, MB, Guo, W, Rossi, SJ, Benet, LZ, Watkins, PB (1997) Role of intestinal P-glycoprotein (mdr1) in interpatient variation in the oral bioavailability of cyclosporine. *Clin Pharmacol Ther* **62**(3)**:** 248-260.

Madin, S, Darby, N (1972) *As catalogued in Registry of Animal Cell-lines of the American*
Type Culture Collection, 2nd ed.

Maglich, JM, Stoltz, CM, Goodwin, B, Hawkins-Brown, D, Moore, JT, Kliewer, SA (2002) Nuclear pregnane x receptor and constitutive androstane receptor regulate overlapping but distinct sets of genes involved in xenobiotic detoxification. *Mol Pharmacol* **62**(3)**:** 638-646.

Mahringer, A, Fricker, G (2010) BCRP at the Blood-Brain Barrier: Genomic Regulation by 17beta-Estradiol. *Mol Pharm* **7**(5)**:** 1835-1847.

Maliepaard, M, Scheffer, GL, Faneyte, IF, van Gastelen, MA, Pijnenborg, AC, Schinkel, AH, van De Vijver, MJ, Scheper, RJ, Schellens, JH (2001) Subcellular localization and distribution of the breast cancer resistance protein transporter in normal human tissues. *Cancer Res* **61**(8)**:** 3458-3464.

Mao, Q, Unadkat, JD (2005) Role of the breast cancer resistance protein (ABCG2) in drug transport. *AAPS J* **7**(1)**:** E118-133.

Marchetti, S, de Vries, NA, Buckle, T, Bolijn, MJ, van Eijndhoven, MA, Beijnen, JH, Mazzanti, R, van Tellingen, O, Schellens, JH (2008) Effect of the ATP-binding cassette drug transporters ABCB1, ABCG2, and ABCC2 on erlotinib hydrochloride (Tarceva) disposition in in vitro and in vivo pharmacokinetic studies employing Bcrp1-/-/Mdr1a/1b-/- (triple-knockout) and wild-type mice. *Mol Cancer Ther* **7**(8)**:** 2280-2287.

Marquez, B, Caceres, NE, Mingeot-Leclercq, MP, Tulkens, PM, Van Bambeke, F (2009) Identification of the efflux transporter of the fluoroquinolone antibiotic ciprofloxacin in murine macrophages: studies with ciprofloxacin-resistant cells. *Antimicrob Agents Chemother* **53**(6)**:** 2410-2416.

Martin, C, Berridge, G, Mistry, P, Higgins, C, Charlton, P, Callaghan, R (2000) Drug binding sites on P-glycoprotein are altered by ATP binding prior to nucleotide hydrolysis. *Biochemistry* **39**(39)**:** 11901-11906.

Martin, CM, Ferdous, A, Gallardo, T, Humphries, C, Sadek, H, Caprioli, A, Garcia, JA, Szweda, LI, Garry, MG, Garry, DJ (2008) Hypoxia-inducible factor-2alpha transactivates Abcg2 and promotes cytoprotection in cardiac side population cells. *Circ Res* **102**(9)**:** 1075-1081.

Matsson, P, Englund, G, Ahlin, G, Bergstrom, CA, Norinder, U, Artursson, P (2007) A global drug inhibition pattern for the human ATP-binding cassette transporter breast cancer resistance protein (ABCG2). *J Pharmacol Exp Ther* **323**(1)**:** 19-30.

Matsson, P, Pedersen, JM, Norinder, U, Bergstrom, CA, Artursson, P (2009) Identification of novel specific and general inhibitors of the three major human ATP-binding cassette transporters P-gp, BCRP and MRP2 among registered drugs. *Pharm Res* **26**(8)**:** 1816-1831.

Merino, G, Alvarez, AI, Pulido, MM, Molina, AJ, Schinkel, AH, Prieto, JG (2006) Breast cancer resistance protein (BCRP/ABCG2) transports fluoroquinolone antibiotics and affects their oral availability, pharmacokinetics, and milk secretion. *Drug Metab Dispos* **34**(4)**:** 690-695.

Merino, G, Jonker, JW, Wagenaar, E, van Herwaarden, AE, Schinkel, AH (2005) The breast cancer resistance protein (BCRP/ABCG2) affects pharmacokinetics, hepatobiliary excretion, and milk secretion of the antibiotic nitrofurantoin. *Mol Pharmacol* **67**(5)**:** 1758-1764.

Meyer zu Schwabedissen, HE, Verstuyft, C, Kroemer, HK, Becquemont, L, Kim, RB (2010) Human multidrug and toxin extrusion 1 (MATE1/SLC47A1) transporter: functional characterization, interaction with OCT2 (SLC22A2), and single nucleotide polymorphisms. *Am J Physiol Renal Physiol* **298**(4)**:** F997-F1005.

Michot, JM, Van Bambeke, F, Mingeot-Leclercq, MP, Tulkens, PM (2004) Active efflux of ciprofloxacin from J774 macrophages through an MRP-like transporter. *Antimicrob Agents Chemother* **48**(7)**:** 2673-2682.

Miller, CA, 3rd (1999) A human aryl hydrocarbon receptor signaling pathway constructed in yeast displays additive responses to ligand mixtures. *Toxicol Appl Pharmacol* **160**(3)**:** 297-303.

Miwa, M, Tsukahara, S, Ishikawa, E, Asada, S, Imai, Y, Sugimoto, Y (2003) Single amino acid substitutions in the transmembrane domains of breast cancer resistance protein (BCRP) alter cross resistance patterns in transfectants. *Int J Cancer* **107**(5)**:** 757-763.

Miyake, K, Mickley, L, Litman, T, Zhan, Z, Robey, R, Cristensen, B, Brangi, M, Greenberger, L, Dean, M, Fojo, T, Bates, SE (1999) Molecular cloning of cDNAs which are highly overexpressed in mitoxantrone-resistant cells: demonstration of homology to ABC transport genes. *Cancer Res* **59**(1)**:** 8-13.

Mizuarai, S, Aozasa, N, Kotani, H (2004) Single nucleotide polymorphisms result in impaired membrane localization and reduced atpase activity in multidrug transporter ABCG2. *Int J Cancer* **109**(2)**:** 238-246.

Morrison, TB, Weis, JJ, Wittwer, CT (1998) Quantification of low-copy transcripts by continuous SYBR Green I monitoring during amplification. *Biotechniques* **24**(6)**:** 954-958, 960, 962.

Muenster, U, Grieshop, B, Ickenroth, K, Gnoth, MJ (2008) Characterization of substrates and inhibitors for the in vitro assessment of Bcrp mediated drug-drug interactions. *Pharm Res* **25**(10)**:** 2320-2326.

Nakamura, Y, Oka, M, Soda, H, Shiozawa, K, Yoshikawa, M, Itoh, A, Ikegami, Y, Tsurutani, J, Nakatomi, K, Kitazaki, T, Doi, S, Yoshida, H, Kohno, S (2005) Gefitinib ("Iressa", ZD1839), an epidermal growth factor receptor tyrosine kinase inhibitor, reverses breast cancer resistance protein/ABCG2-mediated drug resistance. *Cancer Res* **65**(4)**:** 1541-1546.

Ni, Z, Bikadi, Z, Rosenberg, MF, Mao, Q (2010) Structure and function of the human breast cancer resistance protein (BCRP/ABCG2). *Curr Drug Metab* **11**(7)**:** 603-617.

Nicolle, E, Boumendjel, A, Macalou, S, Genoux, E, Ahmed-Belkacem, A, Carrupt, PA, Di Pietro, A (2009) QSAR analysis and molecular modeling of ABCG2-specific inhibitors. *Adv Drug Deliv Rev* **61**(1)**:** 34-46.

Ohtake, F, Takeyama, K, Matsumoto, T, Kitagawa, H, Yamamoto, Y, Nohara, K, Tohyama, C, Krust, A, Mimura, J, Chambon, P, Yanagisawa, J, Fujii-Kuriyama, Y, Kato, S (2003) Modulation of oestrogen receptor signalling by association with the activated dioxin receptor. *Nature* **423**(6939)**:** 545-550.

Ozvegy-Laczka, C, Hegedus, T, Varady, G, Ujhelly, O, Schuetz, JD, Varadi, A, Keri, G, Orfi, L, Nemet, K, Sarkadi, B (2004) High-affinity interaction of tyrosine kinase inhibitors with the ABCG2 multidrug transporter. *Mol Pharmacol* **65**(6)**:** 1485-1495.

Ozvegy, C, Litman, T, Szakacs, G, Nagy, Z, Bates, S, Varadi, A, Sarkadi, B (2001) Functional characterization of the human multidrug transporter, ABCG2, expressed in insect cells. *Biochem Biophys Res Commun* **285**(1)**:** 111-117.

Pan, G, Winter, TN, Roberts, JC, Fairbanks, CA, Elmquist, WF (2009) Organic cation uptake is enhanced in bcrp1-transfected MDCKII cells. *Mol Pharm* **7**(1)**:** 138-145.

Parry, MF, Smego, DA, Digiovanni, MA (1988) Hepatobiliary kinetics and excretion of ciprofloxacin. *Antimicrob Agents Chemother* **32**(7)**:** 982-985.

Pascussi, JM, Gerbal-Chaloin, S, Duret, C, Daujat-Chavanieu, M, Vilarem, MJ, Maurel, P (2008) The tangle of nuclear receptors that controls xenobiotic metabolism and transport: crosstalk and consequences. *Annu Rev Pharmacol Toxicol* **48:** 1-32.

Paulusma, CC, Kool, M, Bosma, PJ, Scheffer, GL, ter Borg, F, Scheper, RJ, Tytgat, GN, Borst, P, Baas, F, Oude Elferink, RP (1997) A mutation in the human canalicular multispecific organic anion transporter gene causes the Dubin-Johnson syndrome. *Hepatology* **25**(6)**:** 1539-1542.

Pavek, P, Merino, G, Wagenaar, E, Bolscher, E, Novotna, M, Jonker, JW, Schinkel, AH (2005) Human breast cancer resistance protein: interactions with steroid drugs, hormones, the dietary carcinogen 2-amino-1-methyl-6-phenylimidazo(4,5-b)pyridine, and transport of cimetidine. *J Pharmacol Exp Ther* **312**(1)**:** 144-152.

Pfaffl, MW (2001) A new mathematical model for relative quantification in real-time RT-PCR. *Nucleic Acids Res* **29**(9)**:** e45.

Pfendner, EG, Vanakker, OM, Terry, SF, Vourthis, S, McAndrew, PE, McClain, MR, Fratta, S, Marais, AS, Hariri, S, Coucke, PJ, Ramsay, M, Viljoen, D, Terry, PF, De Paepe, A, Uitto, J, Bercovitch, LG (2007) Mutation detection in the ABCC6 gene and genotype-phenotype analysis in a large international case series affected by pseudoxanthoma elasticum. *J Med Genet* **44**(10)**:** 621-628.

Polli, JW, Wring, SA, Humphreys, JE, Huang, L, Morgan, JB, Webster, LO, Serabjit-Singh, CS (2001) Rational use of in vitro P-glycoprotein assays in drug discovery. *J Pharmacol Exp Ther* **299**(2)**:** 620-628.

Prime-Chapman, HM, Fearn, RA, Cooper, AE, Moore, V, Hirst, BH (2004) Differential multidrug resistance-associated protein 1 through 6 isoform expression and function in human intestinal epithelial Caco-2 cells. *J Pharmacol Exp Ther* **311**(2)**:** 476-484.

Rabindran, SK, He, H, Singh, M, Brown, E, Collins, KI, Annable, T, Greenberger, LM (1998) Reversal of a novel multidrug resistance mechanism in human colon carcinoma cells by fumitremorgin C. *Cancer Res* **58**(24)**:** 5850-5858.

Raub, TJ (2006) P-glycoprotein recognition of substrates and circumvention through rational drug design. *Mol Pharm* **3**(1)**:** 3-25.

Reid, G, Wielinga, P, Zelcer, N, De Haas, M, Van Deemter, L, Wijnholds, J, Balzarini, J, Borst, P (2003a) Characterization of the transport of nucleoside analog drugs by the human multidrug resistance proteins MRP4 and MRP5. *Mol Pharmacol* **63**(5)**:** 1094-1103.

Reid, G, Wielinga, P, Zelcer, N, van der Heijden, I, Kuil, A, de Haas, M, Wijnholds, J, Borst, P (2003b) The human multidrug resistance protein MRP4 functions as a prostaglandin efflux transporter and is inhibited by nonsteroidal antiinflammatory drugs. *Proc Natl Acad Sci U S A* **100**(16)**:** 9244-9249.

Ren, S, Das, A, Lien, EJ (1996) QSAR analysis of membrane permeability to organic compounds. *J Drug Target* **4**(2)**:** 103-107.

Ritter, CA, Jedlitschky, G, Meyer zu Schwabedissen, H, Grube, M, Kock, K, Kroemer, HK (2005) Cellular export of drugs and signaling molecules by the ATP-binding cassette transporters MRP4 (ABCC4) and MRP5 (ABCC5). *Drug Metab Rev* **37**(1)**:** 253-278.

Rius, M, Nies, AT, Hummel-Eisenbeiss, J, Jedlitschky, G, Keppler, D (2003) Cotransport of reduced glutathione with bile salts by MRP4 (ABCC4) localized to the basolateral hepatocyte membrane. *Hepatology* **38**(2)**:** 374-384.

Robey, RW, Medina-Perez, WY, Nishiyama, K, Lahusen, T, Miyake, K, Litman, T, Senderowicz, AM, Ross, DD, Bates, SE (2001) Overexpression of the ATP-binding cassette half-transporter, ABCG2 (Mxr/BCrp/ABCP1), in flavopiridol-resistant human breast cancer cells. *Clin Cancer Res* **7**(1)**:** 145-152.

Rohwedder, RW, Bergan, T, Thorsteinsson, SB, Scholl, H (1990) Transintestinal elimination of ciprofloxacin. *Diagn Microbiol Infect Dis* **13**(2)**:** 127-133.

Rosenberg, MF, Bikadi, Z, Chan, J, Liu, X, Ni, Z, Cai, X, Ford, RC, Mao, Q (2010) The human breast cancer resistance protein (BCRP/ABCG2) shows conformational changes with mitoxantrone. *Structure* **18**(4)**:** 482-493.

Russel, FG, Koenderink, JB, Masereeuw, R (2008) Multidrug resistance protein 4 (MRP4/ABCC4): a versatile efflux transporter for drugs and signalling molecules. *Trends Pharmacol Sci* **29**(4)**:** 200-207.

Safa, AR (2004) Identification and characterization of the binding sites of P-glycoprotein for multidrug resistance-related drugs and modulators. *Curr Med Chem Anticancer Agents* **4**(1)**:** 1-17.

Saito, H, Hirano, H, Nakagawa, H, Fukami, T, Oosumi, K, Murakami, K, Kimura, H, Kouchi, T, Konomi, M, Tao, E, Tsujikawa, N, Tarui, S, Nagakura, M, Osumi, M, Ishikawa, T (2006) A new strategy of high-speed screening and quantitative structure-activity relationship analysis to evaluate human ATP-binding cassette transporter ABCG2-drug interactions. *J Pharmacol Exp Ther* **317**(3)**:** 1114-1124.

Sambuy, Y, De Angelis, I, Ranaldi, G, Scarino, ML, Stammati, A, Zucco, F (2005) The Caco-2 cell line as a model of the intestinal barrier: influence of cell and culture-related factors on Caco-2 cell functional characteristics. *Cell Biol Toxicol* **21**(1)**:** 1-26.

Scharenberg, CW, Harkey, MA, Torok-Storb, B (2002) The ABCG2 transporter is an efficient Hoechst 33342 efflux pump and is preferentially expressed by immature human hematopoietic progenitors. *Blood* **99**(2)**:** 507-512.

Scheffer, GL, Maliepaard, M, Pijnenborg, AC, van Gastelen, MA, de Jong, MC, Schroeijers, AB, van der Kolk, DM, Allen, JD, Ross, DD, van der Valk, P, Dalton, WS, Schellens, JH, Scheper, RJ (2000) Breast cancer resistance protein is localized at

the plasma membrane in mitoxantrone- and topotecan-resistant cell lines. *Cancer Res* **60**(10)**:** 2589-2593.

Schinkel, AH (1999) P-Glycoprotein, a gatekeeper in the blood-brain barrier. *Adv Drug Deliv Rev* **36**(2-3)**:** 179-194.

Schmitz, G, Langmann, T, Heimerl, S (2001) Role of ABCG1 and other ABCG family members in lipid metabolism. *J Lipid Res* **42**(10)**:** 1513-1520.

Seithel, A, Karlsson, J, Hilgendorf, C, Bjorquist, A, Ungell, AL (2006) Variability in mRNA expression of ABC- and SLC-transporters in human intestinal cells: comparison between human segments and Caco-2 cells. *Eur J Pharm Sci* **28**(4)**:** 291-299.

Sesink, AL, Arts, IC, de Boer, VC, Breedveld, P, Schellens, JH, Hollman, PC, Russel, FG (2005) Breast cancer resistance protein (Bcrp1/Abcg2) limits net intestinal uptake of quercetin in rats by facilitating apical efflux of glucuronides. *Mol Pharmacol* **67**(6)**:** 1999-2006.

Shiozawa, K, Oka, M, Soda, H, Yoshikawa, M, Ikegami, Y, Tsurutani, J, Nakatomi, K, Nakamura, Y, Doi, S, Kitazaki, T, Mizuta, Y, Murase, K, Yoshida, H, Ross, DD, Kohno, S (2004) Reversal of breast cancer resistance protein (BCRP/ABCG2)-mediated drug resistance by novobiocin, a coumermycin antibiotic. *Int J Cancer* **108**(1)**:** 146-151.

Sorgel, F, Naber, KG, Jaehde, U, Reiter, A, Seelmann, R, Sigl, G (1989) Gastrointestinal secretion of ciprofloxacin. Evaluation of the charcoal model for investigations in healthy volunteers. *Am J Med* **87**(5A)**:** 62S-65S.

Sorgel, F, Naber, KG, Kinzig, M, Mahr, G, Muth, P (1991) Comparative pharmacokinetics of ciprofloxacin and temafloxacin in humans: a review. *Am J Med* **91**(6A)**:** 51S-66S.

Sparreboom, A, Gelderblom, H, Marsh, S, Ahluwalia, R, Obach, R, Principe, P, Twelves, C, Verweij, J, McLeod, HL (2004) Diflomotecan pharmacokinetics in relation to ABCG2 421C>A genotype. *Clin Pharmacol Ther* **76**(1)**:** 38-44.

Sparreboom, A, Loos, WJ, Burger, H, Sissung, TM, Verweij, J, Figg, WD, Nooter, K, Gelderblom, H (2005) Effect of ABCG2 genotype on the oral bioavailability of topotecan. *Cancer Biol Ther* **4**(6)**:** 650-658.

Sparreboom, A, van Asperen, J, Mayer, U, Schinkel, AH, Smit, JW, Meijer, DK, Borst, P, Nooijen, WJ, Beijnen, JH, van Tellingen, O (1997) Limited oral bioavailability and active epithelial excretion of paclitaxel (Taxol) caused by P-glycoprotein in the intestine. *Proc Natl Acad Sci U S A* **94**(5)**:** 2031-2035.

Stampfer, MR (1982) Cholera toxin stimulation of human mammary epithelial cells in culture. *In Vitro* **18**(6)**:** 531-537.

Staud, F, Vackova, Z, Pospechova, K, Pavek, P, Ceckova, M, Libra, A, Cygalova, L, Nachtigal, P, Fendrich, Z (2006) Expression and transport activity of breast cancer resistance protein (Bcrp/Abcg2) in dually perfused rat placenta and HRP-1 cell line. *J Pharmacol Exp Ther* **319**(1)**:** 53-62.

Stewart, CF, Leggas, M, Schuetz, JD, Panetta, JC, Cheshire, PJ, Peterson, J, Daw, N, Jenkins, JJ, 3rd, Gilbertson, R, Germain, GS, Harwood, FC, Houghton, PJ (2004) Gefitinib enhances the antitumor activity and oral bioavailability of irinotecan in mice. *Cancer Res* **64**(20)**:** 7491-7499.

Stulnig, TM, Steffensen, KR, Gao, H, Reimers, M, Dahlman-Wright, K, Schuster, GU, Gustafsson, JA (2002) Novel roles of liver X receptors exposed by gene expression profiling in liver and adipose tissue. *Mol Pharmacol* **62**(6)**:** 1299-1305.

Su, SF, Huang, JD (1996) Inhibition of the intestinal digoxin absorption and exsorption by quinidine. *Drug Metab Dispos* **24**(2)**:** 142-147.

Su, Y, Hu, P, Lee, SH, Sinko, PJ (2007) Using novobiocin as a specific inhibitor of breast cancer resistant protein to assess the role of transporter in the absorption and disposition of topotecan. *J Pharm Pharm Sci* **10**(4)**:** 519-536.

Suzuki, M, Suzuki, H, Sugimoto, Y, Sugiyama, Y (2003) ABCG2 transports sulfated conjugates of steroids and xenobiotics. *J Biol Chem* **278**(25)**:** 22644-22649.

Szatmari, I, Vamosi, G, Brazda, P, Balint, BL, Benko, S, Szeles, L, Jeney, V, Ozvegy-Laczka, C, Szanto, A, Barta, E, Balla, J, Sarkadi, B, Nagy, L (2006) Peroxisome proliferator-activated receptor gamma-regulated ABCG2 expression confers cytoprotection to human dendritic cells. *J Biol Chem* **281**(33)**:** 23812-23823.

Taipalensuu, J, Tornblom, H, Lindberg, G, Einarsson, C, Sjoqvist, F, Melhus, H, Garberg, P, Sjostrom, B, Lundgren, B, Artursson, P (2001) Correlation of gene expression of ten drug efflux proteins of the ATP-binding cassette transporter family in normal human jejunum and in human intestinal epithelial Caco-2 cell monolayers. *J Pharmacol Exp Ther* **299**(1)**:** 164-170.

Tammur, J, Prades, C, Arnould, I, Rzhetsky, A, Hutchinson, A, Adachi, M, Schuetz, JD, Swoboda, KJ, Ptacek, LJ, Rosier, M, Dean, M, Allikmets, R (2001) Two new genes from the human ATP-binding cassette transporter superfamily, ABCC11 and ABCC12, tandemly duplicated on chromosome 16q12. *Gene* **273**(1)**:** 89-96.

Tamura, A, Wakabayashi, K, Onishi, Y, Takeda, M, Ikegami, Y, Sawada, S, Tsuji, M, Matsuda, Y, Ishikawa, T (2007) Re-evaluation and functional classification of non-synonymous single nucleotide polymorphisms of the human ATP-binding cassette transporter ABCG2. *Cancer Sci* **98**(2)**:** 231-239.

Tan, KP, Wang, B, Yang, M, Boutros, PC, Macaulay, J, Xu, H, Chuang, AI, Kosuge, K, Yamamoto, M, Takahashi, S, Wu, AM, Ross, DD, Harper, PA, Ito, S (2010) Aryl hydrocarbon receptor is a transcriptional activator of the human breast cancer resistance protein (BCRP/ABCG2). *Mol Pharmacol* **78**(2)**:** 175-185.

Tatsuta, T, Naito, M, Oh-hara, T, Sugawara, I, Tsuruo, T (1992) Functional involvement of P-glycoprotein in blood-brain barrier. *J Biol Chem* **267**(28)**:** 20383-20391.

Thiebaut, F, Tsuruo, T, Hamada, H, Gottesman, MM, Pastan, I, Willingham, MC (1987) Cellular localization of the multidrug-resistance gene product P-glycoprotein in normal human tissues. *Proc Natl Acad Sci U S A* **84**(21)**:** 7735-7738.

Thwaites, DT, Hirst, BH, Simmons, NL (1994) Substrate specificity of the di/tripeptide transporter in human intestinal epithelia (Caco-2): identification of substrates that undergo H^+-coupled absorption. *Br J Pharmacol* **113**(3)**:** 1050-1056.

Tichopad, A, Dilger, M, Schwarz, G, Pfaffl, MW (2003) Standardized determination of real-time PCR efficiency from a single reaction set-up. *Nucleic Acids Res* **31**(20)**:** e122.

Toyoda, Y, Hagiya, Y, Adachi, T, Hoshijima, K, Kuo, MT, Ishikawa, T (2008) MRP class of human ATP binding cassette (ABC) transporters: historical background and new research directions. *Xenobiotica* **38**(7-8)**:** 833-862.

Ueda, A, Hamadeh, HK, Webb, HK, Yamamoto, Y, Sueyoshi, T, Afshari, CA, Lehmann, JM, Negishi, M (2002) Diverse roles of the nuclear orphan receptor CAR in regulating hepatic genes in response to phenobarbital. *Mol Pharmacol* **61**(1)**:** 1-6.

van Aubel, RA, Smeets, PH, Peters, JG, Bindels, RJ, Russel, FG (2002) The MRP4/ABCC4 gene encodes a novel apical organic anion transporter in human kidney proximal tubules: putative efflux pump for urinary cAMP and cGMP. *J Am Soc Nephrol* **13**(3)**:** 595-603.

van Herwaarden, AE, Schinkel, AH (2006) The function of breast cancer resistance protein in epithelial barriers, stem cells and milk secretion of drugs and xenotoxins. *Trends Pharmacol Sci* **27**(1)**:** 10-16.

van Herwaarden, AE, Wagenaar, E, Merino, G, Jonker, JW, Rosing, H, Beijnen, JH, Schinkel, AH (2007) Multidrug transporter ABCG2/breast cancer resistance protein secretes riboflavin (vitamin B2) into milk. *Mol Cell Biol* **27**(4)**:** 1247-1253.

Verschraagen, M, Koks, CH, Schellens, JH, Beijnen, JH (1999) P-glycoprotein system as a determinant of drug interactions: the case of digoxin-verapamil. *Pharmacol Res* **40**(4)**:** 301-306.

Volpe, DA (2004) Permeability classification of representative fluoroquinolones by a cell culture method. *AAPS J* **6**(2)**:** 1-6.

Vore, M, Leggas, M (2008) Progesterone acts via progesterone receptors A and B to regulate breast cancer resistance protein expression. *Mol Pharmacol* **73**(3)**:** 613-615.

Wacher, VJ, Silverman, JA, Zhang, Y, Benet, LZ (1998) Role of P-glycoprotein and cytochrome P450 3A in limiting oral absorption of peptides and peptidomimetics. *J Pharm Sci* **87**(11)**:** 1322-1330.

Wakabayashi, K, Tamura, A, Saito, H, Onishi, Y, Ishikawa, T (2006) Human ABC transporter ABCG2 in xenobiotic protection and redox biology. *Drug Metab Rev* **38**(3)**:** 371-391.

Wall, AM, Gajjar, A, Link, A, Mahmoud, H, Pui, CH, Relling, MV (2000) Individualized methotrexate dosing in children with relapsed acute lymphoblastic leukemia. *Leukemia* **14**(2)**:** 221-225.

Wang, H, Lee, EW, Zhou, L, Leung, PC, Ross, DD, Unadkat, JD, Mao, Q (2008a) Progesterone receptor (PR) isoforms PRA and PRB differentially regulate expression of the breast cancer resistance protein in human placental choriocarcinoma BeWo cells. *Mol Pharmacol* **73**(3)**:** 845-854.

Wang, JS, Zhu, HJ, Markowitz, JS, Donovan, JL, Yuan, HJ, Devane, CL (2008b) Antipsychotic drugs inhibit the function of breast cancer resistance protein. *Basic Clin Pharmacol Toxicol* **103**(4)**:** 336-341.

Wang, M (2007) Extending the good diet, good health paradigm: modulation of breast cancer resistance protein (BCRP) by flavonoids. *Toxicol Sci* **96**(2)**:** 203-205.

Wang, X, Furukawa, T, Nitanda, T, Okamoto, M, Sugimoto, Y, Akiyama, S, Baba, M (2003) Breast cancer resistance protein (BCRP/ABCG2) induces cellular resistance to HIV-1 nucleoside reverse transcriptase inhibitors. *Mol Pharmacol* **63**(1)**:** 65-72.

Wang, X, Morris, ME (2007) Effects of the flavonoid chrysin on nitrofurantoin pharmacokinetics in rats: potential involvement of ABCG2. *Drug Metab Dispos* **35**(2)**:** 268-274.

Ward, A, Reyes, CL, Yu, J, Roth, CB, Chang, G (2007) Flexibility in the ABC transporter MsbA: Alternating access with a twist. *Proc Natl Acad Sci U S A* **104**(48)**:** 19005-19010.

Wattenberg, LW, Page, MA, Leong, JL (1968) Induction of increased benzpyrene hydroxylase activity by flavones and related compounds. *Cancer Res* **28**(5)**:** 934-937.

Weiss, J, Rose, J, Storch, CH, Ketabi-Kiyanvash, N, Sauer, A, Haefeli, WE, Efferth, T (2007) Modulation of human BCRP (ABCG2) activity by anti-HIV drugs. *J Antimicrob Chemother* **59**(2)**:** 238-245.

Weiss, J, Sauer, A, Herzog, M, Boger, RH, Haefeli, WE, Benndorf, RA (2009) Interaction of thiazolidinediones (glitazones) with the ATP-binding cassette transporters P-glycoprotein and breast cancer resistance protein. *Pharmacology* **84**(5)**:** 264-270.

Wielinga, PR, Reid, G, Challa, EE, van der Heijden, I, van Deemter, L, de Haas, M, Mol, C, Kuil, AJ, Groeneveld, E, Schuetz, JD, Brouwer, C, De Abreu, RA, Wijnholds, J, Beijnen, JH, Borst, P (2002) Thiopurine metabolism and identification of the thiopurine metabolites transported by MRP4 and MRP5 overexpressed in human embryonic kidney cells. *Mol Pharmacol* **62**(6)**:** 1321-1331.

Wijnholds, J, Mol, CA, van Deemter, L, de Haas, M, Scheffer, GL, Baas, F, Beijnen, JH, Scheper, RJ, Hatse, S, De Clercq, E, Balzarini, J, Borst, P (2000) Multidrug-resistance protein 5 is a multispecific organic anion transporter able to transport nucleotide analogs. *Proc Natl Acad Sci U S A* **97**(13)**:** 7476-7481.

Woehlecke, H, Pohl, A, Alder-Baerens, N, Lage, H, Herrmann, A (2003) Enhanced exposure of phosphatidylserine in human gastric carcinoma cells overexpressing the half-size ABC transporter BCRP (ABCG2). *Biochem J* **376**(Pt 2)**:** 489-495.

Wu, CP, Calcagno, AM, Hladky, SB, Ambudkar, SV, Barrand, MA (2005) Modulatory effects of plant phenols on human multidrug-resistance proteins 1, 4 and 5 (ABCC1, 4 and 5). *FEBS J* **272**(18)**:** 4725-4740.

Xia, CQ, Liu, N, Miwa, GT, Gan, LS (2007a) Interactions of cyclosporin a with breast cancer resistance protein. *Drug Metab Dispos* **35**(4)**:** 576-582.

Xia, CQ, Liu, N, Yang, D, Miwa, G, Gan, LS (2005) Expression, localization, and functional characteristics of breast cancer resistance protein in Caco-2 cells. *Drug Metab Dispos* **33**(5)**:** 637-643.

Xia, CQ, Milton, MN, Gan, LS (2007b) Evaluation of drug-transporter interactions using in vitro and in vivo models. *Curr Drug Metab* **8**(4)**:** 341-363.

Xiao, Y, Davidson, R, Smith, A, Pereira, D, Zhao, S, Soglia, J, Gebhard, D, de Morais, S, Duignan, DB (2006) A 96-well efflux assay to identify ABCG2 substrates using a stably transfected MDCK II cell line. *Mol Pharm* **3**(1)**:** 45-54.

Xu, J, Liu, Y, Yang, Y, Bates, S, Zhang, JT (2004) Characterization of oligomeric human half-ABC transporter ATP-binding cassette G2. *J Biol Chem* **279**(19)**:** 19781-19789.

Yabuuchi, H, Shimizu, H, Takayanagi, S, Ishikawa, T (2001) Multiple splicing variants of two new human ATP-binding cassette transporters, ABCC11 and ABCC12. *Biochem Biophys Res Commun* **288**(4)**:** 933-939.

Yanase, K, Tsukahara, S, Mitsuhashi, J, Sugimoto, Y (2006) Functional SNPs of the breast cancer resistance protein-therapeutic effects and inhibitor development. *Cancer Lett* **234**(1)**:** 73-80.

Yoshioka, S, Katayama, K, Okawa, C, Takahashi, S, Tsukahara, S, Mitsuhashi, J, Sugimoto, Y (2007) The identification of two germ-line mutations in the human breast cancer resistance protein gene that result in the expression of a low/non-functional protein. *Pharm Res* **24**(6)**:** 1108-1117.

Zakelj, S, Sturm, K, Kristl, A (2006) Ciprofloxacin permeability and its active secretion through rat small intestine in vitro. *Int J Pharm* **313**(1-2)**:** 175-180.

Zamber, CP, Lamba, JK, Yasuda, K, Farnum, J, Thummel, K, Schuetz, JD, Schuetz, EG (2003) Natural allelic variants of breast cancer resistance protein (BCRP) and

their relationship to BCRP expression in human intestine. *Pharmacogenetics* **13**(1)**:** 19-28.

Zelcer, N, Reid, G, Wielinga, P, Kuil, A, van der Heijden, I, Schuetz, JD, Borst, P (2003) Steroid and bile acid conjugates are substrates of human multidrug-resistance protein (MRP) 4 (ATP-binding cassette C4). *Biochem J* **371**(Pt 2)**:** 361-367.

Zelcer, N, van de Wetering, K, Hillebrand, M, Sarton, E, Kuil, A, Wielinga, PR, Tephly, T, Dahan, A, Beijnen, JH, Borst, P (2005) Mice lacking multidrug resistance protein 3 show altered morphine pharmacokinetics and morphine-6-glucuronide antinociception. *Proc Natl Acad Sci U S A* **102**(20)**:** 7274-7279.

Zhang, S, Wang, X, Sagawa, K, Morris, ME (2005) Flavonoids chrysin and benzoflavone, potent breast cancer resistance protein inhibitors, have no significant effect on topotecan pharmacokinetics in rats or mdr1a/1b (-/-) mice. *Drug Metab Dispos* **33**(3)**:** 341-348.

Zhang, W, Yu, BN, He, YJ, Fan, L, Li, Q, Liu, ZQ, Wang, A, Liu, YL, Tan, ZR, Fen, J, Huang, YF, Zhou, HH (2006) Role of BCRP 421C>A polymorphism on rosuvastatin pharmacokinetics in healthy Chinese males. *Clin Chim Acta* **373**(1-2)**:** 99-103.

Zhang, Y, Guo, X, Lin, ET, Benet, LZ (1998) Overlapping substrate specificities of cytochrome P450 3A and P-glycoprotein for a novel cysteine protease inhibitor. *Drug Metab Dispos* **26**(4)**:** 360-366.

Zhao, YH, Abraham, MH, Le, J, Hersey, A, Luscombe, CN, Beck, G, Sherborne, B, Cooper, I (2002) Rate-limited steps of human oral absorption and QSAR studies. *Pharm Res* **19**(10)**:** 1446-1457.

Zhou, L, Schmidt, K, Nelson, FR, Zelesky, V, Troutman, MD, Feng, B (2009) The effect of breast cancer resistance protein and P-glycoprotein on the brain penetration of flavopiridol, imatinib mesylate (Gleevec), prazosin, and 2-methoxy-3-(4-(2-(5-methyl-2-phenyloxazol-4-yl)ethoxy)phenyl)propanoic acid (PF-407288) in mice. *Drug Metab Dispos* **37**(5)**:** 946-955.

Zhou, S, Schuetz, JD, Bunting, KD, Colapietro, AM, Sampath, J, Morris, JJ, Lagutina, I, Grosveld, GC, Osawa, M, Nakauchi, H, Sorrentino, BP (2001) The ABC transporter Bcrp1/ABCG2 is expressed in a wide variety of stem cells and is a molecular determinant of the side-population phenotype. *Nat Med* **7**(9)**:** 1028-1034.

Appendix

Appendix table 1. Table showing bi-directional flux of potential BCRP substrates in native MDCKII cells

Summary table of bi-directional flux in the apical to basal direction, basal to apical direction, net secretion (J_{net} = J_{b-a} - J_{a-b}), efflux ratio (J_{b-a} / J_{a-b}) and permeability coefficient (LogP) of potential BCRP substrates across native MDCKII cell monolayers. Cells were grown to confluency on 96-well permeable Transwell supports and assays were conducted via automation on a Hamilton StarPlus Robot. Compounds were used at a concentration of 10µM. Data points are means of n = 4-6 wells, data were pooled and normalised from 2 independent experiments ± SEM.

	Bidirectional Flux ($pmol.cm^{-2}.hr^{-1}$)				
Compound	**J_{a-b}**	**J_{b-a}**	**J_{net}**	**Efflux Ratio**	**logP**
Cimetidine	13.1 ± 0.7	141.9 ± 21.6	128.8 ± 21.3	10.8 ± 1.4	0.4
Clozapine	74.9 ± 7.1	251.3 ± 29.4	176.3 ± 29.5	3.4 ± 0.5	3.2
Diclofenac	332.3 ± 197.2	464 ± 276.4	131.7 ± 137.7	1.4 ± 0.3	4.5
Flavopiridol	296.6 ± 10.1	1168.7 ± 58.6	872.1 ± 50.2	3.9 ± 0.1	3.3
Gefitinib	1.4 ± 0.9	83 ± 30.1	81.6 ± 29.4	59.3 ± 11.9	4.9
Nitrofurantoin	172.6 ± 35.4	91.3 ± 15	-81.3 ± 25.4	0.5 ± 0.1	0.5
Novobiocin	17.4 ± 5.4	206.1 ± 26.8	188.8 ± 24.7	11.9 ± 3.9	2.5
Prazosin	242 ± 22.7	1281.6 ± 112	1039.5 ± 92.1	5.3 ± 0.2	1.3
Progesterone	390 ± 10.6	845.4 ± 29.7	455.4 ± 21.5	2.2 ± 0.1	3.9
Quinidine	112.2 ± 9.3	1961.2 ± 24.9	1849 ± 25.2	17.5 ± 1.4	3.4
Risperidone	307.7 ± 18.4	964.2 ± 32.7	656.4 ± 19.3	3.1 ± 0.1	3.5

Appendix table 2. Table showing bi-directional flux of potential BCRP substrates in hBCRP-MDCKII cells

Summary table of bi-directional flux in the apical to basal direction, basal to apical direction, net secretion (J_{net} = J_{b-a} - J_{a-b}), efflux ratio (J_{b-a} / J_{a-b}) and permeability coefficient (LogP) of potential BCRP substrates across human BCRP transfected MDCKII cell monolayers. Cells were grown to confluency on 96-well permeable Transwell supports and assays were conducted via automation on a Hamilton StarPlus Robot. Compounds were used at a concentration of 10µM. Data points are means of n = 4-6 wells, data were pooled and normalised from 2 independent experiments ± SEM.

	Bidirectional Flux ($pmol.cm^{-2}.hr^{-1}$)				
Compound	**J_{a-b}**	**J_{b-a}**	**J_{net}**	**Efflux Ratio**	**logP**
Cimetidine	72.1 ± 29	242.9 ± 141	187.4 ± 48.1	3.4 ± 1	0.4
Clozapine	103.8 ± 34.3	341.7 ± 88.5	237.9 ± 51	3.3 ± 0.5	3.2
Diclofenac	411.4 ± 35.4	1090.2 ± 64.4	678.8 ± 57	2.6 ± 0.2	4.5
Flavopiridol	165.7 ± 43.2	2134.9 ± 357.4	1969.2 ± 315.1	12.9 ± 1.1	3.3
Gefitinib	7.3 ± 5.3	273.1 ± 49.6	265.8 ± 45	37.6 ± 15.9	4.9
Nitrofurantoin	1.2 ± 0.2	270.9 ± 31	269.7 ± 31	217.3 ± 30.1	0.5
Novobiocin	10.9 ± 0.7	247 ± 18.5	236.1 ± 18	22.6 ± 3.4	2.5
Prazosin	110.1 ± 17.1	1763.8 ± 190.8	1653.7 ± 117	16 ± 2.6	1.3
Progesterone	333.2 ± 48.8	802 ± 94.3	468.9 ± 131.1	2.4 ± 0.5	3.9
Quinidine	68.9 ± 13.7	2492 ± 643.8	2423.1 ± 640	36.2 ± 8.8	3.4
Risperidone	282.4 ± 19.3	1392.9 ± 211	1110.6 ± 218.1	4.9 ± 0.9	3.5

Appendix table 3. Tables showing bi-directional flux of potential BCRP substrates in mBcrp1-MDCKII cells

Summary table of bi-directional flux in the apical to basal direction, basal to apical direction, net secretion (J_{net} = J_{b-a} - J_{a-b}), efflux ratio (J_{b-a} / J_{a-b}) and permeability coefficient (LogP) of potential BCRP substrates across mouse Bcrp transfected MDCKII cell monolayers. Cells were grown to confluency on 96-well permeable Transwell supports and assays were conducted via automation on a Hamilton StarPlus Robot. Compounds were used at a concentration of 10µM. Data points are means of n = 4-6 wells, data were pooled and normalised from 2 independent experiments ± SEM.

	Bidirectional Flux ($pmol.cm^{-2}.hr^{-1}$)				
Compound	**J_{a-b}**	**J_{b-a}**	**J_{net}**	**Efflux Ratio**	**logP**
Cimetidine	1.4 ± 0.5	222.1 ± 48.1	220.8 ± 93.1	161.1 ± 25.1	0.4
Clozapine	60 ± 6.8	286.7 ± 20.4	226.7 ± 14.1	4.8 ± 0.5	3.2
Diclofenac	356.6 ± 23	1021.7 ± 27.5	665.1 ± 37.2	2.9 ± 0.2	4.5
Flavopiridol	0.5 ± 0.1	1625.7 ± 87.7	1625.2 ± 87.7	3078.2 ± 203.9	3.3
Gefitinib	6.4 ± 3.9	1202.8 ± 622.5	1196.4 ± 418.6	187.5 ± 16.3	4.9
Nitrofurantoin	1.5 ± 0.1	234.4 ± 93.7	232.9 ± 93.7	156.4 ± 21.1	0.5
Novobiocin	0.6 ± 0.1	163.3 ± 23	162.7 ± 23.1	258.2 ± 30.8	2.5
Prazosin	1.8 ± 0.5	1428.4 ± 49.7	1426.5 ± 50.2	792.2 ± 64.2	1.3
Progesterone	52.4 ± 8.6	189.7 ± 56.8	137.3 ± 52.6	3.6 ± 0.5	3.9
Quinidine	1440 ± 115.4	3830 ± 306	2390 ± 421.4	2.6 ± 0.2	3.4
Risperidone	247.7 ± 28.2	654.8 ± 53.6	407.1 ± 75.5	2.6 ± 0.2	3.5

Appendix table 4. Tables showing bi-directional flux of potential BCRP substrates in MDR1-MDCKII cells

Summary table of bi-directional flux in the apical to basal direction, basal to apical direction, net secretion (J_{net} = J_{b-a} - J_{a-b}), efflux ratio (J_{b-a} / J_{a-b}) and permeability coefficient (LogP) of potential BCRP substrates across human MDR1 transfected MDCKII cell monolayers. Cells were grown to confluency on 96-well permeable Transwell supports and assays were conducted via automation on a Hamilton StarPlus Robot. Compounds were used at a concentration of 10µM. Data points are means of n = 4-6 wells, data were pooled and normalised from 2 independent experiments ± SEM.

	Bidirectional Flux ($pmol.cm^{-2}.hr^{-1}$)				
Compound	**J_{a-b}**	**J_{b-a}**	**J_{net}**	**Efflux Ratio**	**logP**
Cimetidine	62.3 ± 7.9	204 ± 49.4	141.1 ± 71.7	3.3 ± 0.4	0.4
Clozapine	225.2 ± 5.7	546.8 ± 28.8	321.5 ± 26.4	2.4 ± 0.1	3.2
Diclofenac	809 ± 80.4	1434.5 ± 193.2	625.6 ± 133.7	1.8 ± 0.2	4.5
Flavopiridol	408.2 ± 48.1	1468.3 ± 148.9	1060.1 ± 145.3	3.6 ± 0.5	3.3
Gefitinib	22.2 ± 10	290.8 ± 18.1	268.6 ± 17.5	13.1 ± 7	4.9
Nitrofurantoin	162.6 ± 12.8	61.3 ± 2.89	-101.3 ± 2.98	0.38 ± 0.1	0.5
Novobiocin	28.5 ± 6	98.5 ± 3.5	69.9 ± 8.3	3.4 ± 0.8	2.5
Prazosin	291.4 ± 8.8	1830 ± 37.3	1538.6 ± 30.9	6.3 ± 0.1	1.3
Progesterone	243.3 ± 28.5	788.5 ± 38.7	545.2 ± 45.3	3.2 ± 0.3	3.9
Quinidine	99.3 ± 4.7	2164.1 ± 34.8	2064.9 ± 38.9	21.8 ± 1.2	3.4
Risperidone	524 ± 68.6	1430.2 ± 91.1	906.1 ± 27.7	2.7 ± 0.2	3.5